THE EFFECTS OF CHEMOTHERAPY AGENTS ON HYPOXIA IN COLORECTAL CANCER

Dr Abul Hassan Siddiky

St. Edmund Hall

A thesis submitted to the Medical Sciences Division of the University of Oxford in partial fulfillment of the requirements for the degree of Doctor of Philosophy

CRUK/MRC Oxford Institute for Radiation Oncology

Department of Oncology

University of Oxford

Trinity Term 2015

Word count: 37,404

ABSTRACT

THE EFFECTS OF CHEMOTHERAPY AGENTS ON HYPOXIA IN COLORECTAL CANCER
Submitted for the degree of Doctor of Philosophy
Dr Abul Hassan Siddiky, St. Edmund Hall, Trinity Term 2015

Tumour hypoxia describes the phenomenon of reduced oxygen tension within solid tumours, resulting in an increase in morbidity, mortality and metastasis. We aim to identify chemotherapy agents that may reduce oxygen consumption and ultimately, improve tumour hypoxia and radiosensitivity.

Four colorectal cancer cell lines (COLO320DM, DLD1, HCT116 and HT29) and a non-transformed cell line (MRC5) were investigated. Clonogenic and cytotoxicity assays of a range of agents were used to determine sub-lethal concentrations that would alter consumption without cytotoxicity. The oxygen consumption and mitochondrial function of treated cells were assessed with the XF96 Analyzer. Flow cytometry, high performance liquid chromatography and western blot were performed to delineate mechanisms of action. The most responsive cell lines were grown as spheroids for hypoxia modelling before being tested *in vivo* for radiation sensitivity. *In vivo* tumour hypoxia analysis was achieved with the *in vivo* imaging system.

The oxygen consumption of all cancer cell lines was markedly reduced after treatment with a number of the agents compared to the non-transformed cell line. DLD1 and HCT116 cell lines showed the greatest balance of resistance to toxicity and reduction in oxygen consumption. Hypoxia imaging of the subsequent spheroids and i*n vivo* tumours further demonstrated a reduction in hypoxia consistent with drug induced decrease in oxygen consumption. This also conferred a relative enhancement in radiosensitivity in both *in vitro* and *in vivo* settings.

Despite decades of clinical use these known chemotherapeutics have not been implicated in alterations in oxidative metabolism. These results raise the prospect of using them in an alternative way to potentially improve clinical outcome.

For Sadia, for her silliness and for Dahlia, the start of a new chapter ...

ACKNOWLEDGEMENTS

First and foremost, I wish to thank Professor Ruth Muschel for giving me the glorious opportunity to pursue a D.Phil at Oxford, for the exposure to an international standard of research and not least for her continued support throughout the project. I will never forget the trust placed in me to develop the research.

I would also to thank Dr. Catherine Kelly and Dr. Thomas Ashton for their support in helping me to adapt from a clinical background to working as a basic scientist and for introducing me to the various scientific techniques that have been employed in the methodology of this dissertation.

I reserve special gratitude to Dr. Pavitra Kannan, who assumed responsibility in guiding me through the latter part of my D.Phil and helped replenish my enthusiasm at a time when all seemed lost.

Finally, immense thanks must go to my wife, who at the commencement of writing, was expecting our first child. It has been a huge sacrifice to live apart for the past 3 years but she has been supportive, enthused and a source of encouragement. Words cannot express the depth of gratitude I have for her. My daughter, Dahlia Seema Siddiky, was born on 9th May 2015 and it was her very arrival that spearheaded the timely completion of the thesis.

This project was jointly funded by both Cancer Research United Kingdom (CRUK) and the Engineering and Physical Sciences Research Council (EPSRC). Without their financial support, it would not have taken place.

ABBREVIATIONS AND ALTERNATIVE NOMENCLATURE

ABC	ATP-binding cassette
Acetyl-CoA	Acetyl-coenzyme A
ADP	Adenosine diphosphate
AMP	Adenosine monophosphate
ANOVA	Analysis of variance
APC	Adenomatous polyposis coli (deleted in polyposis 2.5 or DP2.5)
ARNT	Aryl hydrocarbon receptor nuclear translocator
ATP	Adenosine triphosphate
BrdU	Bromodeoxyuridine
CCD	Charge-coupled device
CDKs	Cyclin-dependent kinases
CIMP	CpG island methylator phenotype
CIN	Chromosomal instability pathway
CPNE	Computerised polarographic needle electrode
CT	Computed tomography
dFdCDP	Gemcitabine diphosphate
dFdCTP	Gemcitabine triphosphate
DFS	Disease free survival
DMEM	Dulbecco's modified Eagle medium
DMSO	Dimethyl sulphoxide
DNA	Deoxyribonucleic acid
dNTP	Deoxynucleotide triphosphate
DTT	Dithiothreitol
ECAR	Extracellular acidification rate
ECM	Extracellular matrix

EDTA	Ethylenediaminetetraacetic acid
EGF	Epidermal growth factor
ELISA	Enzyme-linked immunosorbent assay
EMT	Epithelial-mesenchymal transition
EPO	Erythropoietin
ErbB1	Epidermal growth factor receptor-1 (Her1)
ERK	Extracellular signal-regulated kinase
FACS	Fluorescence activated cell sorting
FAD	Flavin adenine dinucleotide
FADH	Flavin adenine dinucleotide (reduced)
FAP	Familial adenomatous polyposis
FBS	Fetal bovine serum
FCCP	Para-trifluoromethoxy carbonyl cyanide phenylhydrazone
FGF	Fibroblast growth factor
FMISO-PET	[18F]-fluoromisonidazole positron emission tomography
FUTP	Fluorouridine-5-triphosphate
G3P	Glyceraldehyde-3-phosphate
GAPDH	Glyceraldehyde-3-phosphate dehydrogenase
GFP	Green fluorescent protein
GLUT1	Glucose transporter 1
GLS1	Glutaminase 1
GREM1	Gremlin 1
GTPase	Guanosine triphosphatase
H&E	Haematoxylin and eosin
HIF	Hypoxia inducible factor
HMPS	Hereditary mixed polyposis syndrome
HNPCC	Hereditary non-polyposis colorectal cancer

HNSCC	Head and neck squamous cell carcinomas
HPLC	High performance liquid chromatography
HRE	HIF response element
IHC	Immunohistochemistry
IFN	Interferon
IL	Interleukin
IVIS	*In-vivo* Imaging System
kDa	Kilodalton
KRAS	Kirsten rat sarcoma
LDH	Lactate dehydrogenase
MAP	MUTYH-associated polyposis
MAPK	Mitogen-activated protein kinase
MCT1	Monocarboxylate transporter 1
MCT4	Monocarboxylate transporter 4
MDR1	Multidrug resistance protein 1
MEM	Minimum essential medium
MHC	Major histocompatibility complex
MLH1	MutL homolog 1
MRI	Magnetic resonance imaging
MS	Mass spectrometry
MSH2	MutS homolog 2
MSI	Microsatellite instability
mTOR	Mammalian target of rapamycin
MTT	3-(4,5-dimethylthiazol-2-yl)-2,5-diphenyltetrazolium bromide
NAD	Nicotinamide adenine dinucleotide
NADH	Nicotinamide adenine dinucleotide (reduced)
NHEJ	Non-homologous end joining

NRAS	Neuroblastoma rat sarcoma
OCR	Oxygen consumption rate
OCT	Optimal cutting temperature
OS	Overall survival
PARP1	Poly(ADP-ribose) polymerase 1
PBS	Phosphate buffered saline
PVDF	Polyvinylidene fluoride
PFA	Paraformaldehyde
PFKFB3	6-phosphofructo-2-kinase/fructose-2,6-biphosphatase isoform 3
PI3K	Phosphatidylinositol 3-kinase
PIK3CA	Phosphatidylinositol-4,5-bisphosphate 3-kinase, catalytic subunit alpha
PTEN	Phosphatase and tensin homolog
qPCR	Quantitative polymerase chain reaction
Ras	Rat sarcoma
RIPA	Radio immunoprecipitation assay
RNA	Ribonucleic acid
RNR	Ribonucleotide reductase
ROI	Region of interest
RPM	Revolutions per minute
RPMI	Roswell Park Memorial Institute medium
SD	Standard deviation
SDS-PAGE	Sodium dodecyl sulfate-polyacrylamide gel electrophoresis
SEM	Standard error of the mean
STAT	Signal transducers and activators of transcription
TGF	Transforming growth factor
THU	Tetrahydrouridine
TIMP-1	Tissue inhibitor of matrix metalloproteinase-1

TNB	Tris-NaCl-blocking buffer
TNF	Tumour necrosis factor
TNM	Tumour, nodes, metastasis
TRAIL	TNF-related apoptosis-inducing ligand
UTP	Uridine triphosphate
VEGF	Vascular endothelial growth factor
VHL	von Hippel Lindau
wt	Wild type
XF	Extracellular flux

TABLE OF CONTENTS

LIST OF FIGURES

CHAPTER 7: SUB-THERAPEUTIC DOSES OF DOCETAXEL AND GEMCITABINE IMPROVE HYPOXIA *IN VIVO*

CHAPTER 8: IMPROVING HYPOXIA BY REDUCING OXYGEN CONSUMPTION CAN IMPROVE RADIOSENSITIVITY

LIST OF TABLES

CHAPTER 1: INTRODUCTION

1.1 The clinical significance of colorectal cancer

1.1.1 The epidemiology of colorectal cancer

Colorectal cancer is a global problem, represented by over 1 million new cases per year worldwide [1]. Within Europe, it remains the second and third most common site of cancer in women and men respectively, with over 447,000 new diagnoses and 215,000 deaths throughout the continent in 2012 (See Fig. 1.1). Nationally, colorectal cancer is the third most common cause of cancer death and accounts for 13% of all new diagnoses of malignancy in the United Kingdom (UK) [2].

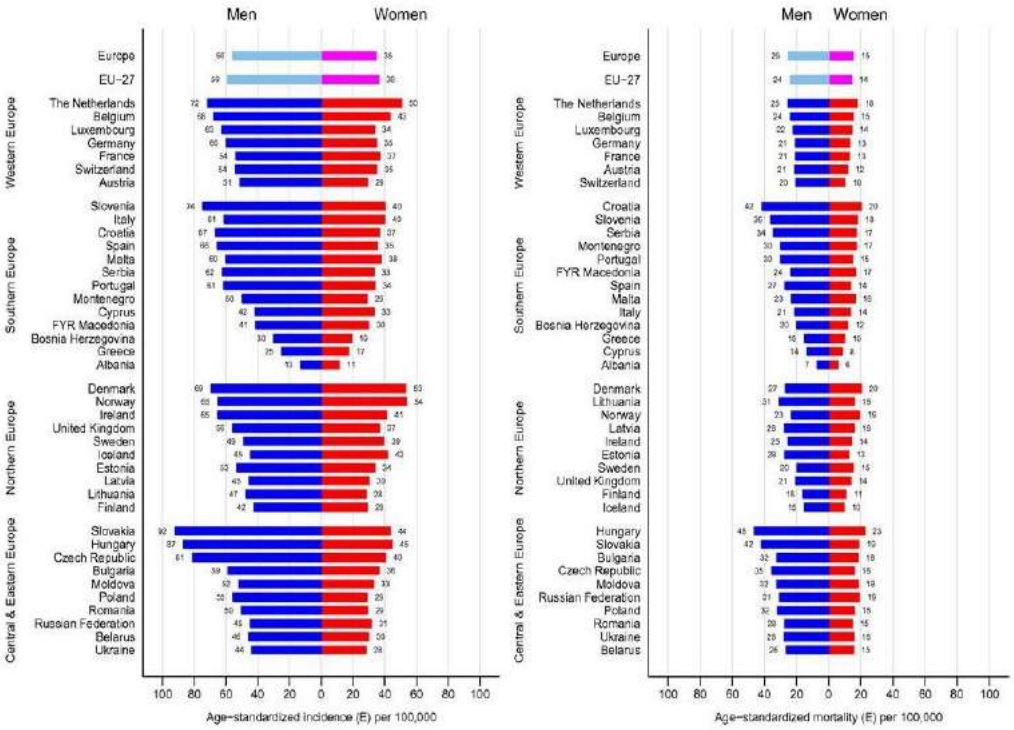

Figure 1.1 Age-standardised colorectal cancer incidence and mortality rates within Europe. Colorectal cancer is the second and third most common cancer in women and men respectively. Reproduced with permission from Ferlay J et al [3].

There is also a marked variation in the incidence of colorectal cancer with ethnicity and geographical location. Age-standardised rates for Caucasian males with colorectal cancer range from 54.1 to 55.3 per 100,000. This is significantly higher than that for Asian and Black males with rates ranging from 19.1 to 28.0 and 29.7 to 43.8 per 100,000 respectively. A similar pattern of incidence rates is also seen in females. The age-standardised rates for Caucasian females range from 34.0 to 34.8 per 100,000, whilst rates for Asian and Black females range from 11.3 to 17.5 and 20.4 to 31.6 per 100,000 respectively [4]. A similarly dramatic difference is seen between Westernised (North America, Europe and Australasia) and non-Westernised (Africa, Asia and South America) countries, with up to a 10-fold higher incidence of colorectal cancer in the former [5]. One possible explanation for this could be socio-economic deprivation, however extrapolation of UK data seems to refute this contention [6]. Another explanation for this geographical variation is the difference in diet, physical activity and body mass index (BMI) between these groups of nations. It is well documented that a diet high in red and processed meats, fat, sugar and low in fibre is associated with a higher risk of developing colorectal cancer [7-10]. Regular physical exercise or activity is also associated with a lower risk of colorectal cancer and this effect may be dose-dependent with increased frequency and intensity inversely associated with risk [11]. Furthermore, high body fat percentage and increased BMI has also been implicated as a risk factor for colorectal cancer [12]. These risk factors are often interrelated and more common in Westernised countries. Further evidence to support this link can be seen with the increased incidence of colorectal cancer in South Korea, Japan and China, which has coincided with the gradual shift in diet to mimic the United States, particularly in more urban areas [5, 13, 14].

Increasing age is also associated with an increased risk of developing colorectal cancer. The probability of developing colorectal cancer increases progressively after the

age of 40 and rises sharply after age 50 [15]. Greater than 90% of colorectal cancer cases occur in people aged 50 and above, whilst the incidence rate is over 50 times higher in persons aged 60 to 79 years than in those under 40 years of age [15]. The median age at diagnosis of colorectal cancer for men and women is 68 and 72 respectively [16]. With these epidemiological statistics, colorectal cancer could be considered primarily a disease of the elderly population. When therefore reviewing the association between diet, age and colorectal cancer, it is possible to surmise that long-term exposure to these risk-inducing foods is required for cancer development. This is further supported by experimental data indicating a minimum 17 year transitional period for benign colorectal polyps to develop into malignant lesions [17].

There is also a significant genetic component in the development of colorectal cancer. Approximately 20% of all patients with colorectal cancer will have a family member with the disease and those with one or more first-degree relatives with the disease are at increased risk [14]. Between 5 to 10% of colorectal cancers are as a result of established hereditary conditions and the best characterised presently are hereditary non-polyposis colorectal cancer (HNPCC) and familial adenomatous polyposis (FAP) [18]. HNPCC is associated with deoxyribonucleic acid (DNA) repair pathway gene mutations, specifically MutL homolog 1 (MLH1) and MutS homolog 2 (MSH2) whilst FAP is caused by mutations in the tumour suppressor gene adenomatous polyposis coli (APC) [19]. The lifetime risk of colorectal cancer in people with HNPCC reaches 80%, whereas this is almost 100% in people with FAP. Indeed, by age 40, colorectal cancer will develop in almost all patients with FAP if the colon is not removed [14]. Other, more recently characterised, hereditary conditions predisposing to colorectal cancer also include MUTYH-associated polyposis (MAP), which is an autosomal recessive disorder appearing to be at least as prevalent as FAP and hereditary mixed polyposis syndrome (HMPS), which is characterised by the development of mixed-morphology colorectal polyps as a

result of a 40-kb genetic duplication creating an aberrant epithelial expression of the gene encoding Gremlin 1 (GREM1), which is an antagonist of bone morphogenetic proteins in the transforming growth factor β signalling pathway [20, 21].

1.1.2 Current treatment modalities and regimes for colorectal cancer

The approaches available to treat colorectal cancer include surgical resection, chemotherapy, radiotherapy or a combination of the three. Endoscopic mucosal resection of early and superficial colorectal cancers is an alternative but relatively new technique and the long-term outcomes from this approach are still being evaluated [22]. The choice of therapy is ultimately a decision between the clinician and patient but evidence and guidance exist to optimise outcome and are largely dependent on the location and tumour, node and metastasis (TNM) stage of the tumour (See Fig. 1.2).

TNM staging for colorectal cancer, 7th edition

Primary tumor (T)	
TX	Primary tumor cannot be assessed
T0	No evidence of primary tumor
Tis	Carcinoma in situ: intraepithelial or invasion of lamina propria*
T1	Tumor invades submucosa
T2	Tumor invades muscularis propria
T3	Tumor invades through the muscularis propria into pericolorectal tissues
T4a	Tumor penetrates to the surface of the visceral peritoneum¶
T4b	Tumor directly invades or is adherent to other organs or structures¶Δ
Regional lymph node (N)◇	
NX	Regional lymph nodes cannot be assessed
N0	No regional lymph node metastasis
N1	Metastasis in 1-3 regional lymph nodes
N1a	Metastasis in one regional lymph node
N1b	Metastasis in 2-3 regional lymph nodes
N1c	Tumor deposit(s) in the subserosa, mesentery, or nonperitonealized pericolic or perirectal tissues without regional nodal metastasis
N2	Metastasis in four or more regional lymph nodes
N2a	Metastasis in 4-6 regional lymph nodes
N2b	Metastasis in seven or more regional lymph nodes
Distant metastasis (M)	
M0	No distant metastasis
M1	Distant metastasis
M1a	Metastasis confined to one organ or site (eg, liver, lung, ovary, nonregional node)
M1b	Metastases in more than one organ/site or the peritoneum

Anatomic stage/prognostic groups§

Stage	T	N	M	Dukes¥	MAC¥
0	Tis	N0	M0	-	-
I	T1	N0	M0	A	A
	T2	N0	M0	A	B1
IIA	T3	N0	M0	B	B2
IIB	T4a	N0	M0	B	B2
IIC	T4b	N0	M0	B	B3
IIIA	T1-2	N1/N1c	M0	C	C1
	T1	N2a	M0	C	C1
IIIB	T3-T4a	N1/N1c	M0	C	C2
	T2-T3	N2a	M0	C	C1/C2
	T1-T2	N2b	M0	C	C1
IIIC	T4a	N2a	M0	C	C2
	T3-T4a	N2b	M0	C	C2
	T4b	N1-N2	M0	C	C3
IVA	Any T	Any N	M1a	-	-
IVB	Any T	Any N	M1b	-	-

Figure 1.2. TNM and Dukes staging for colorectal cancer. Shown are the different staging systems for colorectal cancer in current clinical use. Reproduced with permission from the American Joint Committee on Cancer (AJCC) [23].

Approximately 80% of colorectal cancers are localised to the colonic or rectal wall and/or regional nodes at time of presentation. Proximal tumours have a greater proportion of high grade tumours, whilst the reverse is true of sigmoid tumours, which have a reduced tumour-specific mortality [24]. The greater proportion of high-grade tumours in the proximal colon

appears to be driven by the loss of DNA mismatch repair activity to result in microsatellite instability (MSI), which will be discussed further in Chapter 3 [25]. Surgery is the only curative modality for localised colonic cancer and provides a potentially curative option for select patients with limited metastatic disease, primarily in liver and lung. Long-term survival can be achieved with metastasectomy in up to 50% of cases, in conjunction with systemic chemotherapy. However, even after complete resection of metastases, most patients who are alive at five years are not cancer free. Approximately 20-30% remain disease free long-term and potentially cured [1, 26-29].

The National Institute for Health and Care Excellence (NICE) offers good practice guidelines based on different levels of clinical evidence [30]. Specific to rectal cancer, short-course neoadjuvant (preoperative) radiotherapy may be offered if the risk of recurrence is deemed moderate and chemotherapy may be added if the risk is deemed between moderate and high. A combination of both radiotherapy and chemotherapy should be considered if the risk is deemed high. Neoadjuvant chemotherapy alone should not routinely be offered for patients with locally advanced rectal cancer; although a new phase II trial evaluating this has been recently designed by the Memorial Sloan Kettering Cancer Center in New York [31]. Risk of recurrence is determined with magnetic resonance imaging (MRI) and TNM staging. Adjuvant (postoperative) chemotherapy should be considered for patients with stage II colonic and rectal cancer who are at high risk of recurrence and all patients with stage III colonic and rectal cancer. The choice of chemotherapy regime also depends on patient choice, their tolerance of the agents and on the stage of the disease. Example regimes include capecitabine as monotherapy, XELOX (capecitabine and oxaliplatin) or FOLFOX (folinic acid, fluorouracil and oxaliplatin). For advanced or stage IV disease, FOLFOX, XELOX or tegafur with uracil may be offered as first line treatment then either irinotecan as monotherapy or FOLFIRI (folinic acid, fluorouracil and irinotecan) as second line treatment. Raltitrexed may be considered for patients who are intolerant to fluorouracil and folinic acid or for whom these drugs are

unsuitable. NICE also has detailed guidelines on the use of biological agents such as cetuximab, bevacizumab and panitumumab for chemotherapy but, on the whole, are not generally recommended as they do not provide enough benefit to patients to justify the high costs, unless in specific circumstances.

1.2 Chemotherapeutics

1.2.1 The goals of chemotherapy

The main goals of chemotherapy can be broadly categorised into three aims: to cure cancer or prevent recurrence; to control non-curable disease and prolong life or to improve quality of life by palliating symptoms. These aims are often achieved in combination with other modalities of cancer treatment such as radiotherapy and surgery.

1.2.2 Classes and mechanisms of action of chemotherapy agents

Chemotherapy offers one modality in the treatment of cancer and generally refers to the use of chemical substances or drugs to do so. They are often sub-divided into cytotoxic therapies (agents that take advantage of the rapidly dividing state of cancer cells to induce cell death but are usually non-specific, resulting in a high side-effect profile); targeted therapies (agents that act on cancer specific molecules or metabolic pathways) and hormonal therapies (agents that manipulate the endocrine system to affect hormone-sensitive tumours).

1.2.2.1 Cytotoxic therapies

Cytotoxic agents cause cell damage or death and are the oldest class of anti-cancer agents. They were first identified as a potential chemotherapy agent during World War I when mustard gas was used as a chemical weapon and affected individuals demonstrated anaemia and bone

marrow suppression [32]. This eventually led to the first trial of derivatives of this agent as a treatment for haematological cancers [33]. Cytotoxic agents can be further broadly categorised as follows:

1.2.2.1.1 Alkylating agents

Alkylating agents bind covalently to nucleic acids and proteins which subsequently induces apoptosis by causing torsional stress and DNA damage during replication [34, 35]. These agents are cell-cycle independent, working at any phase of the cell-cycle. Consequently, their effect on the cell is dose-dependent and the fraction of cells that die is directly proportional to the dose of drug [36]. This dose-dependent effect also correlates with the risk of developing acute leukaemia, with the risk highest about 5 to 10 years after treatment [37]. Alkylating agents include nitrogen mustards (e.g. cyclophosphamide, ifosfamide, and melphalan); nitrosoureas (e.g. streptozocin, carmustine, and lomustine); tetrazines (e.g. dacarbazine, mitozolomide and temozolomide) and aziridines (e.g. thiotepa, mytomycin and diaziquone) [35]. Platinum based drugs (e.g. cisplatin, carboplatin, and oxalaplatin) are sometimes grouped with alkylating agents as they exert their cytotoxic effect through a similar mechanism [38].

1.2.2.1.2 Anti-metabolites

Anti-metabolites are a group of agents that disrupt DNA and ribonucleic acid (RNA) synthesis. They structurally resemble either nucleobases or nucleosides and induce cytotoxicity or cytostasis by either inhibiting enzymes required for DNA synthesis or becoming incorporated into DNA or RNA [39]. By impeding DNA synthesis, the agents prevent mitosis, whereas by incorporating into DNA, they cause double-strand DNA breakage and cell death. Anti-metabolites typically cause S phase arrest in the cell-cycle. Consequently, upon reaching a certain dose, the effect of the agent on cell death reaches a plateau and no more cell death occurs with increased doses [35]. Anti-metabolites include anti-folates (e.g. methotrexate,

raltitrexed and pemetrexed); fluoropyrimidines (e.g. fluorouracil and capecitabine); deoxynucleoside analogues (e.g. gemcitabine and pentostatin) and thiopurines (e.g. thioguanine and mercaptopurine) [35, 39].

1.2.2.1.3 Antibiotics

Cytotoxic antibiotics are a diverse group of agents that have principally been derived from the bacterium genus *Streptomyces* and encompass a variety of mechanisms of action to exert their anti-tumour effect. These include DNA intercalation, free radical production and topoisomerase inhibition [35, 40]. Like alkylating agents, they are also cell-cycle independent drugs. Sub-groups of cytotoxic antibiotics include the anthracyclines (e.g. doxorubicin, daunorubicin and mitoxantrone) and chromomycins (e.g. dactinomycin and plicamycin). Other common agents not in these groups include mitomycin and bleomycin.

1.2.2.1.4 Topoisomerase inhibitors

Topoisomerases, which comprise of the enzymes topoisomerase I and topoisomerase II, produce reversible single-strand breaks in DNA during replication, necessary to relieve torsional strain and allow DNA replication to proceed. Topoisomerase inhibitors therefore impede this function and prevent DNA replication and transcription [41]. Drugs targeting topoisomerase I and causing inhibition include irinotecan and topotecan, whereas those targeting topoisomerase II either cause inhibition (e.g. novobiocin and merbarone) or increased expression to saturate DNA binding and prevent replication (e.g. etoposide and teniposide) [42].

1.2.2.1.5 Anti-microtubule agents

Microtubules are important cellular structures and are a component of the cytoskeleton. They are found throughout the cytoplasm and are composed of α-tubulin and β-tubulin proteins, essential in maintaining the structure of the cell. Microtubules are also involved in

chromosome separation during mitosis and meiosis, forming the major constituents of mitotic spindles [43]. Anti-microtubule agents are plant-derived chemicals that interfere with cell division by preventing microtubule function, which are usually in a state of assembly and disassembly. They are cell-cycle specific and cause G_2/M or M phase arrest but can damage cells at all phases of the cell-cycle. The two main sub-groups of anti-microtubule agents are the vinca alkaloids (e.g. vincristine and vinblastine), derived from the Madagascar periwinkle, *Catharanthus roseus* and taxanes (e.g. docetaxel and paclitaxel), derived from the Pacific Yew tree, *Taxus brevifolia* or *Taxus baccata* [44]. The vinca alkaloids interfere with microtubule assembly, whereas the taxanes prevent microtubule disassembly. Both mechanisms block tumour cells from completing mitosis, causing cell-cycle arrest and apoptosis [35].

1.2.2.2 Targeted (biological) therapies

Targeted therapies are a relatively new chemotherapeutic option for cancer and offer tumour-specific or patient-specific treatment. Targeted therapies are designed to affect tumour-specific cellular proteins or processes such as mutant genes or transcription factors, allowing focused treatment with high concentrations being delivered to tumour cells with a relatively low concentration to other tissues. This approach consequently has a much lower side-effect profile when compared to cytotoxic therapies [45]. They can be further grouped into small molecules (e.g. imatinib, gefitinib and sunitinib) or monoclonal antibodies (e.g. rituximab, trastuzumab and cetuximab) [35].

1.2.2.3 Hormonal therapies

Hormone therapy for cancer involves the manipulation of the endocrine system through exogenous administration of specific hormones or agents that inhibit specific hormone activity or production. As steroid hormones are significant drivers of gene expression in certain tumour types, altering their levels or activity can result in tumour cell arrest or apoptosis. It is a

particularly effective treatment in tumours which arise from hormone sensitive tissue or express genes that are hormone responsive such as the breast, prostate, endometrium and adrenal cortex. Hormonal therapy may also be used in the palliative setting to ameliorate certain cancer and/or chemotherapy-associated symptoms, such as anorexia. Hormonal therapy comprises a number of different agents which include anti-oestrogens (e.g. fulvestrant, tamoxifen, and toremifene); aromatase inhibitors (e.g. anastrozole, exemestane and letrozole); progestogens (e.g. megestrol acetate); oestrogens (e.g. diethylstilbestrol); anti-androgens (e.g. flutamide and bicalutamide); gonadotropin-releasing hormone (GnRH) analogues (e.g. leuprolide and goserelin) and somatostatin analogues (e.g. octreotide) [35].

1.3 Tumour hypoxia

1.3.1 Tumour hypoxia – a historical and modern day issue

Hypoxia, the phenomenon whereby the metabolic requirements of tissues are not met due to insufficient availability of oxygen, is a core feature of the solid tumour microenvironment [46]. Hypoxic tumours have proven to be a great challenge in the modern day medical management of affected patients, with an associated increase in morbidity, mortality and metastatic phenotype [47, 48].

First proposed in 1955, human tumours were thought to contain regions of hypoxic cells following observations that the distribution of necrosis relative to blood vessels in human tumours had a comparatively uniform distance of approximately 100 to 150 μM from the vessels. This distance was then theorised to approximate the diffusion distance of oxygen [49]. From this finding, it was further proposed that necrosis was the result of cells being at zero or near zero levels of oxygen whereas adjacent cells would likely be viable but at hypoxic levels of oxygen. These findings correlated with the work of Gray and colleagues, who identified that low

levels of oxygenation conferred a cytoprotective effect against X-rays and led them to conclude that hypoxic cells in tumours could impede radiocurability (Fig. 1.3) [50]. Considerable research into this phenomenon followed but it was not until the late 1980s before it was possible for the first time to measure tumour oxygenation status in vivo following the development of a computerised polarographic needle electrode (CPNE) system [51]. This innovation enabled rapid identification and characterisation of tumour hypoxia followed by its relevance to clinical outcome. Hypoxia was found to be prevalent in approximately 50% of all locally advanced solid tumours, regardless of their size, histology and phenotype [52]. This was followed by clinical studies in carcinomas of the cervix and head and neck which showed a direct correlation between hypoxia and a poor response to chemoradiotherapy [53-56].

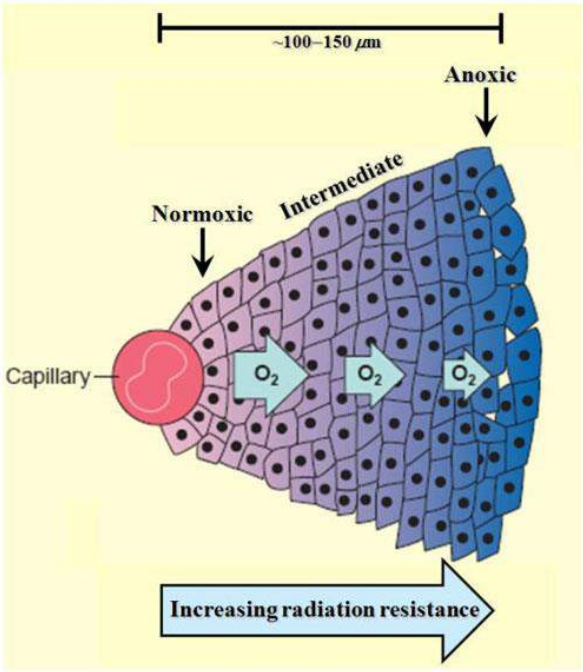

Fig 1.3. Increasing cellular hypoxia is associated with increased radiation resistance. Decreases in oxygen availability due to perfusion-limited hypoxia can protect against the effects of radiotherapy. Reproduced with permission Carlson DJ et al [57].

1.3.2 The effect of hypoxia on tumour biology

Hypoxia has many effects on tumour biology which promote a more aggressive phenotype. These include inhibiting DNA repair, suppressing apoptosis and promoting autophagy, inhibiting the immune response, initiating the anabolic switch in metabolism and supporting genotypes that favour survival in hypoxia–re-oxygenation injury, such as *TP53* mutations [58-63]. Furthermore, hypoxia also contributes to the loss of genomic stability and enhances the epithelial-mesenchymal transition, tumour invasiveness and metastasis, angiogenesis and tyrosine kinase-mediated signalling [64-69].

1.3.2.1 Hypoxia and the HIF reactome

Hypoxia-inducible factor (HIF) is a transcription factor that responds to decreases in oxygen, or hypoxia and is a heterodimer composed of an alpha and a beta subunit. The beta subunit is an aryl hydrocarbon receptor nuclear translocator (ARNT). In oxygenated cells HIF-α subunits are rapidly destroyed by the ubiquitin-proteasome pathway. Ubiquitylation of HIF-α involves the von Hippel Lindau (VHL) tumour suppressor protein which interacts with HIF-α as the recognition component of an E3 ubiquitin ligase complex by hydroxylating the asparagine and proline residues in the HIF-α subunits. Under hypoxic conditions, this process is suppressed resulting in stable, transcriptionally active HIF and HIF-α accumulates. Nuclear entry and retention allow heterodimerisation with the constitutively nuclear HIF-β subunit, binding to hypoxia response elements (HREs) and recruitment of co-activators such as p300 (Fig. 1.4). This leads to a variety of effects, which, alongside their role in tumour metabolism, is discussed in section 1.4.2.

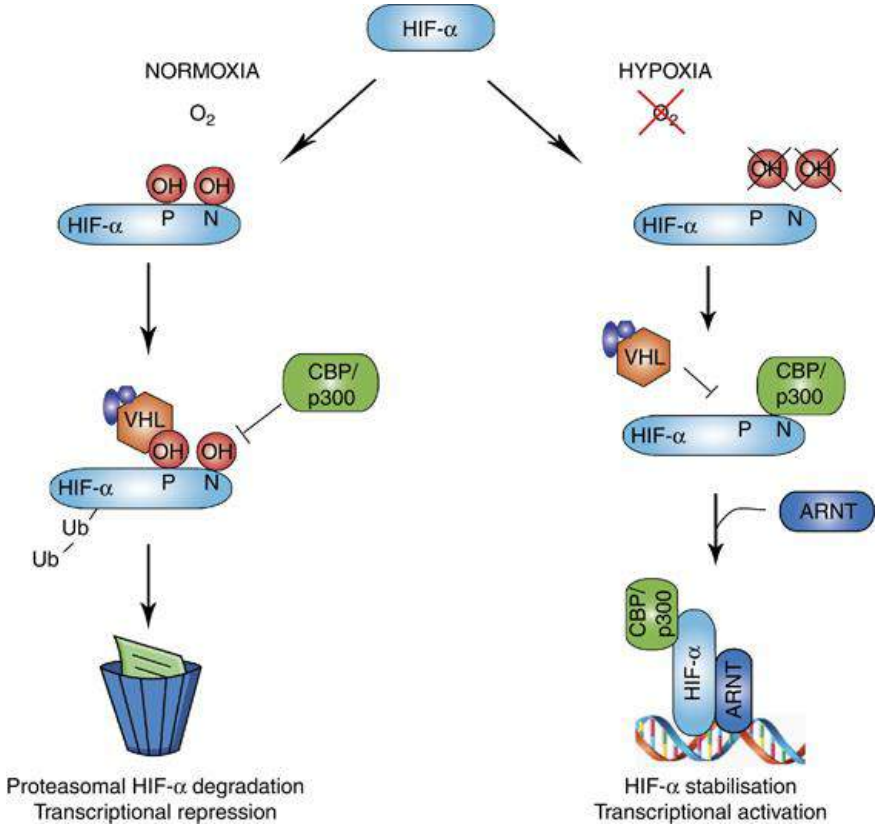

Fig .1.4. The hypoxia mediated regulation of the HIF complex. Stabilisation of the HIF complex through hypoxia leads to a variety of effects that promote a more aggressive tumour phenotype.

1.3.3 Mechanisms for the development of hypoxia

As discussed, a mismatch between oxygen supply and demand inevitably results in tissue hypoxia. Although the partial pressure of oxygen at which this occurs varies at the measured endpoint, hypoxia is present in tumours when the partial pressure drops below a critical value to elicit a reduction in the adenosine triphosphate (ATP) production rate of the cell [70]. In normal subcutaneous tissue, the median value for oxygen partial pressure is usually between 40 and 60 mmHg. However, the average solid tumour might have a median oxygen partial pressure of approximately 10 mmHg. A recent review showed that most human tumours have median oxygen levels lower than their normal tissue of origin [71]. Studies in breast cancer xenografts have demonstrated hypoxia can occur when the partial pressure drops below 40-50

mmHg at the venous end of capillaries (end-capillary blood) [72, 73]. However, on a global tissue level, detrimental changes usually occur at a partial pressure between 8-10 mmHg [74, 75]. From these diverse values, we know that oxygen concentrations in human tumours are highly heterogeneous with some regions at less than 5 mmHg partial pressure of oxygen. A partial pressure of 5 mmHg corresponds to approximately 0.7% oxygen in the gas phase or 7 μM in solution.

The aetiology of hypoxia can be broadly categorised into the following types. However, there may be considerable overlap and one or more, or indeed all, may contribute to the overall hypoxia:

1.3.3.1 Hypoxaemic hypoxia

Hypoxaemic hypoxia occurs when the arterial concentration of oxygen is low with or without adequate perfusion of the tissue by blood. This may occur through disease states such as chronic obstructive pulmonary disease (COPD) or environmental surroundings such as altitude sickness [76].

1.3.3.2 Anaemic hypoxia

Almost all oxygen in the blood is bound to haemoglobin, which increases the oxygen-carrying capacity of blood by about 40-fold [77]. Anaemic hypoxia occurs when the ability of the blood to carry oxygen is compromised with or without normal ambient oxygen levels. This phenomenon occurs in states such as anaemia, where there is a reduced number of red cells capable of transporting oxygen or carbon monoxide (CO) poisoning, when haemoglobin is saturated with CO and unable to bind to oxygen [78].

1.3.3.3 Cytotoxic hypoxia

Certain drugs can induce hypoxia through ingestion or poisoning by preventing the ability of the cells to use oxygen. The quantity of oxygen reaching the cells may be normal but the cells are unable to use the oxygen effectively, due to interruption of oxidative phosphorylation. An example of such an agent is cyanide, which inhibits Complex IV in the mitochondria [79].

1.3.3.4 Ischaemic hypoxia

Insufficient blood flow and reduced tissue perfusion can result in hypoxia and subsequent ischaemia [80]. Systemic causes include myocardial infarction, leading to reduced pump efficiency and thromboembolic events, which can occlude normal flow to tissues such as the brain following a stroke [81].

1.3.3.5 Diffusional hypoxia

Increasing tissue bulk can result in the deterioration of the diffusion geometry, resulting in a rate-limiting effect on the diffusion of oxygen from blood vessels into the tissue [82, 83].

1.3.4 The classical causes of tumour hypoxia

Although each of these mechanisms may contribute to the overall hypoxia within tumours, ischaemic hypoxia and diffusional hypoxia remain the principal causes at a local level. Classically, they are described as steady-state (diffusion-limited) hypoxia and cycling (perfusion-modulated) hypoxia and are associated with permanent and transient limitations in oxygen diffusion respectively (Fig. 1.5) [83].

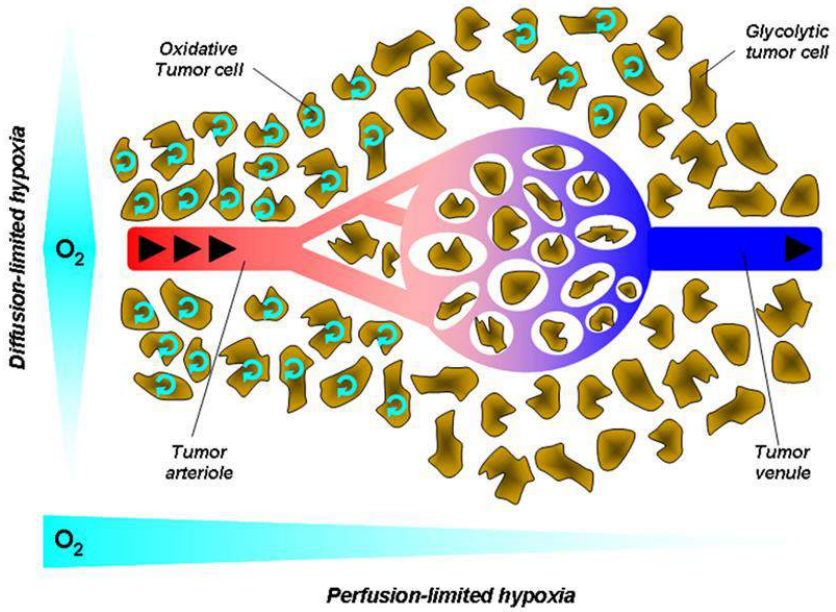

Figure 1.5. The two main forms of tumour hypoxia: Diffusion-limited and perfusion-limited. Hypoxia within tumours are principally caused by these two mechanism but may also be compounded by systemic causes. Reproduced with permission from Jordan BF et al [84].

As a tumour develops and grows beyond its blood supply, it may acquire a proangiogenic phenotype to allow the tumour to develop new vessels and to expand rapidly. This 'angiogenic switch' is regulated by a number of factors that may either upregulate proangiogenic factors such as vascular endothelial growth factor 3 (VEGF3), fibroblast growth factor-β (FGF-β) and transforming growth factors such as TGF-α and TGF-β and/or downregulate angiogenesis inhibitors such as angiostatin and interferon-α (IFN-α) [85, 86]. However, despite the generation of new vascular networks, blood flow in the tumour may not necessarily increase as vasculature evolution is chaotic; resulting in blind ends, leaky vessel walls, arteriovenous shunting, stenoses and aneurysm formation (Fig. 1.6) [71, 87, 88]. These features result in transient limitations in blood perfusion and invariably, hypoxic cells downstream of the perfusion-impairing vessel abnormalities. These cells are acutely hypoxic and are thought to be subjected to intermittent periods of hypoxia during their lifetime [89].

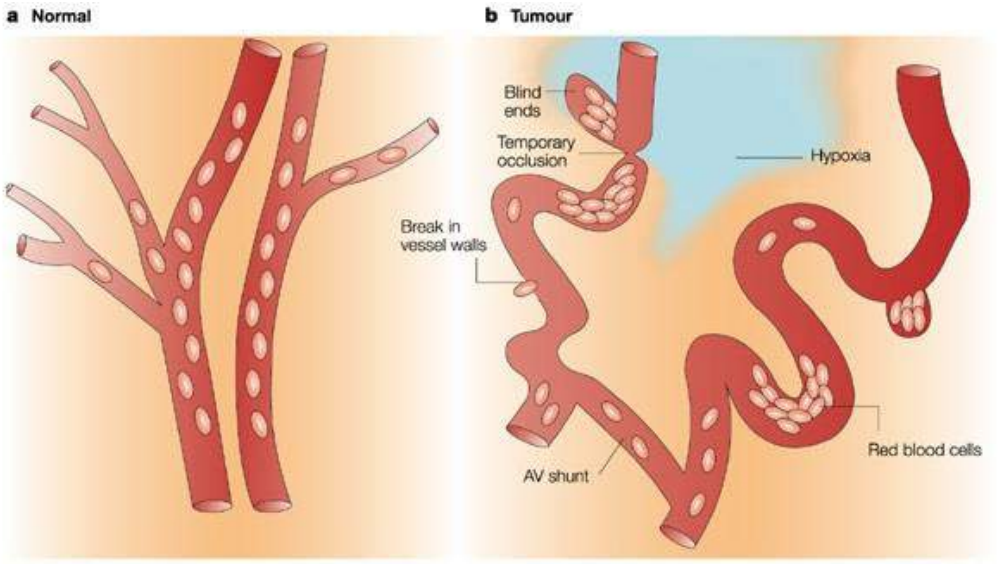

Figure 1.6. Abnormal vasculature formation in tumours is a chief cause for tumour hypoxia. Disordered vessel formation is a key feature of solid tumours, caused by a number of gene abnormalities. Reproduced with permission from Brown JM et al [71].

Diffusion-limited hypoxia occurs as a result of distance from vessels, with hypoxic cells in regions beyond the diffusion distance of oxygen and typically adjacent to necrotic areas (Fig. 1.4) [49]. These cells are chronically hypoxic and have a lifetime within the range of 4 to 10 days in most experimental models [90].

These two mechanisms of tumour hypoxia are biologically distinct and cells in regions with transient hypoxia may differ metabolically from those in regions with diffusion-limited hypoxia [90-92]. Consequently, they may offer different targets for therapy to improve tumour hypoxia.

1.3.5 The clinical significance of tumour hypoxia

Hypoxic tumours offer a great challenge to clinicians due to the effects of hypoxia on tumour biology that promote a more aggressive phenotype, which result in both a worse prognosis and resistance to therapy. By focusing on tumour hypoxia to improve outcome, it provides an alternative and supplementary target for treatment.

1.3.5.1 Hypoxic tumours have a worse prognosis

Tumour hypoxia is associated with a poorer prognosis. This has been identified from several studies looking at the outcome of hypoxic tumours on overall survival (OS) and disease free survival (DFS) from a variety of different primary tumours (Fig. 1.7). Head and neck squamous cell carcinomas (HNSCC) were one of the earliest tumours to be characterised for hypoxia and has been extensively studied. Worse OS has been demonstrated in a number of studies, including the Continuous, Hyperfractionated Accelerated Radiotherapy (CHART) trial, whilst worse local control and DFS has been seen in trials with both neoadjuvant and adjuvant radiotherapy [47, 48, 55, 93, 94]. However, when these tumours were treated with nimorazole as a hypoxic radiosensitiser as part of the Danish Head and Neck Cancer Study (DAHANCA) phase III trial, there was a considerable improvement in outcome and further evidence that tumour hypoxia is a possible therapeutic target [95]. Hypoxia also predisposes tumours to metastatic spread, with a worse DFS seen in soft tissue sarcomas, breast, cervical and colorectal carcinomas [52, 96-100].

Measure of hypoxia	Probe	Clinical setting	Outcome for hypoxic tumours
Oxygen concentration	Eppendorf oxygen electrode	Chemoradiation of advanced HNSCC	Worse OS
		Radiotherapy of soft tissue sarcomas before surgery	Worse DFS owing to a higher rate of distant metastasis
		Brachytherapy of localized prostate cancer	Decreased biochemical control (shown by PSA levels)
		Cervical carcinoma	Worse DFS in node-negative patients owing to a higher rate of distant metastases
Endogenous markers	HIF1α	Node-negative breast cancer	Worse OS
	HIF1α	BRCA1 mutant breast cancer	Worse DFS
	HIF2α, CA9	CHART trial in HNSCC	Worse local control and OS
	CA9	Adjuvant chemotherapy of breast cancer	Worse OS
	Osteopontin	Radiotherapy for HNSCC	Nimorazole (hypoxic radiosensitizer) improved local control and OS
	Lysyl oxidase	Breast cancer	Worse metastasis-free survival
	Hypoxic gene signature	HNSCC and breast cancer	Worse outcome, multiple end points
	Hypoxic gene signature	Hepatocellular carcinoma	Worse OS
Exogenous probes	Pimonidazole	Radiotherapy for advanced HNSCC	Worse local control
	EF5	Post-surgical radiotherapy of HNSCC	Worse DFS

CA9, carbonic anhydrase 9; CHART, continuous hyperfractionated accelerated radiotherapy; DFS, disease-free survival; EF5, etanidazole pentafluoride; HIF, hypoxia-inducible factor; HNSCC, head and neck squamous cell carcinoma; OS, overall survival; PSA, prostate specific antigen.

Figure 1.7. Prognostic and predictive significance of hypoxia in human tumours. Table summarising the clinical significance of hypoxic tumours. Reproduced with permission from Wilson WR et al [101].

1.3.5.2 Treatment resistance

Many of the mechanisms that lead to tumour hypoxia, both at a cellular and physical level, also result in an overall increase in treatment resistance.

1.3.5.2.1 Chemotherapy

Hypoxic cells can confer a level of chemoresistance through a number of different mechanisms. Firstly, due to the physical properties of diffusional and ischaemic hypoxia, anti-tumour agents are unable to reach the target cells and their effect is minimal or nullified (Fig. 1.4) [102, 103]. Furthermore, cellular proliferation decreases as a function of distance from blood vessels and cytotoxic agents targeting the cell cycle become limited [104]. Secondly, hypoxia upregulates genes involved in drug resistance, such as those encoding multidrug resistance protein 1 (MDR1) [105, 106]. Thirdly, limited oxidation of DNA by oxygen free radicals in the hypoxic tumour microenvironment can result in the failure to induce DNA breaks. As a result, chemotherapy agents that rely on this mechanism, such as bleomycin, become relatively ineffective [107]. In other words, some agents require oxygen to exert their cytotoxic effect and tumour hypoxia can therefore protect against this. Fourthly, hypoxia also selects for cells that have lost sensitivity to p53-mediated apoptosis, increasing their resistance to cytotoxic chemotherapy agents [63]. Finally and by no means complete, tumour hypoxia can stabilise hypoxia-inducible factor 1 (HIF-1) and increase the expression of ATP-binding cassette (ABC) transporters, promoting drug resistance and downregulate non-homologous end joining (NHEJ), impeding agents that target DNA double strands [105, 108].

However, although hypoxic changes within tumours can confer chemoresistance, it is also important to note that some hypoxic changes can result in increased drug sensitivity. Hypoxic tumour cells commonly arrest in the S phase of the cell cycle, which can lead to the collapse of stalled replication forks and consequently improve the efficacy of chemotherapy agents such as

poly(ADP-ribose) polymerase 1 (PARP-1) inhibitors [109]. An indirect effect of hypoxia is extracellular acidification, which can lead to increased uptake of acidic agents such as chlorambucil [110]. Furthermore, hypoxia downregulates nucleotide excision repair and homologous recombination, which can improve the sensitivity to DNA crosslinking agents such as the platinum-based drugs [111].

1.3.5.2.2 Radiotherapy

As previously noted, Gray and colleagues established that in the absence of oxygen, the effects of ionising radiation on cells and on tissues were markedly reduced [50]. However, the association between low oxygen levels and radioresistance was not a new observation and had been known since the 1920s [112, 113]. Hypoxic cells can be three-fold more resistant to radiation than normoxic cells [47, 48]. Ionising radiation works by creating highly reactive oxygen free radicals that lead to DNA damage and disruption of the tumour cell membrane. Oxygen stabilises these free radicals to perpetuate their action; therefore, in the presence of limited or no oxygen, these radicals are short-lived and a greater amount of radiation is required to have the same effect. Additionally, proteomic changes from hypoxia can lead to the alteration of proliferation kinetics which may also protect against radiation, although this mechanism is not clearly understood [114]. Further investigation into this phenomenon has identified that oxygen has to be present at the time of irradiation for radiation sensitisation of hypoxic cells; with no effect observed even if oxygen is present immediately before or after the radiation exposure [115]. These findings gave rise to the physicochemical oxygen fixation hypothesis whereby oxygen perpetuates radiation damage as a consequence of its high affinity for the unpaired electron of the free radical produced by radiation. This hypothesis also appears to explain the mechanism of radioresistance *in vivo*. Studies using nitroimidazole and various analogues as hypoxic cell radiosensitisers have shown that tumours can become sensitised to radiation by a significant amount [116, 117]. Nitroimidazoles are electrophilic agents that substitute for oxygen in the physicochemical reaction but unlike oxygen, they are

not involved in normal metabolism and therefore do not suffer the problem of diffusion through tumour tissue. These agents thus penetrate to the hypoxic cells in the tumour.

1.3.6 Approaches to alleviate tumour hypoxia

There have been several approaches to alleviate hypoxia within tumours, with a varied evidence base and outcome. One such approach has been to correct hypoxia caused by anaemia, which is a common paraneoplastic syndrome. The relationship between anaemia, tumour hypoxia and outcome has been extensively reviewed in both *in vitro* and *in vivo* studies [118-120]. Kelleher and colleagues demonstrated that paraneoplastic anaemia resulted in a substantial worsening of tumour oxygenation in rats when measured with the CPNE system [120]. When this was corrected with either a blood transfusion or erythropoietin (EPO), the tumour hypoxia was only partially improved. This relatively modest change is seen in some clinical studies whilst others show significant improvements, which has led to a contentious debate over the influence of haemoglobin level on tumour oxygenation [53, 118, 121-123]. However, at a molecular level, there appears to be no association between haemoglobin level and the upregulation of HIF, the activation of proangiogenic pathways or vascular density [124, 125]. Despite this controversy, there is evidence suggesting that treating anaemia may enhance both radiosensitivity and chemosensitivity of solid tumours and thus use of either EPO or blood transfusion could be a treatment option [120]. However, results from clinical trials thus far have failed to demonstrate any discernible improvement in patient outcome [126, 127].

Another approach has been to increase the arterial concentration of oxygen so that more oxygen is available to tumour tissue. Techniques have ranged from the use of hyperbaric chambers, which use pressures higher than atmospheric pressure to deliver oxygen, to the use of hyperoxic gases such as carbogen, which has an oxygen concentration between 95-98%. Hyperbaric oxygen therapy (HBOT) has shown good results with local tumour control in HNSCC and cervical cancer, with an improvement in both OS and DFS [128]. However, it has been a

considerable challenge to combine delivery of radiotherapy with HBOT and consequently, an increased incidence of late radiation morbidity has been observed. This was thought to be as a result of both delaying radiotherapy until after initiating HBOT and hypofractionation, where larger doses of radiation were given over a shorter time. This has resulted in poor uptake of the technique in clinical practice [129]. Carbogen, however, has been more promising. Hill and colleagues demonstrated that exposing mice to high levels of oxygen for as little as 5 minutes prior to irradiation, was sufficient enough to radiosensitise tumours [130]. This finding was also replicated in the clinical setting. When carbogen was combined with the vasoactive agent, nicotinamide and accelerated radiotherapy (collectively known as ARCON), radiosensitivity of HNSCC and outcome were significantly improved [131]. ARCON addresses the classic causes of tumour hypoxia by targeting diffusion-limited hypoxia (carbogen) and perfusion-limited hypoxia (nicotinamide), whilst accelerated fractionated radiotherapy protects against tumour cell repopulation [132, 133].

The use of hypoxic cell radiosensitisers has also been beneficial. As discussed, nitroimidazoles substitute for oxygen in the physicochemical reaction and confer a radiosensitising effect on hypoxic tumours [116, 117]. However, due to the dose-limiting toxicity of many of the agents in this class, only nimorazole has been incorporated into regular clinical practice, being used to treat HNSCC in Denmark following the success of the DAHANCA-5 trial [95].

Perhaps one of the most promising advancements in targeting tumour hypoxia has been the development of bioreductive produgs or hypoxic cytotoxins. These agents selectively target and kill hypoxic cells by undergoing intracellular reduction to form active cytotoxic compounds. The prodrug is converted into a free radical species by a one-electron reduction, which then becomes a substrate for reverse oxidation by O_2 to form a superoxide and return to the original compound. This redox cycle prevents buildup of the prodrug radical in normoxic cells. In

hypoxic cells, however, the prodrug radical accumulates and if it is more cytotoxic than the superoxide species, then cell death occurs [71]. Several types of agents that have the potential to be metabolised by enzymatic reduction under hypoxic conditions and thus employ this or a similar mechanism to target tumour hypoxia include the transition metals, nitro groups, aliphatic N-oxides, quinone antibiotics and aromatic N-oxides. One of the earliest examples of use of this type of agent in the clinical setting was with the drug tirapazamine [134]. Tirapazamine is an aromatic N-oxide which is up to 200-fold more toxic to hypoxic than normoxic cells in *in vitro* settings [135]. However, when tirapamazine was used in clinical trials, there has been mixed success [136]. The drug has been shown to be very effective in enhancing the chemotherapeutic action of cisplatin by increasing the sensitivity of tumour cells to cisplatin [137]. Early clinical trials showed promise, with an improved response rate and prolonged survival seen in advanced non-small-cell lung cancer and improved survival in HNSCC in combination with cisplatin therapy [138, 139]. However, an update of a Phase III trial looking at tirapazamine, cisplatin, and radiation versus cisplatin and radiation for advanced HNSCC found no evidence that the addition of the agent to standard chemoradiotherapy improved OS [140]. Despite the disappointing results, clinical trials have continued with newer bioreductive agents following several criticisms of the HNSCC trial which identified poor radiotherapy compliance, poor management of drug toxicity and lack of patient selection based on tumour hypoxia, which meant that cohorts of patients with hypoxic tumours that could have been benefiting from the treatment were not easily identified [141]. Rischin and colleagues, however, did demonstrate an improvement in local recurrence when the drug was combined with [18F]-fluoromisonidazole positron emission tomography (FMISO-PET) as part of a substudy of the original trial [142]. The FMISO-PET imaging specifically identified patients with hypoxic tumours, which allayed some of the aforementioned criticisms.

More recently, there has been a growing movement towards targeting the tumour microenvironment and metabolism to improve tumour hypoxia. The relationship

between tumour cell metabolism and tumour hypoxia is a complicated one and will be discussed in greater detail later but it does provide a number of potential therapeutic targets. Cells respond to hypoxia by regulating the expression of many genes and the induction of subsequent pathways. By targeting different components of these pathways, more specific and effective therapies can be developed. A good example and one that is relatively well understood is the HIF-1 hypoxic response pathway and has been a focus for chemotherapy [143]. HIF-1 is implicated in tumour cell survival, glucose utilisation and angiogenesis and is associated with a poorer clinical prognosis [144, 145]. A number of approaches exist for inhibiting the HIF-1 pathway, which include targeting pathways responsible for HIF-1 synthesis, HIF-1 itself, or HIF-1 activated downstream pathways [146]. Focusing on HIF-1 synthesis, inhibitors against the epidermal growth factor (EGF) receptor, phosphatidylinositol 3-kinase (PI3K), the mitogen-activated protein kinase (MAPK) pathway and their downstream protein kinases, such as mammalian target of rapamycin (mTOR) have been shown to reduce tumour hypoxia [147]. Inhibiting these biological response pathways have garnered considerable interest and has led to a number of phase I and II trials [143, 148]. However, other components of the tumour microenvironment have also been exploited, including targeting the proangiogenenic growth factor, VEGF [149-151]. Hypoxia-induced angiogenesis is crucial in the development and metastasis of solid tumours and by suppression of HIF-1α/VEGF-A pathways, this mechanism can be inhibited and be of potential clinical benefit [149]. The scope of targeting tumour cell metabolism to improve hypoxia is vast but one that is both promising and ever developing.

1.4 Tumour cell metabolism

1.4.1 The Warburg Effect

Tumour metabolism, specifically metabolism of glucose, was first shown to be distinct from that of cells in normal tissues by Otto Warburg in 1924 [152]. Translating Pasteur's observations on glucose fermentation to ethanol in yeast, Warburg determined that tumour cells preferentially 'fermented' glucose into lactate despite the presence of sufficient oxygen to support mitochondrial oxidative phosphorylation. This was an observation that appeared unique to tumour tissue and the fact that tumour cells mainly generate energy (ATP) by non-oxidative breakdown of glucose (aerobic glycolysis) came to be known as the Warburg Effect. This observation led to Warburg's hypothesis that postulated that the driver of carcinogenesis was an insufficient cellular respiration caused by insult to the mitochondria. However, although this theory has since been shown to be mistaken, a definitive explanation for the Warburg Effect has remained elusive, principally because the energy requirements of cell proliferation appear to be better met by complete catabolism of glucose, using mitochondrial oxidative phosphorylation to maximise ATP production [153]. Proposed explanations, however, include the fact that it could simply be the consequence of mitochondrial damage in cancer or as an adaptation to the hypoxic tumour microenvironment. It may also be as a result of cancer genes disabling the mitochondria as they are integral to the apoptosis of malignant cells or as an effect associated with cell proliferation. As glycolysis is essential in providing the substrates necessary for cell proliferation, tumour cells may need to activate glycolysis, with or without oxygen, to proliferate.

To put all of this into context, it is important to first review the steps of cellular metabolism and respiration that lead to the production of energy.

1.4.1.1 The glycolytic pathway

The glycolytic pathway, as the name suggest, describes a sequence of steps that lead to the metabolism of glucose, which is a derivative product of carbohydrate. The pathway takes place in the cell cytoplasm and comprises a series of ten steps involving a variety of intermediate structures and enzymatic reactions, where essentially the 6-carbon molecule glucose is broken down to two 3-carbon pyruvate molecules (See Fig. 1.8). This is an exergonic reaction, which requires 2 ATP molecules to be broken down to drive the splitting of glucose into the 2 pyruvates but overall actually produces 4 ATP molecules and a net gain of 2 ATP in total. Glycolysis also produces 2 reduced nicotinamide adenine dinucleotide (NADH) molecules, which are subsequently fed into the electron transport chain and oxidative phosphorylation. The whole process can be broadly divided into two phases; the investment phase, where ATP is consumed and the pay-off phase, where ATP is produced. During the investment phase, glucose is metabolised into glyceraldehyde-3-phosphate (G3P) through a sequence of five separate and consecutive processes. The following five processes comprise of the pay-off phase, where G3P is metabolised to pyruvate and a net gain of NADH and ATP. The metabolism of glucose is an anaerobic process and depending on the availability of oxygen, the cell can either move into the process of aerobic respiration and proceed to the citric acid cycle or continue with the less efficient process of anaerobic respiration called homolactic fermentation. In the latter, hypoxia forces NADH to remain in its reduced form and transfers the hydrogen to pyruvate through the action of the enzyme lactate dehydrogenase (LDH) and produce lactate.

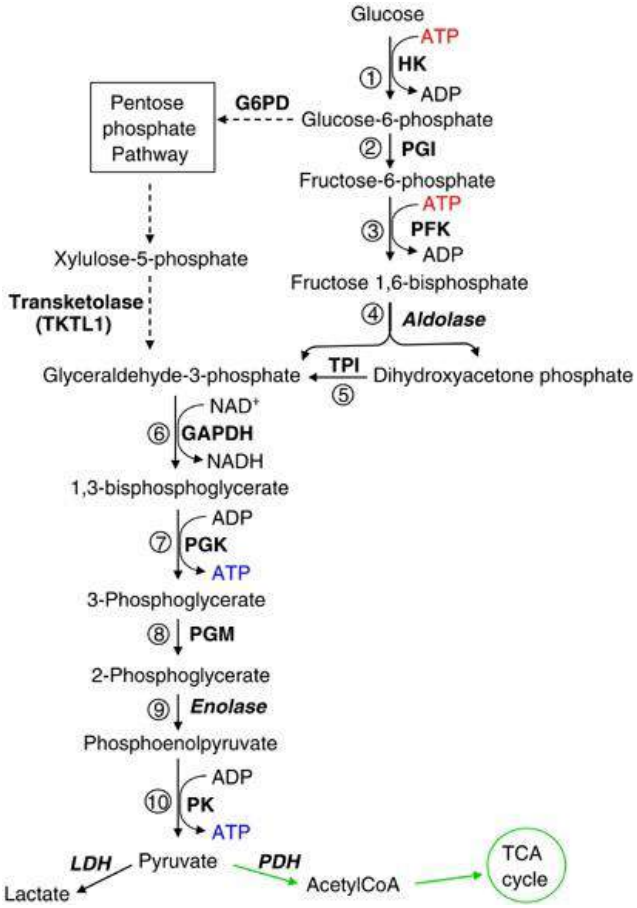

Figure 1.8. Overview of the glycolytic pathway. Glycolysis can be separated into two phases: the investment phase (steps 1-5) and the pay-off phase (steps 6-10). Reproduced with permission from Pelicano H et al [154].

1.4.1.2 The citric acid cycle (Krebs cycle)

The citric acid cycle is a highly efficient and integral metabolic pathway that combines fat, carbohydrate and protein metabolism. It is an amphibolic pathway because it is involved in both the synthesis and degradation of biomolecules. Alongside the synthesis of acetyl-coenzyme A (acetyl-CoA), which is generated from glucose, fatty acids or amino acids, other molecules are metabolised by the cycle. Several amino acids are degraded to become various intermediates of the cycle, whilst fatty acids are metabolised to form succinyl coenzyme A. In normoxia, pyruvate, the end product of preceding glycolysis, enters the mitochondrial matrix and is converted into acetyl-CoA, NADH and carbon dioxide (CO_2). Acetyl-CoA then enters the

citric acid cycle and reacts with oxaloacetate to form citric acid. Citric acid undergoes a series of enzymatic reactions to ultimately yield oxaloacetate, which is then used again in the first step of the next cycle (See Fig. 1.9). After citrate has been formed, the cycle machinery continues through eight distinct enzymatic reactions that produce, in order, aconitate, isocitrate, α-ketoglutarate, succinyl coenzyme A, succinate, fumarate, malate and oxaloacetate. During the eight reactions that take place, for every molecule of acetyl-CoA that enter the cycle, three NADH, one reduced flavin adenine dinucleotide (FADH) and one molecule of ATP are produced. The NADH and FAD/FADH generated by the citric acid cycle is in turn fed into the oxidative phosphorylation pathway. The citric acid cycle is present in virtually all mitochondria containing cells but functions only as part of aerobic metabolism, owing to the close association with oxidative phosphorylation. The net result is the oxidation of nutrients to produce usable chemical energy in the form of ATP.

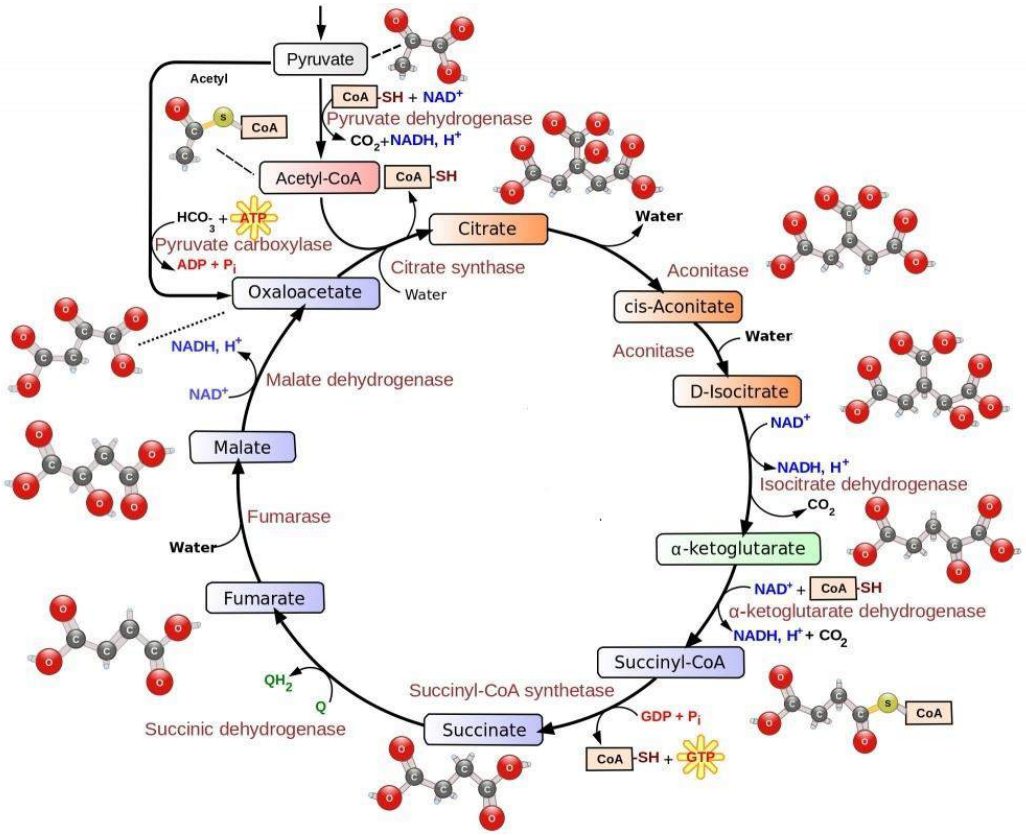

Figure 1.9. Overview of the citric acid (Krebs) cycle. A highly efficient metabolic process, the cycle is a rare example of a genuine cycle where citrate is both the starting and end product.

1.4.1.3 Oxidative phosphorylation and the electron transport chain

Oxidative phosphorylation represents the final stage of cellular respiration. The NADH and FADH produced in glycolysis, the citric acid cycle and pyruvate metabolism now enter the mitochondrial inner membrane and are oxidised, which results in the release of electrons. These electrons then pass through the electron transport chain, which comprise of a series of four protein complexes known as Complexes I-IV. This flow of electrons produces energy which then drives the phosphorylation of adenosine diphosphate (ADP) into ATP (See Fig. 1.10). NADH and FADH act as electron transporters as they flow through the inner membrane space. In Complex I (NADH dehydrogenase), electrons are passed from NADH (being oxidised to NAD) to the electron transport chain, where they cycle through the remaining complexes. Complex II (succinate dehydrogenase) oxidises FADH, cycling more electrons for the chain. Complex III ($CoQH_2$-cytochrome c reductase) facilitates the transfer of the electrons from Complexes I and II to Complex IV (cytochrome c oxidase), where they are transferred to a molecule of oxygen, which is then reduced to water. Throughout this process of sequential reduction and oxidation, energy is released which then drives the pumping of protons out of the intermembrane space into the cytosol. This results in a net negative charge in the matrix and a net positive charge in the intermembrane space, establishing an electrochemical gradient. Positive hydrogen ions flow back across the membrane through ion channels supported by Complex V (ATP synthase), using the energy created by this exergonic process to phosphorylate ADP into ATP. The transport of just two electrons through the electron transport chain generates enough free energy in the form of the electrochemical gradient to drive the synthesis of one molecule of ATP. In total, oxidative phosphorylation produces approximately 90% of the body's total ATP.

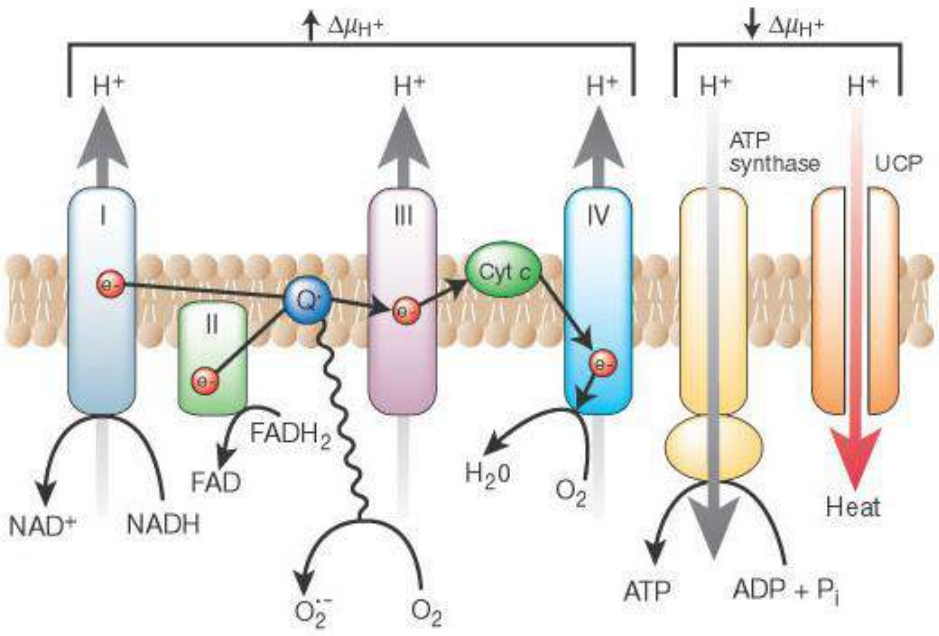

Figure 1.10. Schematic of the electron transport chain in mitochondria. The transfer of electrons across the various complexes generate energy, resulting in a significant ATP payload. Reproduced with permission from Brownlee M et al [155].

1.4.1.4 Summary

Essentially, in the presence of oxygen, non-proliferating (differentiated) tissues metabolise glucose to pyruvate via glycolysis and then completely oxidise most of that pyruvate in the mitochondria via the electron transport chain, to generate approximately 36 molecules of ATP per molecule of glucose (See Fig. 1.11). When oxygen is limiting, cells can redirect the pyruvate away from mitochondrial oxidative phosphorylation by generating lactate in a process known as anaerobic glycolysis (homolactic fermentation). This generation of lactate allows glycolysis to continue but results in minimal ATP production. In tumour cells and in normal proliferative tissues, however, cells tend to convert most glucose to lactate regardless of whether oxygen is present in a process known as aerobic glycolysis (Warburg Effect). The mitochondria remain functional and some oxidative phosphorylation continues but overall ATP production remains lower than normal cellular respiration.

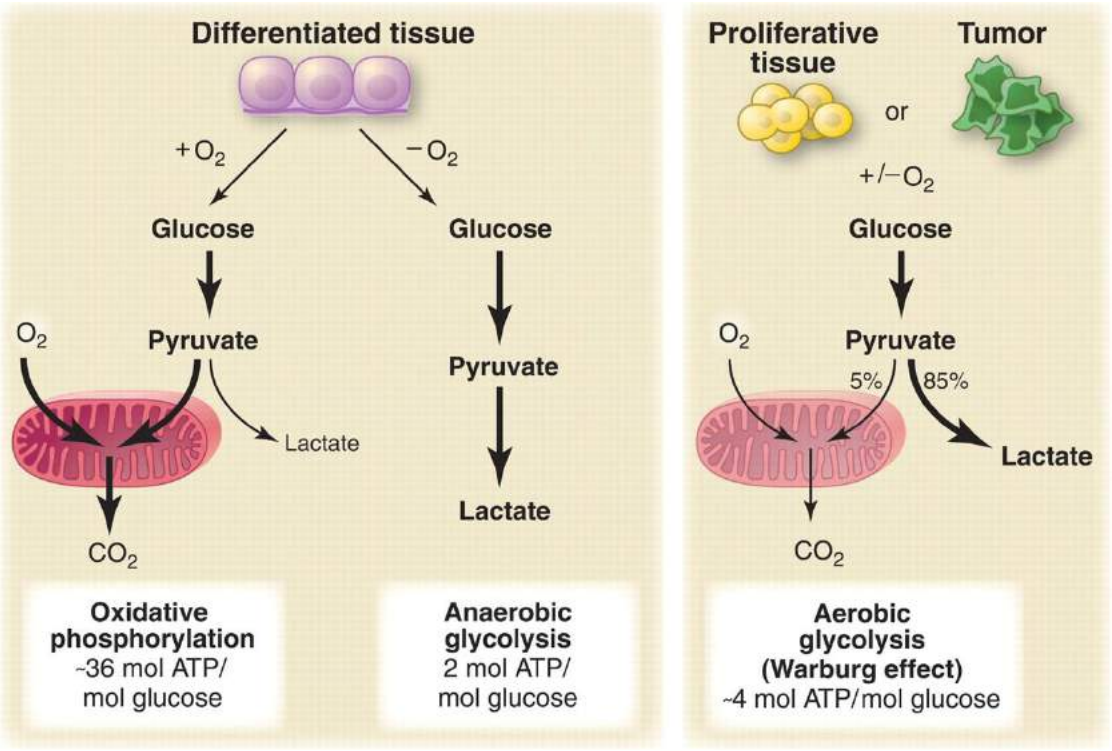

Figure 1.11. Differences between oxidative phosphorylation, anaerobic glycolysis and aerobic glycolysis (Warburg effect). Reproduced with permission from Vander Heiden MG et al [153].

1.4.2 The effect of hypoxia on tumour metabolism

As briefly mentioned, the relationship between tumour cell metabolism and tumour hypoxia is complex. The Warburg Effect demonstrates that changes in metabolism are apparent in tumour cells. Sustained hypoxia can result in changes in the proteome and genome of neoplastic and surrounding stromal cells, altering the tumour microenvironment leading to local growth, dissemination and propagation [46]. These changes may occur from post-transcriptional and post-translational effects and from inhibition or stimulation of gene expression. For example, hypoxia induces expression of HIF-1, which is a transcription factor that promotes tumour survival through its impact on several metabolic pathways and genes and has consequently been a focus for chemotherapy [143, 156]. Specifically, HIF-1 has been identified to affect genes involved in the glycolytic pathway in order to cope with reductions in

oxygen availability and consumption. These include but are not limited to, glucose transporter 1 (GLUT1), pyruvate kinase, glyceraldehyde-3-phosphate dehydrogenase (GAPDH), hexokinase, phosphoglucose isomerase, phosphofructokinase, LDH and pyruvate dehydrogenase kinase. GLUT1 is a glucose transporter, facilitating the movement of hexose sugars along the concentration gradient and has been shown to be upregulated by HIF-1 with changes occurring at both the mRNA and protein levels [157]. This upregulation increases the uptake of glucose into the tumour cells allowing for a higher rate of glycolysis and proliferation [158]. Hexokinase is also upregulated by HIF-1 with both protein and mRNA levels significantly increased. As the first enzyme involved in the glycolytic pathway and therefore an initiator of glycolysis, this results in an increased flux of glucose through the glycolytic pathway following the increased uptake by GLUT1 [159, 160]. Activation of phosphoglucose isomerase through HIF-1 also results in increased cell motility and invasion during metastasis alongside increasing availability and conversion of glucose 6-phosphate to fructose 6-phosphate [161]. These intermediates can then be shuffled into the pentose phosphate pathway to engage in nucleotide synthesis, which is crucial for tumour cell division [162]. Significantly, HIF-1 increases expression of both pyruvate dehydrogenase kinase and LDH. These changes suppress mitochondrial metabolism by directing pyruvate away from entering the citric acid cycle and oxidative phosphorylation and towards LDH, lactate production and acidification, all of which are associated with a more aggressive tumour phenotype [160, 163]. Lactate is then transported out of the hypoxic cell by monocarboxylate transporter 4 (MCT4) which is a hypoxia induced transporter. The free lactate in the extracellular space is then taken up by monocarboxylate transporter 1 (MCT1) into aerobic tumour cells, which convert it back to pyruvate and then use it as an energy source. This mechanism allows hypoxic cells to take up the majority of available nutrients without requiring large quantities of glucose [160]. However, it must be noted that generally the level of glycolysis in tumour cells is high, regardless of the level of oxidative phosphorylation activity and can also be upregulated in response to downregulation of oxidative phosphorylation. This is shown through relatively low

Complex V activity in tumours at raised levels of glycolysis [164]. Suffice to say, hypoxia has innumerable effects on tumour cell metabolism, making it a prime target for focusing anti-tumour therapy.

1.5 The cell cycle and cancer

1.5.1 The regulation of the cell cycle

As previously discussed, the majority of cytotoxic agents have a degree of cell cycle arrest or inhibition either directly or indirectly. Loss of control of the cell cycle machinery is one of the earliest hallmarks of cancer but the rapid proliferative state of malignant cells also provide a target for therapy [165].

The cell cycle is divided into four distinct and sequential phases (see Fig. 1.12) [166]. Perhaps most important are the Synthesis (S) and Mitosis (M) phases which represent the stages of DNA replication and cell division respectively. They are separated by two Gap (G) phases, G_1 and G_2. G_1 follows M phase and is also known as the growth phase. During this phase the cellular activities, which are almost stationary during M phase, resume at a high rate and is marked by an increase in protein and enzymes synthesis required for S phase. Importantly, it is under the control of the *TP53* gene. G_2 follows S phase and is marked by the production of microtubules, necessary for mitosis. Progression through this cycle is driven by cyclins and cyclin-dependent kinases (CDKs) and are essential in the function of the checkpoints. The major function of checkpoints is to assess DNA damage. There are 3 checkpoints within the cell cycle: at the end of G_1 (restriction checkpoint), at the end of G_2 and at the metaphase stage of M phase (metaphase/spindle checkpoint). The restriction checkpoint is responsible for making

the key decision of whether the cell should divide, delay division or enter quiescence. The majority of cells stop at this stage and enter a resting state called G_0.

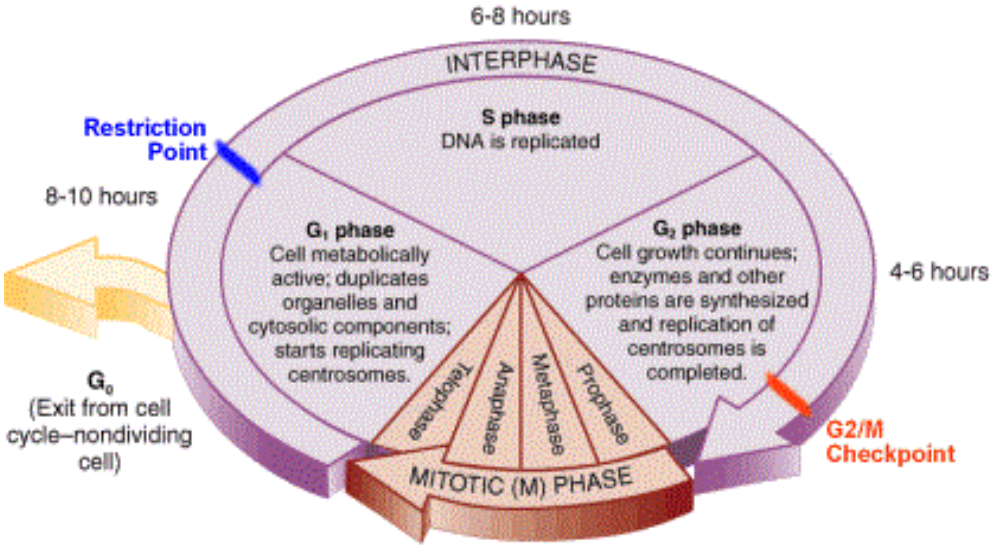

Figure 1.12. Overview of the phases and checkpoints of the cell cycle.

1.5.2 The cell cycle and tumour metabolism

The association between tumour metabolism, hypoxia and the cell cycle is relatively novel and only recently been investigated. Nutrient availability and metabolic status are crucial factors in the decision of a cell to proliferate or enter quiescence and this has certainly been well described at the G_1 checkpoint but less so at different stages of the cycle [167]. It has, however, been demonstrated that both glutaminase 1 (GLS1) and 6-phosphofructo-2-kinase/fructose-2,6-biphosphatase isoform 3 (PFKFB3) are involved in the regulation of the G_1/S checkpoint and both increase during cell division [167, 168]. Interestingly, inhibition of either of these glycolytic enzymes prevents cell progression towards S phase. Further supportive evidence associating cell cycle control and metabolism can be seen with the rise and fall of various other glycolytic pathway biomolecules throughout the different phases of the cell cycle, affecting the control of both glycolysis and glutaminolysis [167]. As elucidated earlier, hypoxia can affect both

metabolism e.g. lactate production and the cell cycle e.g. HIF-1 suppression of p53, thus a link between these three areas is perhaps not a surprise. Considering this relationship alongside oxidative phosphorylation, targeting the cell cycle to reduce oxygen demand and therefore improve tumour hypoxia, provides another potential therapeutic avenue.

1.6 Summary

Colorectal cancer continues to be a significant cause of worldwide mortality and the modalities of cytotoxic chemotherapy, radiotherapy and surgery remain the mainstay of treatment options. However, whilst morbidity and mortality rates have improved, it is important to strive towards different therapeutic options and improvements in current therapies. Tumour hypoxia has been recognised as a chief contributor to poorer outcomes and a number of different approaches to address this have been investigated. By better understanding the association between tumour hypoxia and tumour metabolism and by exploiting these hypoxia response and metabolic pathways we can hope to improve patient outcomes.

1.7 Research aims

1. To identify agents from established chemotherapeutics that may reduce oxygen consumption independent of toxicity.

2. To investigate whether it is possible to reduce hypoxia by manipulating oxygen consumption/respiration.

3. To determine whether an improvement in tumour hypoxia, via this approach, improves radiosensitivity.

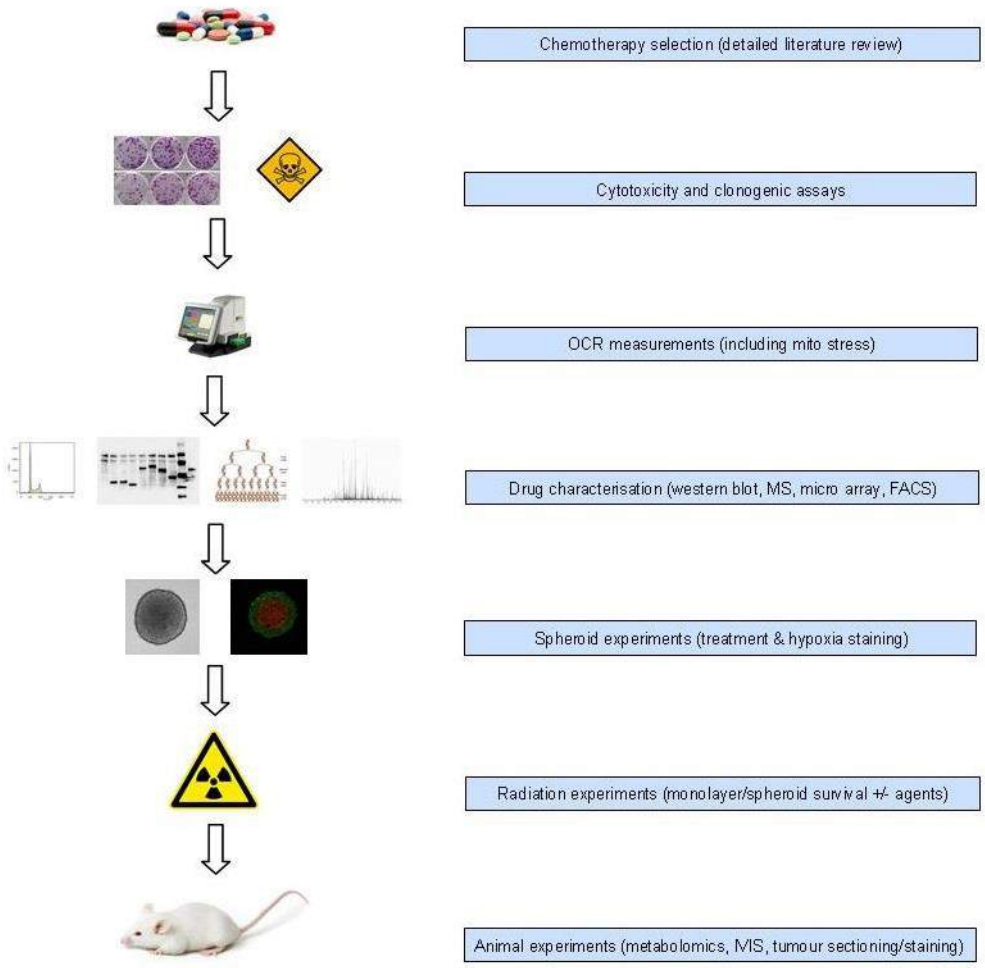

Figure 1.13. Simplified overview of D.Phil project. Each step was subject to several repeats to ensure validity and reproducibility.

CHAPTER 2: MATERIALS AND METHODS

2.1 Cell lines, cell culture, passaging and seeding

2.1.1 Cell lines

The following cancer cell lines were used: MRC5 (human lung fibroblasts), COLO320DM, DLD1, HCT116 and HT29 (all human colon cancer). Cancer cell lines were purchased from the American Type Culture Collection. MRC5 was cultured in F-12 HAM medium (N6658, Sigma-Aldrich UK) with 10% fetal bovine serum (FBS) (F6178, Sigma-Aldrich UK) and 5% penicillin-streptomycin (P4333, Sigma-Aldrich UK). COLO320DM, DLD1, HCT116 and HT29 were grown in Roswell Park Memorial Institute 1640 (RPMI 1640) medium (R8758, Sigma-Aldrich UK) supplemented with 10% FBS and 5% penicillin-streptomycin. The colorectal cancer cell lines were selected based on their molecular characteristics and will be discussed in Chapter 3.

2.1.2 Cell culture, passaging and seeding

All cell culture experiments were performed under sterile conditions in a laminar flow hood and grown in a sterile incubator (Binder) at 5% CO_2 and 37°C. All cells were used at 70-80% confluency and kept for no more than 10 passages. Experiments were conducted with cells between passages 6-8. Cells were dissociated for passage using trypsin (T3924, Sigma-Aldrich UK). Cell numbers were determined using the NucleoCounter NC-100 automated cell counter (Chemometec). The doubling time for DLD1 and HCT116 cell lines was ~24-28 hours and for COLO320DM and HT29 cell lines ~28-32 hours..

2.2 Chemotherapy agents

2.2.1 Source of agents

Table 2.1. Summary of chemotherapy agents used and their solubilities *in vitro*.

Drug	Solubility (*in vitro*)	Source	Catalogue Code
Docetaxel	162 mg/ml DMSO	Selleckchem UK	S1148
Etoposide	30 mg/ml DMSO	Sigma-Aldrich UK	E1383
Fluorouracil	26 mg/ml DMSO	Selleckchem UK	S1209
Gemcitabine HCl	19 mg/ml H_2O	Selleckchem UK	S1149
Hydroxyurea	50 mg/ml H_2O	Sigma-Aldrich UK	H8627
Irinotecan HCl Trihydrate (SN38)	100 mg/ml DMSO	Selleckchem UK	S2217
Mitomycin C	15 mg/ml DMSO	Sigma-Aldrich UK	Y0000378
L-Mimosine	15 mg/ml 10% $NaHCO_3$	Sigma-Aldrich UK	M0253
Mitoxantrone HCl	89 mg/ml DMSO	Selleckchem UK	S2485
Nocodazole	7 mg/ml DMSO	Sigma-Aldrich UK	M1404
Oxaliplatin	14 mg/ml DMSO	Selleckchem UK	S1224
Vincristine	100 mg/ml DMSO	Selleckchem UK	S1241
VX-680	93 mg/ml DMSO	Selleckchem UK	S1048

2.2.2 Creating concentrations for *in vitro* testing

A stock solution of each drug was made up with either dimethyl sulphoxide (DMSO) (472301, Sigma-Aldrich UK) or distilled water, dependent on the solubilities of each agent (See

Table 2.1) and serially diluted to achieve desired concentrations. Solutions were stored at -80°C and allowed to thaw at 37°C in a water bath when required for *in vitro* testing.

2.2.3 Creating doses for *in vivo* testing

Docetaxel was prepared for intraperitoneal injection by creating a stock solution of 20 mg/ml in DMSO and adding an equal volume of Tween 80 (P4780, Sigma-Aldrich UK) and diluting with 5% dextrose in water (S2123, Selleckchem UK) to the final volume. This solution was diluted with 0.9% saline (S8776, Sigma-Aldrich UK) to give doses of 0.1 and 1 mg/kg in 100 µl of 0.9% saline. Gemcitabine was prepared for intraperitoneal injection by dissolving 20 mg/ml in 0.9% saline and diluted to desired doses of 1 and 5 mg/kg in 100 µl of 0.9% saline. Solutions were stored at -80°C and allowed to thaw at room temperature when required for *in vivo* injection.

2.3 Clonogenic survival and cytotoxicity assays

2.3.1 Clonogenic survival assay

Clonogenic survival was used to measure the replicative capacity of cells after treatment. 300 cells of each tumour line were plated per well of a 6-well flat-bottom plate (CLS3516, Sigma-Aldrich UK) in 2 mls of RPMI 1640. After cells were allowed to adhere for 4 hours, they were exposed for 24 hours to a treatment and concentration. After treatment, the medium was replaced with fresh untreated medium and plates were allowed to incubate undisturbed for 14 days at 5% CO_2 and 37°C. The resultant colonies were fixed and stained with 1% crystal violet in pure ethanol (S1917, Selleckchem UK) for several seconds, which was then poured off and the plates washed with distilled water before being allowed to air dry on the work bench at room

temperature. The colonies were then counted on the GelCount Tumour Colony Counter (Oxford Optronix) and the data plotted and analysed with GraphPad Prism 5.0.

2.3.2 Cytotoxicity assays

Different cytotoxicity assays were performed and optimised to determine and confirm ideal sub-cytotoxic concentrations for testing as accurately as possible. These included the 3-(4,5-dimethylthiazol-2-yl)-2,5-diphenyltetrazolium bromide (MTT) and resazurin sodium assays. The data presented in the thesis is from the resazurin assay.

2.3.2.1 MTT assay

The MTT assay is a colourimetric assay for assessing cell metabolic activity as an indirect measure of number of viable cells present. Intracellular enzymes reduce the tetrazolium dye, MTT, to insoluble formazan, which has a deep purple colour. DLD1 and HCT116 cells were seeded in 96-well flat-bottom plates (CLS3585, Sigma-Aldrich UK) at a concentration of 2000 and 5000 cells/well in 100 µl of RPMI 1640 respectively and were allowed to incubate for 24 hours for cells to adhere. The technique of serial dilutions to create exponentially increasing drug concentrations for cytotoxicity testing was performed as follows. 1 ml of medium was added to the first ten wells of a dilution tray (6015, Pires Track), followed by a further 1 ml addition to the first well. 5 µl/ml of 20 mM drug stock was added to the first well to achieve a starting drug concentration of 100 µM. 1:2 dilutions from well 1 to 2 was performed, mixed, and then repeated for well 2 to 3 and so on to well 9. Well 10 was kept as an untreated control lane. This effectively resulted in well concentrations of: 100, 50, 25, 12.5, 6.25, 3.125, 1.5625, 0.78125, 0.39, and 0 µM. Using a multi-well pipette, 100 µl of drug dilution was dispensed into each well of the 96-well plate in triplicate. This resulted in a further 1:2 dilution of drug, giving effective well concentrations of: 50, 25, 12.5, 6.25, 3.125, 1.5625, 0.78125, 0.39, 0.195 and 0 µM (See Fig.

2.1 – courtesy of Dr. Matthew Hall, National Institutes of Health, USA). The plate was then allowed to incubate for 72 hours at 5% CO_2 and 37°C.

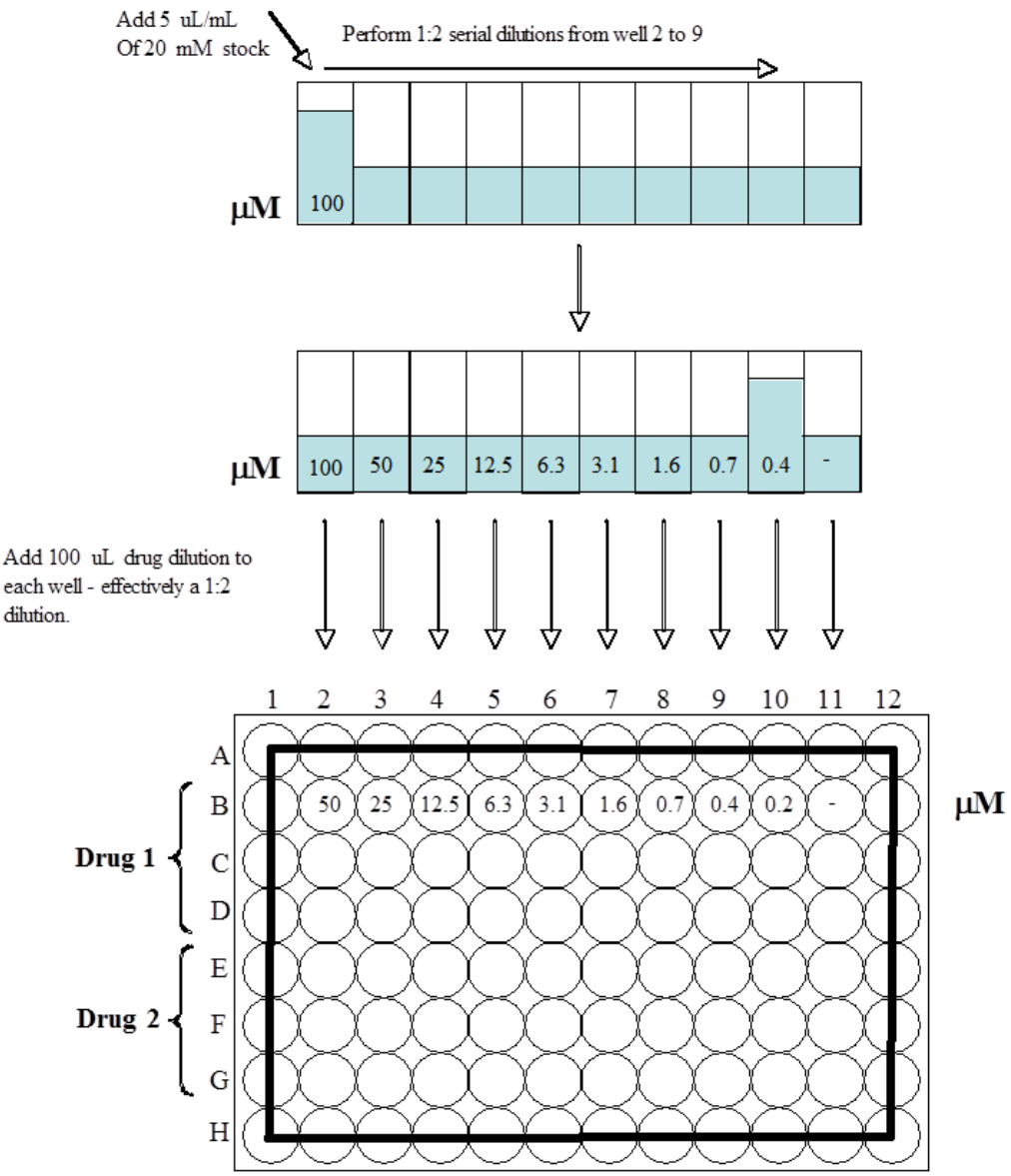

Figure 2.1. Technique of serial dilutions to create exponentially increasing drug concentrations for testing. The starting concentration of drug stock varied dependent on tested agent and were adjusted to encompass nanomolar range when required.

A 10x MTT (M2128, Sigma-Aldrich UK) stock solution was created by dissolving 5 mg/ml of MTT in PBS. This was diluted to 1x concentration by making a 1:10 dilution in IMEM cell growth

media (10373017, Life Technologies). The medium was then removed from the wells of the 96-well plate and replaced immediately with 100 µl of 1x MTT solution per well and allowed to incubate for 2-4 hours at 5% CO_2 and 37°C, until control cells were visibly purple in colour. The MTT solution was removed and replaced with 100 µl of solubilisation buffer (80% ethanol in 0.1 M HCl) per well and left for 10-15 minutes at room temperature. Finally, the absorbance was measured at 570 nm via the microplate reader (Tecan Infinite 200 Pro) and the values plotted, analysed and the IC50 values calculated with GraphPad Prism 5.0. Initial cell seeding concentrations were determined following optimisation studies (See Fig. 2.2).

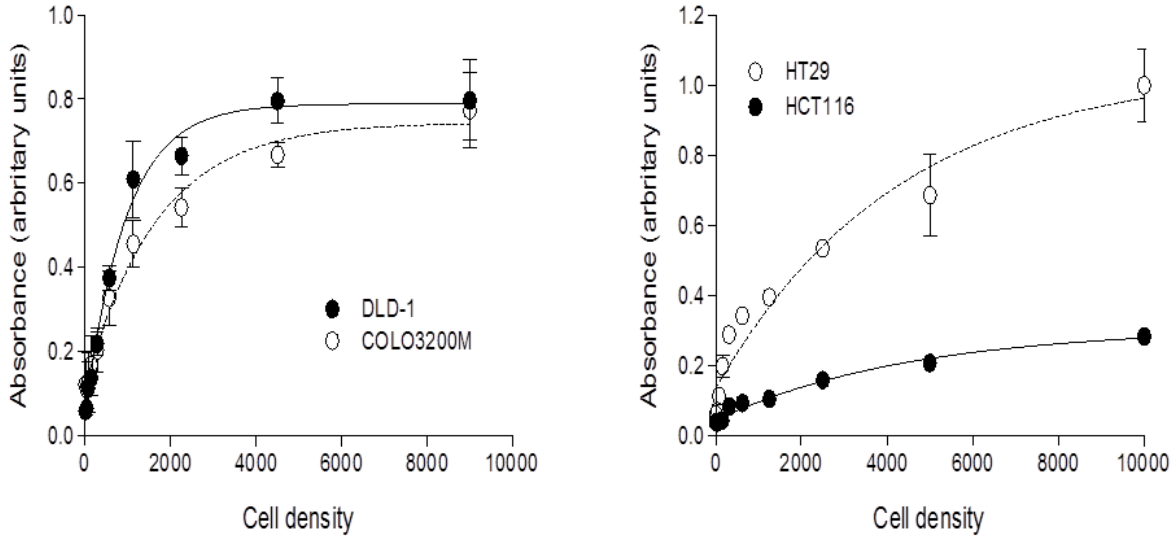

Figure 2.2. Cell seeding optimisation curves for COLO320DM, DLD1, HCT116 and HT29 cell lines for calculating cytotoxicity for selected chemotherapy agents using the MTT assay. Data points represent the mean of 8 wells and error bars represent standard error.

2.3.2.2 Resazurin sodium assay

The Resazurin sodium assay measures the ability of living cells to convert resazurin (blue redox dye) into resofurin (pink end product). Non-viable cells that lose the metabolic capacity to reduce this dye do not generate a fluorescent signal. 1 mg/ml of resazurin sodium (R7017, Sigma-Aldrich UK) was dissolved in sterile PBS and then filter sterilised using 0.22 µM syringe

filters (Z359904, Sigma-Aldrich UK) to create a 10x stock. Tumour cells seeded in 96-well flat-bottom plates at a concentration of 10,000 cells/well in 200 µl of RPMI 1640, were treated for 24 hours with the tested drug before being removed and replaced with fresh media. 20 µl of 1x resazurin was pipetted into each well and the plate incubated for 1-2 hours at 5% CO_2 and 37°C. Plates were then visually inspected after an hour for a pink/purple colour change, being returned to the incubator and reviewed every 20 minutes until this was apparent. Following incubation, the fluorescence was measured at 590 nm via the microplate reader and the values plotted, analysed and the IC50 values calculated with GraphPad Prism 5.0.

2.4 Oxygen consumption rate (OCR) and mitochondrial stress experiments

2.4.1 OCR testing

Oxygen consumption testing was performed with the Extracellular Flux (XF) 96 Analyzer (Seahorse Bioscience), which was able to measure in real time the uptake and excretion of metabolic end products. This was achieved through use of the XF96 FluxPaks (102416-100, Seahorse Bioscience), which contained a disposable sensor cartridge and a XF96-well microplate. The sensor cartridge was embedded with 96 pairs of fluorescent biosensors for oxygen and pH, coupled to a fibre-optic waveguide to measure the extracellular flux changes of oxygen and protons in the media immediately surrounding adherent cells cultured in the XF96-well microplate. The waveguide delivers light at various excitation wavelengths (oxygen at 532 nm and pH at 470 nm) and transmits a fluorescent signal, through optical filters (oxygen at 650 nm and pH at 530 nm) to a set of highly sensitive photodetectors. Each fluorophore is specifically designed to measure a particular analyte and the instrument allows simultaneous measurement of pH and oxygen. Oxygen consumption and proton extrusion cause rapid, measurable changes in oxygen tension and pH (within 3–5 minutes) within a transient microchamber (formed from a vacuum created between the media in the well and the sensor) in

each of the 96 wells. Analyte levels are measured every 22 seconds until the oxygen concentration drops ~30 mmHg and the media pH declines up to 0.4 pH units.

Drug effect on cellular oxygen consumption was performed in two ways. Tumour cells were seeded at 10,000 cells per well in 200 µl of RPMI 1640 in a XF96-well plate for 24 hours to allow cells to attach. This was followed by either exposing the cells to treatment for 24 hours and then measuring the OCR or proceeding to measure the OCR immediately and injecting the treatment to measure the effect in real time over 24 hours. In both approaches, one hour prior to measuring OCR, the culture medium was replaced with XF Assay Medium (102365-100, Seahorse Bioscience) supplemented with 5 mM sodium pyruvate (11360-070, Life Technologies) and 4 mM L-glutamine (25030-081, Life Technologies) at a pH of 7.4 and rested for 1 hour at 5% CO_2 and 37°C. Additionally, prior to measuring the OCR, all the wells of a sensor cartridge was filled with 200 µl of XF Calibrant Solution (100840-000, Seahorse Bioscience) and allowed to rest for at least 4 hours to a maximum of 72 hours at 5% CO_2 and 37°C before being placed into the XF96 Analyzer to calibrate the machine for approximately 30 minutes. The calibration step was done whilst the XF96-well plate was resting for the 1 hour, to maximise efficiency and minimise any potential discrepancies in the readings. Following calibration, a preset programme of timings, duration and frequency of measurements were set and run. Firstly, the XF96 Analyzer would mix the assay media in each well for approximately 20 minutes to allow the oxygen partial pressure to reach equilibrium. This was followed by measuring the OCR and extracellular acidification rate (ECAR) simultaneously for 4 minutes to establish a baseline rate. The assay medium was then gently mixed again for 3 minutes between each rate measurement to restore normal oxygen tension and pH in the microenvironment surrounding the cells. This cycle was repeated for a period of 4 hours if the cells had been treated for 24 hours prior to reading or for a continuous 24 hours if the cells were being treated in real time. In the latter, after the baseline measurement, 25 µl of drug prepared in XF Assay Medium was injected into each well to reach the desired concentration. This was followed by a once-only

mixing for 7 min to expedite compound exposure to cellular proteins, after which OCR and ECAR measurements were then made. To account for any potential variation in cell number brought about by any drug-induced cell death; all raw OCR values were normalised to both the baseline readings and to cell density measurements as determined by Hoechst fluorescence, on a well-by-well basis. At the end of the assay, plates were fixed with 4% paraformaldehyde (PFA) (158127, Sigma-Aldrich UK) and stained with 2 μg/ml Hoechst 33342 (H3570, Invitrogen) prior to measuring fluorescence with the microplate reader.

2.4.2 Mitochondrial stress tests

Mitochondrial stress testing was performed via use of the XF Cell Mito Stress Test Kit (103015-100, Seahorse Bioscience). Tumour cells were seeded on XF96-well plates and processed for OCR and ECAR measurements as described in section 2.4.1 Four measurements were taken before and three after each sequential injection of oligomycin (1 μM), FCCP (0.8 μM) and rotenone and antimycin A (both 1 μM), each at 25 μl volumes in XF Assay Medium. The OCR linked to coupled respiration was calculated by subtracting OCR after the addition of oligomycin from basal OCR. OCR after addition of the mitochondrial uncoupler FCCP reflected the maximal respiratory rate. Non-mitochondrial respiration was determined after rotenone/antimycin A injection and was calculated by subtracting the OCR values from the basal OCR to determine the mitochondrial OCR. Rotenone and oxamate (O2751, Sigma-Aldrich UK) were used to determine whether tumour cell lines were primarily oxidative or glycolytic in phenotype.

2.5 Spheroids

2.5.1 Spheroid creation

Formation of spheroids for experiments between July 2012 and November 2013 were via the liquid overlay technique and from December 2013 to thesis completion were via use of the

lipidure plates. All DLD1 spheroids were generated via the hanging drop method due to difficulties in creating them via either the liquid overlay technique or use of the lipidure plates.

2.5.1.1 Liquid overlay

24-well flat-bottom plates (CLS3526, Sigma-Aldrich UK) were coated with 250 µl of 1% (w/v) agarose (A9539; Sigma-Aldrich UK) and allowed to set for 5-10 minutes. 200 µl of RPMI 1640 were added to each well and allowed to diffuse into the agarose for 20 minutes before being removed and the process repeated again. Tumour cells were then seeded at a concentration of 10,000 cells per well in 200 µl of RPMI 1640 and cultured for 4 days without disturbance in a sterile incubator at 5% CO_2 and 37°C. Treatments were commenced in fresh medium on day 5 for 24 hours before being removed and proceeding with the next stage of the experiment.

2.5.1.2 Lipidure plates

Tumour cells were seeded in 96-well U-bottom lipidure-coat (51011610, NOF Europe) plates at a concentration of 10,000 cells per well in 200 µl of RPMI 1640 and then centrifuged at 800 revolutions per minute (rpm) for 10 minutes. The cells were then cultured for 4 days without disturbance in a sterile incubator at 5% CO_2 and 37°C. Treatments were commenced in fresh medium on day 5 for 24 hours before being removed and proceeding with the next stage of the experiment.

2.5.1.3 Hanging drop

10 µl drops of a DLD1 cell suspension of 2.5 x 10^6 cells/ml in RPMI 1640 was pipetted onto the underside of the lid of 48-well flat-bottom plates (SIAL0548, Sigma-Aldrich UK). Each well was filled with 200 µl of sterile PBS and the lid was inverted and placed on top of the plate, taking care not to disturb the droplets. The cells were then cultured for 4 days without

disturbance in a sterile incubator at 5% CO_2 and 37°C. Spheroids were then removed by pipette and transferred to 96-well round-bottom plates (SIAL079, Sigma-Aldrich UK) and treatments commenced in fresh medium for 24 hours before being removed and proceeding with the next stage of the experiment.

2.5.2 EF5 incubation

To quantify hypoxia, spheroids were incubated with EF5, which was a gift from Dr. Cameron Koch (University of Pennsylvania, Philadelphia, USA). The EF5 was dissolved in PBS to obtain a 3 mM concentration. 20 µl of this stock solution was then added to 180 µl of medium in each spheroid culture well to obtain the final concentration of 300 µM per spheroid. Spheroids were allowed to incubate with EF5 for four hours.

2.5.3 Spheroid processing for immunohistochemistry

Following EF5 incubation, spheroids were aspirated from the wells with a de-tipped 200 µl pipette into 1.5 ml Eppendorf tubes. Any excess media in the tubes were aspirated and discarded and the spheroids then washed with PBS before again being aspirated and discarded. 500 µl of 4% PFA was added to each tube to fix the spheroids at 4°C overnight, following which the PFA was removed and the spheroids again washed with PBS and removed. The spheroids were then subject to preservation in 500 µl of 30% sucrose (S9378, Sigma-Aldrich UK) in PBS at 4°C for 3 hours. Once the spheroids were visibly at the bottom of each Eppendorf tube, the sucrose was removed and the spheroids aspirated with a de-tipped 1000 µl pipette and placed onto a pre-layer of optimal cutting temperature (OCT) compound (Tissue-Tek) in a cryomold (Tissue-Tek). Further OCT compound was placed on top of the spheroids and the cryomolds stored at -80°C, ready for sectioning and staining (See Section 2.8).

2.5.4 Mathematical modelling of OCR

Quantifying reduction in OCR via mathematical modelling was kindly performed by Dr. David Grimes (University of Oxford, Oxford, UK). Spheroids were dual stained with EF5, which binds between 0.8 and 10 mmHg and the proliferation marker Ki-67. The spheroids were grown and the central cross-section of the spheroids were subsequently taken. Images of the sectioned and stained spheroids were then analysed with a MATLAB script, which measured the spheroid radius r_o and the interface between the Ki-67 and EF5, r_{10}. It has been shown previously that if the external oxygen partial pressure around a spheroid p_o is known, then the oxygen partial pressure can be calculated at any point in the viable and oxygenated spheroid rim by:

$$p(r) = p_O + \frac{a\Omega}{6D}\left(r^2 - r_o^2 + 2r_n^3\left(\frac{1}{r} - \frac{1}{r_O}\right)\right)$$

where a is the oxygen consumption rate, D is the oxygen diffusion constant in water (approximately $2\ x\ 10^{-9} m^2 s^{-1}$) and r_n is the anoxic radius of the spheroid. The constant Ω arises from Henry's law and is given by $\Omega = 3.0318\ x\ 10^7\ mmHg\ kg\ m^{-3}$. As the spheroids in this work are sufficiently small that they do not exhibit any central anoxia, we set $r_n = 0$ which simplifies the equation. The interface between the Ki-67 and EF5 occurs at the edge of the EF5 binding threshold so that $(r_{10}) \cong 10\ mmHg$. Thus we can re-arrange the equation above to estimate oxygen consumption rate a, which yields:

$$a = \frac{6D(p_o - 10)}{\Omega(r_o^2 - r_{10}^2)}$$

This identity allows estimation of oxygen consumption rate given the parameters of spheroid radius r_o and EF5 boundary radius r_{10}, and facilitates cross-comparison of spheroids treated with different agents. Whilst the above equations presume oxygen consumption rate a remains constant throughout the spheroid, it should be noted that only very minor differences

would be expected were the oxygen consumption rate hyperbolic rather than constant and thus the equations above will still hold to a high degree even in this case.

2.6 Drug effect characterisation

2.6.1 Western blot

Following optimisation, western blots were performed to the following protocol with the kind assistance of Dr. Pavitra Kannan (University of Oxford, Oxford, UK) to generate the results presented in Chapter 6.

2.6.1.1 Antibodies

Table 2.2. Summary of antibodies and dilutions used for western blot experiments.

Antibodies	Species	Dilution	Source	Catalogue Code
β-actin	Mouse	1:20,000	Sigma-Aldrich UK	A1978
Citrate synthase	Rabbit	1:500	Alpha Diagnostic	CISY11-A
OXPHOS complexes	Human	1:500	Abcam	Ab110411
Phospho-Chk1	Rabbit	1:1000	New England Biolabs	8191S
p21 Waf1/Cip1	Rabbit	1:1000	New England Biolabs	2947S
p27 Kip1	Rabbit	1:1000	New England Biolabs	3688S

2.6.1.2 Extraction of proteins

Tumour cells were seeded in 2 mls of RPMI 1640 at a density of 2 x 10^5 cells/ml in a 6-well plate for 24-48 hours. Wells were then treated with docetaxel or gemcitabine at tested concentrations for 24 hours following which, the media was aspirated off and the wells washed with ice cold PBS and removed. 100 µl of lysis buffer containing radio immunoprecipitation assay (RIPA) buffer (R0278, Sigma-Aldrich UK), protease and phosphatase inhibitors (Roche), was added to each well and the cells scraped off and placed in Eppendorf tubes on ice for 25

minutes with the occasional vortex. Lysates were then spun at 13,000 rpm for 10 minutes and the supernatant transferred to new tubes and kept on ice.

2.6.1.3 Quantification of protein concentration

The total protein present in the lysates was determined using The Pierce® BCA Protein Assay Kit (Thermo Scientific). 2 mg/ml bovine serum albumin (BSA) standard, provided in the kit, was serially diluted at a ratio of 1:12.5 with RIPA buffer to prepare standards in the range from 0 mg/ml to 2 mg/ml. A standard curve of concentrations was created by adding 25 µl each of these standards to a 96-well transparent, flat bottom plate in duplicate. Lysate samples were then diluted 1:12.5 with water (2 µl lysate to 23 µl water) and added to the same 96-well plate. Reagent A (containing sodium bicarbonate, bicinchoninic acid and sodium tartrate in 0.1 M sodium hydroxide) and reagent B (containing 4% cupric sulfate) were combined at a ratio of 50:1 to prepare the BCA Working Reagent, 200 µl of which was added to each sample and standard on the 96-well plate. The plate was then incubated at 5% CO_2 and 37°C for 20-30 minutes. Following incubation, the absorbance was measured at 562 nm via the microplate reader. The results were then normalised against the background reading and then plotted to estimate the protein concentration (µg/µl). These values were then multiplied by 12.5 (to account for dilution) and the actual protein concentration of the lysates was determined.

2.6.1.4 Sample preparation

Samples of 20 µl each were prepared in Eppendorf tubes as follows: 1 µl of 1 M dithiothreitol (DTT); 5 µl of RunBlue LDS Sample Buffer (Expedeon); appropriate volume of lysate which corresponded to 15 µg of protein and water to make up the remaining volume. Samples were then lightly centrifuged and denatured at 70°C for 10 minutes on a heat block.

2.6.1.5 Gel electrophoresis

Proteins were separated by sodium dodecyl sulphate-polyacrylamide gel electrophoresis (SDS-PAGE). 10 µl of the protein sample was loaded onto 12-well RunBlue Pre-cast gels (Expedeon) of 4-12% acrylamide concentration, which were washed with distilled water prior to use. The gels were placed into a Novex mini-cell tank (Invitrogen) filled with SDS running buffer, supplied by RunBlue (Expedeon). 2.5 µl of Precision Plus Protein Kaleidoscope standards (161-0375, Bio-Rad) was loaded into the first and last wells on the gel, followed by the protein samples using loading tips. The gel was then run for 1 hour at 150 Volts.

2.6.1.6 Blotting protocol

Separated proteins were transferred from the gel onto a 48 cm^2 polyvinylidene fluoride (PVDF) transfer membrane (Immobilon from Millipore). The PVDF membrane was activated by immersion for 10 seconds in 100% methanol and then rinsed with transfer buffer (25 mM Tris, 192 mM glycine, 20% methanol and 0.1% SDS). Two sheets of Whatman paper and several sponges were soaked in transfer buffer. The membrane was placed onto the gel and sandwiched between two sheets of Whatman paper and sponges and then inserted into a XCell IITM blot module (Invitrogen), filled with transfer buffer. The transfer was then run for 1 hour at 30 Volts. The membrane was immersed in 5% milk in TBS-T (prepared by dissolving Marvel skimmed milk powder in Tris-buffered saline supplemented with 0.1% Tween-20) and blocked on a roller (SRT6, Stuart Equipment) for 1 hour at room temperature. The membrane was then incubated with primary antibody (See Table 2.2) diluted in 5% milk in TBS-T overnight at 4°C on a roller. Following incubation, the membrane was washed three times with TBS-T for 5 minutes each and then incubated with an appropriate secondary antibody diluted in 5% milk in TBS-T at room temperature on a roller for 1 hour. This was followed by a further three times wash for 5 minutes each with TBS-T before development.

2.6.1.7 Membrane development

Depending on the sensitivity of the primary antibody used, the membrane was developed by using either the Amersham enhanced chemiluminescence (ECL) or ECL+ kit (RPN2232/RPN2133, GE healthcare). ECL comprises Solution A (Tris buffer in 3.2% ethanol) and Solution B (proprietary substrate in Tris buffer) and were mixed at a ratio of 1:1. The membrane was then soaked in this solution for ~20 seconds and placed into an autoradiography cassette (Fisher). Finally, the membrane was exposed to film (Fuji) and developed (XoGraph Imaging Systems).

2.6.2 Flow cytometry

DLD1 and HCT116 spheroids were formed and allowed to grow for 4 days as described in section 2.5 and then subjected to docetaxel (1 nM and 3 nM) or gemcitabine (20 nM and 50 nM) treatment for 24 hours. On day 5, the treatment was removed and replaced with fresh media (RPMI 1640). Spheroids of each treatment group were put together and mechanically disaggregated with micro pipette into a single cell suspension and aliquoted into fluorescence activated cell sorting (FACS) tubes. The tubes were then centrifuged at 1300 rpm for 5 minutes and the supernatant removed and discarded. The cells were washed with 1 ml of PBS and vortexed followed by a further centrifuge at 1300 rpm for 5 minutes. The supernatant was again removed and discarded and the cells then fixed with 1 ml of ice cold 70% ethanol (02877, Sigma-Aldrich UK) for 10 minutes, followed by a centrifuge at 2000 rpm for 5 minutes. The ethanol was aspirated off and the cells washed with 1 ml of PBS before a final centrifuge at 2000 rpm for 5 minutes. The PBS was removed and 1 ml of staining solution containing PBS, 50 µg/ml of propidium iodide (P4170, Sigma-Aldrich UK) and 200 µg/ml of RNase (R5503, Sigma-Aldrich UK) was added, vortexed and incubated at room temperature in the dark for 30 minutes. FACS was performed using a FACSCalibur flow cytometer (BD Biosciences) and the G_1, S, G_2 and apoptotic populations analysed with FlowJo software version 7.6.5.

2.6.3 High performance liquid chromatography (HPLC)

To determine nucleotide populations, tumour cells in RPMI 1640 were seeded into 1 x T175 flasks per treatment and placed in a sterile incubator at 5% CO_2 and 37°C to reach 60-80% confluency, in order attain a minimum of 1 x 10^7 cells per sample. Flasks were then treated with either DMSO or drug (docetaxel, gemcitabine or hydroxyurea) for 24 hours. Following this, the media was aspirated and the cells washed with ice cold PBS before being lifted with trypsin and placed into 10 ml falcon tubes on ice. Tubes were spun at 2000 rpm for 5 minutes at 4°C in the centrifuge and the supernatant carefully removed and discarded with a pipette. 50 µl of 6% trichloroacetic acid (TCA) (T9159; Sigma-Aldrich UK) was added to the cell suspension to lyse the cells and vortexed for 1 minute. The tubes were then spun again at 13,000 rpm for 5 minutes at 4°C and the supernatant transferred into Eppendorfs and stored at -80°C before processing for nucleotide pools. Analysis was kindly performed by Dr. Lisa Folkes (University of Oxford, Oxford, UK).

2.7 Animal work

2.7.1 Animals

All animal procedures were conducted in accordance with the UK Animal Scientific Procedures Act 1986 and approved by a local ethics committee. Animals were housed in specific pathogen-free facilities with temperature and humidity control and on a 14 hour light-10 hour dark cycle, with food and beverage provided *ad libitum*. Female BALB/c nude mice aged 6-8 weeks were purchased from Charles River Laboratories (Kent, UK). Tumour-free mice were weighed twice weekly and mice on an experimental protocol were weighed every two days. All mice were reviewed daily by myself or members of the Biomedical Science facility.

2.7.2 Subcutaneous tumour model

Xenografts were generated on the right flank of each mouse via subcutaneous injection of 100 µl of FBS-free RPMI 1640 containing 1 x 10^6 DLD1 HRE-luciferase cells. DLD1 HRE-luciferase cells were kindly created and gifted by Dr Yunhong Cao (University of Oxford, Oxford, UK). Xenografts were allowed to develop to reach a volume of 80 mm^3 before being randomised and entered into an experimental protocol. Docetaxel and gemcitabine in 0.9% saline was delivered at 0.1 mg/kg and 1 mg/kg and 1 mg/kg and 5 mg/kg concentrations in 100 µl of 0.9% saline respectively, three times per week (days 0, 3 and 6). Untreated mice were injected with 100 µl of 0.9% saline alone. Tumour volume was measured every two days and the mice were imaged with IVIS on days 0, 3 and 6 (See section 2.9.2). Mice were sacrificed on day 7 and processed (See section 2.7.3). In the growth-delay experiments, mice were subject to a single dose of radiation at 6 gray (Gy) on day 7 and the tumours allowed to develop to a maximum volume of 300 mm^3 or for a maximum period of 28 days after first treatment before being sacrificed (See section 2.10.3).

2.7.3 Collection of murine plasma and subcutaneous tumours

Two and half hours prior to sacrifice on day 7, mice were given 0.01 ml/g body weight of 10 mM EF5 dissolved in saline via intraperitoneal injection. Thirty minutes prior to sacrifice, mice were given 50 µl of CD31 antibody via intravenous injection into the lateral tail vein. Mice were sacrificed via intraperitoneal injection of 200 mg/kg sodium pentobarbital. Shortly afterwards, the thoracic cage was opened and the inferior vena cava incised just superior to the diaphragm. Blood was aspirated from the thoracic cavity using a 1 ml insulin syringe and placed in Eppendorf tubes containing 1.5 mg/ml of 0.5 M ethylenediaminetetraacetic acid (EDTA) (E7889, Sigma-Aldrich UK) on ice. Blood samples taken from mice treated with gemcitabine were placed in Eppendorf tubes additionally containing 5 µl of tetrahydrouridine (THU) (Ab142080, Abcam)

to prevent deamination. Blood samples were then kindly analysed by Dr. Michael Stratford (University of Oxford, Oxford, UK).

The subcutaneous tumours were carefully dissected from the flanks of the mice post mortem and divided into two. One half of each tumour was immediately snap frozen in liquid nitrogen for analysis for drug metabolites. The other half of each tumour was placed in OCT compound before snap freezing in liquid nitrogen for sectioning for immunohistochemistry (See section 2.8). All samples were stored at -80°C prior to analysis.

2.8 Immunohistochemistry

2.8.1 Antibodies and stains

Table 2.3. Summary of antibodies and stains used for immunohistochemistry.

Antibodies/Stain	Target	Source	Catalogue Code
Hoechst 33342	Nucleic acids	Invitrogen	H3570
Anti-EF5-Cy3	EF5-bound hypoxic cells	Dr. Cameron Koch (University of Pennsylvania, Philadelphia, USA)	N/A
Alexa Fluor 488 anti-mouse CD31	Endothelial cells	BioLegend	102514
Anti-human Ki-67	Ki-67 protein (expressed exclusively in proliferating cells)	AbD Serotec	HCA053A
Alexa Fluor 647 anti-mouse CD34	Vascular adventitia	eBioscience	51-0341

2.8.2 Hypoxia staining of spheroid sections

The protocol for staining for hypoxia in spheroids (See Table 2.4) was adapted from the protocol devised by Dr. Kasia Bloch (University of Oxford, Oxford, UK), who optimised the technique as part of her D.Phil thesis. Spheroids in OCT compound were cut at 6-8 μm sections with the Bright 5040 microtome (Bright Instruments) and placed onto Superfrost Plus microscope slides (12727307, Fisher Scientific). Slides were then dried in an incubator for 1 hour at 5% CO_2 and 37°C before being stored at -20°C.

Table 2.4. Protocol for staining of spheroid sections for immunohistochemistry.

Step	**Procedure**	**Duration**
1. Slides thawing	Incubate at room temperature	5 min
2. Antigen retrieval	Place in a microwave oven in 10 mM sodium citrate with 0.05% Tween 20	4 min at 300W, then 16 min at 80W
3. Wash	Immerse in PBS	3 min
4. Suppression of endogenous peroxidase activity	Immerse in 0.3% freshly prepared H_2O_2 in PBS	20 min
5. Wash	Immerse in PBS	2 x 3 min
6. Endogenous biotin block	Incubate with streptavidin reagent (Vectashield) in a humidifying chamber	12 min
7. Wash	Immerse in PBS	3 min
8. Endogenous Streptavidin block	Incubate with biotin (Vectashield) in a humidifying chamber	12 min
9. Wash	Immerse in PBS	3 min
10. Blocking	Incubate with tris-NaCl-blocking (TNB) buffer	45 min

	(FP1020, PerkinElmer) in a humidifying chamber	
11. Primary antibody (Ki-67)	Incubate with mouse anti-human Ki-67 primary antibody diluted in TNB buffer at 1:100 dilution in a humidifying chamber at 4°C	Overnight at 4°C
12. Wash	Immerse in PBS	3 x 3 min
13. Secondary antibody (Ki-67)	Incubate with goat anti-mouse biotinylated antibody in a dilution of 1:500 in TNB buffer and incubated in a humidifying chamber	30 min
14. Wash	Immerse in PBS	3 x 3 min
15. Streptavidin-HRP	Incubate with streptavidin-HRP Reagent (PerkinElmer) in a dilution of 1:200 in TNB buffer and incubated in a humidifying chamber	30 min
16. Wash	Immerse in PBS	2 x 3 min
17. Detection of Ki-67	TSA-fluorescein isothiocyanate (FITC) conjugated amplification reagent in a dilution 1:100 in Amplification Diluent and incubated in a humidifying chamber	5 min
18. Wash	Immerse in PBS	1 x 3 min
19. Fixation	Incubate with 4% PFA under the fume hood	20 min
20. Wash	Immerse in PBS	3 x 3 min
21. Blocking	Incubate with TNB buffer in a humidifying chamber	30 min
22. Wash	Immerse in PBS supplemented with 0.3% Tween 20	5 min
23. Primary antibody (EF5)	Incubate with anti-EF5-Cy3 antibody	Overnight at 4°C
24. Wash	Immerse in ice-cold PBS supplemented with 0.3% Tween 20	3 x 3 min
25. Wash	Immerse in PBS	1 x PBS

26. Nuclear staining	Incubate with Hoechst 33342 in a dilution 1:1000 in PBS in a humidifying chamber	5 min
27. Wash	Ice-cold 0.3% Tween 20 in PBS	3 x 45 min
28. Mounting sections	One drop of Vectashield mounting medium and coverslips placed on slides.	

2.8.3 Hypoxia staining of tumour sections

Subcutaneous tumours in OCT compound were cut at 10-12 μm sections with the Bright 5040 microtome and placed onto Superfrost Plus microscope slides. Slides were then dried in an incubator for 1 hour at 5% CO_2 and 37°C before being stored at -20°C. Anti-mouse CD31 was injected into mice as described in section 2.7.3. The protocol for staining for hypoxia in tumours is outlined in Table 2.5.

Table 2.5. Protocol for staining of tumour sections for immunohistochemistry.

Step	**Procedure**	**Duration**
1. Slides thawing	Incubate at room temperature	5 min
2. Fixation	Incubate with 4% PFA under the fume hood	10 min
3. Wash	Immerse in PBS supplemented with 0.3% Tween 20	2 x 10 min
4. Wash	Immerse in PBS	10 min
5. Blocking	Incubate with TNB buffer in a humidifying chamber	60 min
6. Primary antibodies (EF5 & CD34)	Incubate with anti-EF5-Cy3 and Anti-CD34 antibodies	Overnight at 4°C
7. Wash	Immerse in PBS supplemented with 0.3% Tween 20	2 x 45 min
8. Wash	Immerse in PBS	45 min
9. Nuclear staining	Incubate with Hoechst 33342 in a dilution 1:1000 in PBS in a humidifying chamber	10 min

10. Wash	Immerse in PBS	15 min
11. Mounting sections	One drop of Vectashield mounting medium and coverslips placed on slides.	

2.9 Imaging

2.9.1 Confocal imaging for hypoxia staining

Images were acquired with a Zeiss 710 Laser Scanning Confocal Microscope (LSM710, Carl Zeiss). EF5-Cy3 emission was written to the red (R) channel, Ki-67-FITC emission was written to the green (G) channel and Hoechst 33342 emission was written to the blue (B) channel of the RGB picture. Each channel was isolated from the RGB picture for separate analysis in ImageJ (http://imagej.nih.gov/ij/) as described in section 2.11.

2.9.2 *In vivo* imaging for real time tumour hypoxia (IVIS)

For *in vivo* imaging, mice were anaesthetised in an anaesthetic chamber using 3% vaporised isoflurane (Piramal Healthcare), before being injected with 150 mg/kg VivoGlo Luciferin (P1041, Promega) intraperitoneally. The animals were immediately transferred to a charge-coupled device (CCD) camera (IVIS system, PerkinElmer), fixed in position and imaged using automatic f/stop, exposure time and binning. A region of interest (ROI) was drawn around the margins of the subcutaneous tumours of each mouse. Mice were imaged every two minutes for a variable period until the signal intensity reached a plateau. The background photon flux was then subtracted from the signal within the ROI to determine the total tumour photon flux *in vivo*. To represent change in photon flux with time as hypoxia developed, the signal for each mouse at each time-point was normalised to the value obtained for the same animal at Day 0. Images were retrieved and analysed with Living Image 3.2.

2.10 Radiation

2.10.1 Monolayer

DLD1 and HCT116 cells were seeded into 6-well plates at seeding densities between 200 and 40,000 cells directly proportional to the radiotherapy dose and incubated for 6 hours in a sterile incubator (Binder) at 5% CO2 at 37°C to allow cells to adhere. Both cell lines were treated with either docetaxel at 1 nM and 3 nM or gemcitabine at 20 nM and 50 nM concentrations for 24 hours before irradiation with Caesium at 0, 2, 4, 6, 8 or 10 Gy. Radiotherapy was delivered at a dose rate of 0.86Gy/minute at 37°C using a ^{137}Cs-laboratory irradiator (IBL 637, CIS bio International) and was performed with the kind assistance of Dr. Jianzhou Chen (University of Oxford, Oxford, UK). After irradiation, plates were maintained in the incubator for 14 days, until visible colonies had formed. Colonies were fixed and stained with 1% crystal violet in pure ethanol and dried on the work bench at room temperature. The colonies were then counted on the GelCount ™ Tumour Colony Counter (Oxford Optronix). The plating efficiency (PE) and survival fraction (SF) were calculated as follows:

PE = 100 x (number of colonies formed in 0 Gy plates / seeding cell number)

SF = number of colonies formed / (seeding cell number x PE)

The SF data was plotted on a $\log_{10}$ scale against the radiation dose in a linear scale and the survival curves fitted on GraphPad Prism 5.0 using the linear quadratic model: $\ln(SF) = -\alpha D - \beta D^2$.

2.10.2 Spheroids

DLD1 and HCT116 spheroids were formed and allowed to grow for 4 days as described in section 2.5 and then subjected to docetaxel (1 nM and 3 nM) or gemcitabine (20 nM and 50 nM)

treatment for 24 hours. On day 5, the treatment was removed and replaced with fresh media (RPMI 1640). DLD1 spheroids were then irradiated with a single dose of Caesium at 6 Gy or 4 Gy for spheroids treated with docetaxel or gemcitabine respectively and HCT116 spheroids were irradiated with a single dose of Caesium at 4 Gy for spheroids treated with either docetaxel or gemcitabine. Spheroids were then allowed to grow in a sterile incubator at 5% CO_2 at 37°C and their diameters recorded every 2-3 days for a period of 2 weeks. 50% of the media was removed and replaced with fresh media every 2-3 days for all spheroids.

2.10.3 *In vivo*

Following tumour inoculation and proceeding as described in section 2.7.2, mice were anaesthetised with 3% vaporised isoflurane in oxygen on day 7 and the subcutaneous tumours isolated and irradiated with Caesium at a single fraction of 6 Gy. Non-tumour parts of the mice were protected with radiation shielding.

2.11 Statistical analysis

Statistical analyses were performed using GraphPad Prism 5.0. Quantitative data were expressed as means ± standard error of the mean (SEM). One-way analysis of variance (ANOVA) followed by post-hoc Bonferroni's multiple comparison test was performed to assess the differences among various treatments unless otherwise stated and was represented as follows: * = $p<0.05$; ** = $p<0.01$; *** = $p<0.001$.

For the statistical analysis of proliferation, hypoxia, functional and non-functional vessel density in spheroids and xenograft tumours, microscopy images were analysed using ImageJ. For quantification of proliferating and hypoxic cells, red, green and blue channels from microscopy images were separated and a black/white threshold generated for each. A ROI was

drawn around the spheroids or hypoxic dense areas of tumour and the number of proliferative and Hoechst 33342 positive cells calculated within the ROI using the ImageJ software. This allowed the percentage of proliferative cells to be determined as a percentage of the total number of cells within a spheroid or tumour section. For quantification of tumour vascularity, a similar approach was used however the area of CD31 and CD34 staining was calculated and expressed as a percentage of the ROI area.

CHAPTER 3: SELECTION OF CHEMOTHERAPEUTIC AGENTS AND DETERMINING SUB-CYTOTOXIC CONCENTRATIONS

3.1 Aims

1. To review the literature and identify agents from current or expected clinical use for investigation.
2. To determine concentrations of these agents that will alter oxygen consumption with minimal cell death.
3. To identify cell lines for investigation that will reflect the genetic heterogeneity of colorectal cancer.

3.2 Introduction

3.2.1 Chemotherapy agents and hypoxia

As discussed earlier, the ultimate focus of chemotherapeutics has been to kill tumour cells, reduce tumour bulk and to cure. These agents are broadly categorised as cytotoxic, hormonal and targeted therapies. The latter has been of great interest in recent times, as it offers patient-specific and tumour-specific treatments with potentially fewer side-effects. When these agents are combined with the current understanding of tumour hypoxia, tumour metabolism and their relationships, the focus of therapy may be expanded beyond that of just cell kill. Indeed, one of the principle aims of the thesis is to evaluate the effects of established chemotherapy agents on tumour hypoxia, which is an issue that was eloquently put by Brown and colleagues in 2004: "These clear links between hypoxia and intrinsic resistance to chemotherapy provide the 'smoking gun', yet, surprisingly, clinical studies investigating the role of hypoxia in response to chemotherapy have not been reported" [71]. Peculiarly, in the decade since this statement, modest progress has been made in exploring this link. Some agents have sought to take advantage of the cellular mechanics of electron transfer in hypoxia by acting as surrogate donors for the physicochemical reaction such as the nitroimidazoles, which aim to improve radiosensitivity, whereas others exploit the redox reactions in hypoxia, by being reduced to form active cytotoxic compounds and are known as bioreductive prodrugs [71, 116, 117]. However, neither of these hypoxia-specific agents has brought about a significant revolution in current treatment modalities and regimens, as highlighted in section 1.3.6. More recently, targeting hypoxia-specific metabolic pathways has been the focus of treatment and most notably, the HIF-1 hypoxic response pathway has garnered much attention. However, there is very little literature on the role of established chemotherapy agents on tumour hypoxia as preference appears to be given to creating novel agents to target this phenomenon. It would be interesting, therefore, to investigate this further as despite decades of clinical use, they have not been implicated in alterations in oxidative metabolism.

3.2.2 Selection of chemotherapy agents

Chemotherapy agents in current or expected clinical use were selected for study based on two specific reasons. Firstly, it was anticipated that known agents would have an extensive literature background which would help in designing the experiments and secondly, clinical testing would be easier, if required. A detailed literature review of chemotherapy agents that have been tested in hypoxia studies and/or colorectal cancer were identified and used as reference for selecting drugs and starting concentrations [107, 169-190]. Drugs selected for investigation were docetaxel, etoposide, fluorouracil, gemcitabine, irinotecan (SN38), mitomycin C, mitoxantrone, oxaliplatin, vincristine and VX-680. All of these agents are cytotoxic compounds and only fluorouracil, irinotecan and oxaliplatin are currently used as agents against colorectal cancer. VX-680 is a non-specific aurora kinase inhibitor and the only agent not in clinical use, although early success in tumour growth retardation did lead to a Phase II clinical trial before being halted due to evidence of electrocardiograph (ECG) changes in one patient [171, 191]. Mitomycin C and mitoxantrone are both antibiotic agents with cytotoxic mechanisms of action. Some studies show that mitomycin C can also be hypoxia-specific and function as a bioreductive prodrug and has been shown to be particularly effective in reducing hypoxia, whereas others found it was less effective in hypoxia in testicular germ cell tumour cell lines [176, 183, 192]. Vincristine also has a variable effect in hypoxia, with evidence that it can inhibit HIF-1α expression in ovarian and breast tumour cell lines but is relatively ineffectual in gastric cancer [180, 190]. The cytotoxic effects of both etoposide and gemcitabine appear to be reduced in the presence of hypoxia in testicular germ cell, breast, prostatic, hepatic and pancreatic tumour cell lines [183-187]. Irinotecan, however, has been shown to inhibit HIF-1α and VEGF in glioma cell lines through the activity of the drug metabolite SN38 [188]. The cytotoxic effects of fluorouracil is less effective in hypoxia in breast and gastric tumour cell lines whilst the activity of docetaxel is unchanged in prostate and ovarian tumour cell lines [178, 179, 181, 182]. Docetaxel, however, has been shown to inhibit HIF-1 in ovarian and breast tumour cell lines [180].

3.2.3 The heterogeneity of colorectal cancer and selection of cancer cell lines

Colorectal cancer was selected as the tissue for investigation as it is a well-recognised and studied solid tumour known to exhibit core hypoxia. Furthermore, it is a cancer where radiotherapy is used as a treatment modality and since an improvement in radiosensitivity was one of the anticipated outcome measures of the project, it was clinically relevant. There is significant heterogeneity in colorectal cancer and Guinney and colleagues have recently sought to achieve a consensus on the molecular subtypes [193]. Essentially, there are three different and partially overlapping, molecular phenotypes that reflect the different forms of DNA instability [194]. These are: 1) the chromosomal instability pathway (CIN) phenotype, which accounts for ~85%, of all sporadic colorectal cancers and is the most common phenotype; 2) the microsatellite instability (MSI) phenotype accounting for ~15% of all colorectal cancers and is caused by interruptions of the DNA mismatch-repair system, leading to a significant increase in the mutation rate and 3) the CpG island methylator phenotype (CIMP), which exhibits aberrant DNA methylation [195-199]. This phenotypical heterogeneity is significant because certain agents are more likely to be helpful in one subtype of colorectal cancer than another and clinical trials are underway to assess the benefit of these agents in these different subtypes in order to create both patient-specific and tumour-specific therapies. One such trial is the FOCUS4 clinical trial which is testing new agents in patients with unresectable and metastatic colorectal cancer but with various different subtypes [200]. Patients receive chemotherapy for a period of up to 16 weeks and during this time a tumour biopsy from the patient is analysed to determine the genetic characteristics of that tumour. This includes identifying genes which are commonly mutated in colorectal cancer such as Kirsten rat sarcoma (KRAS), neuroblastoma rat sarcoma (NRAS), BRAF and phosphatidylinositol-4,5-bisphosphate 3-kinase, catalytic subunit alpha (PIK3CA). These results allow patients to be assigned into one of five subtypes: the BRAF subtype for cancers with a mutated BRAF gene; the RAS subtype for cancers with mutated KRAS/NRAS genes; the PIK3CA subtype for cancers with a mutated PIK3CA or loss of phosphatase and tensin homolog (PTEN) from tumour cells; a 'no mutation' subtype for

tumours where no mutation has been identified and unclassified for tumours that do not fit the criteria for the other four groups. Therefore, in order to reflect this known heterogeneity in colorectal cancer in the design of the experiments for this study, a panel of four colorectal cancer cell lines from different anatomical regions of the colon, different sexes and with different mutation status were investigated (see Table 3.1).

Table 3.1. Origin, genetic and mutational characteristics of investigated colorectal cancer cell lines. The chosen cell lines are from different anatomical regions of the colon, different sexes and with varied mutation status to represent the heterogeneity of tumours in clinical practice. Adapted with permission from Ahmed D et al. [194].

	COLO320DM	DLD-1	HCT-116	HT-29
Patient	55-Year-old female	Male	48-Year-old male	44-Year-old female
Site	Sigmoid	Colon	Ascending colon	Colon
Stage			Dukes' D	Dukes' C
Source	Primary tumour	Primary tumour	Primary tumour	Primary tumour
Microsatellite	Stable	Unstable	Unstable	Stable
CIMP	–	+	+	+
CIN	+	–	–	+
KRAS	wt	G13D	G13D	wt
BRAF	wt	wt	wt	V600E
PIK3CA	wt	E545K;D549N	H1047R	P449T
PTEN	wt	wt	wt	wt
TP53	R248W	S241F	wt	R273H

3.3. Results

3.3.1 *Colorectal tumour cell lines have a concentration-dependent replicative capacity with tested chemotherapy agents*

To determine the replicative capacity of the selected panel of colorectal cancer cell lines with the agents to be tested, a clonogenic survival assay was performed. All the cancer cell lines demonstrated a decrease in replicative capacity with increasing concentrations of the drugs (See Fig. 3.1). Etoposide and oxaliplatin appeared to be toxic for all cell lines at the tested concentrations. Gemcitabine appeared relatively less so, with a similar profile seen for all cell lines. Docetaxel also appeared to have less toxicity at the tested concentrations for the COLO320DM, DLD1 and HCT116 cell lines whilst VX-680 was less toxic for all but COLO320DM.

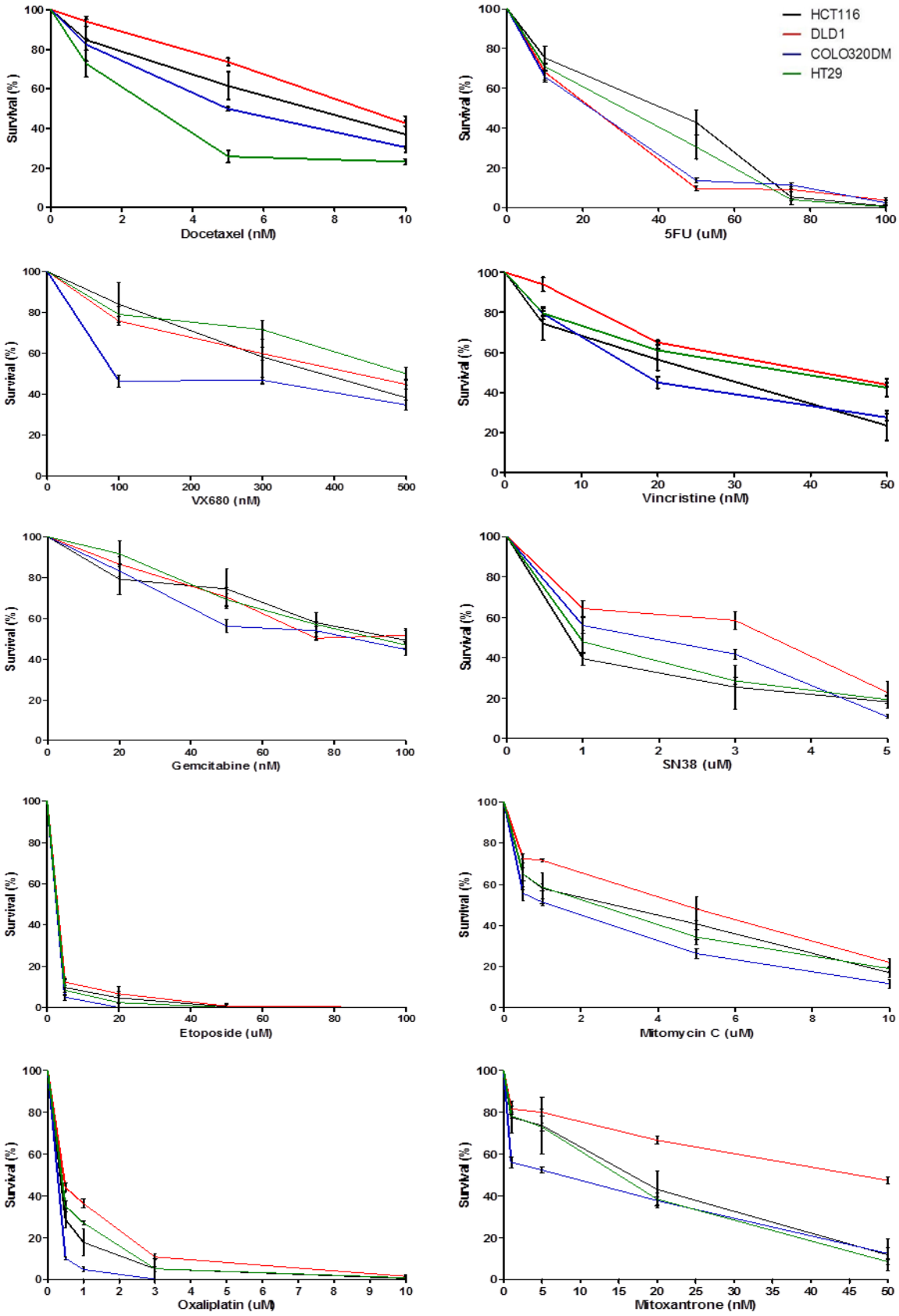

Figure 3.1. Clonogenic studies demonstrating replicative capacity of a panel of colorectal cancer cell lines against various chemotherapy agents at increasing concentrations. Data represents mean ± SEM from three replicates from three repeat experiments.

3.3.2 Colorectal tumour cell lines show a variable sensitivity to tested chemotherapy agents

There appeared to be variability in sensitivity of the different cell lines to a number of the agents. The DLD1 cell line appeared to be least sensitive and COLO320DM most sensitive overall (See Fig. 3.2). This is best reflected in the clonogenicity graphs of vincristine, mitoxantrone, mitomycin C and oxaliplatin (See Fig. 3.1).

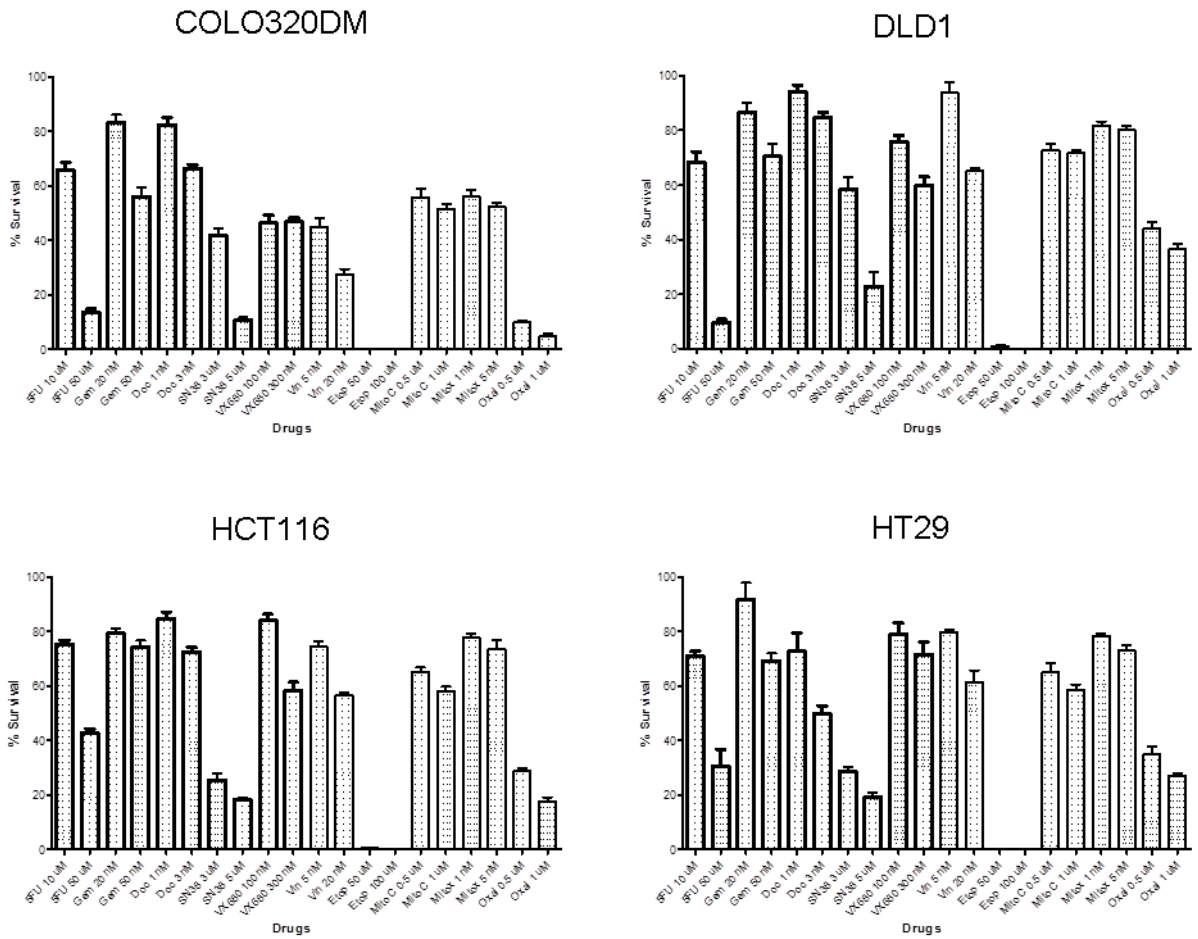

Figure 3.2. % survival of various chemotherapy agents at differing concentrations of 4 different colorectal cancer cell lines. Some agents were toxic for all cell lines at tested concentrations e.g. Etoposide, whereas others had variable responses e.g. Fluorouracil. Data represents mean ± SEM from three replicates from three repeat experiments.

3.3.3 Selection of agents for oxygen consumption studies

The results from the clonogenic assays (See Figs. 3.1 and 3.2) were summarised and an arbitrary 'traffic light' scoring system was applied to help select appropriate drugs and concentrations for further testing (See Table 3.2). Following 24 hours of treatment, drugs and concentrations that resulted in greater than 70% cell survival were highlighted green and thus deemed well tolerated, whilst those between 50 and 70% and those less than 50% were highlighted amber and red respectively and thus less so. Docetaxel and gemcitabine at both concentrations for the DLD1 and HCT116 cell lines were relatively well tolerated and mitoxantrone at both concentrations was well tolerated by DLD1, HCT116 and HT29 cell lines. VX-680 at both 100 nM and 300 nM concentrations was only well tolerated by the HT29 cell line. As earlier discussed, the DLD1 cell line had the greatest overall replicative capacity whereas the COLO320DM cell line had the least. Docetaxel and gemcitabine were then selected for study on their effect on oxygen consumption due to their tolerability across all four cell lines.

Table 3.2. Summary of clonogenic data for tested agents against DLD1, HT29, HCT116 and COLO320DM cell lines. Agents and cell lines selected for further investigation should demonstrate the greatest balance of resistance to toxicity and reduction in OCR.

	DLD1	HT29	HCT116	COLO320DM
Docetaxel 1 nM	94.02 ± 2.51	72.72 ± 6.75	84.69 ± 2.47	82.36 ± 2.71
Docetaxel 3 nM	84.32 ± 1.96	49.03 ± 3.09	72.71 ± 1.63	66.14 ± 1.00
Etoposide 50 µM	0.67 ± 0.67	0.00 ± 0.00	0.33 ± 0.33	0.00 ± 0.00
Etoposide 100 µM	0.00 ± 0.00	0.00 ± 0.00	0.00 ± 0.00	0.00 ± 0.00
5FU 10 µM	68.15 ± 3.96	71.03 ± 1.70	75.36 ± 1.39	65.81 ± 2.77
5FU 50 µM	9.55 ± 1.22	30.43 ± 6.17	42.77 ± 1.44	13.55 ± 1.31
Gemcitabine 20 nM	86.57 ± 3.41	91.70 ± 6.21	79.24 ± 1.77	83.24 ± 2.94
Gemcitabine 50 nM	70.42 ± 4.83	69.17 ± 2.77	74.42 ± 2.26	56.09 ± 3.22
Mitomycin C 0.5 µM	72.67 ± 2.33	65.00 ± 3.22	65.00 ± 1.73	55.67 ± 3.38
Mitomycin C 1 µM	71.67 ± 0.88	58.67 ± 1.86	58.00 ± 1.73	51.33 ± 1.86
Mitoxantrone 1 nM	81.67 ± 1.45	78.33 ± 0.88	77.67 ± 1.76	56.00 ± 2.51
Mitoxantrone 5 nM	80.00 ± 1.73	73.00 ± 2.08	73.67 ± 3.18	52.33 ± 1.45
Oxaliplatin 0.5 µM	44.00 ± 2.31	35.00 ± 2.52	28.67 ± 0.88	10.00 ± 0.58
Oxaliplatin 1 µM	36.33 ± 2.19	27.00 ± 1.00	17.67 ± 1.45	4.67 ± 1.20
SN38 3 µM	58.43 ± 4.62	28.26 ± 1.81	25.46 ± 2.53	41.76 ± 2.50
SN38 5 µM	22.75 ± 5.26	19.16 ± 1.66	18.16 ± 0.71	10.75 ± 0.98
VX680 100 nM	75.71 ± 2.38	78.95 ± 4.14	83.95 ± 2.43	46.38 ± 2.76
VX680 300 nM	59.81 ± 3.21	71.54 ± 4.56	58.21 ± 3.08	46.81 ± 1.30
Vincristine 5 nM	93.98 ± 3.47	79.57 ± 1.27	74.42 ± 1.91	79.32 ± 2.74
Vincristine 20 nM	65.02 ± 1.17	61.09 ± 4.60	56.43 ± 1.24	45.02 ± 2.90

% Survival >70 50-70 <50

3.3.4 Determining sub-cytotoxic concentrations for docetaxel and gemcitabine

Sub-cytotoxic concentrations of docetaxel and gemcitabine were determined from cell viability curves for both DLD1 and HCT116 cell lines, calculated from the Resazurin assay (See Fig. 3.3 A and B). The half maximal inhibitory concentration (IC50) values of the agents for each cell line were determined from fitting non-linear regression (See Fig. 3.3 C). The IC50 for docetaxel was approximately 20 nM and 30 nM for the HCT116 and DLD1 cell lines respectively whilst the IC50 for gemcitabine was approximately 140 nM and 163 nM for the HCT116 and DLD1 cell lines respectively. This confirmed that the concentrations for testing on OCR for docetaxel (1 nM and 3 nM) and gemcitabine (20 nM and 50 nM) should be sub-cytotoxic and therefore minimally lethal.

A

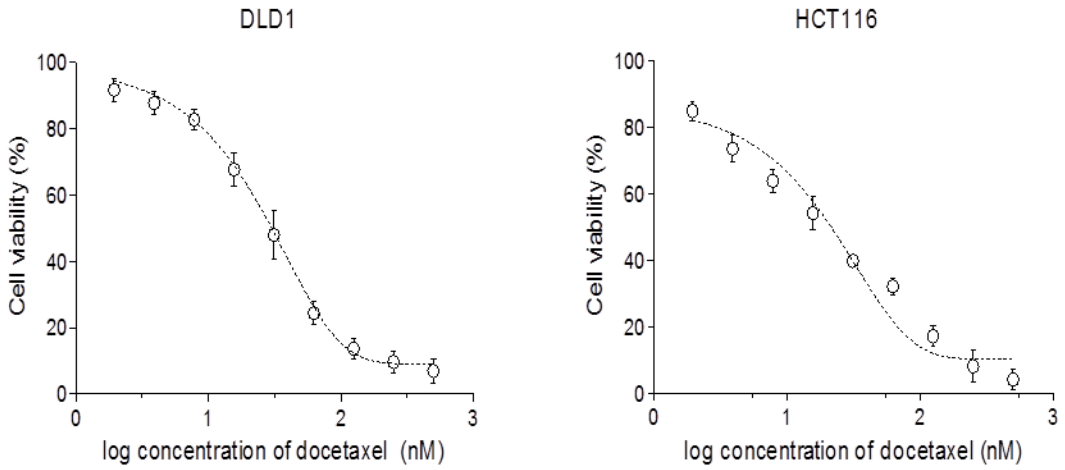

B

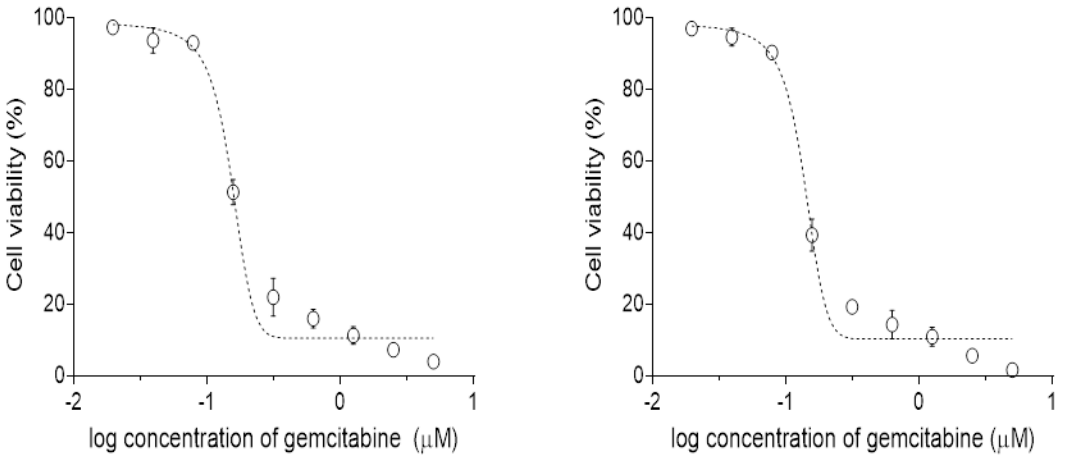

C

	IC50 Docetaxel (nM)	IC50 Gemcitabine (μM)
DLD1	29.66128622 ± 2.851	0.163134661 ± 0.010
HCT116	20.34858369 ± 1.883	0.139685765 ± 0.007

Figure 3.3. Representative cell viability curves for DLD1 and HCT116 cell lines treated with a range of doses of docetaxel and gemcitabine. Cells were treated with the tested agents for 24 hours and the Resazurin assay performed immediately. Non-linear regression was applied using GraphPad Prism 5.0 to determine the IC50. Data points represent mean ± standard deviation from six replicates. Three repeat experiments were performed.

A. Treatment with docetaxel.
B. Treatment with gemcitabine.
C. Calculated IC50 values for docetaxel and gemcitabine.

3.4 Discussion

Both the clonogenic and cytotoxicity assays demonstrate an inverse relationship between increasing concentrations of the agents and tumour cell survival (See Figs. 3.1 and 3.3). This is consistent with the pharmacodynamics of cytotoxic drugs [201, 202]. The calculated IC50 values for docetaxel and gemcitabine for DLD1 and HCT116 cells was consistent with literature findings [203, 204]. All the cell lines appeared to be particularly sensitive to fluorouracil, irinotecan and oxaliplatin, which was not unexpected considering the colorectal-tumour-specific nature of these agents [205].

The variability in sensitivity of certain cell lines to different agents may be explained through the differing genetic mutations and heterogeneous nature of the tumour cells (See Table 3.1 and Fig. 3.2). Both the DLD1 and HCT116 cell lines, which were the least sensitive to the tested agents, have a KRAS G13D mutation (an amino acid substitution at position 13 in KRAS from a glycine to an aspartic acid) which has been demonstrated as being strongly associated with a poorer clinical outcome and may be an explanation for their relative resistance [206-208]. Furthermore, right-sided colonic tumours have also been shown to be associated with a poorer prognosis and the HCT116 cell line is sourced from an ascending colonic tumour, which may also help explain the cell line's impaired sensitivity [206]. However, the evidence for this appears conflicting, with some papers demonstrating no difference in mortality rates between right and left-sided tumours [209, 210]. The HCT116 cell line, however, is sourced from a metastatic phenotype which is associated with a poorer prognosis and may also affect sensitivity [209, 210]. The COLO320DM cell line appeared to be most sensitive to the agents. This may be explained through the fact that the cell line is essentially part of the all-wild-type subgroup, which has been shown to have a very good patient survival and therefore possibly very chemosensitive [206]. Contradicting these theories, per contra, is the stability of microsatellites in the cell lines. MSI is closely associated with prognosis, with tumours with high MSI having a more positive prognosis by 15% compared to tumours with

low MSI or microsatellite stable (MSS) tumours [211-213]. Both DLD1 and HCT116 cell lines have high MSI, so one would perhaps expect greater sensitivity in this regard, whilst the COLO320DM cell line is MSS and therefore should perhaps display greater resistance. One possible explanation may be that KRAS and PI3KCA mutations have a greater impact on a cell lines sensitivity and resistance as compared to MSI. MSI has also been shown to be associated with responsiveness to fluorouracil therapy, with some debate in the literature. Both Sargent and colleagues and Gallinger and colleagues have demonstrated negativity of response with MSI [214]. However, a direct correlation between level of instability and positivity in response has been shown by Shiovitz and colleagues and Sinicrope and colleagues [207, 215]. This discrepancy may be explained by the differences in stage of the tumour, the impact of sporadic versus germline origin and other genetic differences as explored by Roth and colleagues [216]. However, the positive association may help to explain the relative toxicity of the agent in both the DLD1 and HCT116 cell lines at the 50 μM concentrations but as a colorectal-tumour-specific agent, toxicity is seen with all 4 cell lines. Oxaliplatin, however, is associated with good activity in MSS tumours and the considerable toxicity seen in COLO320DM and HT29 cell lines, may be explained from this observation [217]. CIMP-positive tumours have been shown to have a worse OS and are a stronger prognostic feature than MSI [218]. It is interesting to note therefore, that the only cell line to be CIMP-negative was COLO320DM, which was the least resistant cell line. The only cell line with a BRAF mutation was HT29, which is associated with both a poor prognosis and a poor response to chemotherapy and radiotherapy [219, 220]. This is particularly true in MSS tumours, which would help explain the relative resistance of the HT29 cell line to the treatments. The interplay between the various mutations within and between all the cell lines is incredibly complex and their outcome on prognosis and pharmacodynamics is highly variable. In light of this, it would appear very difficult to conclusively confirm an association between a mutation and an outcome considering most tumours have more than a single mutation and their relationships are variable from tumour to tumour and from patient to patient. This viewpoint appears validated by Strese and colleagues

who found that impaired chemosensitivity was not universal when testing a panel of cell lines with 19 different agents in both normoxic and hypoxic conditions [176].

The results of this chapter were vital in helping to lay the foundations for the experiments outlined in the following chapters. The selection of the agents, concentrations and cell lines (which will be discussed in greater detail in Chapter 4) for subsequent investigation were determined from the work presented here.

CHAPTER 4: SUB-CYTOTOXIC CONCENTRATIONS OF CHEMOTHERAPY AGENTS REDUCE OXYGEN CONSUMPTION *IN VITRO*

4.1 Aims

1. To investigate the effects of chemotherapy agents on oxygen consumption in a panel of colorectal tumour cell lines and a non-transformed cell line.
2. To identify chemotherapy agents and cell lines that demonstrate the greatest balance of resistance to toxicity and reduction in OCR.

4.2 Introduction

4.2.1 Evolution and relevance of measuring the oxygen consumption rate

The oxygen consumption rate (OCR) of cells is an important indicator and measurement of normal cellular function. It can be used as a parameter to study mitochondrial function and as a marker of factors triggering the switch from normal oxidative phosphorylation to aerobic glycolysis in tumour cells. Historically, calculation of the cellular OCR was not amenable to high throughput usage and data was often unreliable [221-223]. Until recently, the most common technique for measuring OCR had been through Clark electrodes, which measured the reduction of oxygen via a catalytic platinum surface [224]. However, this technique was not without limitations, with problems such as signal drift, low sensitivity and consumption of oxygen by the electrode itself reported [224]. Other alternative techniques have included the use of scanning electrochemical microscopy and nanosensors, which are attached to the outer cellular membrane [225, 226]. Although theoretically, direct oxygen levels could be detected through this approach, in reality, only intermittent oxygen flux near the cell membrane or the sensor is detected, since these techniques are usually employed in openly diffusible environments. More recently, optical methods of determining OCR have been a promising development in addressing the low throughput issue of previous techniques [227]. This approach adapted a well-established technique of using transition-metal-based phosphores as oxygen sensing dyes [228]. The phosphorescent signal is quenched by oxygen and usually results in a signal that is inversely proportional to the amount of oxygen present. Often, the signal lifetime is also quenched by oxygen. Although the problems of low throughput assessment of OCR are addressed, the technique has issues with reproducible sealing which presents additional variability. Ultimately, the signal acquired for optical probes is, as is found in the scanning electrochemical microscopy technique, that of intermittent oxygen flux near the sensor and presents significant variability. However, it is not necessary for cells to be within a sealed environment to measure their oxygen consumption. In monolayers, oxygen reaches the cells

strictly by diffusion and the relationship between cellular OCR and the dissolved oxygen concentration at equilibrium is described by the steady-state solution to Fick's Law [223].

The latest development in measuring OCR in cells has been through the invention of the extracellular flux (XF) analyser technology and has been the method employed for experiments in this thesis. The XF Analyzer measures OCR and ECAR at intervals of approximately 2-5 minutes and improves on previous technology by reducing variability through multiple sensors. The OCR is an indicator of mitochondrial respiration and ECAR is an indicator of glycolytic activity. Real-time measurements of OCR and ECAR are made by isolating a minute volume (less than 7 μl) of medium above the monolayer of cells within a well. Cellular respiration and proton excretion (glycolysis) causes rapid, measurable changes to the concentrations of dissolved oxygen and free protons in the isolated media, which are measured every few seconds by solid-state sensor probes residing 200 μm above the cell monolayer. The probe measures the concentrations until the rate of change is linear and then able to determine OCR and ECAR. The equipment also allows for real-time introduction of agents and inhibitors to test oxidative phosphorylation and glycolysis as well as the effect of drugs on these pathways. Since the measurements are non-destructive, the metabolic rate of the same cell population can be measured repeatedly over time and other types of biological assays such as cell viability can be performed on the same plate.

4.3 Results

4.3.1 Sub-cytotoxic concentrations of docetaxel and gemcitabine reduce OCR in vitro

To determine whether docetaxel and gemcitabine affect oxygen consumption in the selected panel of colorectal tumour cell lines and in a non-transformed cell line (MRC5 – human lung fibroblasts), the OCR was measured for 24 hours with the XF96 Analyzer shortly after injection of the agents. Cells were seeded at ~80% confluency. Docetaxel significantly reduced the % OCR at both 1 nM and 3 nM concentrations in the COLO320DM and DLD1 cell lines but only at the 3 nM concentration in the HCT116, HT29 and MRC5 cell lines (See Fig. 4.1). Gemcitabine significantly reduced the % OCR in DLD1, HCT116 and HT29 cell lines at 50 nM concentration but no significant effect was observed at 20 nM concentration in any of the cell lines. Additionally, no significant effect was observed in the COLO320DM and MRC5 cell lines at 50 nM concentration (See Fig. 4.2).

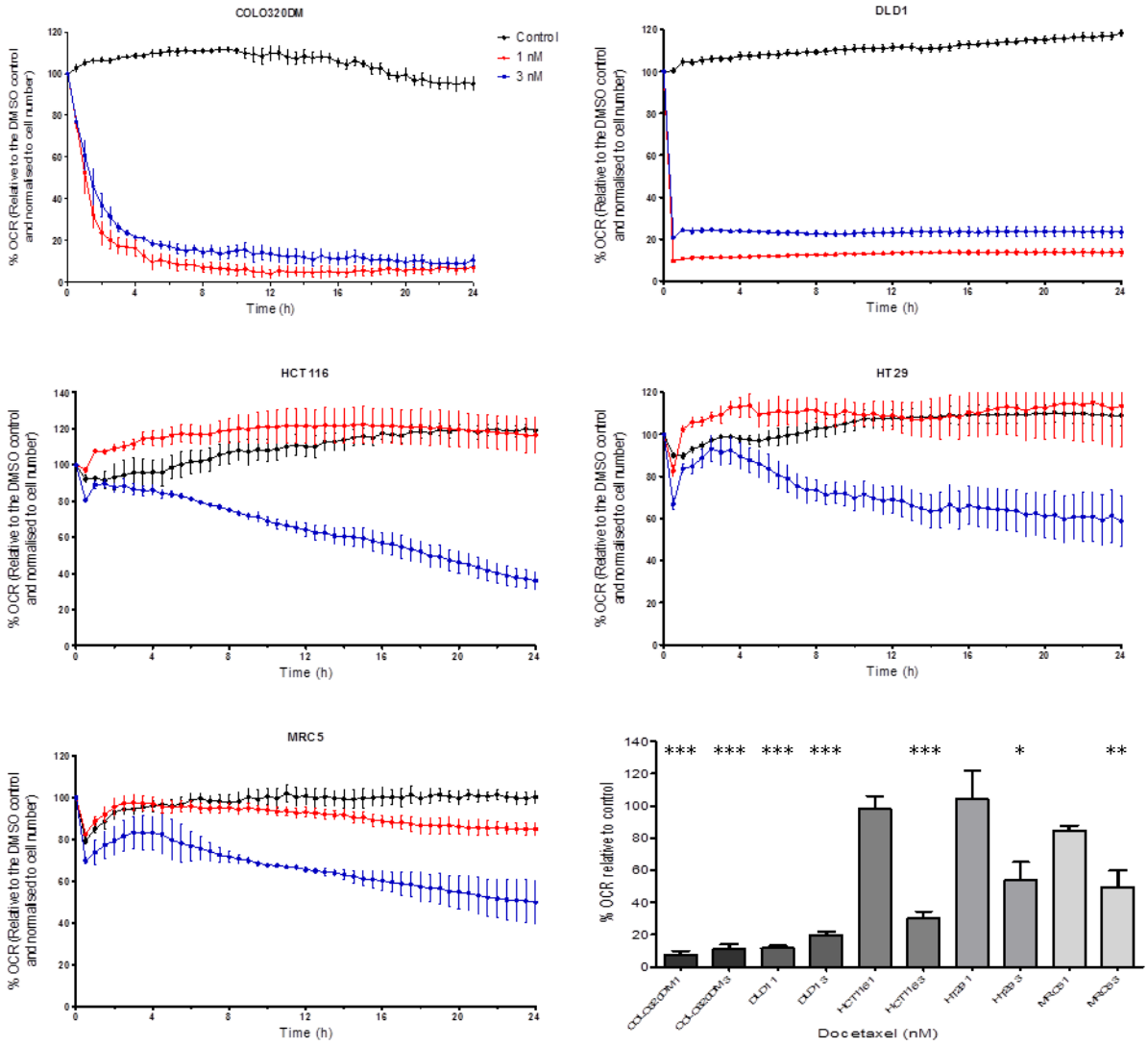

Figure 4.1. Sub-cytotoxic concentrations of docetaxel reduce oxygen consumption. The oxygen consumption rates (OCR) of COLO320DM, HCT116, HT29, DLD1 and MRC5 cells were measured for 24 hours after injection of docetaxel at either 1 nM or 3 nM concentrations using the Seahorse XF96 Analyzer. Cells were seeded at 20,000 per well. A greater reduction is seen in the cancer cell lines versus the non-transformed (MRC5) cell line. The % OCR post injection is shown relative to the DMSO control and normalised to the cell number. The data is an average of at least 3 independent experiments. Data points represent the mean value of the OCR and error bars represent standard error of the mean. One way ANOVA was performed to assess statistical significance with Bonferroni post correction (* = $p<0.05$; ** = $p<0.01$; *** = $p<0.001$)

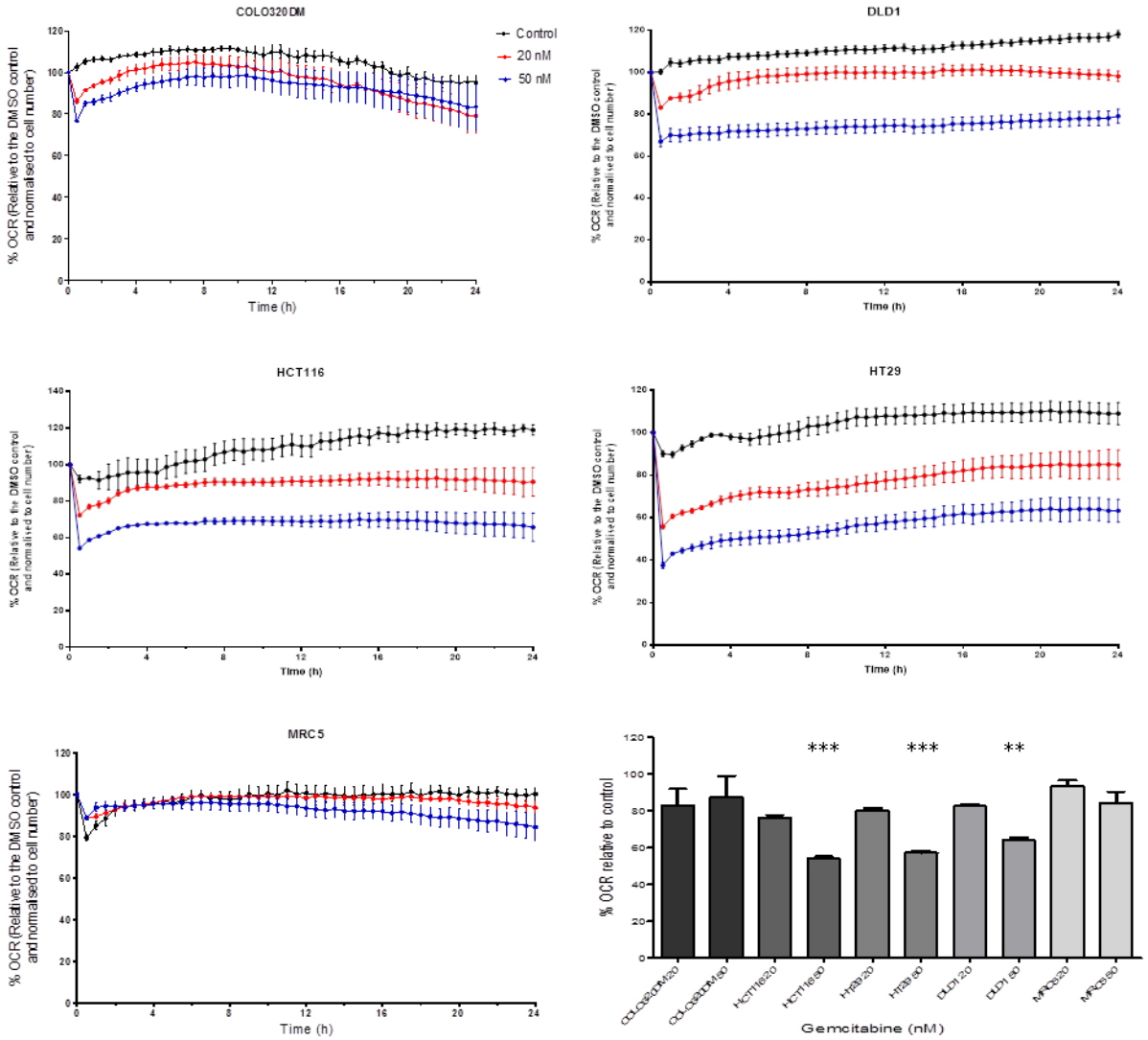

Figure 4.2. Sub-cytotoxic concentrations of gemcitabine reduce oxygen consumption. The oxygen consumption rates (OCR) of COLO320DM, HCT116, HT29, DLD1 and MRC5 cells were measured for 24 hours after injection of gemcitabine at either 20 nM or 50 nM concentrations using the Seahorse XF96 Analyzer. Cells were seeded at 20,000 per well. A greater reduction is seen in the cancer cell lines versus the non-transformed (MRC5) cell line. The % OCR post injection is shown relative to the DMSO control and normalised to the cell number. The data is an average of at least 3 independent experiments. Data points represent the mean value of the OCR and error bars represent standard error of the mean. One way ANOVA was performed to assess statistical significance with Bonferroni post correction (* = $p<0.05$; ** = $p<0.01$; *** = $p<0.001$)

4.3.2 Tested chemotherapy agents have a greater effect in reducing OCR in tumour cell lines than in the non-transformed (MRC5) cell line

The effects of all tested chemotherapy agents on OCR in COLO320DM, DLD1, HCT116, HT29 and MRC5 cell lines was performed for comparison as described in section 4.3.1 and the data summarised (See Fig. 4.3). The reduction of OCR was not limited to docetaxel and gemcitabine. Most agents reduced OCR to a variable degree across all cell lines. However, of the 20 tested conditions (10 agents, 2 concentrations), 13 had a less than 20% reduction in oxygen consumption in the MRC5 cell line. Mitomycin C increased OCR in the HCT116 cell line.

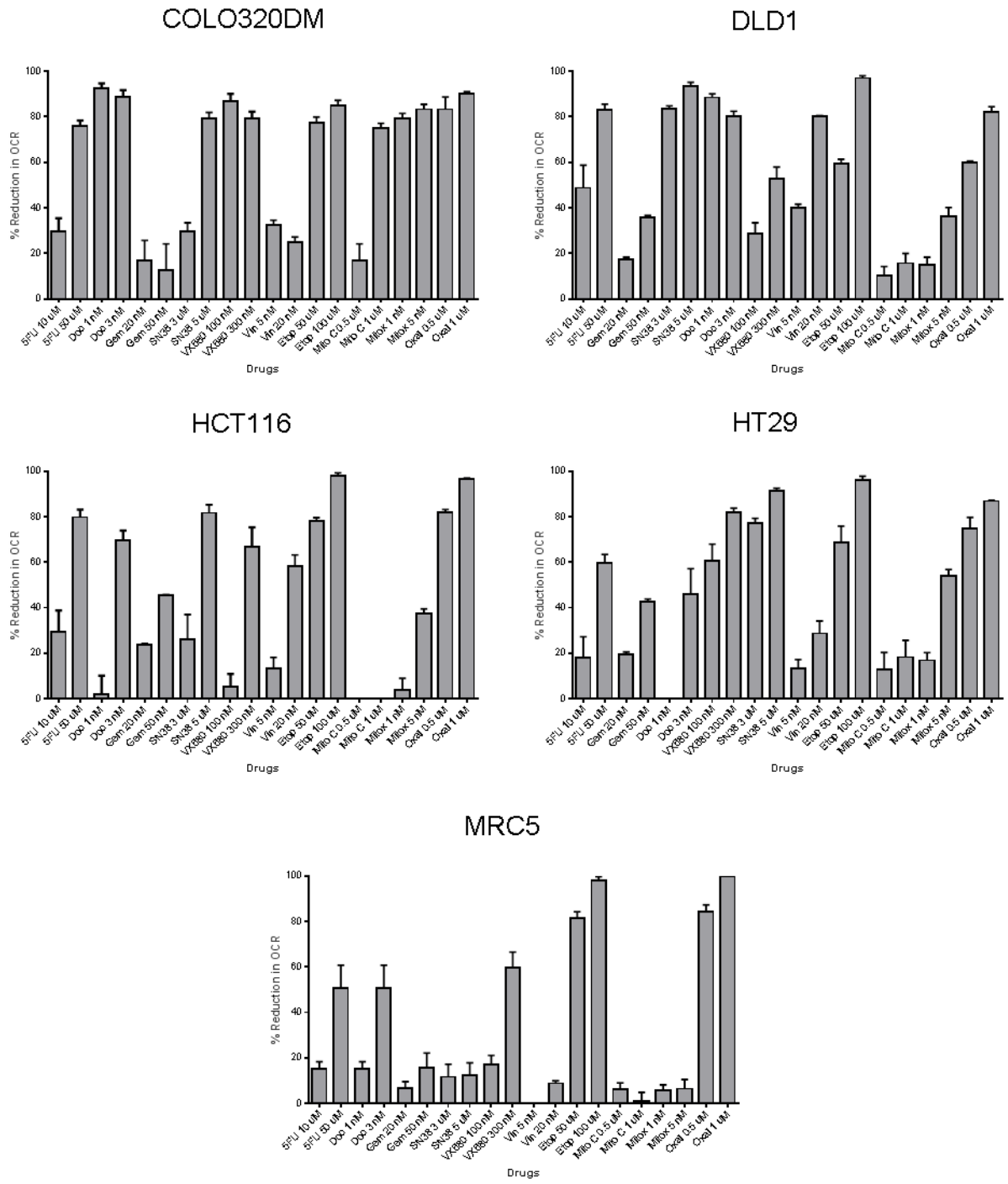

Figure 4.3. Summary of the effects of tested chemotherapy agents on OCR in COLO320DM, DLD1, HCT116, HT29 and MRC5 cells. Most of the chemotherapy agents reduced OCR to a variable degree across all cell lines. Many agents had a greater effect in reducing OCR in the tumour cell lines as compared to the non-transformed cell line (MRC5), suggesting a tumour-specific enhancing effect. Some agents appeared to increase OCR in some of the cell lines e.g. Mitomycin C in the HCT116 cell line. The data is an average of 3 independent experiments. Error bars represent standard error of the mean.

4.3.3 Determining glycolytic phenotype of colorectal tumour cells

To determine whether a tumour cell line exhibited a glycolytic phenotype, the OCR was measured with the XF96 Analyser shortly after injection of different concentrations of glucose. The first measure was done at 4 minutes and subsequent measures every 7 minutes for a total of 6 measures. The baseline % OCR was reduced with increasing concentrations of glucose in a concentration-dependent fashion in both COLO320DM and HCT116 cell lines (See Fig. 4.4). The reverse, however, was observed in the DLD1 cell line, with increasing % OCR alongside the increase in glucose concentration.

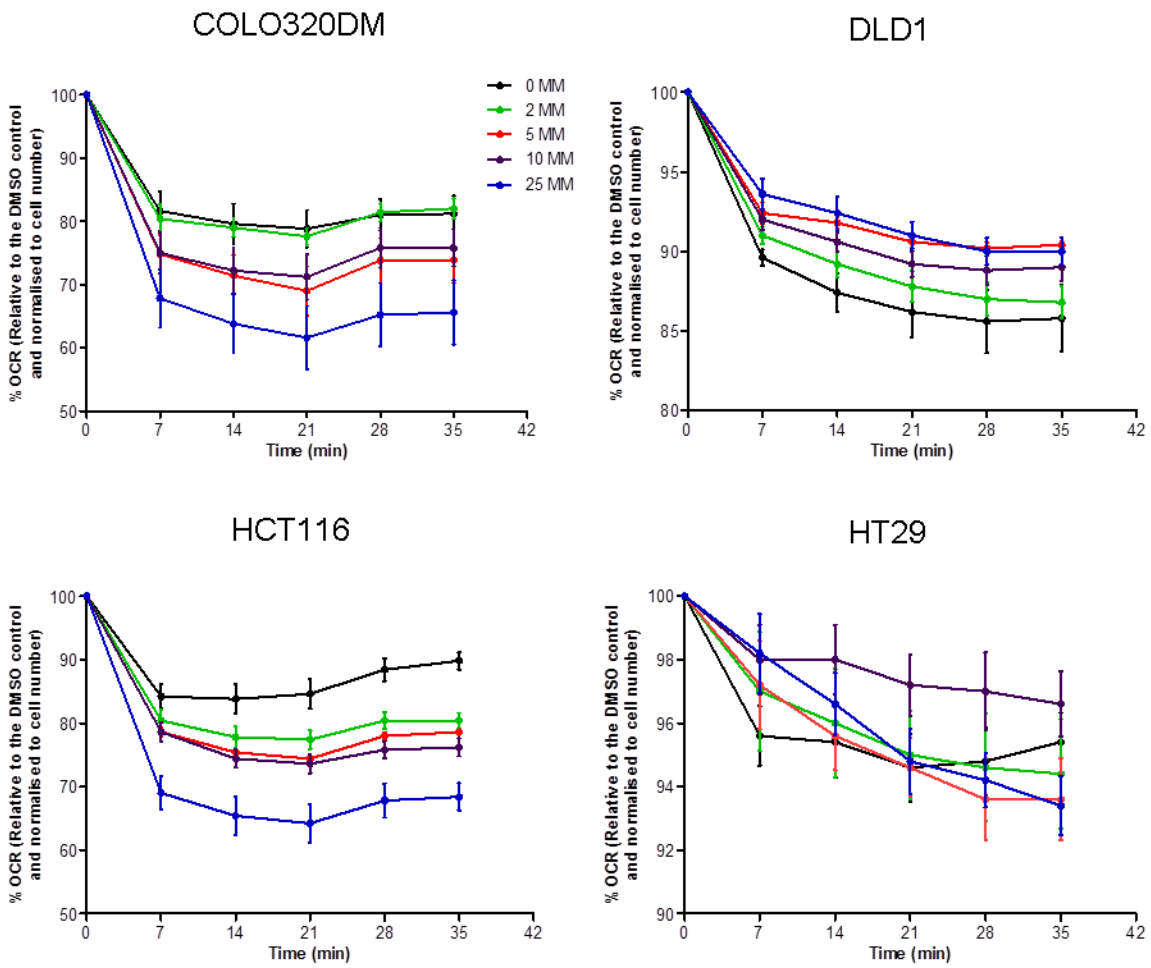

Figure 4.4. The effect of increasing glucose concentration on % OCR in COLO320DM, DLD1, HCT116 and HT29 cell lines. The % OCR generally decreases with time for all cell lines. Both COLO320DM and HCT116 cell lines share a similar profile, with increasing glucose concentrations reducing baseline % OCR whereas the DLD1 cell line sees the opposite, with a rise in % OCR. Data is representative of 3 replicates and from 3 repeat experiments. Error bars represent standard error of the mean.

4.3.4 Contribution of mitochondrial respiration to total cellular oxygen consumption rates and of glycolysis to total extracellular acidification rate in DLD1 and HCT116 cells

To assess these parameters, the basal cellular OCR and ECAR were determined initially for DLD1 and HCT116 cells, using rotenone (an inhibitor of the electron transport chain) and oxamate (an inhibitor of LDH) respectively. The cellular respiration rate was higher in the DLD1 cell line than in the HCT116 cell line (See Fig. 4.5 A). The observed ECAR of HCT116 cells was higher than that of DLD1 cells (See Fig. 4.5 B), suggesting that the former is more glycolytic than the latter. Rotenone reduced the OCR of the DLD1 and HCT116 cell lines to approximately 22% and 34% of their respective baseline rates (See Fig. 4.5 C), whilst oxamate reduced the ECAR to approximately 17% and 20% of their respective baseline rates (See Fig. 4.5 D).

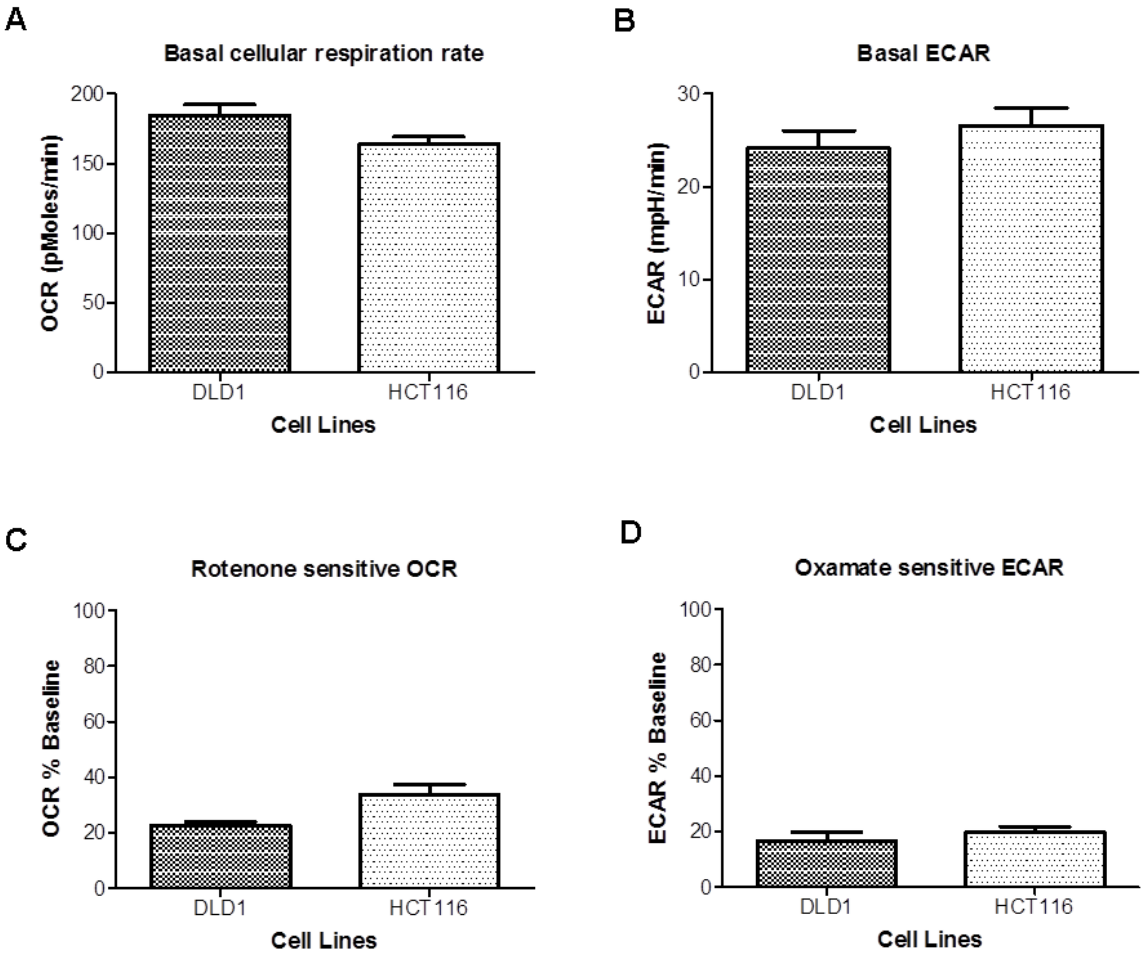

Figure 4.5. Mitochondrial respiration rate and glycolysis rate of DLD1 and HCT116 cells. A. Basal cellular respiration rate (OCR) of the two cell lines. B. Basal extracellular acidification rate (ECAR) of the two cell lines. Both rates were normalised against cell number. C. Mitochondrial respiration rate, rotenone-sensitive total respiration. D. Glycolysis rate, oxamate-sensitive total ECAR. The data is representative of at least 3 independent experiments. Error bars represent standard error of the mean.

4.3.5 Sub-cytotoxic concentrations of docetaxel and gemcitabine increase ECAR in vitro

To determine the effect of docetaxel and gemcitabine on glycolytic activity in the DLD1 and HCT116 tumour cell lines, the ECAR was measured with the XF96 Analyzer following incubation of the cell lines with two concentrations of each drug for 24 hours. The first measure was done at 4 minutes and subsequent measures every 7 minutes for a total of 6 measures. Both docetaxel and gemcitabine increased ECAR in both cell lines in a concentration-dependent fashion (See Fig. 4.6). A greater increase in ECAR was observed with gemcitabine than with docetaxel in both cell lines.

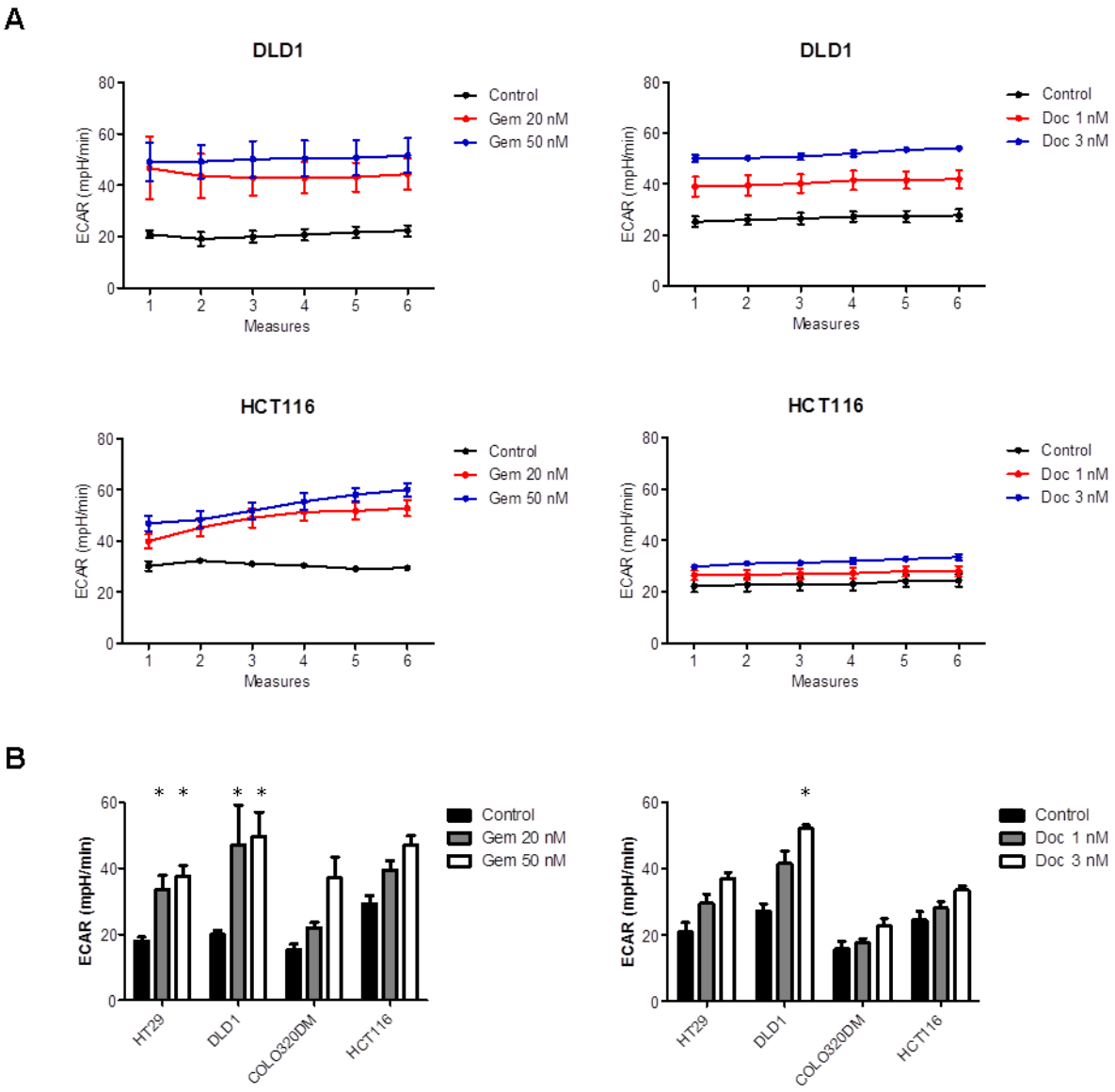

Figure 4.6. Sub-cytotoxic concentrations of docetaxel and gemcitabine increase ECAR in a panel of colorectal tumour cell lines. A. ECAR increases in DLD1 and HCT116 cell lines following treatment with different concentrations of docetaxel and gemcitabine. B. Bar charts summarising the effects on ECAR in COLO320DM, DLD1, HCT116 and HT29 cell lines following treatment with docetaxel and gemcitabine. The data is representative of at least 3 independent experiments. Error bars represent standard error of the mean. One way ANOVA was performed to assess statistical significance with Bonferroni post correction (* = $p<0.05$)

4.3.6 Stratifying agents by their effect on reducing OCR

The results from the O_2 consumption assays (See Fig. 4.3) were summarised and an arbitrary 'traffic light' scoring system was applied (See Table 4.1). Drugs and concentrations that resulted in greater than 50% reduction in OCR were highlighted green whilst those between 30 and 50% and those less than 30% were highlighted amber and red respectively. The COLO320DM and DLD1 cell lines appeared to have the greatest sensitivity to reduction in OCR whereas the MRC5 cell line the least. Etoposide and oxaliplatin had very good reduction in OCR across all cell lines. Docetaxel and gemcitabine, selected for their minimal toxicity at their investigated concentrations (See section 3.3.3), had variable results. Gemcitabine reduced OCR in all tumour cell lines but had less of an effect on COLO320DM. Docetaxel significantly reduced OCR in COLO320DM and DLD1 cell lines but had little effect on HCT116 and HT29 cell lines at the lower concentration.

Table 4.1. Stratifying reduction in OCR in COLO320DM, DLD1, HCT116, HT29 and MRC5 cell lines from tested chemotherapy agents. Agents and cell lines selected for further investigation should demonstrate the greatest balance of resistance to toxicity and reduction in OCR. Most agents had <30% reduction in OCR in the non-transformed (MRC5) cell line. Negative values represent an increase in OCR. Data represents the mean % reduction in OCR and error values are the standard error of the mean.

	DLD1	HT29	HCT116	COLO320DM	MRC5
Docetaxel 1 nM	88.41 ± 1.60	-4.13 ± 17.62	2.07 ± 8.10	92.30 ± 2.30	15.31 ± 3.04
Docetaxel 3 nM	80.25 ± 2.13	46.10 ± 11.14	69.74 ± 4.16	88.80 ± 2.87	50.47 ± 10.32
Etoposide 50 µM	59.41 ± 1.92	68.81 ± 7.13	78.15 ± 1.50	77.17 ± 2.69	81.50 ± 2.78
Etoposide 100 µM	96.90 ± 1.02	96.02 ± 1.86	98.11 ± 1.21	84.78 ± 2.37	98.00 ± 1.68
5FU 10 µM	48.77 ± 9.93	17.92 ± 9.36	29.18 ± 9.65	29.55 ± 5.92	15.31 ± 3.04
5FU 50 µM	82.88 ± 2.59	59.61 ± 3.88	79.83 ± 3.36	75.85 ± 2.50	50.47 ± 10.32
Gemcitabine 20 nM	17.41 ± 0.98	19.48 ± 1.10	23.71 ± 1.23	16.92 ± 8.84	6.45 ± 3.14
Gemcitabine 50 nM	35.81 ± 0.88	42.74 ± 1.05	45.60 ± 0.37	12.53 ± 11.70	15.79 ± 6.36
Mitomycin C 0.5 µM	10.15 ± 4.14	12.87 ± 7.49	-15.79 ± 6.71	16.86 ± 7.33	6.19 ± 2.86
Mitomycin C 1 µM	15.73 ± 4.32	18.28 ± 7.35	-16.63 ± 5.92	74.80 ± 2.23	1.06 ± 3.75
Mitoxantrone 1 nM	14.96 ± 3.39	16.84 ± 3.39	3.76 ± 5.21	79.27 ± 2.16	5.63 ± 2.50
Mitoxantrone 5 nM	36.28 ± 3.89	53.93 ± 2.93	37.59 ± 1.89	83.20 ± 2.19	6.41 ± 4.11
Oxaliplatin 0.5 µM	59.83 ± 0.732	75.00 ± 4.74	81.93 ± 1.31	83.21 ± 5.46	84.25 ± 3.09
Oxaliplatin 1 µM	82.24 ± 2.16	86.93 ± 0.24	96.43 ± 0.63	90.11 ± 0.83	100.06 ± 0.96
SN38 3 µM	83.66 ± 1.05	77.28 ± 2.10	26.08 ± 10.93	29.45 ± 4.05	11.61 ± 5.60
SN38 5 µM	93.29 ± 1.75	91.38 ± 1.21	81.72 ± 3.62	79.35 ± 2.45	12.38 ± 5.44
VX680 100 nM	28.67 ± 4.79	60.50 ± 7.52	5.296 ± 5.60	86.70 ± 3.34	17.12 ± 3.95
VX680 300 nM	52.68 ± 5.25	82.01 ± 1.86	66.66 ± 8.67	79.35 ± 2.87	59.74 ± 6.81
Vincristine 5 nM	39.88 ± 1.78	13.45 ± 3.76	13.29 ± 4.84	32.55 ± 2.07	-7.20 ± 4.51
Vincristine 20 nM	79.94 ± 0.56	28.67 ± 5.48	58.14 ± 5.07	24.76 ± 2.45	8.79 ± 1.11

% OCR Reduction >50 30-50 <30

4.4 Discussion

The results ascertained in Chapter 3 suggested that docetaxel and gemcitabine at the selected concentrations would be well tolerated by the colorectal tumour cell lines, causing minimal toxicity. Both agents are shown to reduce OCR, albeit to a variable degree dependent on both concentration and cell line.

Docetaxel is a chemotherapy agent used in the treatment of non-small-cell lung, hormone-refractory prostate, gastric, head and neck and locally advanced or metastatic breast cancer [229-233]. Although the agent has been shown to have a cytotoxic effect on colorectal cancer in clinical studies, doses required to achieve this are often associated with a debilitating side-effect profile [234]. Docetaxel significantly reduced the % OCR at both concentrations in the COLO320DM and DLD1 cell lines but only at the 3 nM concentration in the HCT116 and HT29 cell lines (See Fig. 4.1). The agent, however, remains promising for further investigation since it has a very good viability profile, particularly for the DLD1 and HCT116 cell lines.

Gemcitabine is a chemotherapy agent primarily used in the treatment of pancreatic cancer but is also an important component in the treatment of non-small-cell lung, breast and bladder cancer [229, 230, 235, 236]. Although it is not usually used in the primary treatment of colorectal cancer, the drug may have a synergistic effect with other agents, particularly anti-metabolites and has become a focus for recent clinical trials in the treatment of late-stage, chemoresistant metastatic disease as a 'salvage' therapy [237-240]. The mechanism by which gemcitabine works in this circumstance is poorly understood but it is thought that it is through the cytotoxic effect of the drug. Cham KK and colleagues suggested that low-dose gemcitabine may improve tumour hypoxia and perfusion in pancreatic tumour xenografts through an alternative mechanism [241]. This will be explored in greater detail with the colorectal xenograft experiments in Chapter 7. In the monolayer studies outlined in this chapter, gemcitabine reduced OCR in DLD1, HCT116 and HT29 cell lines at the higher concentration but

had minimal effect in the COLO320DM cell line (See Fig. 4.2). This is promising considering we can be confident that any reduction in OCR is relatively independent of cell death. As discussed in Chapter 3, COLO320DM is a cell line which is part of the all-wild-type subgroup and the minimal effect of gemcitabine on OCR may be as a consequence of that.

The majority of agents and concentrations had less of an effect on the OCR in the MRC5 cell line when compared to the tumour cell lines (See Fig. 4.3). As discussed in Chapter 1, mitochondria, oxidative phosphorylation and glycolysis are often atypical in tumour cells and this finding may suggest a tumour-specific enhancing effect on the activity of the agents in reducing OCR. Kelly CJ and colleagues demonstrated that targeting aberrant PI3K and mTOR pathways in tumour cell metabolism reduced oxygen consumption, which was not significantly seen in the non-transformed control cell line [147].

Considering tumour cells may exhibit alterations in their ability to metabolise glucose and use oxidative phosphorylation, it was important to preliminarily ascertain the phenotype of the colorectal tumour cell lines. Increasing glucose concentrations reduced the OCR of all cell lines (See Fig. 4.4). This is perhaps not unexpected as an increase in glucose substrate would drive the cells to glycolysis and consequently reduce oxidative phosphorylation and OCR. The baseline % OCR was reduced with increasing concentrations of glucose in a concentration-dependent fashion in both COLO320DM and HCT116 cell lines, suggesting a more glycolytic phenotype in these cell lines. Conversely, the DLD1 cell line had less of a reduction in OCR with increasing glucose concentrations suggesting that glycolysis would saturate and the cell line relied more on oxidative phosphorylation. These results are supported by the data in Fig. 4.5, with OCR higher in DLD1, reflecting a higher oxidative phosphorylation (See Fig. 4.5 A) and ECAR higher in HCT116, reflecting a higher glycolytic activity (See Fig. 4.5 B).

Rotenone, an inhibitor of the electron transport chain, was used to determine the contribution of mitochondrial respiration to total cellular oxygen consumption. Mitochondrial respiration, on the whole, accounts for ~90% of cellular oxygen consumption [242]. The remaining 10% is comprised of non-mitochondrial respiration and cell surface oxygen consumption [242, 243]. The rotenone-sensitive oxygen consumption rate specifically identifies mitochondrial respiration, while the rotenone-resistant rate reflects the non-mitochondrial respiration rate. The OCR of the DLD1 and HCT116 cell lines was reduced to approximately 22% and 34% of their respective baseline rates, suggesting that mitochondrial respiration accounted for 78% and 66% of their total cellular respiration, respectively (See Fig. 4.5 C). This further supports the reliance of oxidative phosphorylation in the DLD1 cell line.

To assess the contribution of lactic acid production from glycolysis to ECAR, oxamate (an inhibitor of LDH) was used. The oxamate-sensitive ECAR reflects the glycolytic rate and the oxamate-insensitive ECAR is due to non-glycolytic acidification, usually by carbon dioxide which can be converted to bicarbonate and contribute to extracellular acidification. The ECAR of the DLD1 and HCT116 cell lines was reduced to approximately 17% and 20% of their respective baseline rates after exposure to oxamate, indicating that glycolysis accounts for about 83% and 80% of their total ECAR (Fig. 4.5 D).

Fig. 4.5 C represents the uncoupled respiration of the DLD1 and HCT116 cell lines. The effects of docetaxel and gemcitabine on the electron transport chain, oxidative phosphorylation and the glycolytic pathway are investigated in detail in Chapter 6 in order to explain the reduction in OCR seen with these agents.

The COLO320DM cell line had very good overall reduction in OCR with most of the drugs and concentrations (see Fig. 4.3 and Table 4.1). This contrasts with the high sensitivity of the cell line to the same agents and suggests perhaps the reduction in the OCR seen is as a

consequence of cell death rather than through any other mechanism. This is also observed with the effect of etoposide and oxaliplatin, which demonstrated a greater than 50% reduction in OCR across all cell lines, including MRC5, yet was highly toxic from the assays seen in Chapter 3. It is likely that reduction in OCR with these agents is from reduction in cell number, despite attempting to normalise for this variable.

With both docetaxel and gemcitabine, the OCR is reduced rapidly but cell viability is not adversely affected within 24 hours (See Figs 4.1, 4.2 and Table 3.2). For the cells to survive and continue to produce ATP, ECAR inevitably increases to counteract the decrease in OCR, indicating that glycolysis is upregulated to continue the production of ATP [244]. This observation is seen with both agents in DLD1 and HCT116 (See Fig. 4.6). Both docetaxel and gemcitabine increase ECAR in both cell lines in a concentration-dependent fashion, with a greater increase seen with gemcitabine than with docetaxel. If an agent was too toxic to cells, one would expect to see a decrease in both OCR and ECAR [244, 245]. As this does not appear to be the case with either docetaxel or gemcitabine, we consider that neither agent at these doses has a considerably toxic effect on the cell lines. Furthermore, the rapid drop in OCR seen with both agents suggests an immediate effect on oxidative phosphorylation and the electron transport chain. This possibility is explored further and discussed in Chapter 6.

Evaluating the results from Chapter 3 and 4, the DLD1 and HCT116 cell lines appear to have a good balance of resistance to toxicity and reduction in OCR to docetaxel and gemcitabine. Both cell lines are also well known to form spheroids *in vitro* and subcutaneous tumours *in vivo* [246-249]. It was therefore concluded that further investigation would be with these agents, concentrations and cell lines.

CHAPTER 5: SUB-CYTOTOXIC CONCENTRATIONS OF DOCETAXEL AND GEMCITABINE REDUCE HYPOXIA IN 3-DIMENSIONAL *IN VITRO* MODELS

5.1 Aims

1. To investigate whether docetaxel and gemcitabine can reduce hypoxia in spheroid models of DLD1 and HCT116 cell lines.
2. To demonstrate that any reduction in hypoxia in spheroid models of DLD1 and HCT116 cell lines occurs independently of cell death.

5.2 Introduction

5.2.1 Using spheroids as a model for investigating core hypoxia

Investigating the relationships between tumour growth, the development of hypoxia and alterations in metabolism requires an appropriate experimental model. Conventional *in vitro* monolayer studies, as demonstrated in Chapter 4, provide a good platform for initial studies but can be physiologically unrealistic. Monolayers are widely used to study the effects of hypoxia on proliferation and metabolism, by being able to manipulate the atmospheric oxygen concentration [250, 251]. However, it is difficult to form physiologically relevant gradients in oxygen in a two-dimensional (2D) environment. First identified by Sutherland and colleagues, the spheroid model offers a unique experimental bridge between conventional 2D monolayer cultures and *in vivo* models such as xenografts, the results of which will be discussed in Chapter 7 [252]. Spheroids are three-dimensional (3D) aggregates of tumour cells that are cultured *in vitro*. Although more challenging to initiate than monolayer cultures, spheroids reproduce crucial tumour characteristics, such as proliferative patterns and histological organisation. They also share signalling and metabolic profiles that are more similar to *in vivo* cells than those in monolayer [253]. Furthermore, in contrast to xenograft models, the effects of agents on diffusion-limited hypoxia can be studied without the need to isolate and separate the potential effects of a heterogeneous vascular network [254].

As discussed in Chapter 1, diffusion-limited hypoxia is one of two principal causes of hypoxia within tumours. Spheroids can offer a unique insight into the potential mechanisms involved in this process. As a spheroid develops, proliferating cells located in its inner region typically become hypoxic. The diffusion of oxygen, glucose and other nutrients restricts spheroid growth, which consequently leads to the development of a necrotic inner core. The potential benefit of using spheroids over monolayers as an *in vitro* model in this instance therefore, is that the artificial maintenance of different oxygen tensions is not necessary. This

leads to reproducible and well defined regions of central hypoxia and necrosis. A major limitation of monolayer studies is that all cells are equally exposed to oxygen and other nutrients, which is a physiologically unrealistic model for tumour hypoxia. Additionally, the microenvironment surrounding cells can significantly influence intracellular signalling so that cells may be more radioresistant in 3D than in 2D systems. This is further explored in Chapter 8. There is also evidence that spheroids have significantly fewer EGF receptors, necessary for mitosis, than corresponding monolayers [255]. This lower density, which is not associated with a lower cell proliferation rate, suggests a more efficient EGF autocrine loop in spheroids than in monolayer cultures. Therefore, 2D models on their own are perhaps inappropriate to study the effect of agents on tumour proliferation.

Spheroid culture also allows for a controlled environment, which can be easily manipulated, tested and repeated. This is particularly a challenge in *in vivo* xenografts, as controlling the number of variables in the experimental process can be very difficult and repeat experiments may not be comparable. Therefore, spheroids offer an alternative and intermediate model for tumour hypoxia studies between 2D culture and 3D *in vivo* xenografts. It is through this niche, that spheroids have become widely used as a model for tumour proliferation, hypoxia and metabolism and for the testing of novel chemotherapy and radiotherapy regimes [147, 253, 256-259].

5.2.2 Mathematical modelling and calculating OCR

As addressed earlier, spheroid models allow investigation of diffusion-limited hypoxia and mathematical modelling provides a relatively accurate way to determine OCR in the 3D setting. With use of oxygen-sensitive markers, such as EF5, hypoxia can be identified in both clinical and preclinical models, such as in spheroids and *in vivo* xenografts, without damaging the cells [260, 261]. Conger and colleagues demonstrated that spheroids generally grew exponentially and then approximately linearly, achieving a roughly constant viable rim thickness [262]. From this

work, various researchers determined several mathematical models of oxygen distribution that considers the oxygen gradient subject to various boundary conditions [263, 264]. Using these principles, Grimes and colleagues described an analytical model which investigates oxygenation through a spheroid and explicitly predicts the consumption rate for a given spheroid, including a prediction of the extent of the hypoxic, necrotic and proliferating regions (See Fig. 5.1) [265]. This model was applied to the spheroid experiments outlined in this chapter.

A

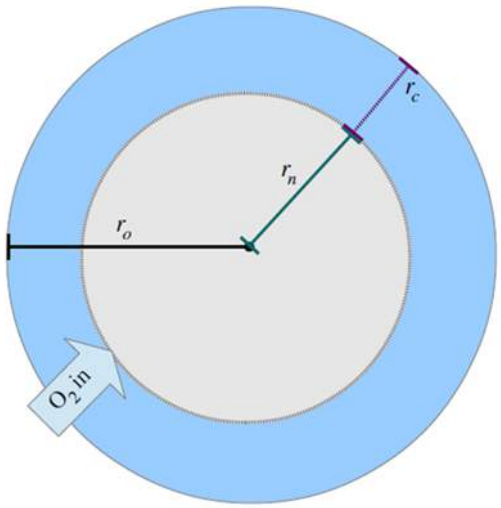

B

$$p(r) = p_o + \frac{a\Omega}{6D}\left(r^2 - r_o^2 + 2r_n^3\left(\frac{1}{r} - \frac{1}{r_o}\right)\right)$$

Figure 5.1. Calculating OCR in spheroids using mathematical modelling. A. Cross section of tumour spheroid of radius r_0. Oxygen partial pressure is non-zero in the region r_c. This region comprises all viable cells both hypoxic and oxic. Oxygen cannot penetrate into region r_n, which is anoxic. B. Formula for calculating OCR in spheroids, the full derivation for which can be found in the paper.

5.3 Results

5.3.1 Optimising immunohistochemistry and identifying region of interest of spheroid sections for hypoxia imaging

In order to image the effects of docetaxel and gemcitabine on hypoxia, spheroids were cultured as described in section 2.5 and incubated with the hypoxia marker EF5 for 4 hours prior to fixation and sectioning. Spheroids were sectioned through the region of interest to ensure specimens representative of core hypoxia (See Fig. 5.2 A). Spheroids of similar size were selected using brightfield microscopy and their approximate diameters were calculated, from which D could be determined and guide sectioning. Sectioned spheroids were treated to a highly optimised staining process, as outlined in section 2.7, with a non-specific nuclear stain (Hoechst 33342), a proliferation marker (Ki-67) and a hypoxia marker (EF5) (See Fig. 5.2 C). Tile images from confocal microscopy gave an overview of all spheroids on each slide (See Fig. 5.2 B).

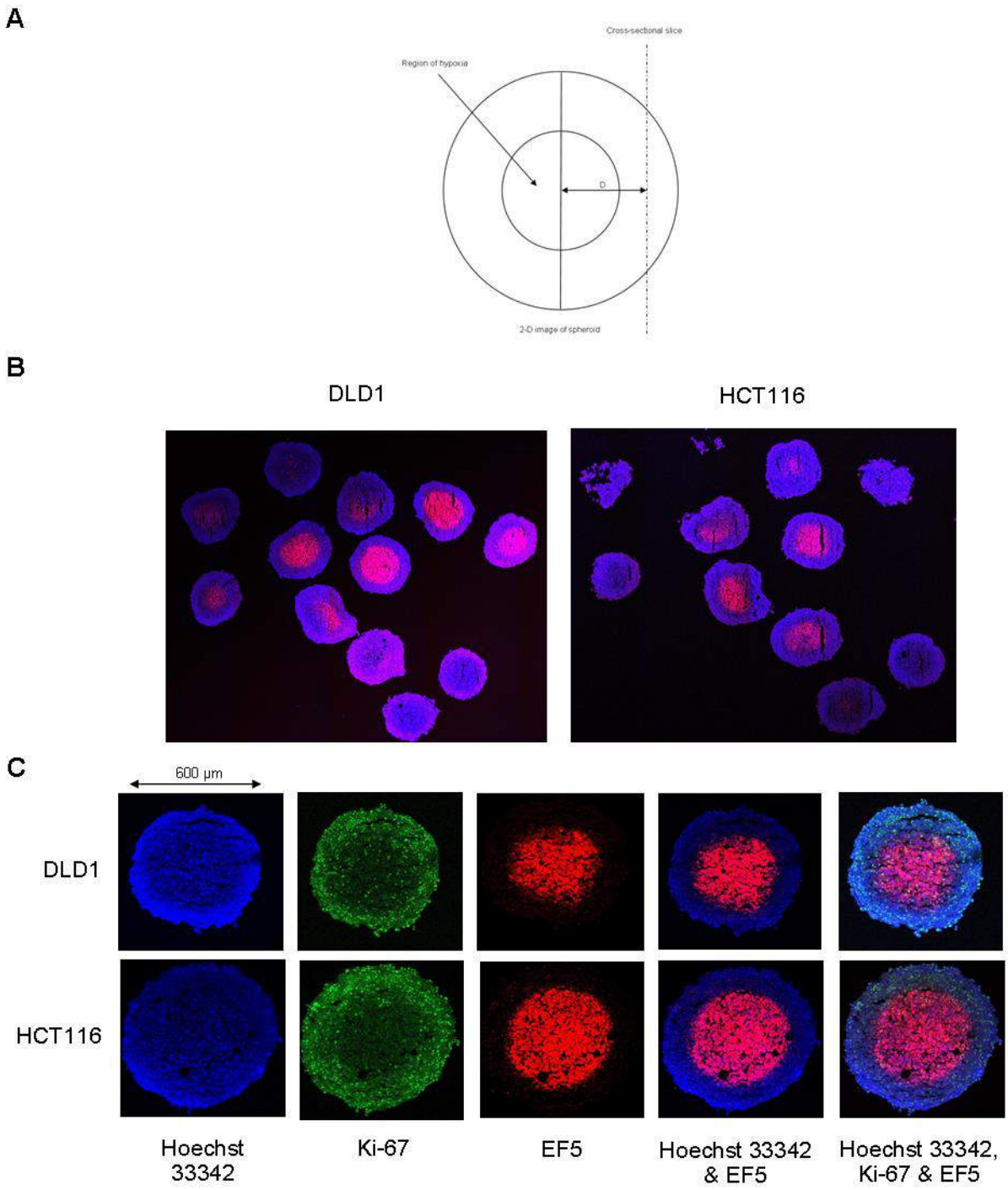

Figure 5.2. Immunohistochemistry of untreated DLD1 and HCT116 spheroids. A. Schematic demonstrating selection of cross-sections analysed where D (distance from centre of spheroid to the cross-section) more than 30% is excluded. B. Representative tile image taken with confocal microscopy of several spheroids sectioned within region of interest. C. DLD1 and HCT116 spheroids stained for cell nuclei (Hoechst 33342, blue), proliferation (Ki-67-FITC, green) and hypoxia (EF5-Cy3, red) with composite images.

5.3.2 Sub-cytotoxic concentrations of docetaxel and gemcitabine reduce spheroid hypoxia

To determine the effect of docetaxel and gemcitabine on hypoxia in DLD1 and HCT116 spheroids; spheroids were treated with each agent and concentration for a 24 hour period, which was inclusive of the 4 hour EF5 incubation period. Spheroids were then fixed, sectioned and stained for hypoxia imaging. Both docetaxel and gemcitabine significantly reduce or eradicate hypoxia (See Figs. 5.3 and 5.4). EF5 staining and thus hypoxia, was not visible in either the DLD1 or HCT116 spheroids treated with docetaxel or gemcitabine at the 3 nM and 50 nM concentrations respectively. However, following removal of the agents and allowing a 24 hour period of recovery in drug-free medium, hypoxia returns (See Figs. 5.3 C and 5.4 C). Quantification of OCR within the spheroids was determined as discussed in section 5.2.2, demonstrating a significant reduction in OCR with treatment as compared to the control spheroids (See Figs. 5.3 B and 5.4 B).

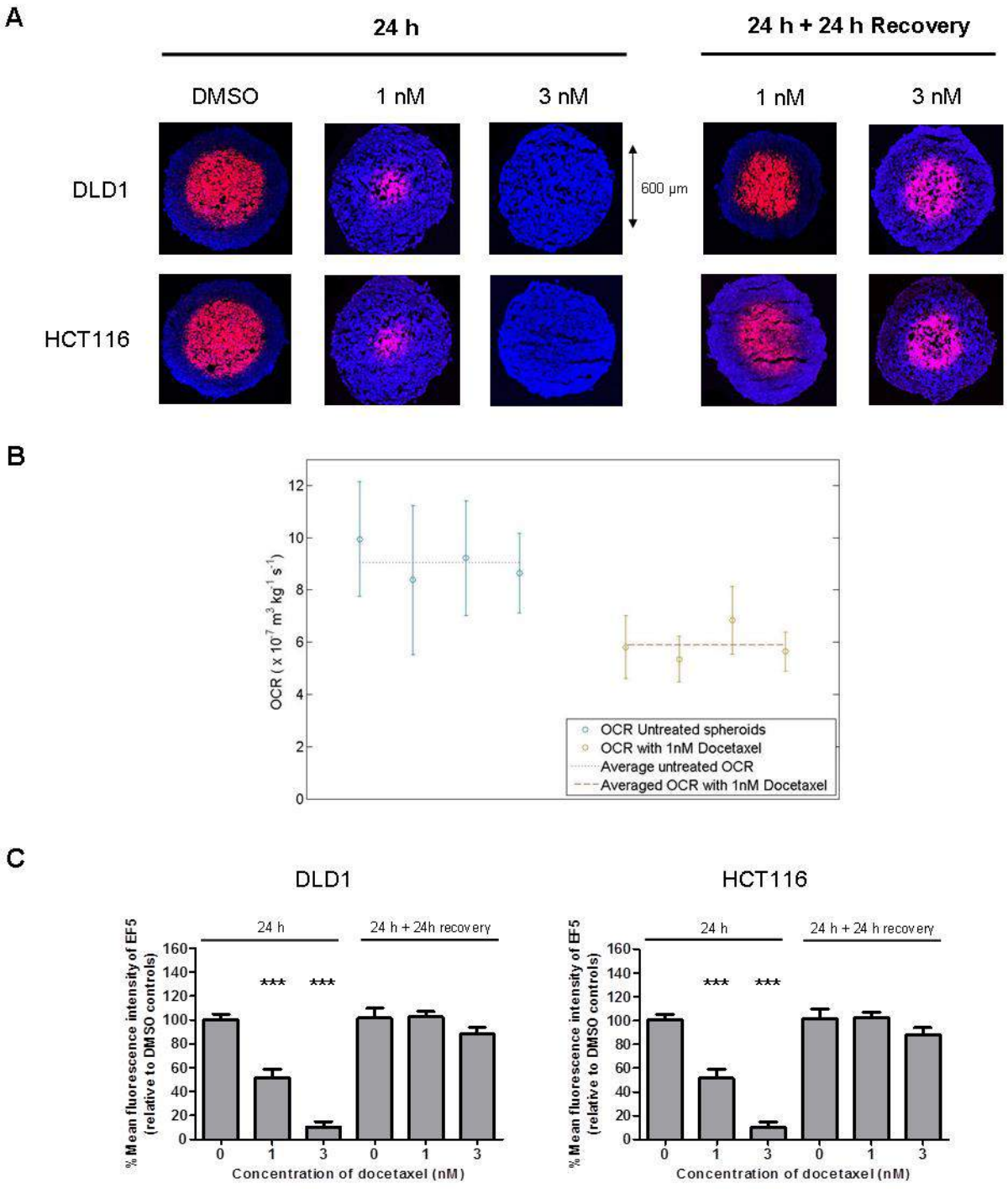

Figure 5.3. Sub-cytotoxic concentrations of docetaxel reduce spheroid hypoxia.

DLD1 and HCT116 spheroids were treated with DMSO or docetaxel either for 24 hours or for 24 hours followed by recovery for 24 hours in drug-free medium, as indicated. A. Hypoxia was assessed by staining central spheroid sections for EF5 (red), with Hoechst as a counterstain (blue). B. Mathematical modelling of the OCR in HCT116 spheroids treated with 1 nM docetaxel. C. Mean fluorescence intensity of treated, untreated and recovered spheroids. The data is representative of 3 independent experiments. Hypoxia was assessed in at least 8 spheroids per treatment per experiment. Values represent mean and SEM. One way ANOVA was performed to assess statistical significance with Bonferroni post correction (*** = $p<0.001$).

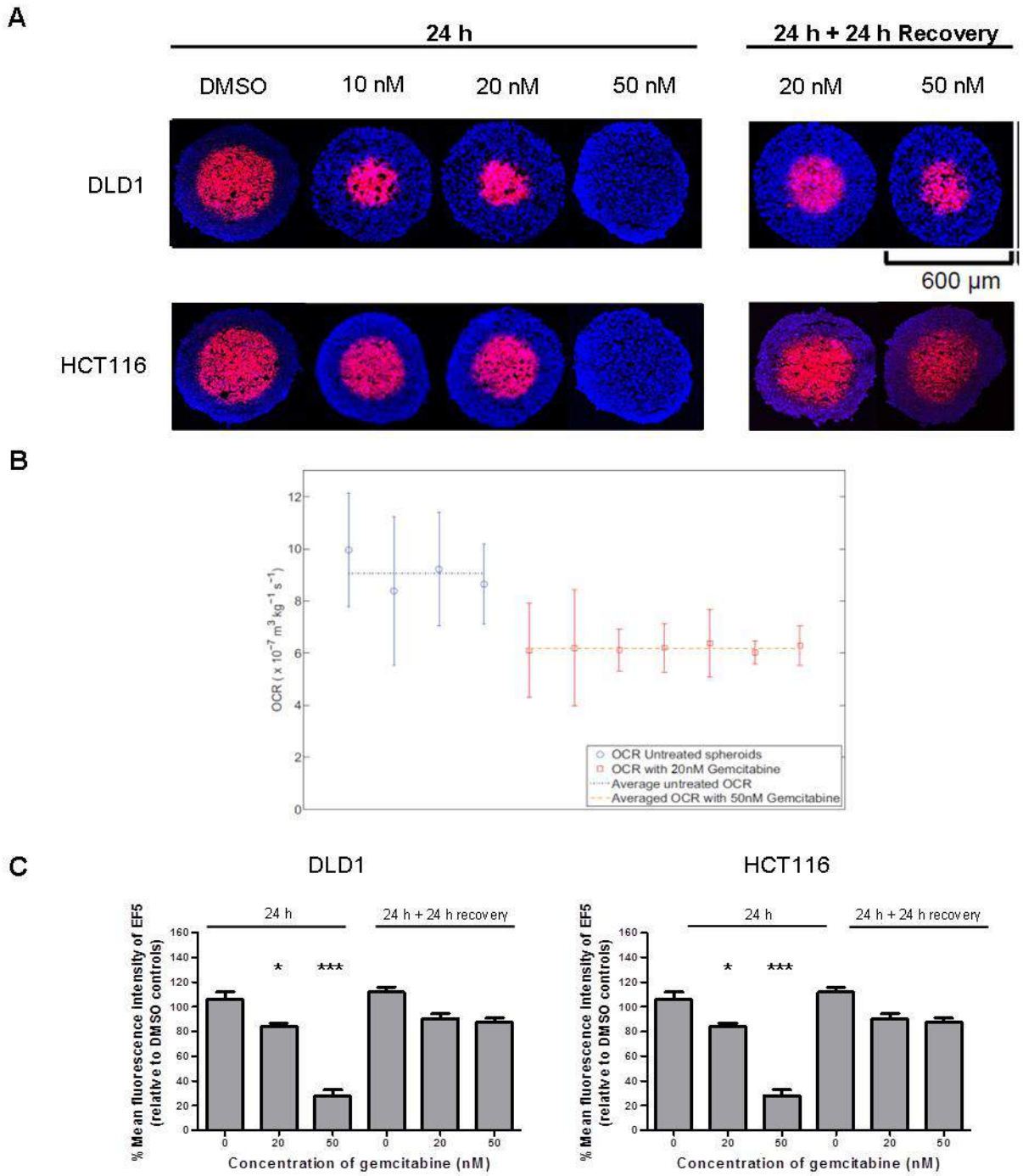

Figure 5.4. Sub-cytotoxic concentrations of gemcitabine reduce spheroid hypoxia.

DLD1 and HCT116 spheroids were treated with DMSO or gemcitabine either for 24 hours or for 24 hours followed by recovery for 24 hours in drug-free medium, as indicated. A. Hypoxia was assessed by staining central spheroid sections for EF5 (red), with Hoechst as a counterstain (blue). B. Mathematical modelling of the OCR in HCT116 spheroids treated with 20 nM gemcitabine. C. Mean fluorescence intensity of treated, untreated and recovered spheroids. The data is representative of 3 independent experiments. Hypoxia was assessed in at least 8 spheroids per treatment per experiment. Values represent mean and SEM. One way ANOVA was performed to assess statistical significance with Bonferroni post correction (* = $p<0.05$, *** = $p<0.001$).

5.3.3 Sub-cytotoxic concentrations of docetaxel and gemcitabine do not affect spheroid diameter

As an indirect indicator of cell death, untreated and treated (following 24 hours incubation with agent) DLD1 and HCT116 spheroids were imaged with brightfield microscopy and their diameters measured and compared (See Figs. 5.5 A and 5.6 A). For both DLD1 and HCT116 spheroids, there was no statistical difference in the average spheroid diameter between untreated and treated groups for either docetaxel or gemcitabine (See Figs 5.5 B and 5.6 B).

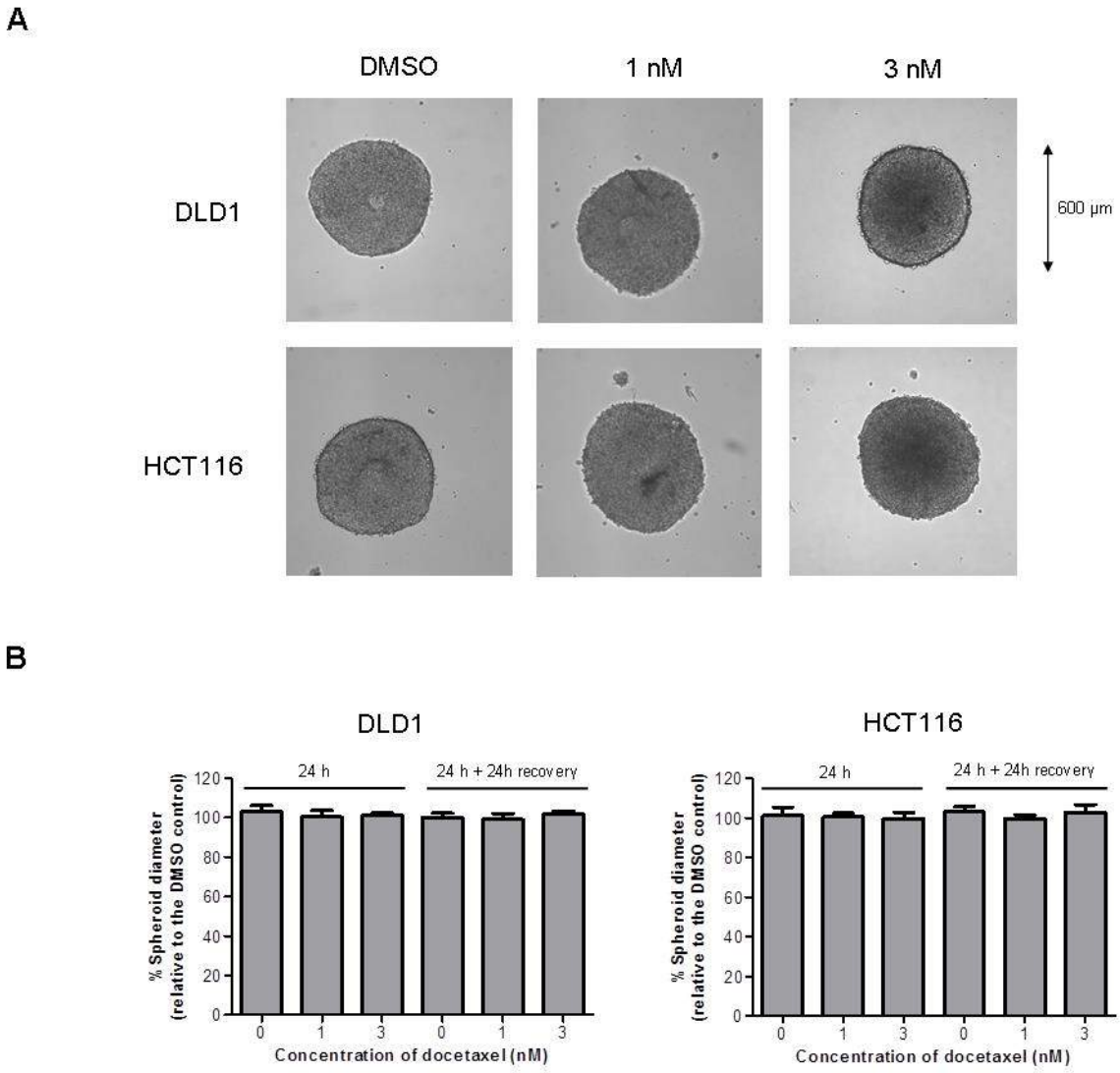

Figure 5.5. Sub-cytotoxic concentrations of docetaxel do not affect the spheroid diameter. A. Brightfield microscopy of representative DLD1 and HCT116 spheroids before and after treatment with different concentrations of docetaxel. B. The average spheroid diameter derived from measurements of spheroid cross-sectional area made prior to sectioning. The measurements are normalised to the DMSO treated spheroids. The data is representative of at least 3 independent experiments. One way ANOVA was performed to assess statistical significance with Bonferroni post correction.

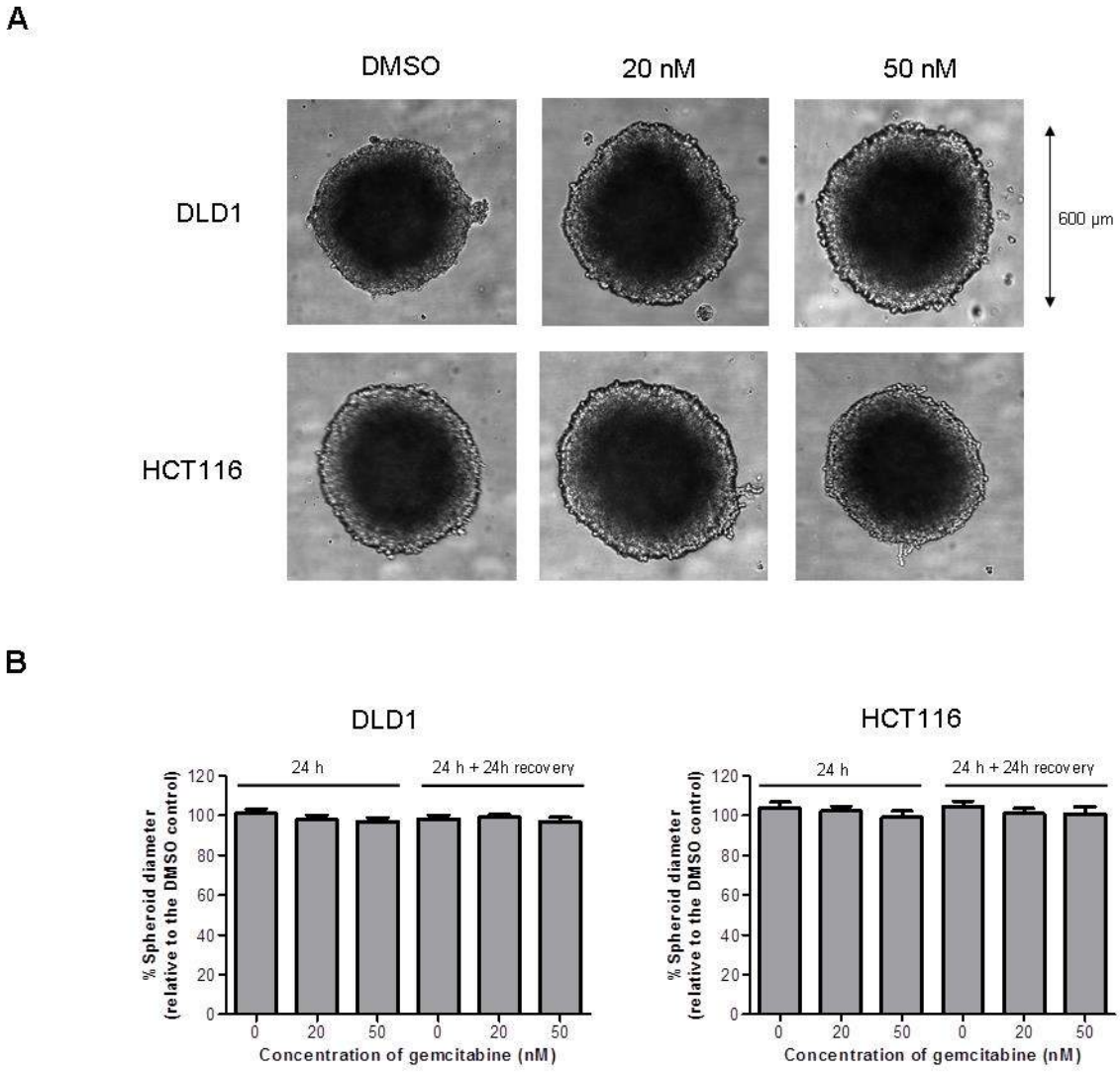

Figure 5.6. Sub-cytotoxic concentrations of gemcitabine do not affect the spheroid diameter. A. Brightfield microscopy of representative DLD1 and HCT116 spheroids before and after treatment with different concentrations of gemcitabine. B. The average spheroid diameter derived from measurements of spheroid cross-sectional area made prior to sectioning. The measurements are normalised to the DMSO treated spheroids. The data is representative of at least 3 independent experiments. One way ANOVA was performed to assess statistical significance with Bonferroni post correction.

5.3.4 Sub-cytotoxic concentrations of docetaxel and gemcitabine reduce the proportion of proliferating cells in spheroids

To determine the effects of sub-cytotoxic concentrations of docetaxel and gemcitabine on the proliferative capacity of DLD1 and HCT116 spheroids, spheroid sections were immunofluorescently stained for Ki-67 (See Fig. 5.2 C). With use of ImageJ (version 1.47) software, the proportion of pixels which were Ki-67 positive were determined and labelled as proliferating. Pixels which were Hoechst 33342-positive but Ki-67 negative were labelled as non-proliferating and an overall percentage of proliferating cells was calculated. Both agents reduced the proportion of proliferating cells in a concentration-dependent manner when compared to untreated spheroids and in both cell lines (See Fig. 5.7).

A

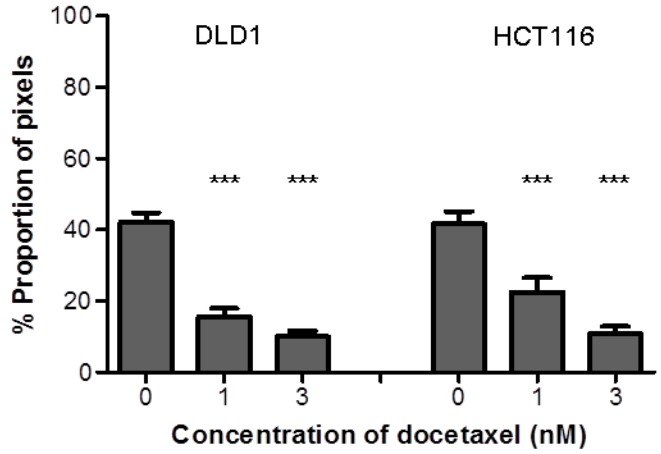

B

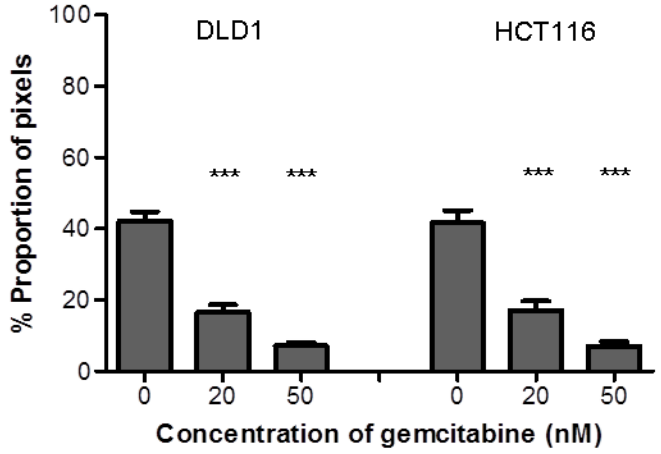

Figure 5.7. Sub-cytotoxic concentrations of docetaxel and gemcitabine reduce proliferation in spheroids. A. Percentage of proliferating cells in DLD1 and HCT116 spheroids treated with docetaxel. B. Percentage of proliferating cells in DLD1 and HCT116 spheroids treated with gemcitabine. Proliferation was assessed in at least 8 spheroids per treatment for each cell line. Data points represent mean of spheroids and SEM. One way ANOVA was performed to assess statistical significance with Bonferroni post correction (*** = $p<0.001$).

5.3.5 Improvement in spheroid hypoxia appears to be independent of drug-induced apoptosis

To determine whether any drug-induced apoptosis could be responsible for the improvement in spheroid hypoxia, the proportion of cells in the sub-G_1 peak on flow cytometric analysis of cells from the spheroids were quantified and compared (See Fig. 5.8 A). Following treatment for 24 hours with either docetaxel or gemcitabine, spheroids were mechanically disaggregated into single cells, fixed in ethanol and treated with propidium iodide and ribonuclease for flow cytometric analysis. The percentage of apoptotic cells between treated and untreated spheroids for both agents and cell lines remained relatively constant and did not reach statistical significance (See Fig. 5.8 B and C).

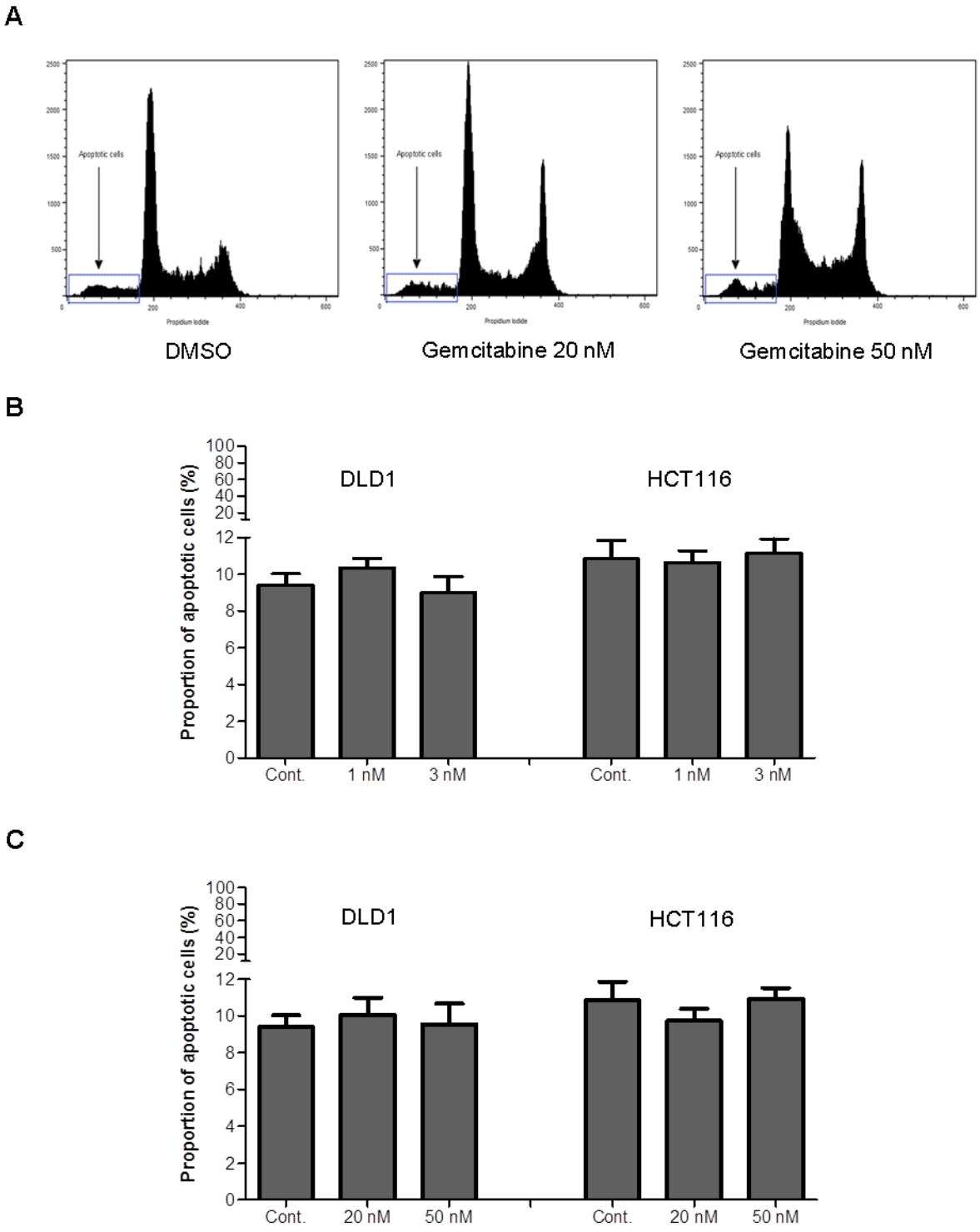

Figure 5.8. Populations of apoptotic cells in spheroids are unchanged between control and docetaxel and gemcitabine treated spheroids. A. Histograms of disaggregated DLD1 spheroids demonstrating little difference in the apoptotic population in the sub-G_1 region. B. Proportion of apoptotic cells in DLD1 and HCT116 spheroids treated with docetaxel. C. Proportion of apoptotic cells in DLD1 and HCT116 spheroids treated with gemcitabine. Apoptosis was assessed in at least 8 spheroids per treatment per cell line. Data points represent mean and SEM. One way ANOVA was performed to assess statistical significance with Bonferroni post correction (no significance).

5.4 Discussion

The results outlined in this chapter reaffirm many of the findings discussed in chapters 3 and 4. Spheroids are an excellent bridge between monolayer and *in vivo* experiments for studying hypoxia and also provide a platform for investigating diffusion-limited hypoxia.

To accurately evaluate any improvements in hypoxia within spheroids, it was essential that immunofluorescence staining was optimised, reproducible and robust. EF5 is a highly specific nitroimidazole developed at the University of Pennsylvania by Dr. Cameron Koch and Dr. Sydney Evans and has become a widely used marker of hypoxia. As a bioreductive dye, EF5 covalently binds all viable hypoxic cells at a rate that is inversely proportional to tissue oxygen level [266, 267]. EF5 binding to hypoxic cells has since been vigorously studied and is now currently used to detect hypoxia in solid tumours in clinical settings [268, 269]. Ki-67 human nuclear antigen is a classical histopathological marker of cell proliferation which is expressed in proliferating cells but not in quiescent cells [270-272]. Ki-67 expression appears to be restricted to late G_1, S, G_2 and M phases and is absent in the quiescent, G_0 phase [272]. Furthermore, increased expression of Ki-67 is related to poor long-term survival and death [273]. Finally, Hoechst 33342, a bisbenzamide dye, was used to stain DNA. Hoechst non-specifically binds to nucleic acids but DNA strands rich in adenine and thymine increase its fluorescence [274]. Within spheroids, the rate of uptake of Hoechst is independent of cell type and distribution is uniform throughout the cross-section, being dependent only on stain delivery [275]. The results of the staining process were successful in delineating the different features of the spheroids and allowed for further investigation to proceed. Clear boundaries of peripheral proliferation and central hypoxia were easily identified and alongside Hoechst staining, allowed for effective quantitative analysis (See Fig. 5.2).

Reducing OCR with docetaxel and gemcitabine improved spheroid hypoxia (See Figs. 5.3 and 5.4). Reduction in OCR was confirmed through mathematical modelling, as discussed in

section 5.2.2 and in keeping with the findings identified in Chapter 4. Several researchers have demonstrated that reducing OCR, whether chemically or otherwise, can improve spheroid or tumour hypoxia and the results identified here are supportive of this [276, 277]. Indeed, it was through the discovery of the role of metformin in reducing OCR and improving tumour hypoxia, that this relatively niche area has now garnered much attention [277].

To confirm that both docetaxel and gemcitabine caused minimal cell death within the spheroids and that apoptosis was not the explanation for improvement in hypoxia, both average spheroid diameter and population of apoptotic cells were assessed (See Figs. 5.5, 5.6 and 5.8). The average diameter of spheroids did not statistically differ between untreated and treated spheroids (See Figs. 5.5 B and 5.6 B), with no visible difference in size or viability measured on brightfield microscopy (See Figs. 5.5 A and 5.6 A). Furthermore, the population of apoptotic cells within untreated and treated spheroids did not change between the groups (See Fig. 5.8). Disaggregated spheroids are fixed, washed with phosphate-citrate buffer and treated with propidium iodide. This results in the extraction of low molecular weight DNA from apoptotic cells, appearing to the left of the normal G_1 peak. Although the technique is quick and relatively easy, it is not a very specific method of detecting apoptosis as cells in late S phase or from G_2 may be missed. It does, however, give a broad overview to what exactly is happening in a population of cells and is particularly useful for studies over a time course.

Spheroids are composed of cells with differing proliferative status which results in a cellular heterogeneity that closely mimics the multiple cell phenotypes found *in vivo*. Several studies in xenograft models from human cancer lines have shown that the populations of proliferating and hypoxic cells can be distinct [278]. However, other experiments have confirmed that hypoxia and proliferation can overlap [279, 280]. This was elegantly demonstrated by Ljungkvist and colleagues in xenograft models of human HNSCC, who showed that there was a significant number of proliferating cells present in the hypoxic region, although

this was reduced when compared to the normoxic region [281]. This also appears to be the case with the spheroid results here, with most of Ki-67 staining present primarily on the periphery and minimal amount within the core hypoxic region (See Fig. 5.2 C). This staining pattern was not unexpected considering that as a spheroid grows, proliferating cells located in the inner region naturally become hypoxic and undergo cell arrest or apoptosis. This was further illustrated by Takagi and colleagues who showed a decrease in proliferation from the spheroid periphery to the inner core in human prostate tumour cells, which was directly related to the level of hypoxia present [282]. Figure 5.7 show that both docetaxel and gemcitabine reduce the proportion of proliferating cells in the spheroid as a whole in a concentration-dependent manner. This is perhaps to be expected considering that both docetaxel and gemcitabine are known to have cell cycle inhibitory effects and is principally the mechanism by which the agents exert cytotoxicity. However, as discussed earlier, neither drug had an effect on the population of apoptotic cells, suggesting that the tested concentrations inhibit proliferation but do not trigger the apoptotic pathways that lead to cell death. These concentrations may leave the cells in a state of senescence although this was not experimentally confirmed. Furthermore, whilst the literature points to an inverse relationship between hypoxia and proliferation in spheroids, some studies have shown that a limited exposure to hypoxia may not affect cell proliferation at all, whereas prolonged exposure to chronic hypoxia can decrease cell proliferation and induce cell death [283]. With this in mind, any improvement in hypoxia may theoretically move cells from a state of quiescence to that of proliferation and this should be evident with a potential increase in Ki-67 positive cells within the core of a spheroid. Unfortunately, this was not observed in these results but this may be explained through the limited opportunity to do so within the 24 hour period of treatment or through the conflicting anti-proliferative effects of the agents themselves. On the other hand, the movement of cells from a proliferative to a quiescent state, which has a lower OCR comparatively, may be a potential explanation for the improvement in hypoxia seen in the spheroids. The specific effects of the drugs on the G_1, S and

G_2 cell populations and their potential relationship with reducing oxygen consumption will be discussed in the next chapter.

CHAPTER 6: DOCETAXEL AND GEMCITABINE IMPROVE HYPOXIA BY ALTERING OXIDATIVE PHOSPHORYLATION

6.1 Aims

1. To determine possible mechanisms of action of docetaxel and gemcitabine in reducing OCR and improving hypoxia.
2. To confirm any determined mechanisms of action with different experimental techniques.

6.2 Introduction

6.2.1 The known mechanisms of action of docetaxel and gemcitabine

As discussed in Chapters 1 and 3, both docetaxel and gemcitabine are broadly classed as cytotoxic chemotherapeutic agents which take advantage of the rapidly dividing state of tumour cells to initiate cell death but are usually non-specific, resulting in a high side-effect profile. Separately, they have different mechanisms of action.

Docetaxel is a plant-derived anti-microtubule agent shown to exhibit cytotoxic activity on a variety of different tumours, including melanoma, breast, colorectal, lung, ovarian, gastric, renal and prostate [44, 284]. Microtubules are an important component of the cytoskeleton within cells. They are essential in maintaining the structure of the cell and are in a constant state of assembly and disassembly [43]. Docetaxel binds specifically, reversibly and with high affinity to β-tubulin at a maximum stoichiometry of 1 mole docetaxel per mole tubulin in microtubules [285]. This binding stabilises microtubules and prevents microtubule disassembly, leading to a gradual and considerable loss of free tubulin, necessary for microtubule formation [286]. Consequently, tumour cells are blocked from completing mitosis and enter cell cycle arrest and apoptosis [35, 286]. It is through this principle mechanism that the cytotoxic effect of docetaxel is exerted. However, docetaxel does not prevent disassembly of microtubules in interphase and therefore does not prevent entry into the cell cycle but blocks mitosis by inhibiting the mitotic spindle assembly. Additionally, apoptosis is also further encouraged by the action of docetaxel on inhibiting the apoptosis-blocking oncoprotein, bcl-2 [285].

Gemcitabine is a deoxynucleoside analogue and part of the anti-metabolite sub-group of cytotoxic agents, which are a group of agents that disrupt DNA and RNA synthesis. The drug is commonly used in the treatment of breast, non-small cell lung, bladder and pancreatic cancer. Gemcitabine is specifically a deoxycytidine analogue and is metabolised intracellularly to two

active metabolites, gemcitabine diphosphate (dFdCDP) and gemcitabine triphosphate (dFdCTP). Cytotoxicity is exerted through incorporation of dFdCTP into DNA with the assistance of dFdCDP, resulting in inhibition of DNA synthesis and induction of apoptosis [35, 39]. By impeding DNA synthesis, the drug prevents mitosis. It also incorporates into DNA, resulting in double-strand DNA breakage and cell death. Gemcitabine typically causes S phase arrest in the cell cycle. Consequently, the efficacy of the drug can reach a therapeutic limit, after which cell death no longer occurs with increased doses [35]. Another target of gemcitabine is the enzyme ribonucleotide reductase (RNR), which catalyses the formation of deoxyribonucleotides from ribonucleotides, used in the synthesis of DNA [287]. The dFdCDP analogue binds to the RNR active site and irreversibly inactivates the enzyme. Once inhibited, the cell cannot produce the deoxyribonucleotides necessary for DNA replication and apoptosis is induced [288]. Additionally, RNR is essential in regulating the DNA synthesis rate so that the ratio of DNA to cell mass is constant during mitosis and DNA repair [289].

6.2.2 The influence of docetaxel and gemcitabine in and on hypoxia

There is great variability in both the efficacy and activity of docetaxel and gemcitabine on hypoxia across different cell lines and tumours [176]. Their actions on hypoxia, however, have not been thoroughly elucidated. Several studies have shown that the cytotoxic effects of gemcitabine appear to be reduced in the presence of hypoxia, particularly in testicular germ cell, breast, prostatic, hepatic and pancreatic tumour cell lines [183, 186, 187]. The activity of docetaxel, on the contrary, appears unchanged in prostate and ovarian tumour cell lines and preserves its tumour cell-killing activity even at lowest concentrations against EGFR-overexpressing carcinoma cells [178, 181, 182, 290, 291]. However, Strese and colleagues demonstrated that docetaxel was associated with increased drug resistance in a panel of varied tumour cell lines in anoxic and hypoxic conditions [176]. Cham and colleagues demonstrated that metronomic gemcitabine could improve tumour hypoxia in xenograft models and reduce tumour volume but the mechanisms for these observations were not discussed in their study

[241]. A number of studies have also used gemcitabine as an adjunct treatment alongside agents that become active in the hypoxia environment such as the hypoxia-activated prodrug TH-302 or agents targeting HIF-1α, such as PX-478 or si-HIF1α and have shown a synergistic effect [292-294]. However, most of these studies have principally been in pancreatic tumour models, as opposed to the colorectal tumour cell lines investigated here. Docetaxel has been shown to have an inhibitory effect in some studies and no effect in others on HIF-1α expression in ovarian and breast tumour cell lines [180, 181].

These conflicting results in the literature show that impaired chemosensitivity in hypoxia is not universal. Indeed, chemotherapy agents have varying efficacies in different cell lines and some agents appear even less effective in normoxia [176, 291]. Chapters 4 and 5 have shown that both docetaxel and gemcitabine lower OCR and improve hypoxia in DLD1 and HCT116 cell lines and the mechanisms by which this is achieved will be explored in this chapter.

6.3 Results

6.3.1 Sub-cytotoxic concentrations of docetaxel and gemcitabine induce G_2/M and S phase arrest respectively

To determine the effect of docetaxel and gemcitabine on cell division, control- and drug-treated DLD1 and HCT116 spheroids were disaggregated into single cells, fixed in ethanol and treated with propidium iodide and ribonuclease for flow cytometric analysis. Docetaxel induced G_2/M arrest in cells from both DLD1 and HCT116 spheroids (See Fig. 6.1). This effects was evidenced by a rise in the G_2 peak with increasing concentration of docetaxel (See Fig. 6.1 A) and by an increase in the proportion of cells in G_2/M in both cell lines (See Fig. 6.1 B). Gemcitabine induced S phase arrest in cells from both DLD1 and HCT116 spheroids (See Fig. 6.2). This effect was evidenced by a change in the distribution of S phase on the histograms with increasing concentration of gemcitabine (See Fig. 6.2 A) and by an increase in the proportion of cells in S phase in both cell lines (See Fig. 6.2 B). Both agents reduced the proportion of cells in G_1.

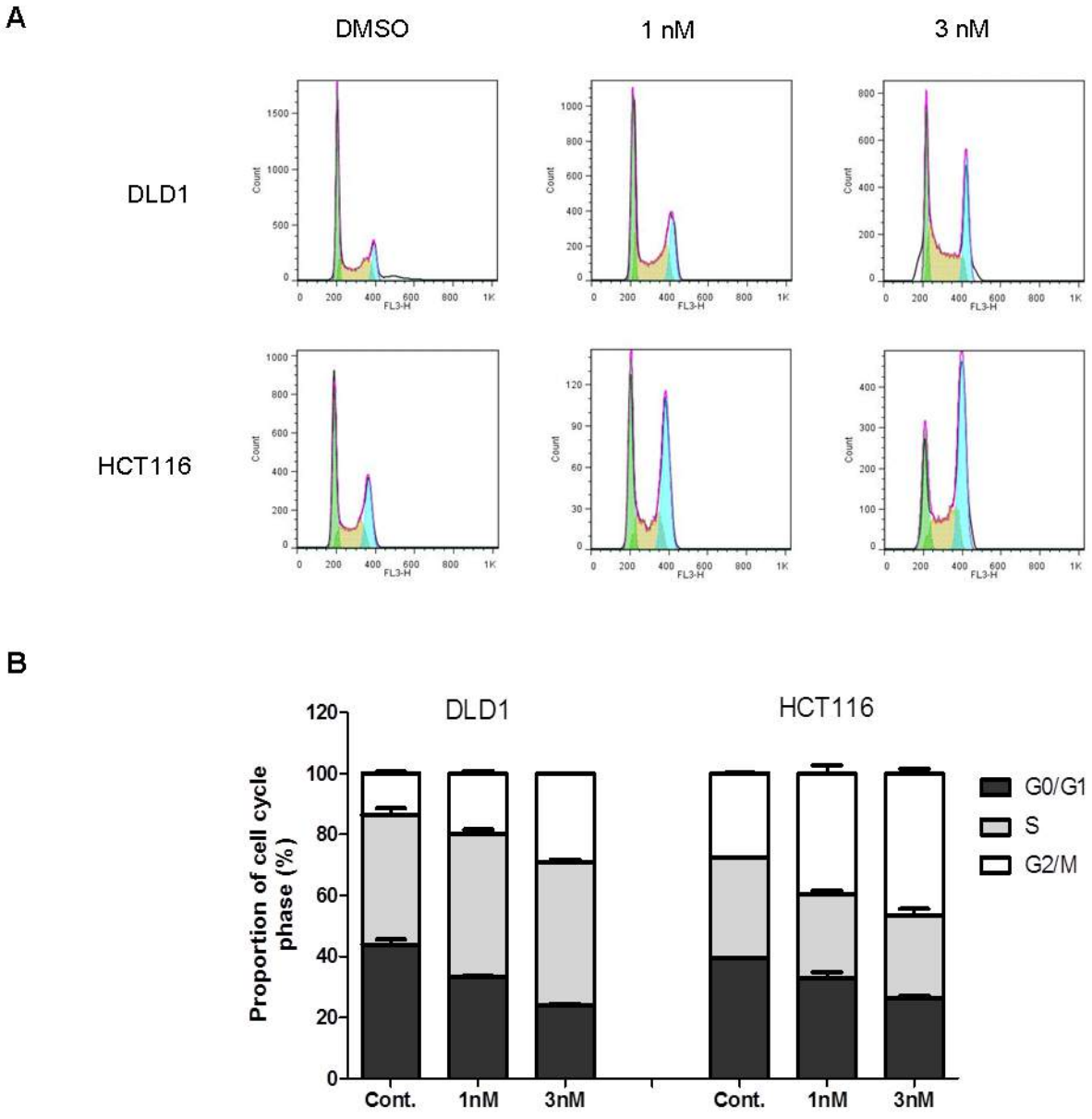

Figure 6.1. Sub-cytotoxic concentrations of docetaxel cause G_2/M phase arrest. A. Histograms of DNA content of disaggregated DLD1 and HCT116 spheroids following treatment with different concentrations of docetaxel. B. Grouped representation of alterations in the cell cycle distributions of DLD1 and HCT116 cell lines following treatment. Data is a mean of at least 3 independent experiments with at least 8 spheroids per experiment and error is SEM.

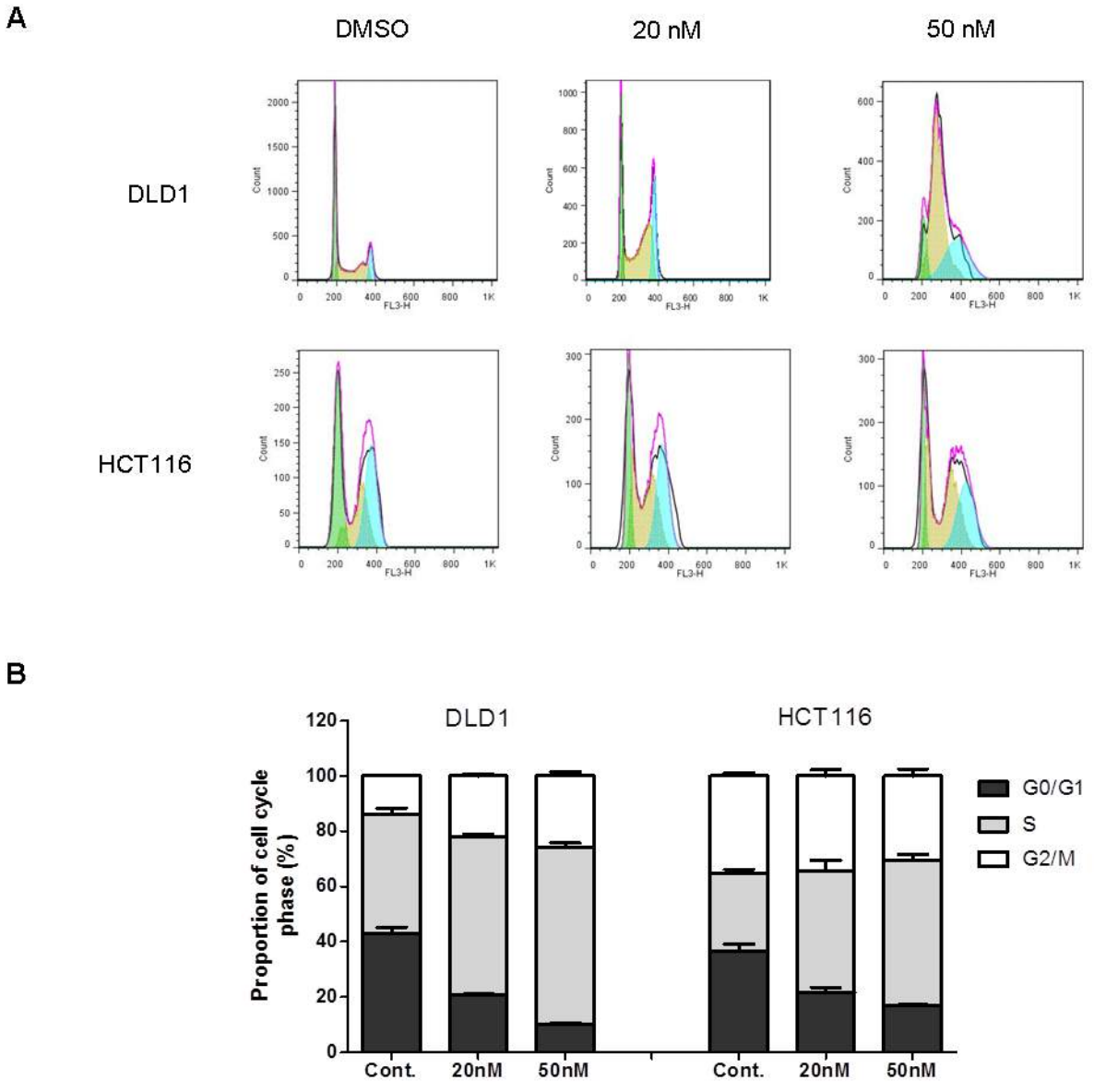

Figure 6.2. Sub-cytotoxic concentrations of gemcitabine cause S phase arrest. A. Histograms of DNA content of disaggregated DLD1 and HCT116 spheroids following treatment with different concentrations of gemcitabine. B. Grouped representation of alterations in the cell cycle distributions of DLD1 and HCT116 cell lines following treatment. Data is a mean of at least 3 independent experiments with at least 8 spheroids per experiment and error is SEM.

6.3.2 Sub-cytotoxic concentrations of docetaxel and gemcitabine alter cell cycle kinase activity

Both docetaxel and gemcitabine are known to have cell cycle inhibitory effects by targeting various kinases involved in cell cycle progression. To determine whether sub-cytotoxic concentrations of each agent affected known kinase targets, protein expression was measured for cyclin-dependent kinase inhibitors p21 and p27 and the protein kinase, Chk1, which coordinate the DNA damage and cell cycle checkpoint responses. Docetaxel at 3 nM concentration increased Chk1 expression in both DLD1 and HCT116 cell lines (See Fig. 6.3 A). Gemcitabine at 50 nM concentration increased p21, p27 and Chk1 expression in both DLD1 and HCT116 cell lines (See Fig. 6.3 B).

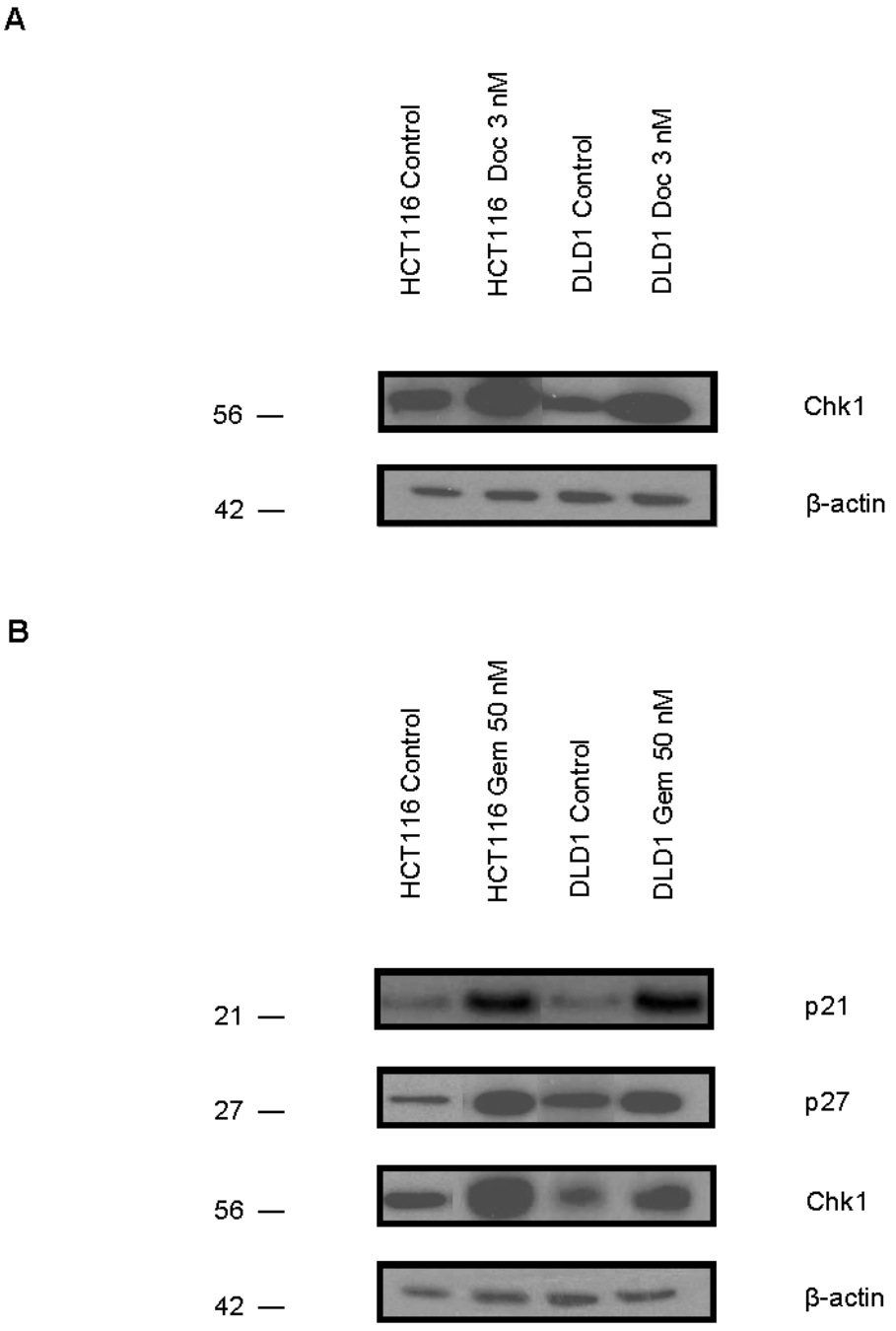

Figure 6.3. Sub-cytotoxic concentrations of docetaxel and gemcitabine alter kinase activity on western blot. A. Western blot demonstrating increased expression of Chk1 following treatment with 3 nM docetaxel in DLD1 and HCT116 cells. B. Western blot demonstrating increased expression of p21, p27 and Chk1 following treatment with 50 nM gemcitabine in DLD1 and HCt116 cells. Data shown is representative of at least three independent experiments

6.3.3 Sub-cytotoxic concentrations of docetaxel and gemcitabine alter mitochondrial function

To determine whether docetaxel and gemcitabine affected mitochondrial respiration, mitochondrial stress testing was performed to assess the key parameters of mitochondrial function (See Fig. 6.4). Untreated or drug-treated DLD1 and HCT116 cells were subjected sequentially to four drugs to calculate coupled and uncoupled respiration: 1) oligomycin (an inhibitor of Complex V); 2) para-trifluoromethoxy carbonyl cyanide phenylhydrazone (FCCP - an uncoupling agent); 3) rotenone (an inhibitor of Complex I) and 4) antimycin A (an inhibitor of Complex III) (See Fig. 6.4 B). Representative graphs of mitochondrial stress test results in untreated and treated DLD1 and HCT116 cells can be seen in Figs 6.5 A and B and 6.6 A and B. Docetaxel significantly reduced coupled respiration at 3 nM concentration in both the DLD1 and HCT116 cell lines and at 1 nM concentration in the DLD1 cell line (See Fig. 6.5 C). Both concentrations of docetaxel significantly reduced uncoupled respiration in the DLD1 cell line but not in the HCT116 cell line (See Fig. 6.5 D). Thus both coupled and uncoupled respiration are inhibited by docetaxel in DLD1 cells but only coupled respiration is inhibited in HCT116 cells. Coupled respiration was also significantly reduced in both cell lines after 24 hours treatment with 20 nM and 50 nM gemcitabine compared to the DMSO-treated control (See Fig. 6.6 C). Gemcitabine reduced uncoupled respiration in the DLD1 cell line but significantly increased it in the HCT116 cell line (See Fig. 6.6 D). Thus both coupled and uncoupled respiration are inhibited by gemcitabine in DLD1 cells but only coupled respiration is inhibited in HCT116 cells and is associated with an increase in uncoupled respiration.

A

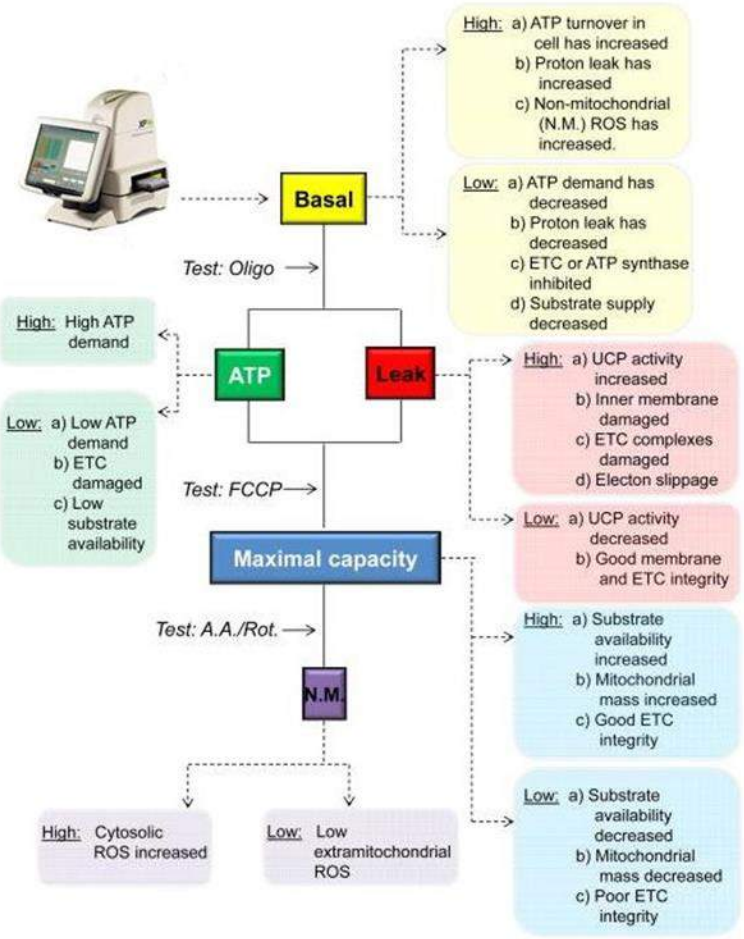

B

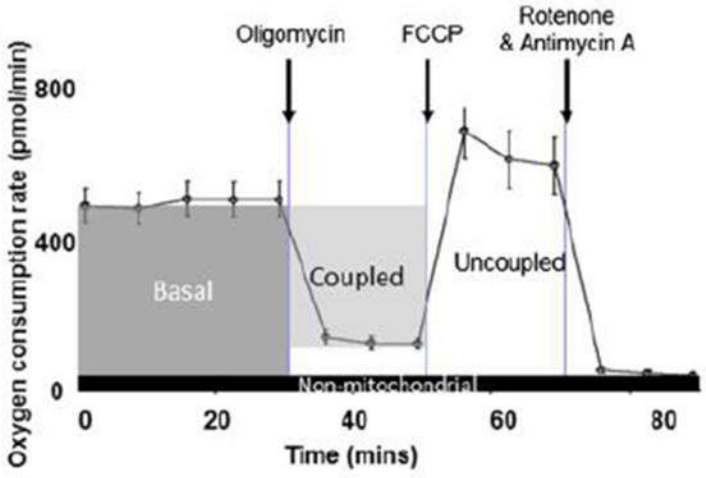

Figure 6.4. Interpreting the key parameters of mitochondrial function. A. Flow diagram summarising the possible results from mitochondrial stress testing. B. Coupled and uncoupled respiration were determined in cells to which either FCCP or oligomycin (respectively) had been added. Subtraction of the post-oligomycin OCR from the basal OCR gives coupled respiration. Uncoupled respiration is determined by subtracting the post-rotenone (non-mitochondrial) OCR from the post-FCCP OCR.

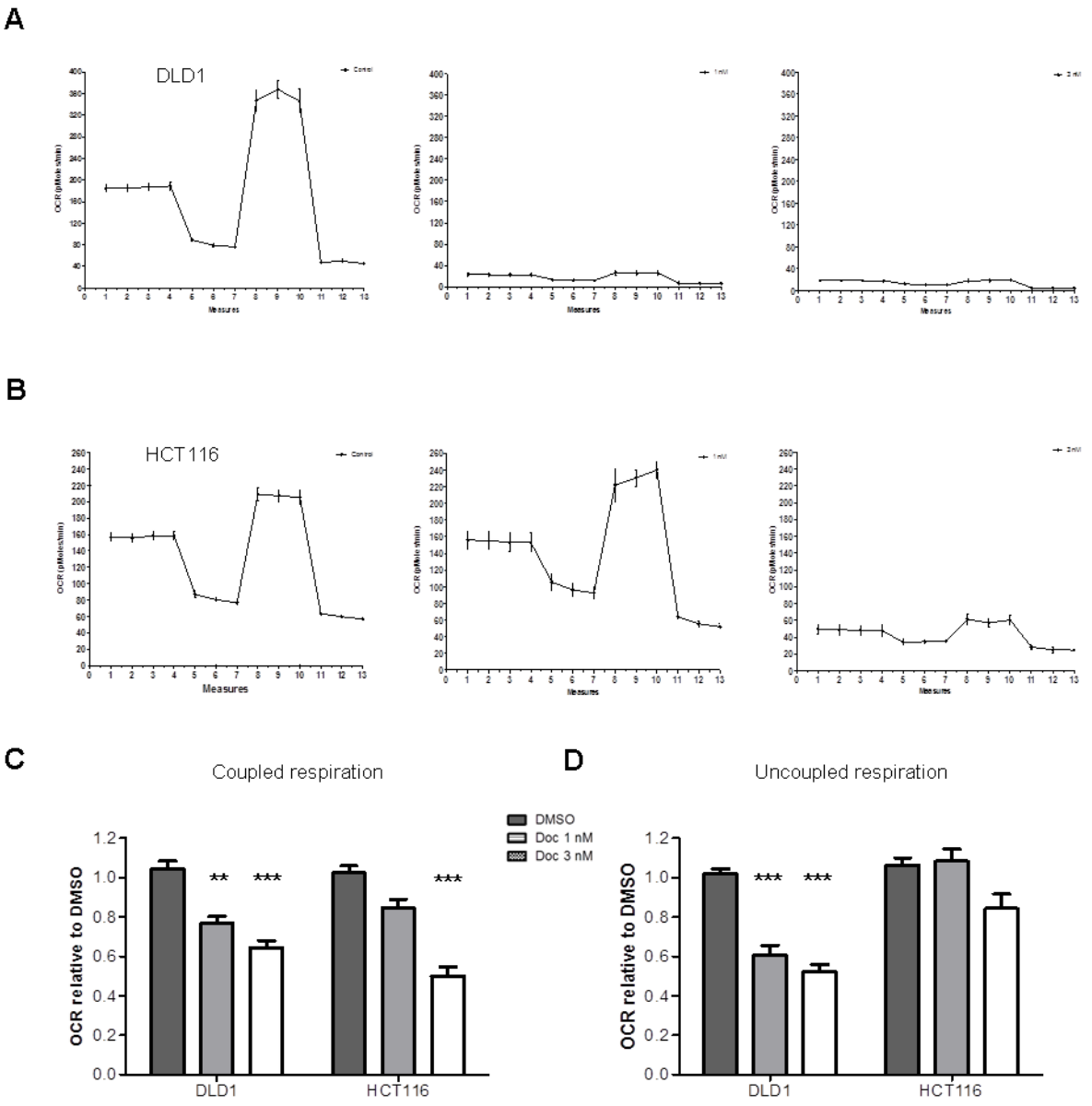

Figure 6.5. Sub-cytotoxic concentrations of docetaxel affect mitochondrial respiration. The OCR of DLD1 and HCT116 cells were measured for a total of 13 readings following injections of oligomycin, FCCP and antimycin A and rotenone at timed intervals. A. Representative graphs of mitochondrial stress test results in the DLD1 cell line. B. Representative graphs of mitochondrial stress test results in the HCT116 cell line. C. Coupled respiration was significantly reduced in both cell lines after 24 h treatment with 3 nM docetaxel and in the DLD1 cell line with 1 nM docetaxel compared to the DMSO-treated control. D. Docetaxel reduced uncoupled respiration in the DLD1 cell line but not in the HCT116 cell line. All data points represent standard error. Data shown are representative of three independent experiments. One-way ANOVAs were performed with Bonferroni-corrected post t-tests comparing treated to DMSO-treated control samples (* = $p<0.05$; ** = $p<0.01$; *** = $p<0.001$).

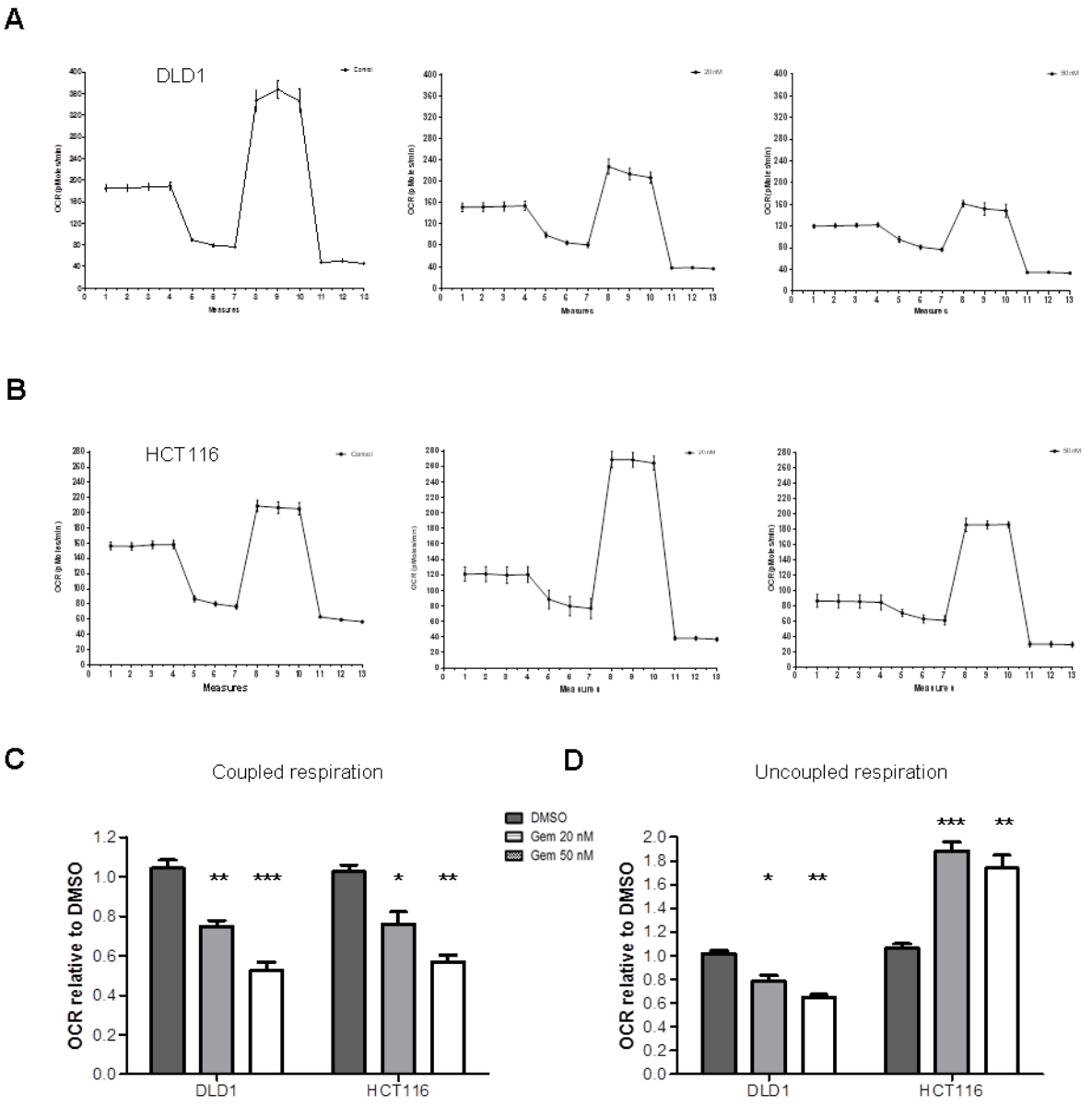

Figure 6.6. Sub-cytotoxic concentrations of gemcitabine affect mitochondrial respiration. The OCR of DLD1 and HCT116 cells were measured for a total of 13 readings following injections of oligomycin, FCCP and antimycin A and rotenone at timed intervals. A. Representative graphs of mitochondrial stress test results in the DLD1 cell line. B. Representative graphs of mitochondrial stress test results in the HCT116 cell line. C. Coupled respiration was significantly reduced in both cell lines after 24 h treatment with 20 nM and 50 nM gemcitabine compared to the DMSO-treated control. D. Gemcitabine reduced uncoupled respiration in the DLD1 cell line but significantly increased it in the HCT116 cell line. All data points represent standard error. Data shown are representative of three independent experiments. One-way ANOVAs were performed with Bonferroni-corrected post t-tests comparing treated to DMSO-treated control samples (* = $p<0.05$; ** = $p<0.01$; *** = $p<0.001$).

6.3.4 Sub-cytotoxic concentrations of docetaxel and gemcitabine do not reduce mitochondrial mass or Complex I-V expression in the electron transport chain

To determine whether the alterations in mitochondrial function were a result of reductions in mitochondrial mass or in expression of mitochondrial complexes, protein expression was measured for citrate synthase and oxidative phosphorylation complexes. No reduction in mitochondrial mass, as assessed by citrate synthase expression, was observed with docetaxel or gemcitabine treatment in either the DLD1 or HCT116 cell lines (See Fig. 6.7 A). Similarly, expression levels of the five mitochondrial complexes did not reduce with either treatment when tested in DLD1 cells (See Fig. 6.7 B).

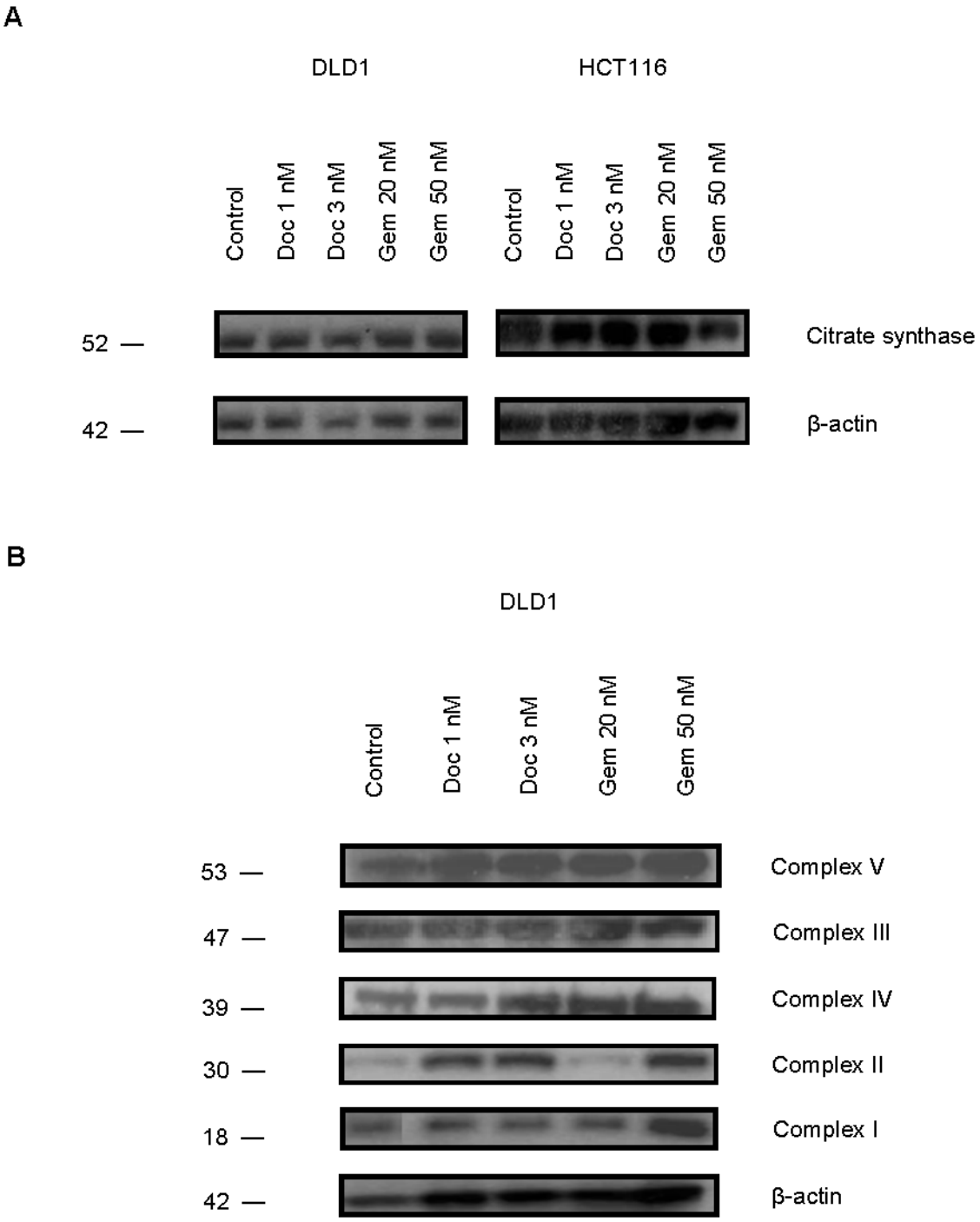

Figure 6.7. Sub-cytotoxic concentrations of docetaxel and gemcitabine do not reduce mitochondrial mass or complex expression. A. Western blot demonstrating no change in mitochondrial mass following treatment with docetaxel or gemcitabine in DLD1 and HCT116 cells as confirmed by immunoblotting for citrate synthase. B. Western blot demonstrating unchanged or increased expression of electron transport chain complexes following treatment with docetaxel or gemcitabine in DLD1 cells. Data shown is representative of at least three independent experiments

6.3.5 Deoxynucleotide triphosphate populations in DLD1 and HCT116 cells treated with docetaxel and gemcitabine

To determine whether docetaxel or gemcitabine alter deoxynucleotide triphosphate (dNTP) populations within DLD1 and HCT116 cells, levels of individual dNTPs were quantified after 24 hours of drug treatment using high performance liquid chromatography (HPLC). At either 1 nM or 3 nM concentrations, docetaxel did not affect the dNTP pools (See Fig. 6.8 A). Gemcitabine increased the dTTP levels in a concentration-dependent manner in both DLD1 and HCT116 cell lines but is more pronounced in the former (See Fig. 6.8 B).

A

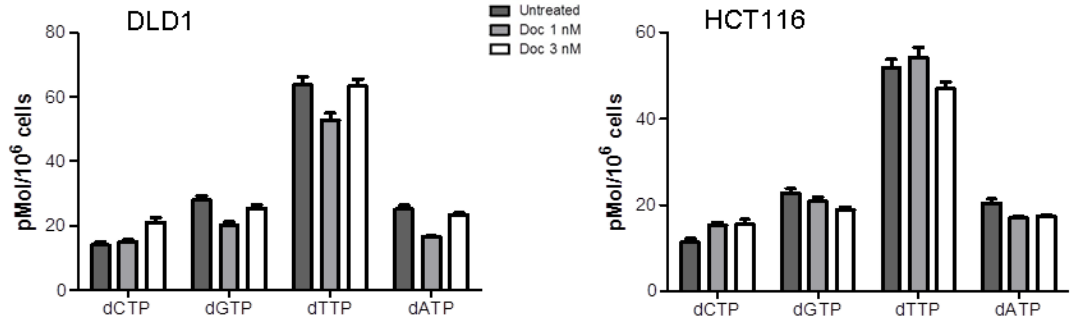

B

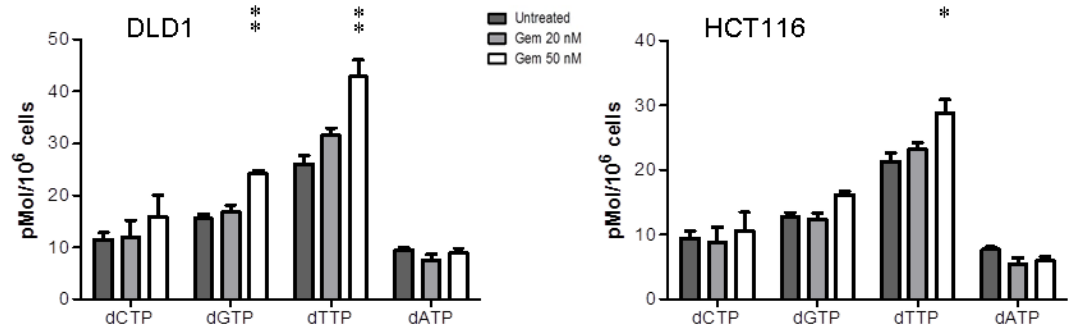

Figure 6.8. HPLC analysis of deoxynucleotide triphosphate levels in untreated versus treated cells. A. Analysis of DLD1 and HCT116 cells treated with 24 hour incubation of 1 nM and 3 nM docetaxel. B. Analysis of DLD1 and HCT116 cells treated with 24 hour incubation of 20 nM and 50 nM gemcitabine. Values were calculated as mean intracellular concentration (pmoles) of dNTPs per 10^6 cells from three independent experiments. Error bars represent the standard error. One way ANOVA was performed to assess statistical significance with Bonferroni post correction (* = $p<0.05$; ** = $p<0.01$).

6.3.6 Gemcitabine reduces OCR and improves hypoxia independent of its effect on RNR

To identify whether gemcitabine reduces OCR and improves hypoxia through its action on RNR, cells were treated with and without hydroxyurea (a known inhibitor of RNR), analysed using OCR assays to measure oxygen consumption and using HPLC analysis to measure the dNTP populations (See Fig. 6.9). Hydroxyurea at 10 μM and 100 μM concentrations did not reduce OCR in DLD1 and HCT116 cells (See Fig. 6.9 A and B) and even increased OCR in HCT116 cells at the 100 μm concentration (See Fig. 6.9 B). The population of all dNTPs were reduced in both cell lines at both 10 μM and 100 μM concentrations, although the reduction in dTTP levels was less marked (See Fig. 6.9 C). This is in contrast with the relatively unaffected levels of dNTPs seen when treated with gemcitabine (See Fig. 6.8 B).

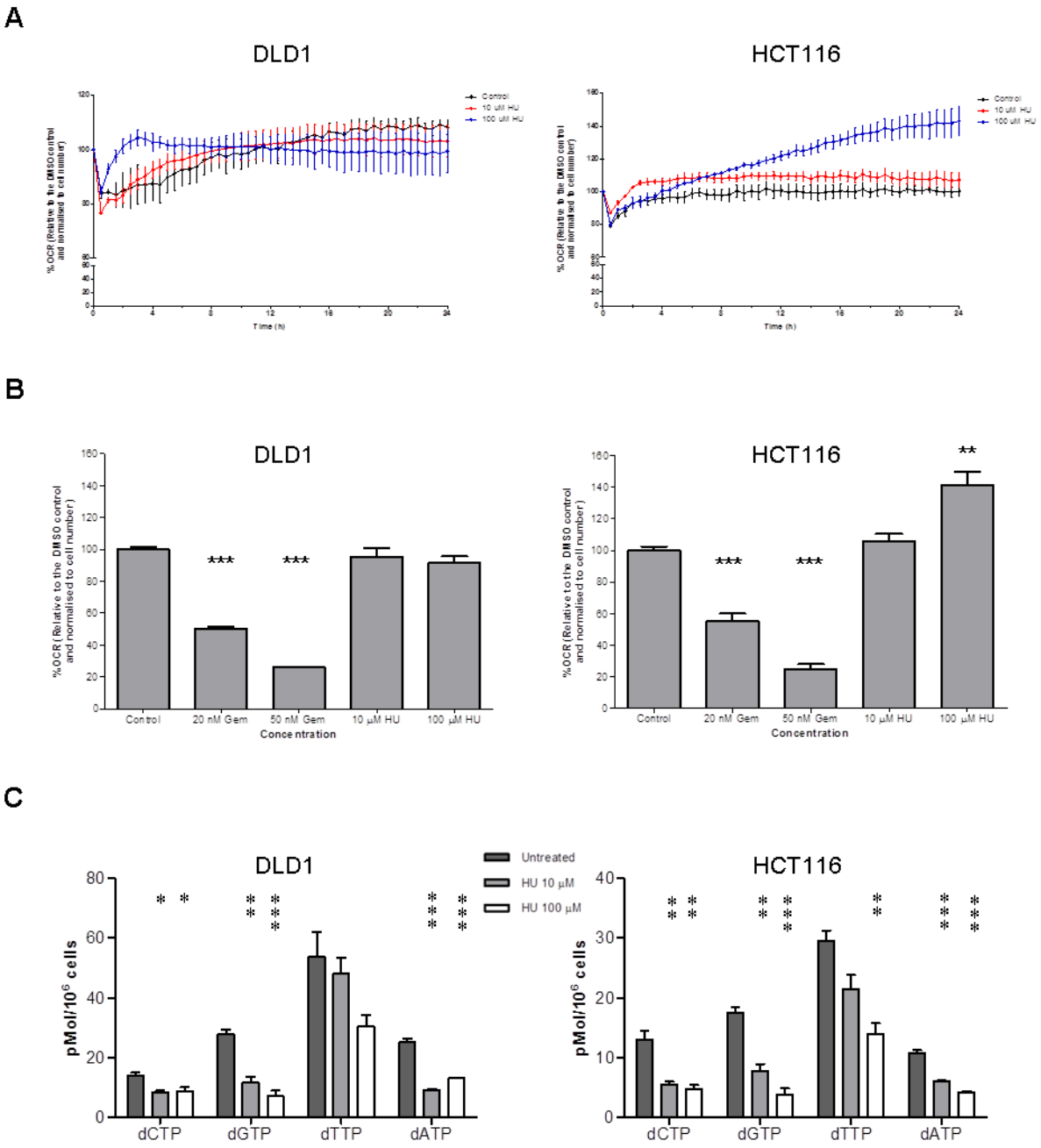

Figure 6.9. The effect of gemcitabine on reducing OCR is independent of its action on RNR. A. The OCR of DLD1 and HCT116 cells measured for 24 hours after injection of either 10 μM or 100 μM hydroxyurea (HU) using the Seahorse XF96 Analyser. B. Comparing % OCR in control, gemcitabine treated and HU treated DLD1 and HCT116 cells. C. HPLC analysis of dNTPs in control and HU treated DLD1 and HCT116 cells. All data points represent standard error. Data shown are representative of three independent experiments. Error bars represent the standard error. One way ANOVA was performed to assess statistical significance with Bonferroni post correction (* = $p<0.05$; ** = $p<0.01$; *** = $p<0.001$).

6.4 Discussion

The different mechanisms of action of docetaxel and gemcitabine in exerting cytotoxicity are both very complex and very effective. The focus of this chapter was to determine whether the drugs reduced OCR and hypoxia through their cytotoxic effect or an alternative mechanism. The work presented in Chapters 3 and 5 illustrated that cell death at these concentrations of docetaxel and gemcitabine were limited and that the cytotoxic effect was unlikely to be a significant contributor to reducing OCR and hypoxia.

A reduction in cellular proliferation within spheroids, as presented in Chapter 5, was hypothesised to be a potential mechanism for the observed improvement in hypoxia, as senescent and G_0 cells have a lower oxygen requirement than proliferating cells [167, 295-298]. Cellular senescence is distinct from quiescence (G_0) as it is an induced state that occurs in response to DNA damage or interruption that would make on going mitosis non-viable. Senescence therefore provides an alternative to a cell's death by apoptosis. This is quite distinct from quiescence, which usually occurs in response to a lack of growth factors or nutrients such as oxygen. Cells remain in G_0 until there is a reason for them to divide and therefore quiescence is reversible whereas senescence is not. Consequently, improvement in hypoxia may be due to the agents moving proliferating cells into a senescent state, as a result of DNA damage, cell cycle inhibition or both. Both docetaxel and gemcitabine are known to have cell cycle inhibitory effects, blocking the process at G_2/M and S phase respectively [35, 286]. Figures 6.1 and 6.2 demonstrate that even at these low concentrations, both drugs affect the cell cycle and arrest the cells at the aforementioned phases. Because the population of apoptotic cells remain unchanged with treatment, one potential explanation for the observed cell cycle arrest is that proliferating cells become senescent after drug treatment. However, due to time constraints, this alternative explanation could not be experimentally tested.

Sub-cytotoxic concentrations of docetaxel and gemcitabine interfered with cell cycle machinery, as demonstrated by the increased expression of p21, p27 and Chk1 measured using western blot analysis. Both p21 and p27 are potent cyclin-dependent kinase inhibitors. The p21 protein binds to and inhibits the activity of cyclins CDK2, CDK1 and CDK4/6 complexes and thus acts as a regulator of cell cycle progression at G_1 and S phase but can affect all phases of the cycle [299]. p21 initiates cell cycle arrest but can also mediate cellular senescence. Therefore agents which affect the cell cycle at S phase would be expected to increase the activity of p21, in line with the observed increase in expression of p21 in both DLD1 and HCT116 cell lines treated with 50 nM gemcitabine (See Fig. 6.3 B). p27 is a protein with a similar mechanism of action and function as p21 and induces cell cycle arrest at G_1 and S phase by binding to and preventing the activation of CDK2 or CDK4 complexes [300]. As with p21, there is increased expression of p27 with gemcitabine in both cell lines (See Fig, 6.3 B). Finally, Chk1 is a serine/threonine protein kinase which co-ordinates the DNA damage and cell cycle checkpoint response [301]. Activation of Chk1 results in the initiation of cell cycle checkpoints, cell cycle arrest, DNA repair, gene transcription and apoptosis which impacts various stages of the cell cycle including the S, G_2/M transition and M phases [302]. As expected, both docetaxel and gemcitabine increase expression of Chk1 in DLD1 and HCT116 cells (See Fig. 6.3 A and B). Together, these findings suggest that sub-cytotoxic concentrations of these agents have an anti-proliferative effect and possibly promote cellular senescence.

However, the anti-mitotic effect of docetaxel and gemcitabine is perhaps not the only possible explanation for the reduction in OCR, as the results from Chapter 4 would suggest. The rapid drop in OCR observed with both agents indicates that the drugs may have an immediate effect on the electron transport chain and oxidative phosphorylation. This certainly appears to be the case, as both drugs significantly reduced coupled respiration in both cell lines on mitochondrial stress testing (See Figs. 6.5 C and 6.6 C). Coupled respiration describes oxygen uptake which is dependent on the presence of ADP and phosphate i.e. one cannot occur without

the other. The flow of electrons through the electron transport chain, from electron donors such as NADH to electron acceptors such as oxygen, is an exergonic process, whereas ATP synthesis is an endergonic process. However, as coupled respiration is dependent on the supply of electrons from the electron transport chain, this does not in itself show that the observed OCR reduction is dependent on Complex V (ATP synthase) activity. It is therefore necessary to also consider uncoupled respiration, which reflects electron transport chain activity. Treatment with docetaxel and gemcitabine reduced uncoupled respiration in the DLD1 cell line but either had no effect or increased it in the HCT116 cell line (See Figs. 6.5 D and 6.6 D). This observation may be explained through results identified in Chapter 4, which showed that the HCT116 cell line had a predominantly glycolytic phenotype.

This reduction in mitochondrial function appears to be independent of mitochondrial mass and complex expression (See Fig. 6.7). DLD1 and HCT116 cells treated with docetaxel and gemcitabine had no effect on the level of mitochondria, as determined by western blot for citrate synthase (See Fig. 6.7 A). Citrate synthase is an essential component of the citric acid cycle and is a commonly used quantitative enzyme marker for mitochondrial mass. This was further supported by the fact that neither drug reduced the expression of the complexes of the electron transport chain, with either similar or increased expression seen with treatment in both cell lines (See Fig. 6.7 B).

At the tested concentrations, neither docetaxel nor gemcitabine negatively affected the dNTP populations (See Fig. 6.8). As discussed, both agents are known to be anti-proliferative but as gemcitabine has a specific effect on RNR, a reduction in the individual dNTPs may be expected. Instead, there was an increase in the population of dTTP with increasing concentrations of gemcitabine (See Fig. 6.8 B). This finding can perhaps be explained through the fact that dTTP is not formed through RNR but through thymidylate synthase, where dUMP is methylated to dTTP. Gemcitabine at these concentrations does not therefore have a significant

effect on RNR, a result similar to those obtained by Kerr and colleagues [303]. In contrast to the effects observed with gemcitabine, treatment of DLD1 and HCT116 cells with hydroxyurea, a known inhibitor of RNR, resulted in a significant drop in all dNTP levels (See Fig. 6.9 C) [304, 305]. Although dTTP levels drop despite being synthesised by a different enzyme, the reduction is less marked as compared to the other dNTPs. This can be explained through the fact that RNR inhibition will deplete dUDP, which is formed from dUMP, to result in a modest fall in dTTP levels. However, hydroxyurea has little effect on the OCR after 24 hours of treatment, suggesting that the activity of gemcitabine in reducing OCR is independent of its action on RNR and that possibly a new mechanism of action, one that affects the electron transport chain and oxidative phosphorylation, is responsible (See Fig. 6.9 A and B).

CHAPTER 7: SUB-THERAPEUTIC DOSES OF DOCETAXEL AND GEMCITABINE IMPROVE HYPOXIA *IN VIVO*

7.1 Aims

1. To determine whether the improvement in hypoxia seen in spheroids with docetaxel and gemcitabine is translated into subcutaneous DLD1 tumours *in vivo*.
2. To confirm that doses of docetaxel and gemcitabine within the murine models are of a sub-therapeutic level.
3. To determine whether sub-therapeutic doses of docetaxel and gemcitabine affect tumour growth and murine weight.

7.2 Introduction

7.2.1 Translating *in vitro* results for *in vivo* testing

In order to best test the validity of the results thus far, it was necessary to proceed with *in vivo* testing via subcutaneous xenograft murine models. This required a shift in the delivery of docetaxel and gemcitabine by moving from administering sub-cytotoxic concentrations to sub-therapeutic doses. Both docetaxel and gemcitabine are administered in the clinical setting at doses based on the surface area of the patient. Docetaxel is typically given for the treatment of breast, prostate, gastric, non-small-cell lung and head and neck cancer as a single agent or in combination with other treatments. It is usually delivered at doses ranging from 60-100 mg/m^2 every three weeks [306]. Gemcitabine is licensed in the UK for the treatment of breast, ovarian, non-small-cell lung and pancreatic cancer and is usually delivered at doses ranging from 1000-1250 mg/m^2 no more than once per week [306]. Both agents require careful monitoring of renal and hepatic function and the dosing may be adjusted accordingly.

7.2.2 Metabolism and *in vivo* dosing of gemcitabine

In humans, gemcitabine has a short half-life of between 8–20 minutes because of rapid deamination to dFdU, which in itself has a long half-life at approximately 50 hours and is mostly excreted in the urine [204, 307]. dFdCTP peak concentrations are obtained within 30 minutes of the end of an infusion and dFdCTP elimination was linear at low concentrations [204]. The long half-life of dFdCTP is possibly the reason why gemcitabine has activity against both rapidly proliferating and slowly dividing tumours. Clinical pharmacokinetic studies have demonstrated that the rate of intracellular accumulation of dFdCTP was saturated at gemcitabine concentrations of 15–20 μM in plasma [204]. A standard 30 minute infusion of gemcitabine at doses of 1000–1,200 mg/m^2 generates gemcitabine plasma concentrations of 20–60 μM, exceeding the levels at which dFdCTP formation becomes saturated and possibly also inhibits gemcitabine phosphorylation [204, 308]. Consequently, a significant portion of gemcitabine is

deaminated to dFdU. Although these findings suggest that a lower dosing regimen may theoretically be optimal, results from clinical trials have shown that dosing at 1000-1250 mg/m^2 gave the best results in progression free survival (PFS) and median survival in pancreatic, lung and breast cancer [309-312]. With these results in mind, determining a dosing regimen for mice that was significantly below the therapeutic levels seen in humans, comparatively, was necessary to support the hypothesis that gemcitabine improves hypoxia independent of cell death. However, given that concentrations thus far had been in molar range as opposed to mg/m^2 and that drug delivery would be intraperitoneal rather than intravenously, considerable review of the literature was required in order to ensure the findings from *in vitro* could be translated and relatable *in vivo*. Because our principle hypothesis was that sub-cytotoxic concentrations have a beneficial effect on hypoxia, we selected a dose that was clearly sub-therapeutic, albeit not necessarily the same concentrations tested *in vitro*. Wang and colleagues demonstrated that intraperitoneal injections of gemcitabine at 160 mg/kg was the equivalent of delivering 480 mg/m^2 whilst Ciccolini and colleagues demonstrated that intraperitoneal injections at 100 mg/kg reached plasma concentrations of 700 μg/ml [313, 314]. Several studies have used doses of gemcitabine at 60-320 mg/kg from between 1-3 times/week via intraperitoneal injection [172, 313, 315, 316]. However, daily dosing at just 5 mg/kg/day was associated with significant morbidity and mortality in mice, causing severe enteropathy [317, 318]. This appears contrary to what you might expect considering 76-86% of the dose is excreted in the first 24 hours and the low level of intraperitoneal absorption of the drug would suggest that daily low-level dosing would be safe [319]. In light of this, gemcitabine dosing at 1 mg/kg and 5 mg/kg, 3 times/week was adjudged to be both safe for mice and sufficiently low so that tumour cell death was unlikely. Indeed, this was up to 320 times less than the doses given in some studies assessing the therapeutic effect of gemcitabine on tumours in mice [172, 313, 315, 316].

7.2.3 Metabolism and *in vivo* dosing of docetaxel

Despite being a well-established chemotherapy agent, the optimal dosing regimen for docetaxel remains unclear. However, most phase II and phase III clinical trials have found greatest patient benefit at doses between 60-100 mg/m^2 given every three weeks by intravenous infusion [203]. Greater than 90% of docetaxel is bound in plasma by lipoproteins, alpha 1-acid glycoprotein and albumin [203, 320]. Significantly, alpha 1-acid glycoprotein is highly variable, particularly in patients with cancer and is the main determinant of docetaxel's plasma binding variability [320]. Consequently, plasma concentrations in patients are highly variable, with pharmacokinetic studies reporting plasma concentrations of 0.1–1.2 μM and maximum concentrations ranging between 0.3 and 6.9 μM within 24 hours post-treatment [321-323]. Increased dosing results in a linear increase of the area under the concentration-time curve and therefore dose is directly proportional to plasma concentration. Metabolism of docetaxel is primarily hepatic, with renal excretion contributing to <5% of elimination [203]. Docetaxel has a relatively short initial (α) half-life with a rapid decline of approximately 4.5 minutes, when the drug moves into the peripheral compartments from the systemic circulation. This is followed by a β half-life of approximately 38 minutes and a relatively slow γ half-life of approximately 12 hours, which represent the slow efflux of docetaxel from the peripheral compartment [203]. The variability of docetaxel dosing is also reflected in murine testing, with intraperitoneal doses given from 10 mg/kg to 50 mg/kg and from once a week to alternate days [324-326]. In mice, a dose at 32 mg/kg is roughly equivalent to the human dose of 100 mg/m^2 on a mg/m^2 basis and a single dose of 50 mg/kg can cause severe toxicity [326]. Yonemura and colleagues deliberately used low-doses of docetaxel at 8 mg/kg, 2 mg/kg and 0.5 mg/kg on days 2, 5, 9, 12, 16 and 19 after tumour inoculation, with no adverse effects seen in any group after 7 days [327]. Consequently, docetaxel dosing at 0.1 mg/kg and 1 mg/kg, 3 times/week was deemed to be both sub-therapeutic and safe to administer.

7.3 Results

7.3.1 Sub-therapeutic doses of docetaxel and gemcitabine can improve tumour hypoxia as measured by IVIS bioluminescent imaging

To determine the effect of docetaxel and gemcitabine at sub-therapeutic doses on tumour hypoxia, mice were inoculated with DLD1 cells containing a HRE-luciferase reporter. Once tumours reached a volume of 80 mm^3, mice were randomised into two groups (drug vs. control) and given either treatment three times/week. Tumours were then imaged for hypoxia using IVIS within two hours of drug administration. Docetaxel significantly reduced hypoxia in the tumours at the 1 mg/kg dose but not at the 0.1 mg/kg dose (See Fig. 7.1 A and B). Gemcitabine significantly reduced tumour hypoxia at both 1 mg/kg and 5 mg/kg doses, with the latter having a greater effect (See Fig. 7.1 A and C).

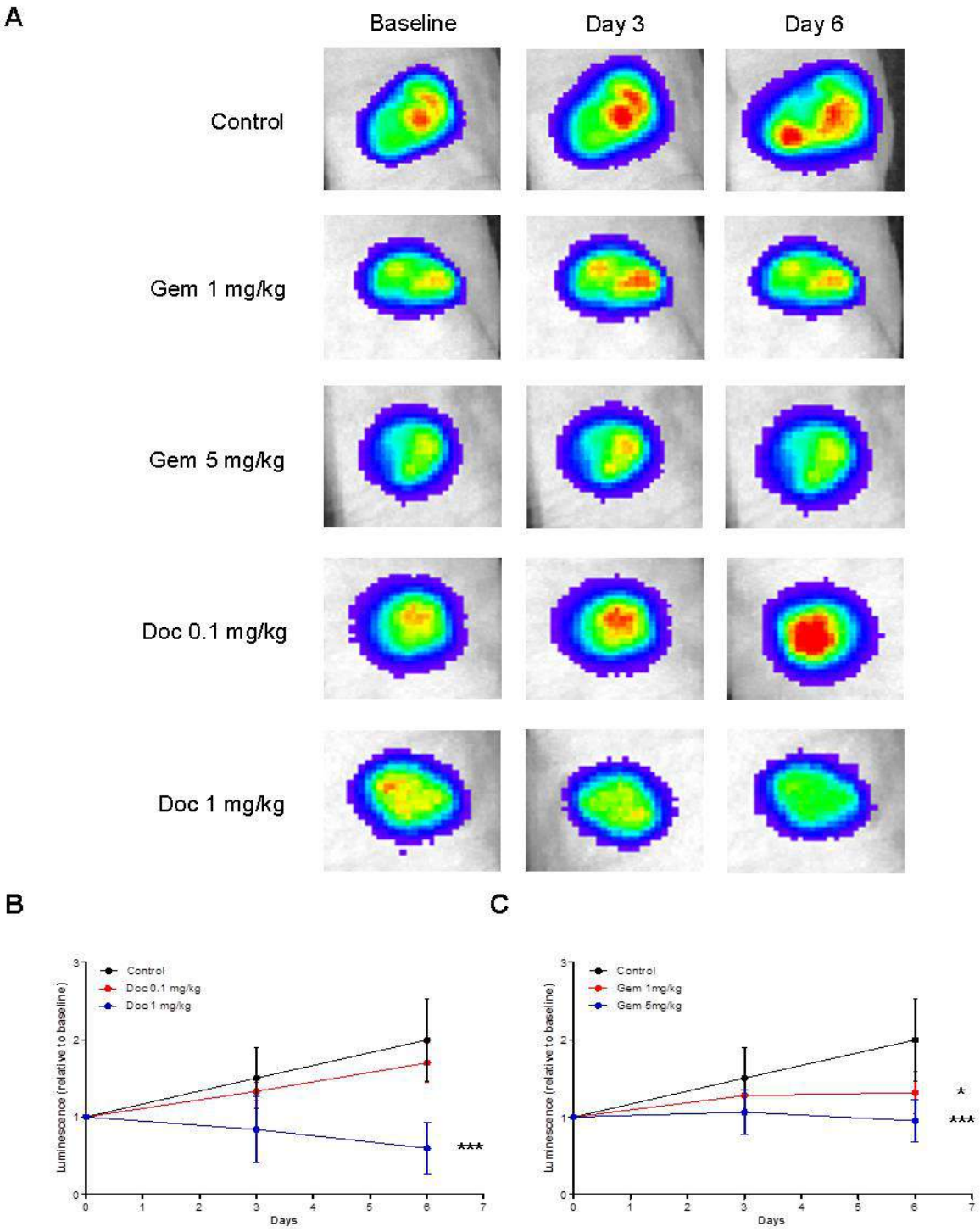

Figure 7.1. Sub-therapeutic doses of docetaxel and gemcitabine can improve tumour hypoxia as seen on IVIS. A. Representative IVIS images of subcutaneous DLD1 tumours recording luminescence intensity in control and treated mice. B. Averaged luminescence normalised to baseline of control versus docetaxel treated mice. C. Averaged luminescence normalised to baseline of control versus gemcitabine treated mice. Treatments were administered 3x/wk via I.P. injection. Each group had at least 6 mice and entered into study once tumour volume reached 80 mm^3. Data points represent mean of at least 6 tumours and error bars represent standard error. Two way ANOVA with repeated measures was performed to assess statistical significance with Bonferroni post correction (* = $p<0.05$; ** = $p<0.01$; *** = $p<0.001$).

7.3.2 The effects of sub-therapeutic doses of docetaxel and gemcitabine on tumour volume and murine weight

Untreated and treated mice had their tumour volume and weight recorded every other day until sacrifice and tumour excision. Excised tumours showed little variation in shape macroscopically, with most tumours spherical in dimension (See Fig. 7.2 A). Despite the low doses of docetaxel, there was a significant reduction in the development of tumour volume at both 0.1 mg/kg and 1 mg/kg dosing, whereas gemcitabine had no statistical reduction in tumour volume at either 1 mg/kg or 5 mg/kg doses (See Fig. 7.2 B). There was a general trend of murine weight loss in all mice over the course of 7 days but there was no difference in rate of loss seen between treated and untreated groups (See Fig. 7.2 C).

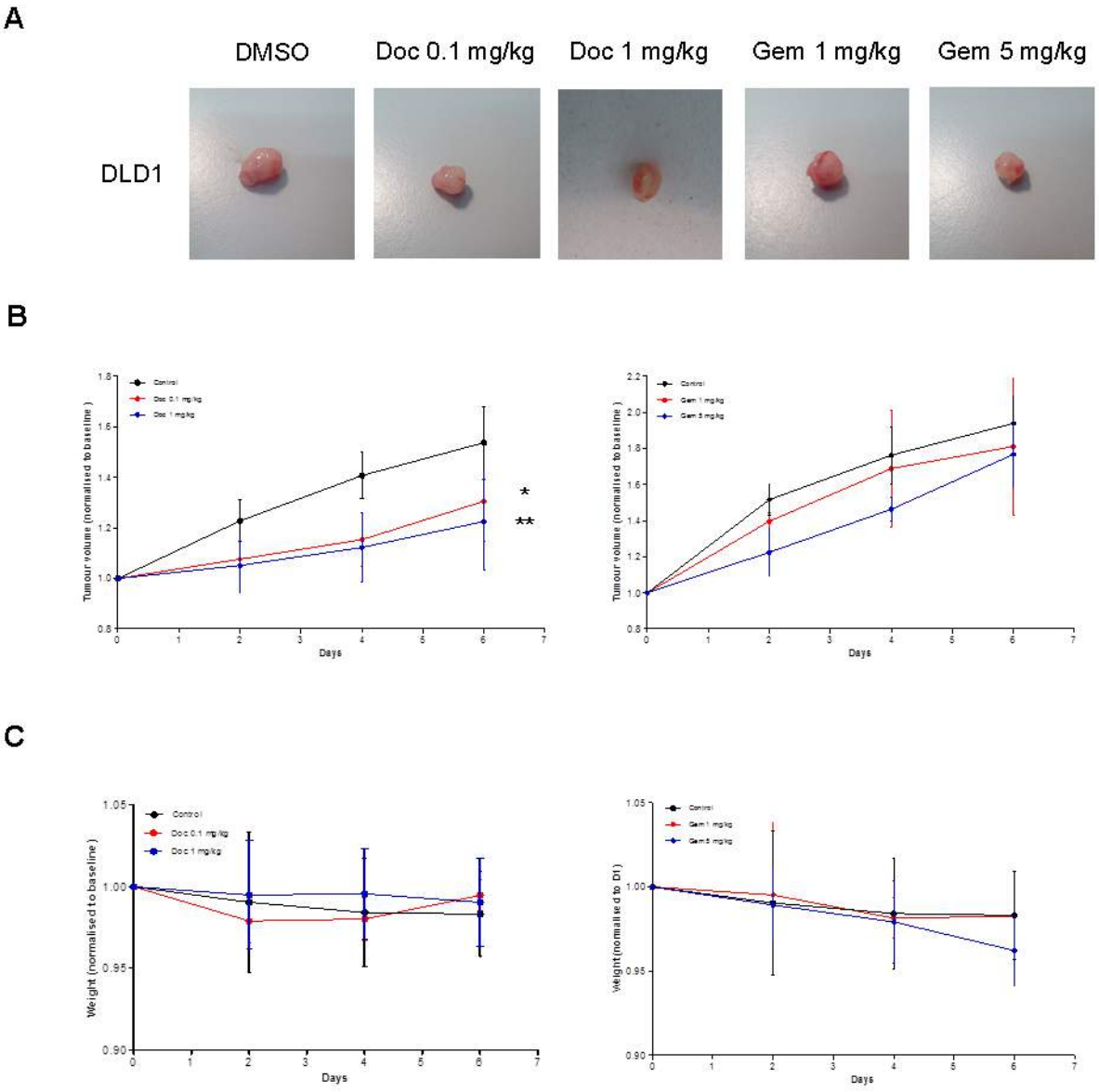

Figure 7.2. The effects of sub-therapeutic doses of docetaxel and gemcitabine on tumour volume and mice weight. A. Representative macroscopic images of excised subcutaneous DLD1 tumours in control and treated mice. B. Averaged tumour volume normalised to baseline of control versus docetaxel and gemcitabine treated mice. C. Averaged weight normalised to baseline of control versus docetaxel and gemcitabine treated mice. Treatments were administered 3x/wk via I.P. injection. Each group had at least 6 mice and entered into study once tumour volume reached 80 mm^3. Error bars represent standard error. Two way ANOVA with repeated measures was performed to assess statistical significance with Bonferroni post correction (* = $p<0.05$; ** = $p<0.01$; *** = $p<0.001$).

7.3.3 Docetaxel and gemcitabine metabolite levels in murine plasma and xenografts following sub-therapeutic dosing

To confirm whether the dosing regimen of docetaxel and gemcitabine was delivering sub-therapeutic levels, the concentrations of drug metabolites were measured in the plasma and xenografts as described in section 2.7.3. The concentration of docetaxel was found to be higher in the tumour than in the plasma and was greater at the 1 mg/kg dosing than in the 0.1 mg/kg dosing (See Fig. 7.3 A). The concentrations found in the plasma and tumours at 1 mg/kg were considerably higher than what was tested *in vitro*. The concentration of gemcitabine was less than 2 nM in both the plasma and tumours but this was attributed to the very short half-life of the drug. The concentration of dFdU, the deaminated inactive by-product of gemcitabine, was higher in the plasma than in the tumours and was greater at the 5 mg/kg dosing than in the 1 mg/kg dosing (See Fig. 7.3 B). The concentrations of both docetaxel and gemcitabine in the plasma and tumours of control mice was zero.

A

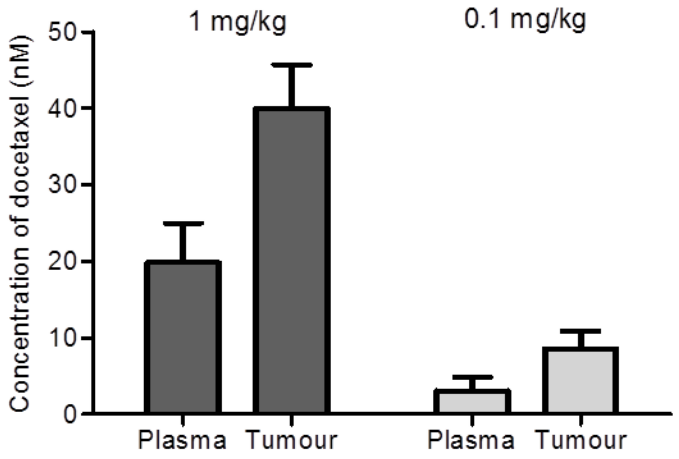

B

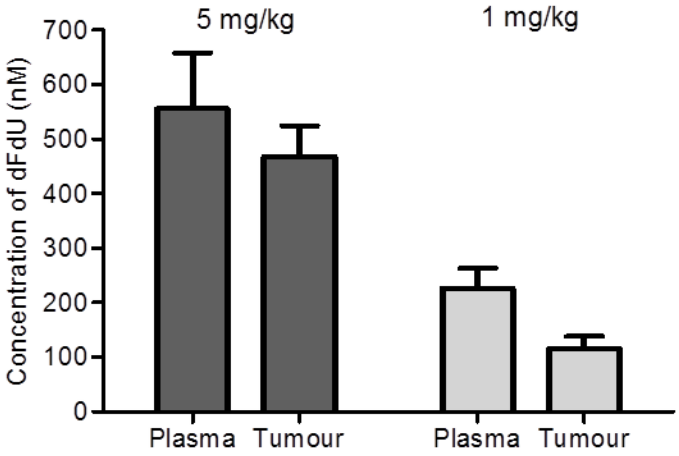

Figure 7.3. Docetaxel and gemcitabine metabolite levels in murine plasma and DLD1 xenografts. A. Metabolite levels in mice treated with docetaxel. B. Metabolite levels in mice treated with gemcitabine. All treatments were administered via intraperitoneal injection 3x/week. Data is an average of 6 mice per treatment group. Error bars represent standard error

7.3.4 Sub-therapeutic doses of docetaxel and gemcitabine can improve tumour hypoxia as seen on immunohistochemistry

To confirm whether sub-therapeutic doses of docetaxel and gemcitabine improved tumour hypoxia at a tissue level, tumours from control and drug-treated mice were sectioned, stained and imaged for blood vessels and hypoxia as described in sections 2.8.3 and 2.9.1. Cell nuclei were stained with Hoechst 33342 (blue), blood vessels with anti-CD31 (green) and hypoxia with anti-EF5 (red) (See Fig. 7.4). Hypoxia appeared to be visibly reduced within the proximity of blood vessels in both control and drug-treated mice. Tumour tissue outside the proximity of blood vessels appeared to have visible levels of hypoxia in the 1 mg/kg gemcitabine, 0.1 mg/kg docetaxel and control sections but this was less prominent in the tumours treated with 1 mg/kg gemcitabine. However, there appeared to be a visible improvement in hypoxia within the tumour tissue outside the proximity of blood vessels in the tumours treated with 5 mg/kg gemcitabine and 1 mg/kg docetaxel.

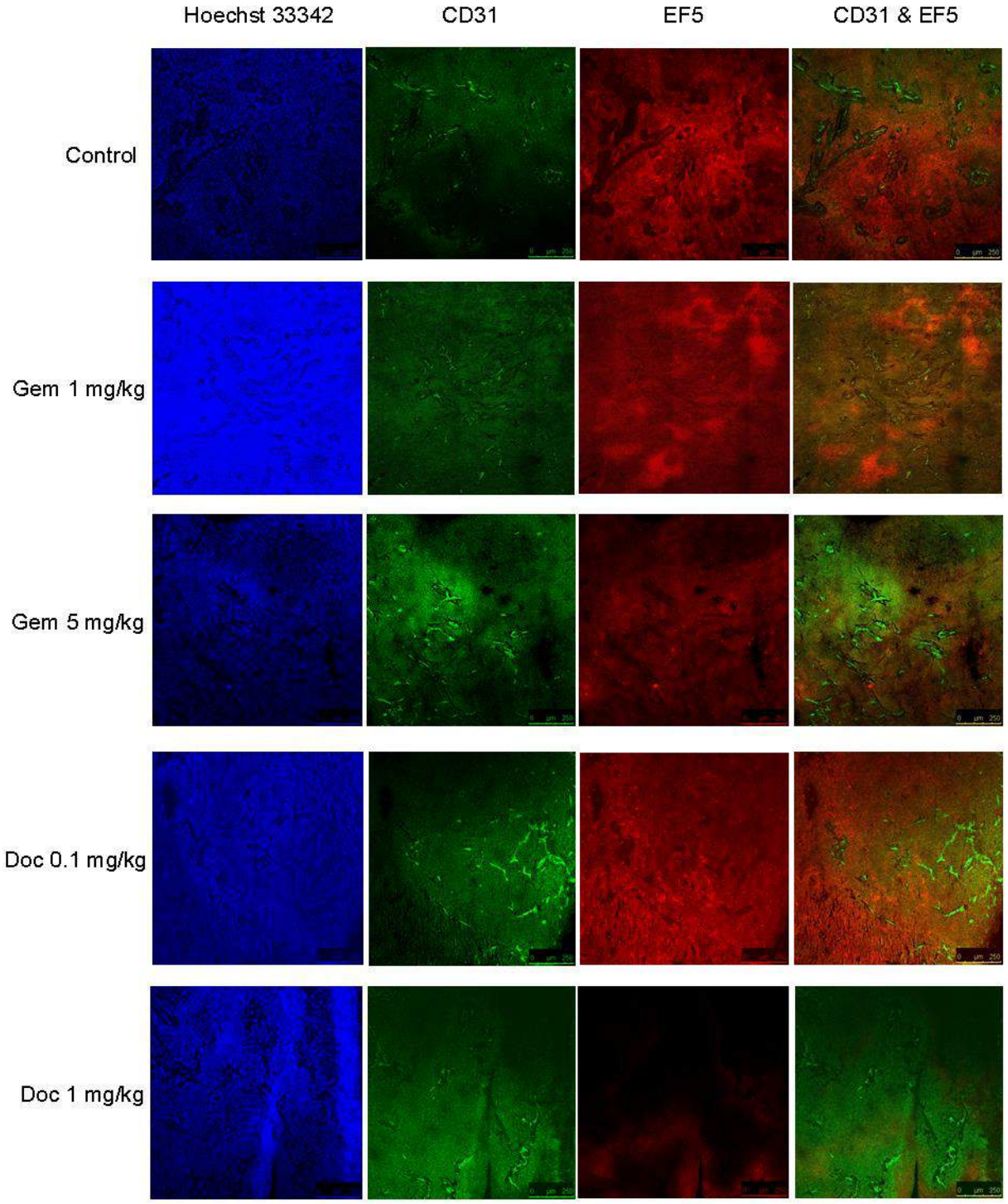

Figure 7.4. Sub-therapeutic doses of docetaxel and gemcitabine can improve tumour hypoxia as seen on immunohistochemistry. Representative immunohistochemistry sections of subcutaneous DLD1 tumours from control and drug-treated mice. Treatments were administered 3x/ wk via intraperitoneal injection. Each group had at least 6 mice and entered into study once tumour volume reached 80 mm^3.

7.4 Discussion

Sub-therapeutic doses of docetaxel and gemcitabine improve hypoxia *in vivo*. However, the concept of administering cytotoxic agents regularly at lower doses relative to using the maximum tolerated dose is not a new one. This dosing regimen is known as 'metronomic chemotherapy' and is now recognised as an alternative option for cancer treatment [241]. Although not wholly sub-cytotoxic in comparison with standard regimens, metronomic dosing has demonstrated a reduced side-effect profile but similar or even increased efficacy in pre-clinical studies [328, 329]. Furthermore, a number of Phase II trials have also shown that metronomic chemotherapy regimens in the absence or presence of anti-angiogenic agents, are active and minimally toxic in breast, ovarian, prostate and colorectal cancer [330-333]. The mechanism by which metronomic chemotherapy works is thought to be anti-angiogenic, either by inducing endothelial cell apoptosis in the tumour vasculature, destruction of endothelial progenitors and/or promotion of endogenous anti-angiogenic factors [328, 334, 335]. The effect on tumour hypoxia by using metronomic chemotherapy has also recently been investigated [315]. FaDu tumours, which are sourced from human nasopharyngeal cancer and known to exhibit hypoxia, were exposed to low dose gemcitabine (25 mg/kg and 15 mg/kg, 3x/week) and had their partial pressure of oxygen (pO_2) measured with electron paramagnetic resonance oximetry. The authors were able to demonstrate a transient improvement from the pre-treatment baseline pO_2 on day 3 following treatment with a conventional schedule of gemcitabine (150 mg/kg given on days 1, 8, and 15) but no significant change in the tumour pO_2 on treatment with metronomic gemcitabine at 25 mg/kg given on days 1, 3 and 5 for 3 weeks. However, tumour pO_2 increased significantly on days 15-18 during treatment with a metronomic gemcitabine at 15 mg/kg given on days 1, 3 and 5 for 3 weeks. Tumour growth was retarded with all the gemcitabine regimens and the authors attributed the improvement in hypoxia to vascular remodelling, which appears to conflict with the anti-angiogenic hypotheses as to how metronomic chemotherapy worked, discussed earlier.

A reduction in hypoxia was seen on both IVIS bioluminescence imaging and on immunohistochemistry (See Figs. 7.1 and 7.4). The effects were greatest with docetaxel at 1 mg/kg and gemcitabine at 5 mg/kg, although most pronounced with the former. Neither dosing regimens were associated with toxicity in the mice, with no change in the rate of weight loss observed, which was used as a surrogate marker (See Fig. 7.2 C). However, there was a significant reduction in the rate of tumour volume growth with both doses of docetaxel (See Fig. 7.2 B). A possible explanation for this can be seen in Fig. 7.3 A, where the concentration of docetaxel measured in both the plasma and tumour at the 1 mg/kg regimen exceeded 20 nM and 40 nM respectively. These concentrations are known to be cytotoxic despite selecting a dose that was considerably lower than what has been used in the literature and is the most likely explanation for the reduction in growth. It is possible that the frequency of dosing (3x/week) may be responsible, since the drug is extensively bound in the plasma and may have resulted in a cumulative effect. Brunsvig and colleagues had demonstrated that median docetaxel plasma levels of 3 nM could be obtained 72 hours after a dose of 20 mg/m^2 but attempting to convert this into a mg/kg dosing regimen was not possible [323]. It is therefore difficult to assess the significance of the improvement in hypoxia in the *in vivo* experiments for docetaxel. On the other hand, there was no significant reduction in tumour volume growth with gemcitabine and levels of the drug in the plasma and tumour were less than 2 nM. However, as discussed previously, gemcitabine has a very short half-life and thus this measurement is difficult to interpret. The inactive metabolite of gemcitabine, dFdU, can be measured and the recordable levels confirm that gemcitabine entered the systemic circulation of the mice. The higher levels in the plasma as compared with the tumours suggest perhaps the drug is saturated within the tissue. Due to the pharmacokinetic properties of gemcitabine, it is very difficult to determine the actual concentration of the gemcitabine from the levels of dFdU but the unchanged tumour growth rate suggests that this did not reach cytotoxic concentrations as seen with docetaxel. Furthermore, it is known that dFdU itself does not have any cytotoxic effects but has been shown to have radiosensitising effects, which will be explored in Chapter 8 [336].

The improvement in tumour hypoxia with low dose gemcitabine is supported in the literature [241, 315]. However, these studies postulate that this improvement is as a result of improved perfusion and did not explore other possible mechanisms for doing so. Furthermore, although gemcitabine at low dose was investigated, none of the studies utilised concentrations or doses as low as the ones we used and thus these findings, along with the data on mitochondrial function and possible senescence as demonstrated in Chapter 6, offer a potential novel discovery.

CHAPTER 8: IMPROVING HYPOXIA BY REDUCING OXYGEN CONSUMPTION CAN IMPROVE RADIOSENSITIVITY

8.1 Aims

1. To investigate the effects of docetaxel and gemcitabine on radiosensitivity in monolayer, spheroids and *in vivo*.
2. To determine whether sub-cytotoxic concentrations/sub-therapeutic doses of docetaxel and gemcitabine confer radiosensitivity.

8.2 Introduction

8.2.1 Radiotherapy as a primary or adjunct cancer treatment option

As briefly mentioned in Chapter 1, radiotherapy offers one of three main therapeutic approaches against cancer. It is commonly delivered as a single therapy or as an adjunct with chemotherapy, surgery or both. Ionising radiation works by creating highly reactive oxygen free radicals which leads to DNA damage and disruption of the tumour cell membrane. Oxygen stabilises these free radicals to perpetuate their action, therefore in hypoxia, these radicals are short-lived and a greater amount of radiation is required to have the same effect. Although cells, malignant and non-malignant, are capable of repairing themselves, apoptosis is induced if the damage is too severe [337]. However, the response to radiation differs between cell types and an understanding of the mechanisms responsible for these differences is required in order to optimise treatment and minimise side-effects [338]. Presently, it is estimated that approximately 50% of all cancer patients will receive radiotherapy at some point through the course of their disease [339]. Comparatively, it remains the most cost-effective treatment modality for cancer, accounting for approximately 5% of total cost of cancer care in many developed countries [340, 341].

8.2.2 Docetaxel and gemcitabine as radiosensitisers

Both docetaxel and gemcitabine have been shown to have radiosensitising effects, although it is uncommon for either to be primarily used for that purpose and even rarer in colorectal cancer [303, 323, 342-348].

The principle behind using docetaxel as a radiation sensitiser comes from its ability to arrest proliferating cells in the G_2/M phase of the cell cycle which is the most radiosensitive phase of the cell cycle [348]. Sulfhydryl containing molecules, which are endogenous radiation protectors, are at their lowest concentrations in the cell during G_2/M. These molecules confer

cytoprotection by free-radical scavenging, which protects against the oxygen free-radical generation by ionising radiation and by hydrogen atom donation to facilitate DNA damage repair. Docetaxel induces mitotic arrest and apoptosis in a concentration-dependent fashion, as shown in Chapter 3 and has also been shown to induce apoptosis without G_2/M arrest at low concentration [349-351]. However, the results in Chapter 6 demonstrated that G_2/M arrest still occurred at 1 nM and 3 nM concentrations. Other mechanisms of enhancing radiosensitivity include docetaxel's ability to: a) cause tumour re-oxygenation; b) eliminate radioresistant S phase cells; c) inhibit tumour angiogenesis at low concentrations by inhibiting endothelial cell differentiation, migration and proliferation and d) stimulate anti-tumour immune resistance mechanisms [352-354]. Finally, docetaxel has been shown to increase the therapeutic index when combined with radiotherapy *in vivo* in murine human xenograft tumour models, as well as in humans with advanced malignancy in Phase I and II trials [355-358].

In contrast, the mechanisms by which gemcitabine improve radiosensitivity are not wholly understood. Current evidence suggests that depletion of dATP nucleotide pools, cell cycle S phase arrest, reduction of the apoptotic threshold, inhibition of DNA synthesis and of DNA repair may contribute to or mediate radiosensitisation [343, 345, 359]. In Chapter 6, gemcitabine induced both an arrest in the cell cycle at S phase and reduced dATP levels on HPLC, albeit modestly in the latter. However, it was concluded that the low concentrations of gemcitabine likely did not affect the activity of RNR, as dNTP levels did not change significantly. Therefore any improvement in radiosensitisation is likely to occur independently from this potential mechanism. As discussed in Chapter 7, gemcitabine rapidly undergoes deamination to dFdU, resulting in a plasma half-life of gemcitabine of between 8-20 minutes, whilst the plasma half-life of dFdU itself is close to 50 hours, at levels known to cause growth inhibition [204]. Crucially, although dFdU has limited cytotoxic activity, it has a dose-dependent radiosensitising effect *in vitro* and potentially contributes to radiosensitisation clinically [345]. dFdU enhances radiation-induced chromosomal aberrations which point towards interruption

of DNA damage repair and has also been shown to impede homologous recombination (HR) [360, 361]. Interruption of HR is associated with increased radiosensitivity and has been observed in HR-knockdown irs1 and irs1SF hamster cell lines and in HR-knockdown *Drosophila melanogaster* [362]. However, increased radiosensitivity was not seen in HR-knockdown mice, suggesting that the role of HR interruption on radiotherapy may be minor [363].

8.2.3 Radiation experiments in spheroids

The benefit of using spheroids as a model for cancer was extensively discussed in Chapter 5 and their role in determining radiotherapy response, sensitivity and cellular interactions remains significant. Sutherland and colleagues were able to demonstrate and obtain multi-component survival curves following irradiation of multi-cell spheroids of a variety of different cell lines [364]. They were able to determine the presence of resistant cell populations through changes in the slope of the survival curves in the regions of high radiation doses. Consequently, spheroids have become an important tool in accessing the effects of cellular dynamics and radiation absorbance owing to the reproducible and consistent spherical geometry, which also facilitates the use of mathematical modelling [365, 366].

8.2.4 Mathematical modelling and radiation response

There are several models that have been used to quantify the effect of radiation on cell survival. Very early attempts at modelling simply looked at the linear growth of tumours in response to radiation, for example, experimental measurements of Jensen's rat tumour were used to calculate the rate of growth of irradiated sarcomas [367]. The linear-quadratic model is now most often used to describe the cell survival curve and has become the *de facto* standard [368]. The model is based on the assumption there are two mechanisms of radiation induced cell death: 1) a single lethal event or 2) the additive effect of multiple harmful but non-lethal events. A single lethal event leads to an exponent that is linearly related to dose. However, the

survival fraction function for multiple events carries an exponent that is proportional to the square of dose; hence the term linear-quadratic. The success of using this model is elegantly demonstrated by Rockne and colleagues who combined it with proliferation and migration rates describing tumour growth and expansion to successfully predict response to radiotherapy [369].

8.3 Results

8.3.1 Sub-cytotoxic concentrations of docetaxel and gemcitabine enhance radiosensitivity in DLD1 and HCT116 cells grown as monolayers

To determine the effects of sub-cytotoxic concentrations of docetaxel and gemcitabine on radiation sensitivity, DLD1 and HCT116 cells were seeded at densities between 200 and 40,000 directly proportional to the radiotherapy dose, allowed to adhere and then treated for 24 hours with either docetaxel at 1 nM and 3 nM or gemcitabine at 20 nM and 50 nM concentrations. The cells were then irradiated at 0, 2, 4, 6, 8 or 10 Gy using a Caesium irradiator and then allowed to form colonies for 14 days. The linear-quadratic formula was used to calculate survival fractions. Docetaxel enhances radiosensitivity in both DLD1 and HCT116 cell lines but only at 3 nM concentration with the former (See Fig. 8.1 A). Gemcitabine enhances radiosensitivity and at both concentrations in both DLD1 and HCT116 cell lines, with the most prominent effect at 50 nM (See Fig. 8.1 B).

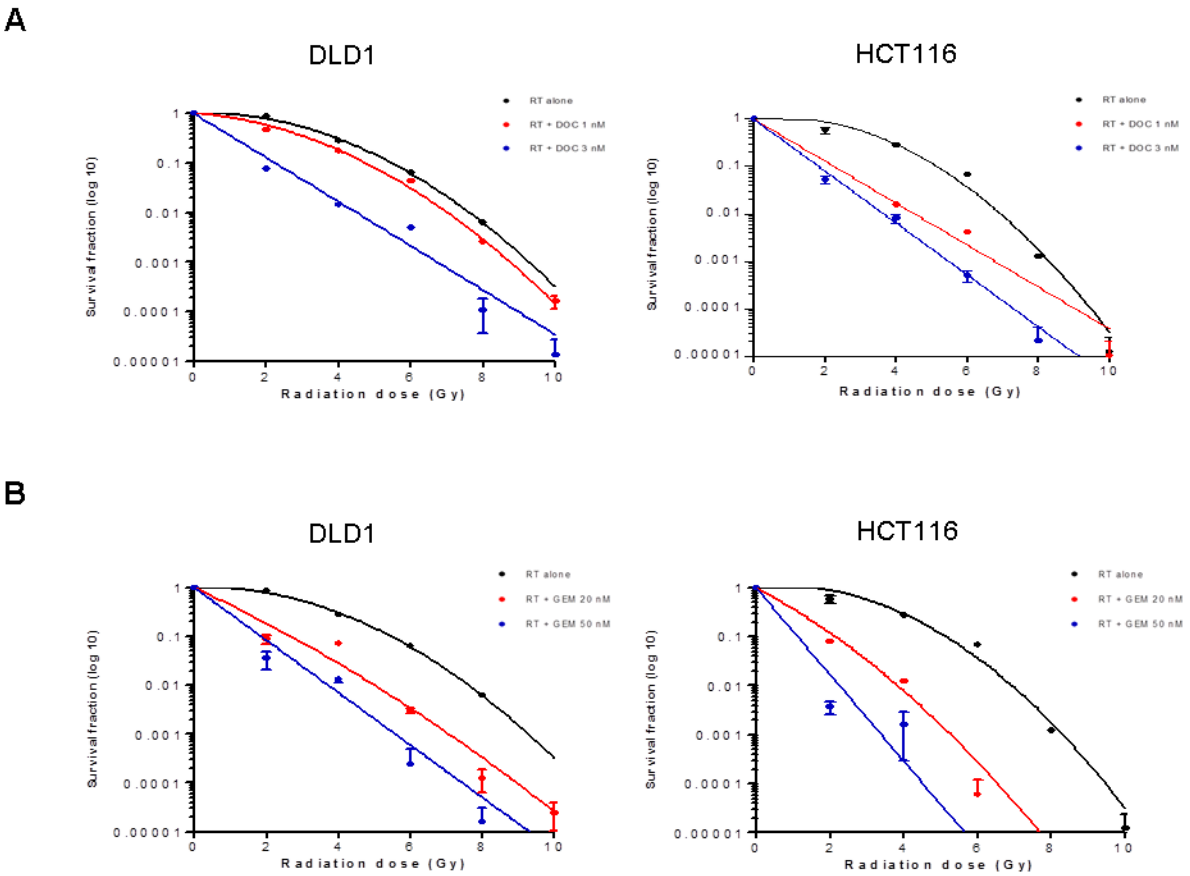

Figure 8.1. Docetaxel and gemcitabine enhance radiosensitivity in DLD1 and HCT116 cells in monolayer. A. Survival curves of DLD1 and HCT116 cells treated with docetaxel and incremental doses of radiation (Gy). B. Survival curves of DLD1 and HCT116 cells treated with gemcitabine and incremental doses of radiation (Gy). Survival curves were generated using the linear-quadratic model. Data is representative of 3 independent experiments, each with at least three replicates. Error bars represent SEM.

8.3.2 Sub-cytotoxic concentrations of docetaxel and gemcitabine enhance radiosensitivity in DLD1 and HCT116 spheroids

To determine whether the radiosensitising effects of docetaxel and gemcitabine were seen in spheroids, spheroids were grown for 4 days and similar sized ones grouped together to receive radiotherapy alone or with treatment. Spheroids were then allowed to grow for a further two weeks and their diameters recorded every 2-3 days. Disaggregated DLD1 and HCT116 spheroids were treated with increasing doses of radiation to determine cell survival curves (See Fig. 8.2 A). All spheroids had a roughly linear reduction in radii with time. Docetaxel enhanced the radiosensitivity of DLD1 spheroids at both concentrations, resulting in greater reduction in radii with time (See Fig. 8.2 B). Gemcitabine also enhanced the radiosensitivity of DLD1 spheroids at both concentrations but with greater effect observed and an even greater reduction in radii with time (See Fig. 8.2 C).

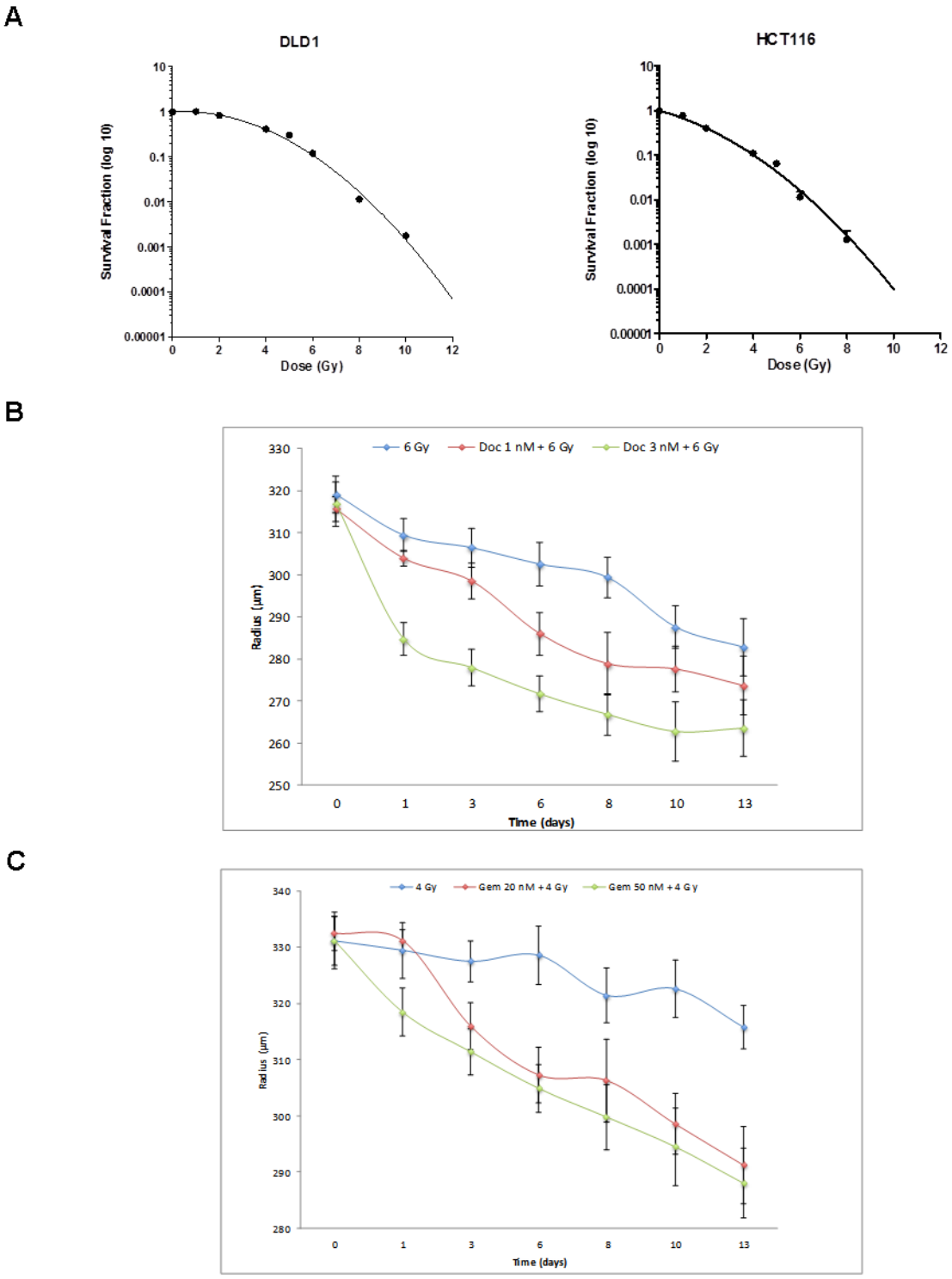

Figure 8.2. Docetaxel and gemcitabine enhance radiosensitivity in DLD1 and HCT116 spheroids. A. Cell survival curves for disaggregated DLD1 and HCT116 spheroids treated with incremental doses of radiation (Gy). B. Growth curves of DLD1 spheroids treated with 6 Gy radiation alone or with docetaxel at 1 nM and 3 nM concentrations. C. Growth curves of DLD1 spheroids treated with 4 Gy radiation alone or with gemcitabine at 20 nM and 50 nM concentrations. The survival curves were generated using the linear quadratic model. Each data point represents at least 8 spheroids. A set of representative spheroids were chosen and their radii averaged. The error bars represent standard deviation.

8.3.3 Sub-therapeutic doses of docetaxel and gemcitabine enhance radiosensitivity in subcutaneous DLD1 xenografts in mice

To determine whether sub-therapeutic doses of docetaxel and gemcitabine enhanced radiosensitivity *in vivo*, mice inoculated with DLD1 HRE-Luciferase cells by subcutaneous injection were allowed to reach a tumour volume of 80 mm^3 before commencing treatment with either agent 3 times/week. Tumours then received a single dose of radiation at 6 Gy on day 7 and allowed to reach a maximum tumour volume of 300 mm^3 or for a maximum period of 28 days, whichever was sooner. Tumour measurements were performed on alternate days. Radiation alone retarded tumour growth whilst both docetaxel and gemcitabine enhanced the effect of radiation in the DLD1 tumours, with a growth delay observed at all tested doses (See Fig. 8.3). Docetaxel appeared to have a greater radiosensitising effect than gemcitabine did. The control group reached maximum tumour volume by day 26-28 whereas the other groups did not.

A

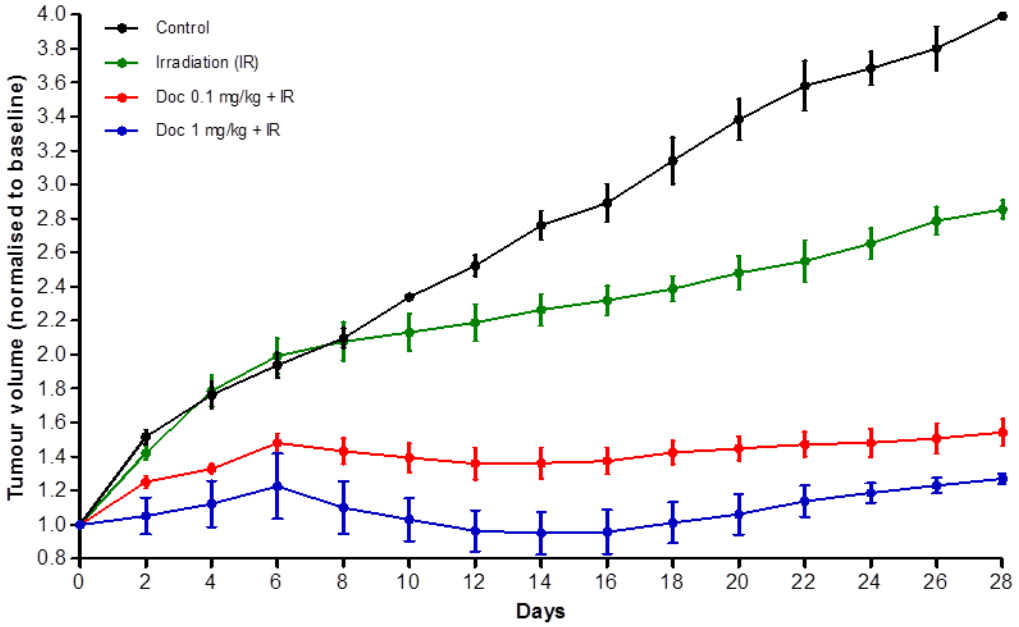

B

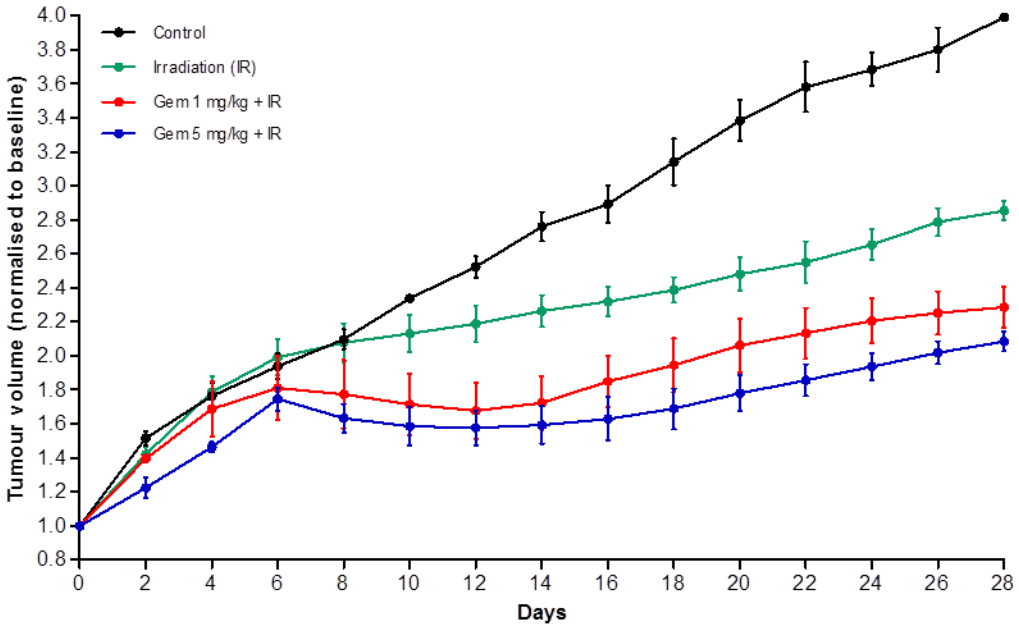

Figure 8.3. Docetaxel and gemcitabine enhance radiosensitivity in subcutaneous DLD1 tumours. A. Tumour volume growth curves of DLD1 tumours treated with radiation alone or with docetaxel at 0.1 mg/kg and 1 mg/kg doses. B. Tumour volume growth curves of DLD1 tumours treated with radiation alone or with gemcitabine at 1 mg/kg and 5 mg/kg doses. Treatments were administered 3x/wk via I.P. injection on days 0, 3 and 6, followed by a single dose of radiation at 6 Gy on day 7. Each group had at least 4 mice and entered into study once tumour volume reached 80 mm^3 and allowed to develop to a maximum volume of 300 mm^3 or for a maximum period of 28 days after first treatment.

8.4 Discussion

Docetaxel and gemcitabine are known radiosensitisers. The results of this chapter demonstrate a radiosensitising effect with both drugs across the monolayer, spheroid and *in vivo* experimental platforms. This is apparent despite evidence in the literature of variable effectiveness in radiosensitising colorectal tumour cell lines [343, 348]. Neither agent is used as a radiosensitiser as its primary role or as a monotherapy in colorectal cancer.

The radiosensitising effect by docetaxel and gemcitabine seen in monolayer and in spheroids was achieved despite using very low, sub-cytotoxic concentrations (See Figs. 8.1 and 8.2). However, there is considerable evidence in the literature that supports these findings [303, 342, 343]. Radiosensitisation with gemcitabine has been achieved at 10 nM and 20 nM concentrations in colorectal and bladder tumour cell lines respectively, with the latter demonstrating little change in the nucleotide pools, corroborating the findings presented in Chapter 6 [303, 343]. The significance of this is that one of the principle proposed mechanisms of action of gemcitabine in improving radiosensitivity is the inhibition of RNR, leading to perturbation of dNTP pools, especially dATP. This is supported with evidence that dATP-pool depletion following gemcitabine treatment occurs with a time course that correlates with radiosensitisation for both colon and pancreatic tumour cells [370, 371]. However, the results of the experiments in Chapter 6 demonstrated that gemcitabine did not appear to significantly affect nucleotide pools at these concentrations and thus this potential explanation is not valid in this circumstance. However, radiosensitisation does appear to be affected by cell cycle phase. Lawrence TS and colleagues demonstrated that the maximum radiosensitisation achieved using a 4 hour exposure to gemcitabine at 10 nM concentration in the HT29 cell line was an enhancement ratio of 1.4, whereas 24 hour exposure achieved an enhancement ratio of 1.8. This longer exposure was accompanied by redistribution of cells into S phase [370]. Since gemcitabine was demonstrated to arrest cells in S phase at 20 nM and 50 nM concentrations, this is a plausible explanation for these results. The same can also be inferred for docetaxel,

which was demonstrated to arrest cells at G_2/M phase and it is through this phase arrest that the drug has been conclusively shown to enhance radiosensitivity [348].

Spheroid radii reduced with time following intervention with docetaxel or gemcitabine and/or radiation (See Fig 8.2). It is not unexpected to see a growth delay with radiation, as cellular arrest and death results in a temporary loss in volume but mitosis eventually resumes. This is supported by evidence that spheroids have been shown to grow according to the exponential law for up to 28 days, even after minor to moderate lethal interruption[372]. However, in this instance, the spheroids continued to shrink with no evidence of a return to growth after two weeks of measurements. The continued loss in size may be due to the interventions being significant enough to prevent regrowth or it can possibly be attributed to cell shedding. It has been theorised that cell shedding occurs due to the loosening of cell-to-cell attachments but the effects of this process are still largely unknown [373]. Cell shedding occurs close to M phase and the detached cells continue to progress through the cell cycle. One study reported that radiation did not have an effect on the number of cells shed from spheroids. However, the number of clonogenic cells decreased significantly with increasing doses of radiation [374]. When mathematical modelling is applied to this phenomenon to investigate the nature of cell shedding, it was demonstrated that this process was unlikely to be intense enough to cause growth saturation of spheroids [375]. Consequently, the growth kinetics observed in this experiment needs to be further investigated.

Docetaxel appeared to have a greater radiosensitising effect than gemcitabine on tumour volume growth retardation over the course of the 21 days post irradiation (See Fig. 8.3 A). However, in the preceding days to irradiation, docetaxel also appeared to have a tumour growth retardation effect that could only really be attributed to the effect of the drug itself. Although the results highlighted in Chapter 7 demonstrated a possible retarding effect of docetaxel, this was not statistically significant. The sub-therapeutic dosing of the agent should minimise cell

death, although it is very difficult to compare the results of sub-cytotoxic concentrations *in vitro* to sub-therapeutic doses *in vivo*. However with the introduction of radiation on day 7, there is a drop in the average tumour volume at both tested doses not seen with radiation alone, which suggests a synergistic, radiosensitising effect. This is similarly observed with gemcitabine although there is no tumour volume growth retardation seen with the drug alone in the first week of measurements (See Fig. 8.3 B).

As the mechanisms by which docetaxel enhances radiosensitivity have been decisively confirmed in the literature and the results presented here are in keeping with these findings, focus on how else gemcitabine may enhance radiosensitivity will be discussed specifically. Ionising radiation causes DNA double-strand breaks and is the critical lesion to induce cell death. However, gemcitabine does not appear to increase radiation-induced damage or decrease damage repair during the first 4 hours after irradiation, suggesting that gemcitabine does not affect the primary DNA lesion but the consequences of this lesion [376, 377].

It has therefore been suggested that gemcitabine could act as a radiation sensitiser by lowering the threshold for radiation-induced apoptosis. There is considerable evidence that several chemotherapeutic drugs, including gemcitabine, can activate the cellular apoptotic machinery [378]. One study looked at comparing human tumour cell lines which had been sensitised by gemcitabine (HT29, SW620 and UMSSCC-6) to those which had not (A549) and found that gemcitabine significantly enhanced apoptosis in the former [343]. The authors also found that although apoptosis played a relatively minor role in the clonogenic death produced by radiation alone, it accounted for a substantial fraction of the loss of clonogenicity produced by the combination of gemcitabine and radiation, suggesting that gemcitabine shifts the pattern of radiation-induced cell death from a non-apoptotic to an apoptotic mechanism. However, the effect of gemcitabine was highly variable across the different cell lines, a phenomenon that has been discussed previously. HT29 and A549 cells showed similar sensitivity to the cytotoxic

concentrations of gemcitabine but A549 cells were not radiosensitised by non-cytotoxic concentrations. Furthermore, exposure to gemcitabine prior to radiation did not result in an increase in radiation-induced apoptosis. This evidence would seem to support that apoptosis plays a key role in gemcitabine-mediated radiosensitisation. However, the experiments shown in Chapter 5 did not correlate with this hypothesis, as there was no statistical difference in the population of apoptotic cells in gemcitabine treated DLD1 spheroids, despite the results in this chapter demonstrating a clear radiosensitising effect.

It is apparent that both docetaxel and gemcitabine have radiosensitising effects in the DLD1 and HCT116 cell lines, which has been extensively demonstrated in and is supported by the literature. The mechanisms by which this occurs has yet to be clearly elucidated, especially with gemcitabine and therefore further research is necessary.

CHAPTER 9: CONCLUDING REMARKS

9.1 Overall conclusions

The first aim of this D.Phil was to identify whether established chemotherapy agents may reduce oxygen consumption independent of toxicity. The work presented in Chapters 3 and 4 demonstrated that some of the agents at very low dose resulted in minimal cell death and that a number of these agents were then capable of reducing OCR in colorectal cancer cell lines. This reduction was variable across the different cell lines and with the different drugs. Docetaxel and gemcitabine were selected for further investigation and characterisation after fulfilling the criteria of sub-cytotoxicity and ability to reduce OCR. The work presented in Chapter 6 attempted to elucidate the mechanisms by which these two agents achieved this and there was evidence to suggest that alterations in oxidative phosphorylation and/or cell cycle interference were responsible.

The second aim of the D.Phil was to investigate whether it was possible to reduce hypoxia in spheroid and xenograft models of colorectal cancer using sub-cytotoxic/sub-therapeutic treatments and whether the findings identified in Chapter 4 were responsible or contributed to the reduction in hypoxia. Both docetaxel and gemcitabine improved hypoxia in spheroids, which was confirmed both mathematically and via immunofluorescence. The mathematical modelling further supported the link between these agents reducing OCR and the consequent improvement in hypoxia. OCR reduction was therefore at least partly responsible for the improvement. There was also an improvement in hypoxia seen within the core of xenograft tumours on IVIS imaging. Sub-therapeutic doses of docetaxel and gemcitabine given 3x/week resulted in a reduction in the extent of tumour hypoxia. For docetaxel, this effect was likely due to cytotoxicity for two reasons: 1) tumour development was retarded with treatment and 2) metabolite concentrations in plasma and in tumours exceeded those tested *in vitro*, reaching

levels used to achieve cytotoxicity. This finding was surprising, as the selected doses were not expected to be cytotoxic. For gemcitabine, the reduction in tumour hypoxia was likely a result of decreased oxygen consumption, as tumour growth rates did not change during treatment.

The final aim of the D.Phil was to determine whether an improvement in tumour hypoxia can lead to an improvement in radiosensitivity. As illustrated in Chapter 8, both docetaxel and gemcitabine improved radiosensitivity across the monolayer, spheroid and *in vivo* experimental platforms. Both agents are known to have radiosensitising effects and although the mechanisms by which this is achieved are reasonably well understood for docetaxel, the same cannot be said for gemcitabine. The main issue arises from attempting to prove that the improvement in hypoxia is the cause for the improved radiosensitisation. Theoretically this stands to reason, as increased availability of oxygen as a consequence of reduced consumption will allow the stabilisation of free radicals generated by the ionising radiation to perpetuate their action. The results from Chapters 5 and 6 did not support existing theories as to how gemcitabine enhances radiosensitivity such as the inhibition of RNR or lowering of the apoptotic threshold because there was no change in either the nucleotide pools (and by inference, activity of RNR) or the population of apoptotic cells in treated spheroids. However, treated tumour cells were confirmed to enter S phase arrest, which did at least support this theory of action.

The results of OCR reduction and the subsequent hypoxia improvement were consistent across all experimental platforms, which seemed to support this hypothesis. The results in Chapter 6 suggested that alterations in mitochondrial function may be responsible for the hypoxia improvement as there was no associated loss in either mitochondrial mass or electron transport complexes, yet there was clearly a change in coupled respiration seen in both DLD1 and HCT116 cell lines. The results, however, maybe cell line dependent as each may have a naturally oxidative or glycolytic phenotype, which in turn may influence the activity of the drugs

on hypoxia. This appeared to be the case for DLD1 and HCT116, with the former more oxidative and the latter more glycolytic.

Another potential explanation as to why these two agents improve tumour hypoxia may indeed be independent of any action on oxidative phosphorylation and mitochondrial function. In Chapter 6, it was demonstrated that sub-cytotoxic concentrations of docetaxel and gemcitabine arrest cells in G_2/M and S phase respectively. However, the results from spheroid experiments in Chapter 5 demonstrated no change in the population of apoptotic cells alongside a reduction in the number of proliferating cells. It is therefore possible that these agents are forcing cells in a proliferative state, in which they are highly oxygen consuming, to a senescent state, in which they are not. This dramatic change in the oxygen consumption dynamics results in more oxygen being available for use by other cells, resulting in the prevention of hypoxia developing. Furthermore, this transition seems to occur independently of any apoptotic-inducing mechanisms: either the cellular arrest does not trigger apoptosis or there is some form of inhibition of the apoptotic pathways, which was not explored in this thesis.

In brief, established chemotherapy agents can be used to improve tumour hypoxia via reduction in the OCR of tumour cells. By using sub-cytotoxic concentrations, simple cell death is an unlikely explanation for this reduction and is likely achieved by interruption of mitochondrial function and/or cell cycle. The improvement in hypoxia is associated with an improvement in radiosensitisation, although both drugs are previously known to act as radiosensitisers. However, the improvement in hypoxia via reducing OCR offers a potential explanation as to how gemcitabine works in this manner.

9.2 Limitations of the project

9.2.1 General limitations

The experiments and submission of the D.Phil had to be concluded within a 3 year period owing to the stipulations of taking an Out of Programme for Research (OOPR) break from my clinical training. This was a significant time constraint and will be addressed in the following sections. The original hypothesis of focusing on cell cycle inhibition and its role in tumour hypoxia was changed to focus on the general effects of chemotherapy agents and this slight change in direction meant the repetition of several experiments and the annulment of the results of others.

9.2.2 Specific limitations

There are several limitations to this work, which are presented below and which should be addressed in future work.

9.2.2.1 Chapter 3

The testing concentrations of the drugs were selected from an appraisal of the literature, identifying common cytotoxic concentrations that have been successfully used and deliberately selecting a significantly lower concentration for the experiments. Ideally, detailed cytotoxicity assays for each of the drugs would have been performed, as was done so for docetaxel and gemcitabine (See Fig. 3.3).

9.2.2.2 Chapter 4

All experiments looking at the effect of chemotherapy agents on OCR in the investigated cell lines were performed in normoxic conditions. Cell lines were cultured at atmospheric oxygen and tested at the same oxygen concentration. Ideally, it would have been interesting to

compare the effects of these agents in cells grown in hypoxic conditions. However, the feasibility of doing so was near impossible as it would be necessary to perform the measurements in a closed, controlled system. The metabolic effects of hypoxia are nullified within moments of exposure to normoxia and the XF96 Analyzer did not have the function to control oxygen concentrations within the system as measurements were recorded. The application of treatments, changing of media and transfer from the incubator to the bench or the XF96 Analyzer would all expose atmospheric oxygen concentration to the cells, making it very difficult to interpret any results.

9.2.2.3 Chapter 5

One of the great benefits of using spheroids to model tumour hypoxia is the ability to apply mathematical modelling. However, this is not without potential issue or limitation. The modelling technique applied to the spheroids discussed in this chapter were robust and repeatable but unfortunately was limited to being able to estimate OCR in spheroids were a clear boundary between normoxic and hypoxic cells were apparent. Therefore, one could not use this model to calculate the OCR in spheroids where there was complete reduction of hypoxia, as EF5 staining did not occur and a boundary did not exist. However, one can assume that the OCR in these spheroids was lower than in those where they could be recorded.

With regards measuring apoptosis, it was briefly discussed that the flow cytometry technique employed in this chapter was not a very specific method of detecting apoptosis as cells in late S phase or from G_2 may be missed. To detect apoptosis more specifically, immunohistochemistry using annexin V staining or using the TUNEL assay should be performed. Furthermore, future work should verify whether cells move into a state of senescence and what role, if any, the anti-apoptotic pathways had in changing the proportion of proliferating cells but not changing the proportion of apoptotic cells.

9.2.2.4 Chapter 6

Definite mechanisms by which docetaxel and gemcitabine may improve hypoxia were not identified. Evidence from this thesis suggests that both agents impact on mitochondrial function and on cell cycle and these effects may be responsible for the reduction in OCR and hypoxia improvement. To elucidate the mechanism, future experiments would include mitotic spindle and DNA staining, mitochondrial permeabilisation studies and gene array and/or mass spectrometry. Furthermore, western blot analysis for the electron transport complexes was only performed in the DLD1 cell line due to time constraints and ideally, would also be performed on the HCT116 cell line.

9.2.2.5 Chapter 7

The *in vivo* experiments were commenced in the final year of the D.Phil and due to time constraints, repeats could not be performed. Although the *in vivo* experiments provided some interesting data, the number of mice in each experimental group (4-6), was less than ideal, as was the number of repeat experiments. Furthermore, only the DLD1 cell line, but not the HCT116 cell line, was tested *in vivo*. Comparison of different frequencies of treatment such as daily injection versus 1x/week versus 3x/week would also have been interesting. One final avenue for this work would be to investigate whether improving tumour hypoxia reduces metastases. These experiments would require a different tumour model to optimise for metastases, such as either intracaecal or intrasplenic tumour inoculation as opposed to the subcutaneous model employed in this thesis. Finally, at the time of submission, the quantification data for the histology of the tumours was not yet complete but it is anticipated that this will be done in due course.

9.2.2.6 Chapter 8

Due to time limitations, the tumour growth delay experiments with radiation in mice had to be concluded by day 28 regardless of whether the tumour had reached a volume of 300 mm^3 or not. Ideally, the tumour volume measurements would have continued until the pre-set maximum tumour volume limit had been reached and the duration and enhancing ratio of the radiosensitising effect of the drugs could not be calculated. Furthermore, it would be interesting to compare differences in using fractionated versus single-dose radiotherapy, along with gemcitabine treatment.

9.3 Potential clinical relevance

As with all basic science research, the critical question of its relevance to clinical practice has to be considered. As discussed in Chapter 1, most chemotherapies aim to cure and the majority of these aim to cause cell death. However, this is usually associated with some form of morbidity as a consequence of the side-effects of the drugs. The results presented in this thesis provide an alternative option, which is to use these agents at low-dose as a radiation sensitiser alongside radiotherapy. This would maximise treatment whilst also minimising the side-effects of the drugs. This is particularly useful in radiosensitive tumours and can be offered as a temporary measure whilst waiting for definitive, usually surgical, treatment. Finally, the techniques used throughout this thesis may be applied to test other drugs that have been identified as promising from high throughput screening. This method may find a number of potential agents that reduce tumour hypoxia that were otherwise designed for a different pathology, as was the case with metformin and is presently being explored by my colleague Dr. Thomas Ashton.

9.4 Future directions

Whilst we attempted to identify the mechanisms that may be responsible for improvements in tumour hypoxia at the tested concentrations, further investigation will be required to elucidate a clearer answer. Furthermore and as discussed, there are several questions and hypotheses that have been raised as a result of this work and it is anticipated that my colleague, Dr. Pavitra Kannan will proceed in further investigating these. Finally, there were several promising agents from preliminary testing such as fluorouracil and VX680, that could have been investigated further alongside or instead of docetaxel and gemcitabine. Future work arising from this thesis will be able to focus on these other promising agents.

REFERENCES

1. Cunningham, D., W. Atkin, H.J. Lenz, H.T. Lynch, B. Minsky, B. Nordlinger, and N. Starling, *Colorectal cancer.* Lancet, 2010. **375**(9719): p. 1030-47.
2. Massat, N.J., P.D. Sasieni, D. Parmar, and S.W. Duffy, *An ongoing case-control study to evaluate the NHS Bowel Cancer Screening Programme.* BMC Cancer, 2014. **14**(1): p. 945.
3. Ferlay, J., E. Steliarova-Foucher, J. Lortet-Tieulent, S. Rosso, J.W. Coebergh, H. Comber, D. Forman, and F. Bray, *Cancer incidence and mortality patterns in Europe: estimates for 40 countries in 2012.* Eur J Cancer, 2013. **49**(6): p. 1374-403.
4. Jones, A.M., E. Morris, J. Thomas, D. Forman, J. Melia, and S.M. Moss, *Evaluation of bowel cancer registration data in England, 1996-2004.* Br J Cancer, 2009. **101**(8): p. 1269-73.
5. Ferlay, J., I. Soerjomataram, R. Dikshit, S. Eser, C. Mathers, M. Rebelo, D.M. Parkin, D. Forman, and F. Bray, *Cancer incidence and mortality worldwide: Sources, methods and major patterns in GLOBOCAN 2012.* Int J Cancer, 2015. **136**(5): p. E359-86.
6. Network, C.R.U.a.N.C.I., *Cancer by deprivation in England: Incidence, 1996-2010, Mortality, 1997-2011.* 2014, NCIN: London.
7. Chan, D.S., R. Lau, D. Aune, R. Vieira, D.C. Greenwood, E. Kampman, and T. Norat, *Red and processed meat and colorectal cancer incidence: meta-analysis of prospective studies.* PLoS One, 2011. **6**(6): p. e20456.
8. Zhivotovskiy, A.S., A.G. Kutikhin, A.Z. Azanov, A.E. Yuzhalin, Y.A. Magarill, and E.B. Brusina, *Colorectal cancer risk factors among the population of South-East Siberia: a case-control study.* Asian Pac J Cancer Prev, 2012. **13**(10): p. 5183-8.
9. Theodoratou, E., S.M. Farrington, A. Tenesa, G. McNeill, R. Cetnarskyj, E. Korakakis, F.V. Din, M.E. Porteous, M.G. Dunlop, and H. Campbell, *Associations between dietary and lifestyle risk factors and colorectal cancer in the Scottish population.* Eur J Cancer Prev, 2014. **23**(1): p. 8-17.
10. Aune, D., D.S. Chan, R. Lau, R. Vieira, D.C. Greenwood, E. Kampman, and T. Norat, *Dietary fibre, whole grains, and risk of colorectal cancer: systematic review and dose-response meta-analysis of prospective studies.* Bmj, 2011. **343**: p. d6617.
11. Lee, K.J., M. Inoue, T. Otani, M. Iwasaki, S. Sasazuki, and S. Tsugane, *Physical activity and risk of colorectal cancer in Japanese men and women: the Japan Public Health Center-based prospective study.* Cancer Causes Control, 2007. **18**(2): p. 199-209.
12. De Pergola, G. and F. Silvestris, *Obesity as a major risk factor for cancer.* J Obes, 2013. **2013**: p. 291546.
13. Shin, A., K.Z. Kim, K.W. Jung, S. Park, Y.J. Won, J. Kim, D.Y. Kim, and J.H. Oh, *Increasing trend of colorectal cancer incidence in Korea, 1999-2009.* Cancer Res Treat, 2012. **44**(4): p. 219-26.
14. Haggar, F.A. and R.P. Boushey, *Colorectal cancer epidemiology: incidence, mortality, survival, and risk factors.* Clin Colon Rectal Surg, 2009. **22**(4): p. 191-7.
15. Howlader N, N.A., Krapcho M, Garshell J, Miller D, Altekruse SF, et al., *SEER Cancer Statistics Review, 1975-2011*. 2014, National Cancer Institute. Bethesda, MD.

16. Siegel, R., C. DeSantis, K. Virgo, K. Stein, A. Mariotto, T. Smith, D. Cooper, T. Gansler, C. Lerro, S. Fedewa, C. Lin, C. Leach, R.S. Cannady, H. Cho, S. Scoppa, M. Hachey, R. Kirch, A. Jemal, and E. Ward, *Cancer treatment and survivorship statistics, 2012.* CA Cancer J Clin, 2012. **62**(4): p. 220-41.
17. Jones, S., W.D. Chen, G. Parmigiani, F. Diehl, N. Beerenwinkel, T. Antal, A. Traulsen, M.A. Nowak, C. Siegel, V.E. Velculescu, K.W. Kinzler, B. Vogelstein, J. Willis, and S.D. Markowitz, *Comparative lesion sequencing provides insights into tumor evolution.* Proc Natl Acad Sci U S A, 2008. **105**(11): p. 4283-8.
18. Jackson-Thompson, J., F. Ahmed, R.R. German, S.M. Lai, and C. Friedman, *Descriptive epidemiology of colorectal cancer in the United States, 1998-2001.* Cancer, 2006. **107**(5 Suppl): p. 1103-11.
19. Wilmink, A.B., *Overview of the epidemiology of colorectal cancer.* Dis Colon Rectum, 1997. **40**(4): p. 483-93.
20. Sampson, J.R. and N. Jones, *MUTYH-associated polyposis.* Best Pract Res Clin Gastroenterol, 2009. **23**(2): p. 209-18.
21. Davis, H., S. Irshad, and M. Bansal, *Aberrant epithelial GREM1 expression initiates colonic tumorigenesis from cells outside the stem cell niche.* 2015. **21**(1): p. 62-70.
22. Sakamoto, T., G. Mori, M. Yamada, Y. Kinjo, E. So, S. Abe, Y. Otake, T. Nakajima, T. Matsuda, and Y. Saito, *Endoscopic submucosal dissection for colorectal neoplasms: a review.* World J Gastroenterol, 2014. **20**(43): p. 16153-8.
23. Edge, S.B. and C.C. Compton, *The American Joint Committee on Cancer: the 7th edition of the AJCC cancer staging manual and the future of TNM.* Ann Surg Oncol, 2010. **17**(6): p. 1471-4.
24. Wray, C.M., A. Ziogas, M.W. Hinojosa, H. Le, M.J. Stamos, and J.A. Zell, *Tumor subsite location within the colon is prognostic for survival after colon cancer diagnosis.* Dis Colon Rectum, 2009. **52**(8): p. 1359-66.
25. Boland, C.R. and A. Goel, *Microsatellite Instability in Colorectal Cancer.* Gastroenterology, 2010. **138**(6): p. 2073-2087.e3.
26. Scheele, J., R. Stang, A. Altendorf-Hofmann, and M. Paul, *Resection of colorectal liver metastases.* World J Surg, 1995. **19**(1): p. 59-71.
27. Fernandez, F.G., J.A. Drebin, D.C. Linehan, F. Dehdashti, B.A. Siegel, and S.M. Strasberg, *Five-year survival after resection of hepatic metastases from colorectal cancer in patients screened by positron emission tomography with F-18 fluorodeoxyglucose (FDG-PET).* Ann Surg, 2004. **240**(3): p. 438-47; discussion 447-50.
28. Hornbech, K., J. Ravn, and D.A. Steinbruchel, *Outcome after pulmonary metastasectomy: analysis of 5 years consecutive surgical resections 2002-2006.* J Thorac Oncol, 2011. **6**(10): p. 1733-40.
29. Inoue, M., Y. Kotake, K. Nakagawa, K. Fujiwara, K. Fukuhara, and T. Yasumitsu, *Surgery for pulmonary metastases from colorectal carcinoma.* Ann Thorac Surg, 2000. **70**(2): p. 380-3.
30. Poston, G.J., D. Tait, S. O'Connell, A. Bennett, and S. Berendse, *Diagnosis and management of colorectal cancer: summary of NICE guidance.* Bmj, 2011. **343**: p. d6751.
31. Yang, T.J. and K.A. Goodman, *Predicting complete response: is there a role for non-operative management of rectal cancer?* Journal of Gastrontestinal Oncology, 2015. **6**(2): p. 241-246.
32. Krumbhaar, E., *Role of the blood and the bone marrow in certain forms of gas poisoning.* Journal of the American Medical Association, 1919. **72**(1): p. 39-41.

33. Goodman, L.S., M.M. Wintrobe, and et al., *Nitrogen mustard therapy; use of methyl-bis (beta-chloroethyl) amine hydrochloride and tris (beta-chloroethyl) amine hydrochloride for Hodgkin's disease, lymphosarcoma, leukemia and certain allied and miscellaneous disorders.* J Am Med Assoc, 1946. **132**: p. 126-32.
34. Corrie, P.G. and G. Pippa, *Cytotoxic chemotherapy: clinical aspects.* Medicine, 2008. **36**(1): p. 24-28.
35. Lind, M.J., *Principles of cytotoxic chemotherapy.* Medicine, 2008. **36**(1): p. 19–23.
36. Malhotra, V. and M.C. Perry, *Classical chemotherapy: mechanisms, toxicities and the therapeutic window.* Cancer Biol Ther, 2003. **2**(4 Suppl 1): p. S2-4.
37. Tucker, M.A., A.T. Meadows, J.D. Boice, Jr., M. Stovall, O. Oberlin, B.J. Stone, J. Birch, P.A. Voute, R.N. Hoover, and J.F. Fraumeni, Jr., *Leukemia after therapy with alkylating agents for childhood cancer.* J Natl Cancer Inst, 1987. **78**(3): p. 459-64.
38. Chen, X., Y. Wu, H. Dong, C.Y. Zhang, and Y. Zhang, *Platinum-based agents for individualized cancer treatment.* Curr Mol Med, 2013. **13**(10): p. 1603-12.
39. Parker, W.B., *Enzymology of purine and pyrimidine antimetabolites used in the treatment of cancer.* Chem Rev, 2009. **109**(7): p. 2880-93.
40. Minotti, G., P. Menna, E. Salvatorelli, G. Cairo, and L. Gianni, *Anthracyclines: molecular advances and pharmacologic developments in antitumor activity and cardiotoxicity.* Pharmacol Rev, 2004. **56**(2): p. 185-229.
41. Goodsell, D.S., *The molecular perspective: DNA topoisomerases.* Stem Cells, 2002. **20**(5): p. 470-1.
42. Nitiss, J.L., *Targeting DNA topoisomerase II in cancer chemotherapy.* Nat Rev Cancer, 2009. **9**(5): p. 338-50.
43. Alberts, B., A. Johnson, J. Lewis, M. Raff, K. Roberts, and P. Walter, *Molecular Biology of the Cell*. 4th ed. 2002, New York: Garland Science.
44. Yue, Q.X., X. Liu, and D.A. Guo, *Microtubule-binding natural products for cancer therapy.* Planta Med, 2010. **76**(11): p. 1037-43.
45. Gerber, D.E., *Targeted therapies: a new generation of cancer treatments.* Am Fam Physician, 2008. **77**(3): p. 311-9.
46. Hoogsteen, I.J., H.A. Marres, A.J. van der Kogel, and J.H. Kaanders, *The hypoxic tumour microenvironment, patient selection and hypoxia-modifying treatments.* Clin Oncol (R Coll Radiol), 2007. **19**(6): p. 385-96.
47. Nordsmark, M., M. Overgaard, and J. Overgaard, *Pretreatment oxygenation predicts radiation response in advanced squamous cell carcinoma of the head and neck.* Radiother Oncol, 1996. **41**(1): p. 31-9.
48. Brizel, D.M., R.K. Dodge, R.W. Clough, and M.W. Dewhirst, *Oxygenation of head and neck cancer: changes during radiotherapy and impact on treatment outcome.* Radiother Oncol, 1999. **53**(2): p. 113-7.
49. Thomlinson, R.H. and L.H. Gray, *The histological structure of some human lung cancers and the possible implications for radiotherapy.* Br J Cancer, 1955. **9**(4): p. 539-49.
50. Gray, L.H., A.D. Conger, M. Ebert, S. Hornsey, and O.C. Scott, *The concentration of oxygen dissolved in tissues at the time of irradiation as a factor in radiotherapy.* Br J Radiol, 1953. **26**(312): p. 638-48.
51. Hockel, M., K. Schlenger, C. Knoop, and P. Vaupel, *Oxygenation of carcinomas of the uterine cervix: evaluation by computerized O2 tension measurements.* Cancer Res, 1991. **51**(22): p. 6098-102.
52. Vaupel, P., A. Mayer, and M. Hockel, *Tumor hypoxia and malignant progression.* Methods Enzymol, 2004. **381**: p. 335-54.

53. Fyles, A.W., M. Milosevic, R. Wong, M.C. Kavanagh, M. Pintilie, A. Sun, W. Chapman, W. Levin, L. Manchul, T.J. Keane, and R.P. Hill, *Oxygenation predicts radiation response and survival in patients with cervix cancer.* Radiother Oncol, 1998. **48**(2): p. 149-56.
54. Knocke, T.H., H.D. Weitmann, H.J. Feldmann, E. Selzer, and R. Potter, *Intratumoral pO2-measurements as predictive assay in the treatment of carcinoma of the uterine cervix.* Radiother Oncol, 1999. **53**(2): p. 99-104.
55. Kaanders, J.H., K.I. Wijffels, H.A. Marres, A.S. Ljungkvist, L.A. Pop, F.J. van den Hoogen, P.C. de Wilde, J. Bussink, J.A. Raleigh, and A.J. van der Kogel, *Pimonidazole binding and tumor vascularity predict for treatment outcome in head and neck cancer.* Cancer Res, 2002. **62**(23): p. 7066-74.
56. Nordsmark, M., S.M. Bentzen, V. Rudat, D. Brizel, E. Lartigau, P. Stadler, A. Becker, M. Adam, M. Molls, J. Dunst, D.J. Terris, and J. Overgaard, *Prognostic value of tumor oxygenation in 397 head and neck tumors after primary radiation therapy. An international multi-center study.* Radiother Oncol, 2005. **77**(1): p. 18-24.
57. Carlson, D.J., P.J. Keall, B.W. Loo, Jr., Z.J. Chen, and J.M. Brown, *Hypofractionation results in reduced tumor cell kill compared to conventional fractionation for tumors with regions of hypoxia.* Int J Radiat Oncol Biol Phys, 2011. **79**(4): p. 1188-95.
58. Bristow, R.G. and R.P. Hill, *Hypoxia and metabolism. Hypoxia, DNA repair and genetic instability.* Nat Rev Cancer, 2008. **8**(3): p. 180-92.
59. Erler, J.T., C.J. Cawthorne, K.J. Williams, M. Koritzinsky, B.G. Wouters, C. Wilson, C. Miller, C. Demonacos, I.J. Stratford, and C. Dive, *Hypoxia-mediated down-regulation of Bid and Bax in tumors occurs via hypoxia-inducible factor 1-dependent and -independent mechanisms and contributes to drug resistance.* Mol Cell Biol, 2004. **24**(7): p. 2875-89.
60. Rouschop, K.M., T. van den Beucken, L. Dubois, H. Niessen, J. Bussink, K. Savelkouls, T. Keulers, H. Mujcic, W. Landuyt, J.W. Voncken, P. Lambin, A.J. van der Kogel, M. Koritzinsky, and B.G. Wouters, *The unfolded protein response protects human tumor cells during hypoxia through regulation of the autophagy genes MAP1LC3B and ATG5.* J Clin Invest, 2010. **120**(1): p. 127-41.
61. Yotnda, P., D. Wu, and A.M. Swanson, *Hypoxic tumors and their effect on immune cells and cancer therapy.* Methods Mol Biol, 2010. **651**: p. 1-29.
62. Cairns, R.A., I.S. Harris, and T.W. Mak, *Regulation of cancer cell metabolism.* Nat Rev Cancer, 2011. **11**(2): p. 85-95.
63. Graeber, T.G., C. Osmanian, T. Jacks, D.E. Housman, C.J. Koch, S.W. Lowe, and A.J. Giaccia, *Hypoxia-mediated selection of cells with diminished apoptotic potential in solid tumours.* Nature, 1996. **379**(6560): p. 88-91.
64. Guzy, R.D., B. Hoyos, E. Robin, H. Chen, L. Liu, K.D. Mansfield, M.C. Simon, U. Hammerling, and P.T. Schumacker, *Mitochondrial complex III is required for hypoxia-induced ROS production and cellular oxygen sensing.* Cell Metab, 2005. **1**(6): p. 401-8.
65. Hill, R.P., D.T. Marie-Egyptienne, and D.W. Hedley, *Cancer stem cells, hypoxia and metastasis.* Semin Radiat Oncol, 2009. **19**(2): p. 106-11.
66. Pennacchietti, S., P. Michieli, M. Galluzzo, M. Mazzone, S. Giordano, and P.M. Comoglio, *Hypoxia promotes invasive growth by transcriptional activation of the met protooncogene.* Cancer Cell, 2003. **3**(4): p. 347-61.

67. Chang, Q., I. Jurisica, T. Do, and D.W. Hedley, *Hypoxia predicts aggressive growth and spontaneous metastasis formation from orthotopically grown primary xenografts of human pancreatic cancer.* Cancer Res, 2011. **71**(8): p. 3110-20.
68. Semenza, G.L., *Hypoxia, clonal selection, and the role of HIF-1 in tumor progression.* Crit Rev Biochem Mol Biol, 2000. **35**(2): p. 71-103.
69. Wang, Y. and M. Ohh, *Oxygen-mediated endocytosis in cancer.* J Cell Mol Med, 2010. **14**(3): p. 496-503.
70. Hockel, M. and P. Vaupel, *Tumor hypoxia: definitions and current clinical, biologic, and molecular aspects.* J Natl Cancer Inst, 2001. **93**(4): p. 266-76.
71. Brown, J.M. and W.R. Wilson, *Exploiting tumour hypoxia in cancer treatment.* Nat Rev Cancer, 2004. **4**(6): p. 437-47.
72. Vaupel, P., H.P. Fortmeyer, S. Runkel, and F. Kallinowski, *Blood flow, oxygen consumption, and tissue oxygenation of human breast cancer xenografts in nude rats.* Cancer Res, 1987. **47**(13): p. 3496-503.
73. Kallinowski, F., K.H. Schlenger, S. Runkel, M. Kloes, M. Stohrer, P. Okunieff, and P. Vaupel, *Blood flow, metabolism, cellular microenvironment, and growth rate of human tumor xenografts.* Cancer Res, 1989. **49**(14): p. 3759-64.
74. Vaupel, P., C. Schaefer, and P. Okunieff, *Intracellular acidosis in murine fibrosarcomas coincides with ATP depletion, hypoxia, and high levels of lactate and total Pi.* NMR Biomed, 1994. **7**(3): p. 128-36.
75. Vaupel, P., *Physiological properties of malignant tumours.* NMR Biomed, 1992. **5**(5): p. 220-5.
76. West, J.B., *Respiratory Physiology: The Essentials*. 8th ed. 2008, Philadelphia: Lippincott Williams & Wilkins.
77. Martin, L., *All you really need to know to interpret arterial blood gases*. 2nd ed. 1999, Philadelphia: Lippincott Williams & Wilkins.
78. Weaver, L.K., *Hyperbaric oxygen therapy for carbon monoxide poisoning.* Undersea Hyperb Med, 2014. **41**(4): p. 339-54.
79. Bickar, D., J. Bonaventura, and C. Bonaventura, *Cytochrome c oxidase binding of hydrogen peroxide.* Biochemistry, 1982. **21**(11): p. 2661-6.
80. Xie, P., S. Jia, R. Tye, C. Chavez-Munoz, M. Vracar-Grabar, S.J. Hong, R. Galiano, and T.A. Mustoe, *Systemic administration of hemoglobin improves ischemic wound healing.* J Surg Res, 2014.
81. Fareed, J., D.A. Hoppensteadt, and R.L. Bick, *Management of thrombotic and cardiovascular disorders in the new millenium. .* Clin Appl Thromb Hemost.
, 2003. **9**: p. 101-108.
82. Olive, P.L., C. Vikse, and M.J. Trotter, *Measurement of oxygen diffusion distance in tumor cubes using a fluorescent hypoxia probe.* Int J Radiat Oncol Biol Phys, 1992. **22**(3): p. 397-402.
83. Koch, C.J., W.T. Jenkins, K.W. Jenkins, X.Y. Yang, A.L. Shuman, S. Pickup, C.R. Riehl, R. Paudyal, H. Poptani, and S.M. Evans, *Mechanisms of blood flow and hypoxia production in rat 9L-epigastric tumors.* Tumor Microenviron Ther, 2013. **1**: p. 1-13.
84. Jordan, B.F. and P. Sonveaux, *Targeting tumor perfusion and oxygenation to improve the outcome of anticancer therapy.* Front Pharmacol, 2012. **3**: p. 94.
85. Hanahan, D. and J. Folkman, *Patterns and emerging mechanisms of the angiogenic switch during tumorigenesis.* Cell, 1996. **86**(3): p. 353-64.
86. Los, M. and E.E. Voest, *The potential role of antivascular therapy in the adjuvant and neoadjuvant treatment of cancer.* Semin Oncol, 2001. **28**(1): p. 93-105.

87. Eberhard, A., S. Kahlert, V. Goede, B. Hemmerlein, K.H. Plate, and H.G. Augustin, *Heterogeneity of angiogenesis and blood vessel maturation in human tumors: implications for antiangiogenic tumor therapies.* Cancer Res, 2000. **60**(5): p. 1388-93.
88. Koukourakis, M.I., *Tumour angiogenesis and response to radiotherapy.* Anticancer Res, 2001. **21**(6b): p. 4285-300.
89. Rofstad, E.K., K. Galappathi, B. Mathiesen, and E.B. Ruud, *Fluctuating and diffusion-limited hypoxia in hypoxia-induced metastasis.* Clin Cancer Res, 2007. **13**(7): p. 1971-8.
90. Dewhirst, M.W., *Concepts of oxygen transport at the microcirculatory level.* Semin Radiat Oncol, 1998. **8**(3): p. 143-50.
91. Brown, J.M. and A.J. Giaccia, *The unique physiology of solid tumors: opportunities (and problems) for cancer therapy.* Cancer Res, 1998. **58**(7): p. 1408-16.
92. Durand, R.E. and E. Sham, *The lifetime of hypoxic human tumor cells.* Int J Radiat Oncol Biol Phys, 1998. **42**(4): p. 711-5.
93. Koukourakis, M.I., S.M. Bentzen, A. Giatromanolaki, G.D. Wilson, F.M. Daley, M.I. Saunders, S. Dische, E. Sivridis, and A.L. Harris, *Endogenous markers of two separate hypoxia response pathways (hypoxia inducible factor 2 alpha and carbonic anhydrase 9) are associated with radiotherapy failure in head and neck cancer patients recruited in the CHART randomized trial.* J Clin Oncol, 2006. **24**(5): p. 727-35.
94. Evans, S.M., K.L. Du, A.A. Chalian, R. Mick, P.J. Zhang, S.M. Hahn, H. Quon, R. Lustig, G.S. Weinstein, and C.J. Koch, *Patterns and levels of hypoxia in head and neck squamous cell carcinomas and their relationship to patient outcome.* Int J Radiat Oncol Biol Phys, 2007. **69**(4): p. 1024-31.
95. Overgaard, J., H.S. Hansen, M. Overgaard, L. Bastholt, A. Berthelsen, L. Specht, B. Lindelov, and K. Jorgensen, *A randomized double-blind phase III study of nimorazole as a hypoxic radiosensitizer of primary radiotherapy in supraglottic larynx and pharynx carcinoma. Results of the Danish Head and Neck Cancer Study (DAHANCA) Protocol 5-85.* Radiother Oncol, 1998. **46**(2): p. 135-46.
96. Le, Q.T., N.C. Denko, and A.J. Giaccia, *Hypoxic gene expression and metastasis.* Cancer Metastasis Rev, 2004. **23**(3-4): p. 293-310.
97. Brizel, D.M., S.P. Scully, J.M. Harrelson, L.J. Layfield, J.M. Bean, L.R. Prosnitz, and M.W. Dewhirst, *Tumor oxygenation predicts for the likelihood of distant metastases in human soft tissue sarcoma.* Cancer Res, 1996. **56**(5): p. 941-3.
98. Fyles, A., M. Milosevic, D. Hedley, M. Pintilie, W. Levin, L. Manchul, and R.P. Hill, *Tumor hypoxia has independent predictor impact only in patients with node-negative cervix cancer.* J Clin Oncol, 2002. **20**(3): p. 680-7.
99. Erler, J.T., K.L. Bennewith, M. Nicolau, N. Dornhofer, C. Kong, Q.T. Le, J.T. Chi, S.S. Jeffrey, and A.J. Giaccia, *Lysyl oxidase is essential for hypoxia-induced metastasis.* Nature, 2006. **440**(7088): p. 1222-6.
100. Baba, Y., K. Nosho, K. Shima, N. Irahara, A.T. Chan, J.A. Meyerhardt, D.C. Chung, E.L. Giovannucci, C.S. Fuchs, and S. Ogino, *HIF1A Overexpression Is Associated with Poor Prognosis in a Cohort of 731 Colorectal Cancers.* Am J Pathol, 2010. **176**(5): p. 2292-301.
101. Wilson, W.R. and M.P. Hay, *Targeting hypoxia in cancer therapy.* Nat Rev Cancer, 2011. **11**(6): p. 393-410.

102. Kyle, A.H., L.A. Huxham, D.M. Yeoman, and A.I. Minchinton, *Limited tissue penetration of taxanes: a mechanism for resistance in solid tumors.* Clin Cancer Res, 2007. **13**(9): p. 2804-10.
103. Durand, R.E., *The influence of microenvironmental factors during cancer therapy.* In Vivo, 1994. **8**(5): p. 691-702.
104. Tannock, I.F., *The relation between cell proliferation and the vascular system in a transplanted mouse mammary tumour.* Br J Cancer, 1968. **22**(2): p. 258-73.
105. Comerford, K.M., T.J. Wallace, J. Karhausen, N.A. Louis, M.C. Montalto, and S.P. Colgan, *Hypoxia-inducible factor-1-dependent regulation of the multidrug resistance (MDR1) gene.* Cancer Res, 2002. **62**(12): p. 3387-94.
106. Wartenberg, M., F.C. Ling, M. Muschen, F. Klein, H. Acker, M. Gassmann, K. Petrat, V. Putz, J. Hescheler, and H. Sauer, *Regulation of the multidrug resistance transporter P-glycoprotein in multicellular tumor spheroids by hypoxia-inducible factor (HIF-1) and reactive oxygen species.* Faseb j, 2003. **17**(3): p. 503-5.
107. Teicher, B.A., J.S. Lazo, and A.C. Sartorelli, *Classification of antineoplastic agents by their selective toxicities toward oxygenated and hypoxic tumor cells.* Cancer Res, 1981. **41**(1): p. 73-81.
108. Wirthner, R., S. Wrann, K. Balamurugan, R.H. Wenger, and D.P. Stiehl, *Impaired DNA double-strand break repair contributes to chemoresistance in HIF-1 alpha-deficient mouse embryonic fibroblasts.* Carcinogenesis, 2008. **29**(12): p. 2306-16.
109. Chan, N., I.M. Pires, Z. Bencokova, C. Coackley, K.R. Luoto, N. Bhogal, M. Lakshman, P. Gottipati, F.J. Oliver, T. Helleday, E.M. Hammond, and R.G. Bristow, *Contextual synthetic lethality of cancer cell kill based on the tumor microenvironment.* Cancer Res, 2010. **70**(20): p. 8045-54.
110. Brophy, G.T. and N.E. Sladek, *Influence of pH on the cytotoxic activity of chlorambucil.* Biochem Pharmacol, 1983. **32**(1): p. 79-84.
111. Chan, N., M. Koritzinsky, H. Zhao, R. Bindra, P.M. Glazer, S. Powell, A. Belmaaza, B. Wouters, and R.G. Bristow, *Chronic hypoxia decreases synthesis of homologous recombination proteins to offset chemoresistance and radioresistance.* Cancer Res, 2008. **68**(2): p. 605-14.
112. Holthusen, H., *Beitrage zur biologie der strahelnwirkung. Untershungen an askarideneiern.* Ptlugers Arch. f.d. ges. Physio, 1921. **187**: p. 1-24.
113. Petry, E., *Zur kenntnis der degingungen der biologischen wirkung der Rontgenstrahlen III Mitteilung. Wirkung von oxydationsmitteln auf die empfindlichkeit.* Biochem. Z, 1923. **135**: p. 353-383.
114. Harrison, L. and K. Blackwell, *Hypoxia and anemia: factors in decreased sensitivity to radiation therapy and chemotherapy?* Oncologist, 2004. **9 Suppl 5**: p. 31-40.
115. Hodgkiss, R.J., I.J. Roberts, M.E. Watts, and M. Woodcock, *Rapid-mixing studies of radiosensitivity with thiol-depleted mammalian cells.* Int J Radiat Biol Relat Stud Phys Chem Med, 1987. **52**(5): p. 735-44.
116. Brown, J.M., *Selective radiosensitization of the hypoxic cells of mouse tumors with the nitroimidazoles metronidazole and Ro 7-0582.* Radiat Res, 1975. **64**(3): p. 633-47.
117. Denekamp, J. and S.R. Harris, *Tests of two electron-affinic radiosensitizers in vivo using regrowth of an experimental carcinoma.* Radiat Res, 1975. **61**(2): p. 191-203.
118. Becker, A., P. Stadler, R.S. Lavey, G. Hansgen, T. Kuhnt, C. Lautenschlager, H.J. Feldmann, M. Molls, and J. Dunst, *Severe anemia is associated with poor tumor*

oxygenation in head and neck squamous cell carcinomas. Int J Radiat Oncol Biol Phys, 2000. **46**(2): p. 459-66.
119. Hirst, D.G., *What is the importance of anaemia in radiotherapy? The value of animal studies.* Radiother Oncol, 1991. **20 Suppl 1**: p. 29-33.
120. Kelleher, D.K., U. Mattheinsen, O. Thews, and P. Vaupel, *Blood flow, oxygenation, and bioenergetic status of tumors after erythropoietin treatment in normal and anemic rats.* Cancer Res, 1996. **56**(20): p. 4728-34.
121. Nordsmark, M. and J. Overgaard, *Tumor hypoxia is independent of hemoglobin and prognostic for loco-regional tumor control after primary radiotherapy in advanced head and neck cancer.* Acta Oncol, 2004. **43**(4): p. 396-403.
122. Dunst, J., T. Kuhnt, H.G. Strauss, U. Krause, T. Pelz, H. Koelbl, and G. Haensgen, *Anemia in cervical cancers: impact on survival, patterns of relapse, and association with hypoxia and angiogenesis.* Int J Radiat Oncol Biol Phys, 2003. **56**(3): p. 778-87.
123. Vaupel, P., A. Mayer, S. Briest, and M. Hockel, *Oxygenation gain factor: a novel parameter characterizing the association between hemoglobin level and the oxygenation status of breast cancers.* Cancer Res, 2003. **63**(22): p. 7634-7.
124. Koukourakis, M.I., A. Giatromanolaki, E. Sivridis, J. Pastorek, I. Karapantzos, K.C. Gatter, and A.L. Harris, *Hypoxia-activated tumor pathways of angiogenesis and pH regulation independent of anemia in head-and-neck cancer.* Int J Radiat Oncol Biol Phys, 2004. **59**(1): p. 67-71.
125. Winter, S.C., K.A. Shah, C. Han, L. Campo, H. Turley, R. Leek, R.J. Corbridge, G.J. Cox, and A.L. Harris, *The relation between hypoxia-inducible factor (HIF)-1alpha and HIF-2alpha expression with anemia and outcome in surgically treated head and neck cancer.* Cancer, 2006. **107**(4): p. 757-66.
126. Henke, M., R. Laszig, C. Rube, U. Schafer, K.D. Haase, B. Schilcher, S. Mose, K.T. Beer, U. Burger, C. Dougherty, and H. Frommhold, *Erythropoietin to treat head and neck cancer patients with anaemia undergoing radiotherapy: randomised, double-blind, placebo-controlled trial.* Lancet, 2003. **362**(9392): p. 1255-60.
127. Lambin, P., B.L. Ramaekers, G.A. van Mastrigt, P. Van den Ende, J. de Jong, D.K. De Ruysscher, and M. Pijls-Johannesma, *Erythropoietin as an adjuvant treatment with (chemo) radiation therapy for head and neck cancer.* Cochrane Database Syst Rev, 2009(3): p. Cd006158.
128. Saunders, M. and S. Dische, *Clinical results of hypoxic cell radiosensitisation from hyperbaric oxygen to accelerated radiotherapy, carbogen and nicotinamide.* Br J Cancer Suppl, 1996. **27**: p. S271-8.
129. Kaanders, J.H., J. Bussink, and A.J. van der Kogel, *Clinical studies of hypoxia modification in radiotherapy.* Semin Radiat Oncol, 2004. **14**(3): p. 233-40.
130. Hill, S.A., D.R. Collingridge, B. Vojnovic, and D.J. Chaplin, *Tumour radiosensitization by high-oxygen-content gases: influence of the carbon dioxide content of the inspired gas on PO2, microcirculatory function and radiosensitivity.* Int J Radiat Oncol Biol Phys, 1998. **40**(4): p. 943-51.
131. Janssens, G.O., S.E. Rademakers, C.H. Terhaard, P.A. Doornaert, H.P. Bijl, P. van den Ende, A. Chin, R.P. Takes, R. de Bree, I.J. Hoogsteen, J. Bussink, P.N. Span, and J.H. Kaanders, *Improved recurrence-free survival with ARCON for anemic patients with laryngeal cancer.* Clin Cancer Res, 2014. **20**(5): p. 1345-54.
132. Kaanders, J.H., J. Bussink, and A.J. van der Kogel, *ARCON: a novel biology-based approach in radiotherapy.* Lancet Oncol, 2002. **3**(12): p. 728-37.

133. Janssens, G.O., S.E. Rademakers, C.H. Terhaard, P.A. Doornaert, H.P. Bijl, P. van den Ende, A. Chin, H.A. Marres, R. de Bree, A.J. van der Kogel, I.J. Hoogsteen, J. Bussink, P.N. Span, and J.H. Kaanders, *Accelerated radiotherapy with carbogen and nicotinamide for laryngeal cancer: results of a phase III randomized trial.* J Clin Oncol, 2012. **30**(15): p. 1777-83.
134. Zeman, E.M., J.M. Brown, M.J. Lemmon, V.K. Hirst, and W.W. Lee, *SR-4233: a new bioreductive agent with high selective toxicity for hypoxic mammalian cells.* Int J Radiat Oncol Biol Phys, 1986. **12**(7): p. 1239-42.
135. Brown, J.M., *SR 4233 (tirapazamine): a new anticancer drug exploiting hypoxia in solid tumours.* Br J Cancer, 1993. **67**(6): p. 1163-70.
136. Reddy, S.B. and S.K. Williamson, *Tirapazamine: a novel agent targeting hypoxic tumor cells.* Expert Opin Investig Drugs, 2009. **18**(1): p. 77-87.
137. Dorie, M.J. and J.M. Brown, *Tumor-specific, schedule-dependent interaction between tirapazamine (SR 4233) and cisplatin.* Cancer Res, 1993. **53**(19): p. 4633-6.
138. von Pawel, J., R. von Roemeling, U. Gatzemeier, M. Boyer, L.O. Elisson, P. Clark, D. Talbot, A. Rey, T.W. Butler, V. Hirsh, I. Olver, B. Bergman, J. Ayoub, G. Richardson, D. Dunlop, A. Arcenas, R. Vescio, J. Viallet, and J. Treat, *Tirapazamine plus cisplatin versus cisplatin in advanced non-small-cell lung cancer: A report of the international CATAPULT I study group. Cisplatin and Tirapazamine in Subjects with Advanced Previously Untreated Non-Small-Cell Lung Tumors.* J Clin Oncol, 2000. **18**(6): p. 1351-9.
139. Rischin, D., L. Peters, R. Fisher, A. Macann, J. Denham, M. Poulsen, M. Jackson, L. Kenny, M. Penniment, J. Corry, D. Lamb, and B. McClure, *Tirapazamine, Cisplatin, and Radiation versus Fluorouracil, Cisplatin, and Radiation in patients with locally advanced head and neck cancer: a randomized phase II trial of the Trans-Tasman Radiation Oncology Group (TROG 98.02).* J Clin Oncol, 2005. **23**(1): p. 79-87.
140. Rischin, D., L.J. Peters, B. O'Sullivan, J. Giralt, R. Fisher, K. Yuen, A. Trotti, J. Bernier, J. Bourhis, J. Ringash, M. Henke, and L. Kenny, *Tirapazamine, cisplatin, and radiation versus cisplatin and radiation for advanced squamous cell carcinoma of the head and neck (TROG 02.02, HeadSTART): a phase III trial of the Trans-Tasman Radiation Oncology Group.* J Clin Oncol, 2010. **28**(18): p. 2989-95.
141. Hicks, K.O., B.G. Siim, J.K. Jaiswal, F.B. Pruijn, A.M. Fraser, R. Patel, A. Hogg, H.D. Liyanage, M.J. Dorie, J.M. Brown, W.A. Denny, M.P. Hay, and W.R. Wilson, *Pharmacokinetic/pharmacodynamic modeling identifies SN30000 and SN29751 as tirapazamine analogues with improved tissue penetration and hypoxic cell killing in tumors.* Clin Cancer Res, 2010. **16**(20): p. 4946-57.
142. Rischin, D., R.J. Hicks, R. Fisher, D. Binns, J. Corry, S. Porceddu, and L.J. Peters, *Prognostic significance of [18F]-misonidazole positron emission tomography-detected tumor hypoxia in patients with advanced head and neck cancer randomly assigned to chemoradiation with or without tirapazamine: a substudy of Trans-Tasman Radiation Oncology Group Study 98.02.* J Clin Oncol, 2006. **24**(13): p. 2098-104.
143. Semenza, G.L., *Targeting HIF-1 for cancer therapy.* Nat Rev Cancer, 2003. **3**(10): p. 721-32.
144. Semenza, G.L., *Involvement of hypoxia-inducible factor 1 in human cancer.* Intern Med, 2002. **41**(2): p. 79-83.
145. Harris, A.L., *Hypoxia--a key regulatory factor in tumour growth.* Nat Rev Cancer, 2002. **2**(1): p. 38-47.

146. Wouters, B.G., T. van den Beucken, M.G. Magagnin, P. Lambin, and C. Koumenis, *Targeting hypoxia tolerance in cancer.* Drug Resist Updat, 2004. **7**(1): p. 25-40.
147. Kelly, C.J., K. Hussien, E. Fokas, P. Kannan, R.J. Shipley, T.M. Ashton, M. Stratford, N. Pearson, and R.J. Muschel, *Regulation of O2 consumption by the PI3K and mTOR pathways contributes to tumor hypoxia.* Radiother Oncol, 2014. **111**(1): p. 72-80.
148. Shaw, R.J. and L.C. Cantley, *Ras, PI(3)K and mTOR signalling controls tumour cell growth.* Nature, 2006. **441**(7092): p. 424-30.
149. Chen, H., J. Feng, Y. Zhang, A. Shen, Y. Chen, J. Lin, W. Lin, T.J. Sferra, and J. Peng, *Pien Tze Huang Inhibits Hypoxia-Induced Angiogenesis via HIF-1 alpha /VEGF-A Pathway in Colorectal Cancer.* Evid Based Complement Alternat Med, 2015. **2015**: p. 454279.
150. Li, G., C. Shan, L. Liu, T. Zhou, J. Zhou, X. Hu, Y. Chen, H. Cui, and N. Gao, *Tanshinone IIA inhibits HIF-1alpha and VEGF expression in breast cancer cells via mTOR/p70S6K/RPS6/4E-BP1 signaling pathway.* PLoS One, 2015. **10**(2): p. e0117440.
151. Wouters, B.G., S.A. Weppler, M. Koritzinsky, W. Landuyt, S. Nuyts, J. Theys, R.K. Chiu, and P. Lambin, *Hypoxia as a target for combined modality treatments.* Eur J Cancer, 2002. **38**(2): p. 240-57.
152. Warburg, O., K. Posener, and E. Negelein, Biochem Z, 1924. **152**: p. 319.
153. Vander Heiden, M.G., L.C. Cantley, and C.B. Thompson, *Understanding the Warburg effect: the metabolic requirements of cell proliferation.* Science, 2009. **324**(5930): p. 1029-33.
154. Pelicano, H., D.S. Martin, R.H. Xu, and P. Huang, *Glycolysis inhibition for anticancer treatment.* Oncogene, 2006. **25**(34): p. 4633-46.
155. Brownlee, M., *Biochemistry and molecular cell biology of diabetic complications.* Nature, 2001. **414**(6865): p. 813-20.
156. Ke, Q. and M. Costa, *Hypoxia-inducible factor-1 (HIF-1).* Mol Pharmacol, 2006. **70**(5): p. 1469-80.
157. Zhang, J.Z., A. Behrooz, and F. Ismail-Beigi, *Regulation of glucose transport by hypoxia.* Am J Kidney Dis, 1999. **34**(1): p. 189-202.
158. Hamanaka, R.B. and N.S. Chandel, *Targeting glucose metabolism for cancer therapy.* J Exp Med, 2012. **209**(2): p. 211-5.
159. Natsuizaka, M., M. Ozasa, S. Darmanin, M. Miyamoto, S. Kondo, S. Kamada, M. Shindoh, F. Higashino, W. Suhara, H. Koide, K. Aita, K. Nakagawa, T. Kondo, M. Asaka, F. Okada, and M. Kobayashi, *Synergistic up-regulation of Hexokinase-2, glucose transporters and angiogenic factors in pancreatic cancer cells by glucose deprivation and hypoxia.* Exp Cell Res, 2007. **313**(15): p. 3337-48.
160. Semenza, G.L., *HIF-1 mediates metabolic responses to intratumoral hypoxia and oncogenic mutations.* J Clin Invest, 2013. **123**(9): p. 3664-71.
161. Funasaka, T., T. Yanagawa, V. Hogan, and A. Raz, *Regulation of phosphoglucose isomerase/autocrine motility factor expression by hypoxia.* Faseb j, 2005. **19**(11): p. 1422-30.
162. Hsu, P.P. and D.M. Sabatini, *Cancer cell metabolism: Warburg and beyond.* Cell, 2008. **134**(5): p. 703-7.
163. Serganova, I., A. Rizwan, X. Ni, S.B. Thakur, J. Vider, J. Russell, R. Blasberg, and J.A. Koutcher, *Metabolic imaging: a link between lactate dehydrogenase A, lactate, and tumor phenotype.* Clin Cancer Res, 2011. **17**(19): p. 6250-61.
164. Gogvadze, V., S. Orrenius, and B. Zhivotovsky, *Mitochondria in cancer cells: what is so special about them?* Trends Cell Biol, 2008. **18**(4): p. 165-73.

165. Hanahan, D. and R.A. Weinberg, *Hallmarks of cancer: the next generation.* Cell, 2011. **144**(5): p. 646-74.
166. Williams, G.H. and K. Stoeber, *The cell cycle and cancer.* J Pathol, 2012. **226**(2): p. 352-64.
167. Duan, S. and M. Pagano, *Linking metabolism and cell cycle progression via the APC/CCdh1 and SCFbetaTrCP ubiquitin ligases.* Proc Natl Acad Sci U S A, 2011. **108**(52): p. 20857-8.
168. Colombo, S.L., M. Palacios-Callender, N. Frakich, J. De Leon, C.A. Schmitt, L. Boorn, N. Davis, and S. Moncada, *Anaphase-promoting complex/cyclosome-Cdh1 coordinates glycolysis and glutaminolysis with transition to S phase in human T lymphocytes.* Proc Natl Acad Sci U S A, 2010. **107**(44): p. 18868-73.
169. Murono, K., N.H. Tsuno, K. Kawai, K. Sasaki, K. Hongo, M. Kaneko, M. Hiyoshi, N. Tada, T. Nirei, E. Sunami, K. Takahashi, and J. Kitayama, *SN-38 overcomes chemoresistance of colorectal cancer cells induced by hypoxia, through HIF1alpha.* Anticancer Res, 2012. **32**(3): p. 865-72.
170. Haug, K., K.L. Kravik, and P.M. De Angelis, *Cellular response to irinotecan in colon cancer cell lines showing differential response to 5-fluorouracil.* Anticancer Res, 2008. **28**(2a): p. 583-92.
171. Harrington, E.A., D. Bebbington, J. Moore, R.K. Rasmussen, A.O. Ajose-Adeogun, T. Nakayama, J.A. Graham, C. Demur, T. Hercend, A. Diu-Hercend, M. Su, J.M. Golec, and K.M. Miller, *VX-680, a potent and selective small-molecule inhibitor of the Aurora kinases, suppresses tumor growth in vivo.* Nat Med, 2004. **10**(3): p. 262-7.
172. Montano, R., R. Thompson, I. Chung, H. Hou, N. Khan, and A. Eastman, *Sensitization of human cancer cells to gemcitabine by the Chk1 inhibitor MK-8776: cell cycle perturbation and impact of administration schedule in vitro and in vivo.* BMC Cancer, 2013. **13**: p. 604.
173. Wiebke, E.A., N.A. Grieshop, P.J. Loehrer, G.J. Eckert, and R.A. Sidner, *Antitumor effects of 5-fluorouracil on human colon cancer cell lines: antagonism by levamisole.* J Surg Res, 2003. **111**(1): p. 63-9.
174. De Angelis, P.M., D.H. Svendsrud, K.L. Kravik, and T. Stokke, *Cellular response to 5-fluorouracil (5-FU) in 5-FU-resistant colon cancer cell lines during treatment and recovery.* Mol Cancer, 2006. **5**: p. 20.
175. Liu, L., X. Ning, L. Sun, Y. Shi, S. Han, C. Guo, Y. Chen, S. Sun, F. Yin, K. Wu, and D. Fan, *Involvement of MGr1-Ag/37LRP in the vincristine-induced HIF-1 expression in gastric cancer cells.* Mol Cell Biochem, 2007. **303**(1-2): p. 151-60.
176. Strese, S., M. Fryknas, R. Larsson, and J. Gullbo, *Effects of hypoxia on human cancer cell line chemosensitivity.* BMC Cancer, 2013. **13**: p. 331.
177. Sermeus, A., M. Rebucci, M. Fransolet, L. Flamant, D. Desmet, E. Delaive, T. Arnould, and C. Michiels, *Differential effect of hypoxia on etoposide-induced DNA damage response and p53 regulation in different cell types.* J Cell Physiol, 2013. **228**(12): p. 2365-76.
178. Sakata, K., T.T. Kwok, B.J. Murphy, K.R. Laderoute, G.R. Gordon, and R.M. Sutherland, *Hypoxia-induced drug resistance: comparison to P-glycoprotein-associated drug resistance.* Br J Cancer, 1991. **64**(5): p. 809-14.
179. Rohwer, N., C. Dame, A. Haugstetter, B. Wiedenmann, K. Detjen, C.A. Schmitt, and T. Cramer, *Hypoxia-inducible factor 1alpha determines gastric cancer chemosensitivity via modulation of p53 and NF-kappaB.* PLoS One, 2010. **5**(8): p. e12038.

180. Escuin, D., E.R. Kline, and P. Giannakakou, *Both microtubule-stabilizing and microtubule-destabilizing drugs inhibit hypoxia-inducible factor-1alpha accumulation and activity by disrupting microtubule function.* Cancer Res, 2005. **65**(19): p. 9021-8.
181. Duyndam, M.C., M.P. van Berkel, J.C. Dorsman, D.A. Rockx, H.M. Pinedo, and E. Boven, *Cisplatin and doxorubicin repress Vascular Endothelial Growth Factor expression and differentially down-regulate Hypoxia-inducible Factor I activity in human ovarian cancer cells.* Biochem Pharmacol, 2007. **74**(2): p. 191-201.
182. Forde, J.C., A.S. Perry, K. Brennan, L.M. Martin, M.P. Lawler, T.H. Lynch, D. Hollywood, and L. Marignol, *Docetaxel maintains its cytotoxic activity under hypoxic conditions in prostate cancer cells.* Urol Oncol, 2012. **30**(6): p. 912-9.
183. Koch, S., F. Mayer, F. Honecker, M. Schittenhelm, and C. Bokemeyer, *Efficacy of cytotoxic agents used in the treatment of testicular germ cell tumours under normoxic and hypoxic conditions in vitro.* Br J Cancer, 2003. **89**(11): p. 2133-9.
184. Sermeus, A., J.P. Cosse, M. Crespin, V. Mainfroid, F. de Longueville, N. Ninane, M. Raes, J. Remacle, and C. Michiels, *Hypoxia induces protection against etoposide-induced apoptosis: molecular profiling of changes in gene expression and transcription factor activity.* Mol Cancer, 2008. **7**: p. 27.
185. Sullivan, R. and C.H. Graham, *Hypoxia prevents etoposide-induced DNA damage in cancer cells through a mechanism involving hypoxia-inducible factor 1.* Mol Cancer Ther, 2009. **8**(6): p. 1702-13.
186. Onozuka, H., K. Tsuchihara, and H. Esumi, *Hypoglycemic/hypoxic condition in vitro mimicking the tumor microenvironment markedly reduced the efficacy of anticancer drugs.* Cancer Sci, 2011. **102**(5): p. 975-82.
187. Kasuya, K., A. Tsuchida, Y. Nagakawa, M. Suzuki, Y. Abe, T. Itoi, H. Serizawa, T. Nagao, M. Shimazu, and T. Aoki, *Hypoxia-inducible factor-1alpha expression and gemcitabine chemotherapy for pancreatic cancer.* Oncol Rep, 2011. **26**(6): p. 1399-406.
188. Kamiyama, H., S. Takano, K. Tsuboi, and A. Matsumura, *Anti-angiogenic effects of SN38 (active metabolite of irinotecan): inhibition of hypoxia-inducible factor 1 alpha (HIF-1alpha)/vascular endothelial growth factor (VEGF) expression of glioma and growth of endothelial cells.* J Cancer Res Clin Oncol, 2005. **131**(4): p. 205-13.
189. Kennedy, K.A., J.M. Siegfried, A.C. Sartorelli, and T.R. Tritton, *Effects of anthracyclines on oxygenated and hypoxic tumor cells.* Cancer Res, 1983. **43**(1): p. 54-9.
190. Liu, L., X. Ning, L. Sun, H. Zhang, Y. Shi, C. Guo, S. Han, J. Liu, S. Sun, Z. Han, K. Wu, and D. Fan, *Hypoxia-inducible factor-1 alpha contributes to hypoxia-induced chemoresistance in gastric cancer.* Cancer Sci, 2008. **99**(1): p. 121-8.
191. Kollareddy, M., D. Zheleva, P. Dzubak, P.S. Brahmkshatriya, M. Lepsik, and M. Hajduch, *Aurora kinase inhibitors: progress towards the clinic.* Invest New Drugs, 2012. **30**(6): p. 2411-32.
192. Rauth, A.M., J.K. Mohindra, and I.F. Tannock, *Activity of mitomycin C for aerobic and hypoxic cells in vitro and in vivo.* Cancer Res, 1983. **43**(9): p. 4154-8.
193. Guinney, J., R. Dienstmann, X. Wang, A. de Reynies, A. Schlicker, C. Soneson, L. Marisa, P. Roepman, G. Nyamundanda, P. Angelino, B.M. Bot, J.S. Morris, I.M. Simon, S. Gerster, E. Fessler, F. De Sousa E Melo, E. Missiaglia, H. Ramay, D. Barras, K. Homicsko, D. Maru, G.C. Manyam, B. Broom, V. Boige, B. Perez-Villamil, T. Laderas, R. Salazar, J.W. Gray, D. Hanahan, J. Tabernero, R. Bernards, S.H.

Friend, P. Laurent-Puig, J.P. Medema, A. Sadanandam, L. Wessels, M. Delorenzi, S. Kopetz, L. Vermeulen, and S. Tejpar, *The consensus molecular subtypes of colorectal cancer.* Nat Med, 2015. **advance online publication**.

194. Ahmed, D., P.W. Eide, I.A. Eilertsen, S.A. Danielsen, M. Eknaes, M. Hektoen, G.E. Lind, and R.A. Lothe, *Epigenetic and genetic features of 24 colon cancer cell lines.* Oncogenesis, 2013. **2**: p. e71.
195. Nowak, M.A., N.L. Komarova, A. Sengupta, P.V. Jallepalli, M. Shih Ie, B. Vogelstein, and C. Lengauer, *The role of chromosomal instability in tumor initiation.* Proc Natl Acad Sci U S A, 2002. **99**(25): p. 16226-31.
196. Hermsen, M., C. Postma, J. Baak, M. Weiss, A. Rapallo, A. Sciutto, G. Roemen, J.W. Arends, R. Williams, W. Giaretti, A. De Goeij, and G. Meijer, *Colorectal adenoma to carcinoma progression follows multiple pathways of chromosomal instability.* Gastroenterology, 2002. **123**(4): p. 1109-19.
197. Lengauer, C., K.W. Kinzler, and B. Vogelstein, *Genetic instability in colorectal cancers.* Nature, 1997. **386**(6625): p. 623-7.
198. Lothe, R.A., *Microsatellite instability in human solid tumors.* Mol Med Today, 1997. **3**(2): p. 61-8.
199. Issa, J.P., *CpG island methylator phenotype in cancer.* Nat Rev Cancer, 2004. **4**(12): p. 988-93.
200. Kaplan, R., T. Maughan, A. Crook, D. Fisher, R. Wilson, L. Brown, and M. Parmar, *Evaluating many treatments and biomarkers in oncology: a new design.* J Clin Oncol, 2013. **31**(36): p. 4562-8.
201. Riddick, D.S., C. Lee, S. Ramji, E.C. Chinje, R.L. Cowen, K.J. Williams, A.V. Patterson, I.J. Stratford, C.S. Morrow, A.J. Townsend, Y. Jounaidi, C.S. Chen, T. Su, H. Lu, P.S. Schwartz, and D.J. Waxman, *Cancer chemotherapy and drug metabolism.* Drug Metab Dispos, 2005. **33**(8): p. 1083-96.
202. Newell, D.R., *Phase I clinical studies with cytotoxic drugs: pharmacokinetic and pharmacodynamic considerations.* Br J Cancer, 1990. **61**(2): p. 189-91.
203. Clarke, S.J. and L.P. Rivory, *Clinical pharmacokinetics of docetaxel.* Clin Pharmacokinet, 1999. **36**(2): p. 99-114.
204. Abbruzzese, J.L., R. Grunewald, E.A. Weeks, D. Gravel, T. Adams, B. Nowak, S. Mineishi, P. Tarassoff, W. Satterlee, M.N. Raber, and et al., *A phase I clinical, plasma, and cellular pharmacology study of gemcitabine.* J Clin Oncol, 1991. **9**(3): p. 491-8.
205. Goyle, S. and A. Maraveyas, *Chemotherapy for colorectal cancer.* Dig Surg, 2005. **22**(6): p. 401-14.
206. Foltran, L., G.D. Maglio, N. Pella, P. Ermacora, G. Aprile, E. Masiero, M. Giovannoni, E. Iaiza, G.G. Cardellino, S.E. Lutrino, M. Mazzer, M. Giangreco, F.E. Pisa, S. Pizzolitto, and G. Fasola, *Prognostic role of KRAS, NRAS, BRAF and PIK3CA mutations in advanced colorectal cancer.* Future Oncol, 2015. **11**(4): p. 629-40.
207. Shiovitz, S. and W.M. Grady, *Molecular markers predictive of chemotherapy response in colorectal cancer.* Curr Gastroenterol Rep, 2015. **17**(2): p. 431.
208. Linnekamp, J.F., X. Wang, J.P. Medema, and L. Vermeulen, *Colorectal cancer heterogeneity and targeted therapy: a case for molecular disease subtypes.* Cancer Res, 2015. **75**(2): p. 245-9.
209. Weiss, J.M., P.R. Pfau, E.S. O'Connor, J. King, N. LoConte, G. Kennedy, and M.A. Smith, *Mortality by stage for right- versus left-sided colon cancer: analysis of surveillance, epidemiology, and end results--Medicare data.* J Clin Oncol, 2011. **29**(33): p. 4401-9.

210. Deliu, I.C., E.F. Georgescu, and M.C. Bezna, *Analysis of prognostic factors in colorectal carcinoma.* Rev Med Chir Soc Med Nat Iasi, 2014. **118**(3): p. 808-16.
211. Popat, S., R. Hubner, and R.S. Houlston, *Systematic review of microsatellite instability and colorectal cancer prognosis.* J Clin Oncol, 2005. **23**(3): p. 609-18.
212. Benatti, P., R. Gafa, D. Barana, M. Marino, A. Scarselli, M. Pedroni, I. Maestri, L. Guerzoni, L. Roncucci, M. Menigatti, B. Roncari, S. Maffei, G. Rossi, G. Ponti, A. Santini, L. Losi, C. Di Gregorio, C. Oliani, M. Ponz de Leon, and G. Lanza, *Microsatellite instability and colorectal cancer prognosis.* Clin Cancer Res, 2005. **11**(23): p. 8332-40.
213. Merok, M.A., T. Ahlquist, E.C. Royrvik, K.F. Tufteland, M. Hektoen, O.H. Sjo, T. Mala, A. Svindland, R.A. Lothe, and A. Nesbakken, *Microsatellite instability has a positive prognostic impact on stage II colorectal cancer after complete resection: results from a large, consecutive Norwegian series.* Ann Oncol, 2013. **24**(5): p. 1274-82.
214. Sinicrope, F.A. and D.J. Sargent, *Molecular pathways: microsatellite instability in colorectal cancer: prognostic, predictive, and therapeutic implications.* Clin Cancer Res, 2012. **18**(6): p. 1506-12.
215. Sinicrope, F.A., N.R. Foster, S.N. Thibodeau, S. Marsoni, G. Monges, R. Labianca, G.P. Kim, G. Yothers, C. Allegra, M.J. Moore, S. Gallinger, and D.J. Sargent, *DNA mismatch repair status and colon cancer recurrence and survival in clinical trials of 5-fluorouracil-based adjuvant therapy.* J Natl Cancer Inst, 2011. **103**(11): p. 863-75.
216. Tejpar, S., Z. Saridaki, M. Delorenzi, F. Bosman, and A.D. Roth, *Microsatellite Instability, Prognosis and Drug Sensitivity of Stage II and III Colorectal Cancer: More Complexity to the Puzzle.* Journal of the National Cancer Institute, 2011.
217. Gavin, P.G., L.H. Colangelo, D. Fumagalli, N. Tanaka, M.Y. Remillard, G. Yothers, C. Kim, Y. Taniyama, S.I. Kim, H.J. Choi, N.L. Blackmon, C. Lipchik, N.J. Petrelli, M.J. O'Connell, N. Wolmark, S. Paik, and K.L. Pogue-Geile, *Mutation profiling and microsatellite instability in stage II and III colon cancer: an assessment of their prognostic and oxaliplatin predictive value.* Clin Cancer Res, 2012. **18**(23): p. 6531-41.
218. Shiovitz, S., M.M. Bertagnolli, L.A. Renfro, E. Nam, N.R. Foster, S. Dzieciatkowski, Y. Luo, V.V. Lao, R.J. Monnat, Jr., M.J. Emond, N. Maizels, D. Niedzwiecki, R.M. Goldberg, L.B. Saltz, A. Venook, R.S. Warren, and W.M. Grady, *CpG island methylator phenotype is associated with response to adjuvant irinotecan-based therapy for stage III colon cancer.* Gastroenterology, 2014. **147**(3): p. 637-45.
219. Clancy, C., J.P. Burke, M.F. Kalady, and J.C. Coffey, *BRAF mutation is associated with distinct clinicopathological characteristics in colorectal cancer: a systematic review and meta-analysis.* Colorectal Dis, 2013. **15**(12): p. e711-8.
220. Roth, A.D., S. Tejpar, M. Delorenzi, P. Yan, R. Fiocca, D. Klingbiel, D. Dietrich, B. Biesmans, G. Bodoky, C. Barone, E. Aranda, B. Nordlinger, L. Cisar, R. Labianca, D. Cunningham, E. Van Cutsem, and F. Bosman, *Prognostic role of KRAS and BRAF in stage II and III resected colon cancer: results of the translational study on the PETACC-3, EORTC 40993, SAKK 60-00 trial.* J Clin Oncol, 2010. **28**(3): p. 466-74.
221. Kindig, C.A., K.M. Kelley, R.A. Howlett, C.M. Stary, and M.C. Hogan, *Assessment of O2 uptake dynamics in isolated single skeletal myocytes.* J Appl Physiol (1985), 2003. **94**(1): p. 353-7.

222. Kunz-Schughart, L.A., J. Doetsch, W. Mueller-Klieser, and K. Groebe, *Proliferative activity and tumorigenic conversion: impact on cellular metabolism in 3-D culture.* Am J Physiol Cell Physiol, 2000. **278**(4): p. C765-80.
223. Mamchaoui, K. and G. Saumon, *A method for measuring the oxygen consumption of intact cell monolayers.* Am J Physiol Lung Cell Mol Physiol, 2000. **278**(4): p. L858-63.
224. Ramamoorthy, R., P.K. Dutta, and S.A. Akbar, *Oxygen sensors: Materials, methods, designs, and applications,.* Journal of Material Science, 2003. **38**: p. 4271-4282.
225. Kuang, Y. and D.R. Walt, *Detecting oxygen consumption in the proximity of Saccharomyces cerevisiae cells using self-assembled fluorescent nanosensors.* Biotechnol Bioeng, 2007. **96**(2): p. 318-25.
226. Saito, T., C.C. Wu, H. Shiku, T. Yasukawa, M. Yokoo, T. Ito-Sasaki, H. Abe, H. Hoshi, and T. Matsue, *Oxygen consumption of cell suspension in a poly(dimethylsiloxane) (PDMS) microchannel estimated by scanning electrochemical microscopy.* Analyst, 2006. **131**(9): p. 1006-11.
227. Warkentin, M., H.M. Freese, U. Karsten, and R. Schumann, *New and fast method to quantify respiration rates of bacterial and plankton communities in freshwater ecosystems by using optical oxygen sensor spots.* Appl Environ Microbiol, 2007. **73**(21): p. 6722-9.
228. Borisov, S.M., G. Nuss, and I. Klimant, *Red light-excitable oxygen sensing materials based on platinum(II) and palladium(II) benzoporphyrins.* Anal Chem, 2008. **80**(24): p. 9435-42.
229. Simon, G.R. and A. Turrisi, *Management of small cell lung cancer: ACCP evidence-based clinical practice guidelines (2nd edition).* Chest, 2007. **132**(3 Suppl): p. 324s-339s.
230. Veronesi, U., P. Boyle, A. Goldhirsch, R. Orecchia, and G. Viale, *Breast cancer.* Lancet, 2005. **365**(9472): p. 1727-41.
231. Scartozzi, M., E. Galizia, L. Verdecchia, R. Berardi, S. Antognoli, S. Chiorrini, and S. Cascinu, *Chemotherapy for advanced gastric cancer: across the years for a standard of care.* Expert Opin Pharmacother, 2007. **8**(6): p. 797-808.
232. de Bono, J.S., S. Oudard, M. Ozguroglu, S. Hansen, J.P. Machiels, I. Kocak, G. Gravis, I. Bodrogi, M.J. Mackenzie, L. Shen, M. Roessner, S. Gupta, and A.O. Sartor, *Prednisone plus cabazitaxel or mitoxantrone for metastatic castration-resistant prostate cancer progressing after docetaxel treatment: a randomised open-label trial.* Lancet, 2010. **376**(9747): p. 1147-54.
233. Colevas, A.D. and M.R. Posner, *Docetaxel in head and neck cancer: a review.* Am J Clin Oncol, 1998. **21**(5): p. 482-6.
234. Sternberg, C.N., W.W. ten Bokkel Huinink, J.F. Smyth, V. Bruntsch, L.Y. Dirix, N.A. Pavlidis, H. Franklin, S. Wanders, N. Le Bail, and S.B. Kaye, *Docetaxel (Taxotere), a novel taxoid, in the treatment of advanced colorectal carcinoma: an EORTC Early Clinical Trials Group Study.* Br J Cancer, 1994. **70**(2): p. 376-9.
235. Vincent, A., J. Herman, R. Schulick, R.H. Hruban, and M. Goggins, *Pancreatic cancer.* Lancet, 2011. **378**(9791): p. 607-20.
236. Cheung, G., A. Sahai, M. Billia, P. Dasgupta, and M.S. Khan, *Recent advances in the diagnosis and treatment of bladder cancer.* BMC Med, 2013. **11**: p. 13.
237. Jimenez-Fonseca, P., M.P. Solis, M. Garrido, L. Faez, D. Rodriguez, A.L. Ruiz, M.L. Sanchez Lorenzo, E. Uriol, M.D. Menendez, and J.M. Vieitez, *Gemcitabine plus capecitabine (Gem-Cape) biweekly in chemorefractory metastatic colorectal cancer.* Clin Transl Oncol, 2014.

238. Lee, K.W., Y.J. Kim, K.H. Lee, S.W. Han, T.Y. Kim, D.Y. Oh, S.A. Im, T.Y. Kim, Y.J. Bang, I.S. Choi, and J.H. Kim, *Phase II trial of gemcitabine plus UFT as salvage treatment in oxaliplatin, irinotecan and fluoropyrimidine-refractory metastatic colorectal cancer.* Cancer Chemother Pharmacol, 2014. **74**(3): p. 447-55.
239. Spindler, K.L., N. Pallisgaard, R.F. Andersen, J. Ploen, and A. Jakobsen, *Gemcitabine and capecitabine for heavily pre-treated metastatic colorectal cancer patients--a phase II and translational research study.* Anticancer Res, 2014. **34**(2): p. 845-50.
240. Correale, P., C. Botta, M.S. Rotundo, A. Guglielmo, R. Conca, A. Licchetta, P. Pastina, E. Bestoso, D. Ciliberto, M.G. Cusi, A. Fioravanti, G.M. Guidelli, M.T. Bianco, G. Misso, E. Martino, M. Caraglia, P. Tassone, E. Mini, G. Mantovani, R. Ridolfi, L. Pirtoli, and P. Tagliaferri, *Gemcitabine, oxaliplatin, levofolinate, 5-fluorouracil, granulocyte-macrophage colony-stimulating factor, and interleukin-2 (GOLFIG) versus FOLFOX chemotherapy in metastatic colorectal cancer patients: the GOLFIG-2 multicentric open-label randomized phase III trial.* J Immunother, 2014. **37**(1): p. 26-35.
241. Cham, K.K., J.H. Baker, K.S. Takhar, J.A. Flexman, M.Q. Wong, D.A. Owen, A. Yung, P. Kozlowski, S.A. Reinsberg, E.M. Chu, C.W. Chang, A.K. Buczkowski, S.W. Chung, C.H. Scudamore, A.I. Minchinton, D.T. Yapp, and S.S. Ng, *Metronomic gemcitabine suppresses tumour growth, improves perfusion, and reduces hypoxia in human pancreatic ductal adenocarcinoma.* Br J Cancer, 2010. **103**(1): p. 52-60.
242. Kraus-Berthier, L., M. Jan, N. Guilbaud, M. Naze, A. Pierre, and G. Atassi, *Histology and sensitivity to anticancer drugs of two human non-small cell lung carcinomas implanted in the pleural cavity of nude mice.* Clin Cancer Res, 2000. **6**(1): p. 297-304.
243. Herst, P.M., A.S. Tan, D.J. Scarlett, and M.V. Berridge, *Cell surface oxygen consumption by mitochondrial gene knockout cells.* Biochim Biophys Acta, 2004. **1656**(2-3): p. 79-87.
244. Wu, M., A. Neilson, A.L. Swift, R. Moran, J. Tamagnine, D. Parslow, S. Armistead, K. Lemire, J. Orrell, J. Teich, S. Chomicz, and D.A. Ferrick, *Multiparameter metabolic analysis reveals a close link between attenuated mitochondrial bioenergetic function and enhanced glycolysis dependency in human tumor cells.* Am J Physiol Cell Physiol, 2007. **292**(1): p. C125-36.
245. Cairns, R.A., *Drivers of the warburg phenotype.* Cancer J, 2015. **21**(2): p. 56-61.
246. Hoffmann, O.I., C. Ilmberger, S. Magosch, M. Joka, K.W. Jauch, and B. Mayer, *Impact of the spheroid model complexity on drug response.* J Biotechnol, 2015.
247. Flatmark, K., G.M. Maelandsmo, M. Martinsen, H. Rasmussen, and O. Fodstad, *Twelve colorectal cancer cell lines exhibit highly variable growth and metastatic capacities in an orthotopic model in nude mice.* Eur J Cancer, 2004. **40**(10): p. 1593-8.
248. Golas, J.M., J. Lucas, C. Etienne, J. Golas, C. Discafani, L. Sridharan, E. Boghaert, K. Arndt, F. Ye, D.H. Boschelli, F. Li, C. Titsch, C. Huselton, I. Chaudhary, and F. Boschelli, *SKI-606, a Src/Abl inhibitor with in vivo activity in colon tumor xenograft models.* Cancer Res, 2005. **65**(12): p. 5358-64.
249. Ayers, G.D., E.T. McKinley, P. Zhao, J.M. Fritz, R.E. Metry, B.C. Deal, K.M. Adlerz, R.J. Coffey, and H.C. Manning, *Volume of preclinical xenograft tumors is more accurately assessed by ultrasound imaging than manual caliper measurements.* J Ultrasound Med, 2010. **29**(6): p. 891-901.

250. Goda, N., H.E. Ryan, B. Khadivi, W. McNulty, R.C. Rickert, and R.S. Johnson, *Hypoxia-inducible factor 1alpha is essential for cell cycle arrest during hypoxia.* Mol Cell Biol, 2003. **23**(1): p. 359-69.
251. Lash, G.E., T.E. Fitzpatrick, and C.H. Graham, *Effect of hypoxia on cellular adhesion to vitronectin and fibronectin.* Biochem Biophys Res Commun, 2001. **287**(3): p. 622-9.
252. Sutherland, R.M., J.A. McCredie, and W.R. Inch, *Growth of multicell spheroids in tissue culture as a model of nodular carcinomas.* J Natl Cancer Inst, 1971. **46**(1): p. 113-20.
253. Hirschhaeuser, F., H. Menne, C. Dittfeld, J. West, W. Mueller-Klieser, and L.A. Kunz-Schughart, *Multicellular tumor spheroids: an underestimated tool is catching up again.* J Biotechnol, 2010. **148**(1): p. 3-15.
254. Brurberg, K.G., J.V. Gaustad, C.S. Mollatt, and E.K. Rofstad, *Temporal heterogeneity in blood supply in human tumor xenografts.* Neoplasia, 2008. **10**(7): p. 727-35.
255. Mansbridge, J.N., W.A. Ausserer, M.A. Knapp, and R.M. Sutherland, *Adaptation of EGF receptor signal transduction to three-dimensional culture conditions: changes in surface receptor expression and protein tyrosine phosphorylation.* J Cell Physiol, 1994. **161**(2): p. 374-82.
256. Olive, P.L. and R.E. Durand, *Drug and radiation resistance in spheroids: cell contact and kinetics.* Cancer Metastasis Rev, 1994. **13**(2): p. 121-38.
257. Bauman, G.S., B.J. Fisher, W. McDonald, V.R. Amberger, E. Moore, and R.F. Del Maestro, *Effects of radiation on a three-dimensional model of malignant glioma invasion.* Int J Dev Neurosci, 1999. **17**(5-6): p. 643-51.
258. Monazzam, A., R. Josephsson, C. Blomqvist, J. Carlsson, B. Langstrom, and M. Bergstrom, *Application of the multicellular tumour spheroid model to screen PET tracers for analysis of early response of chemotherapy in breast cancer.* Breast Cancer Res, 2007. **9**(4): p. R45.
259. Herrmann, R., W. Fayad, S. Schwarz, M. Berndtsson, and S. Linder, *Screening for compounds that induce apoptosis of cancer cells grown as multicellular spheroids.* J Biomol Screen, 2008. **13**(1): p. 1-8.
260. Waleh, N.S., M.D. Brody, M.A. Knapp, H.L. Mendonca, E.M. Lord, C.J. Koch, K.R. Laderoute, and R.M. Sutherland, *Mapping of the vascular endothelial growth factor-producing hypoxic cells in multicellular tumor spheroids using a hypoxia-specific marker.* Cancer Res, 1995. **55**(24): p. 6222-6.
261. Woods, M.L., C.J. Koch, and E.M. Lord, *Detection of individual hypoxic cells in multicellular spheroids by flow cytometry using the 2-nitroimidazole, EF5, and monoclonal antibodies.* Int J Radiat Oncol Biol Phys, 1996. **34**(1): p. 93-101.
262. Conger, A.D. and M.C. Ziskin, *Growth of mammalian multicellular tumor spheroids.* Cancer Res, 1983. **43**(2): p. 556-60.
263. Mueller-Klieser, W., *Method for the determination of oxygen consumption rates and diffusion coefficients in multicellular spheroids.* Biophys J, 1984. **46**(3): p. 343-8.
264. Groebe, K. and W. Mueller-Klieser, *Distributions of oxygen, nutrient, and metabolic waste concentrations in multicellular spheroids and their dependence on spheroid parameters.* Eur Biophys J, 1991. **19**(4): p. 169-81.
265. Grimes, D.R., C. Kelly, K. Bloch, and M. Partridge, *A method for estimating the oxygen consumption rate in multicellular tumour spheroids.* J R Soc Interface, 2014. **11**(92): p. 20131124.

266. Koch, C.J., *Measurement of absolute oxygen levels in cells and tissues using oxygen sensors and 2-nitroimidazole EF5.* Methods Enzymol, 2002. **352**: p. 3-31.
267. Koch, C.J., S.M. Evans, and E.M. Lord, *Oxygen dependence of cellular uptake of EF5 [2-(2-nitro-1H-imidazol-1-yl)-N-(2,2,3,3,3-pentafluoropropyl)a cet amide] : analysis of drug adducts by fluorescent antibodies vs bound radioactivity.* Br J Cancer, 1995. **72**(4): p. 869-74.
268. Koch, C.J., S.M. Hahn, K. Rockwell, Jr., J.M. Covey, W.G. McKenna, and S.M. Evans, *Pharmacokinetics of EF5 [2-(2-nitro-1-H-imidazol-1-yl)-N-(2,2,3,3,3-pentafluoropropyl) acetamide] in human patients: implications for hypoxia measurements in vivo by 2-nitroimidazoles.* Cancer Chemother Pharmacol, 2001. **48**(3): p. 177-87.
269. Marotta, D., J. Karar, W.T. Jenkins, M. Kumanova, K.W. Jenkins, J.W. Tobias, D. Baldwin, A. Hatzigeorgiou, P. Alexiou, S.M. Evans, R. Alarcon, A. Maity, C. Koch, and C. Koumenis, *In vivo profiling of hypoxic gene expression in gliomas using the hypoxia marker EF5 and laser-capture microdissection.* Cancer Res, 2011. **71**(3): p. 779-89.
270. Goodson, W.H., 3rd, D.H. Moore, 2nd, B.M. Ljung, K. Chew, C. Florendo, B. Mayall, H.S. Smith, and F.M. Waldman, *The functional relationship between in vivo bromodeoxyuridine labeling index and Ki-67 proliferation index in human breast cancer.* Breast Cancer Res Treat, 1998. **49**(2): p. 155-64.
271. Schluter, C., M. Duchrow, C. Wohlenberg, M.H. Becker, G. Key, H.D. Flad, and J. Gerdes, *The cell proliferation-associated antigen of antibody Ki-67: a very large, ubiquitous nuclear protein with numerous repeated elements, representing a new kind of cell cycle-maintaining proteins.* J Cell Biol, 1993. **123**(3): p. 513-22.
272. Gerdes, J., H. Lemke, H. Baisch, H.H. Wacker, U. Schwab, and H. Stein, *Cell cycle analysis of a cell proliferation-associated human nuclear antigen defined by the monoclonal antibody Ki-67.* J Immunol, 1984. **133**(4): p. 1710-5.
273. Colozza, M., E. Azambuja, F. Cardoso, C. Sotiriou, D. Larsimont, and M.J. Piccart, *Proliferative markers as prognostic and predictive tools in early breast cancer: where are we now?* Ann Oncol, 2005. **16**(11): p. 1723-39.
274. Latt, S.A. and G. Stetten, *Spectral studies on 33258 Hoechst and related bisbenzimidazole dyes useful for fluorescent detection of deoxyribonucleic acid synthesis.* J Histochem Cytochem, 1976. **24**(1): p. 24-33.
275. Olive, P.L., D.J. Chaplin, and R.E. Durand, *Pharmacokinetics, binding and distribution of Hoechst 33342 in spheroids and murine tumours.* Br J Cancer, 1985. **52**(5): p. 739-46.
276. Diepart, C., O. Karroum, J. Magat, O. Feron, J. Verrax, P.B. Calderon, V. Gregoire, P. Leveque, J. Stockis, N. Dauguet, B.F. Jordan, and B. Gallez, *Arsenic trioxide treatment decreases the oxygen consumption rate of tumor cells and radiosensitizes solid tumors.* Cancer Res, 2012. **72**(2): p. 482-90.
277. Zannella, V.E., A. Dal Pra, H. Muaddi, T.D. McKee, S. Stapleton, J. Sykes, R. Glicksman, S. Chaib, P. Zamiara, M. Milosevic, B.G. Wouters, R.G. Bristow, and M. Koritzinsky, *Reprogramming metabolism with metformin improves tumor oxygenation and radiotherapy response.* Clin Cancer Res, 2013. **19**(24): p. 6741-50.
278. Durand, R.E. and J.A. Raleigh, *Identification of nonproliferating but viable hypoxic tumor cells in vivo.* Cancer Res, 1998. **58**(16): p. 3547-50.

279. Amellem, O., M. Loffler, and E.O. Pettersen, *Regulation of cell proliferation under extreme and moderate hypoxia: the role of pyrimidine (deoxy)nucleotides.* Br J Cancer, 1994. **70**(5): p. 857-66.
280. Pettersen, E.O. and T. Lindmo, *Inhibition of cell-cycle progression by acute treatment with various degrees of hypoxia: modifications induced by low concentrations of misonidazole present during hypoxia.* Br J Cancer, 1983. **48**(6): p. 809-17.
281. Ljungkvist, A.S., J. Bussink, P.F. Rijken, J.H. Kaanders, A.J. van der Kogel, and J. Denekamp, *Vascular architecture, hypoxia, and proliferation in first-generation xenografts of human head-and-neck squamous cell carcinomas.* Int J Radiat Oncol Biol Phys, 2002. **54**(1): p. 215-28.
282. Takagi, A., M. Watanabe, Y. Ishii, J. Morita, Y. Hirokawa, T. Matsuzaki, and T. Shiraishi, *Three-dimensional cellular spheroid formation provides human prostate tumor cells with tissue-like features.* Anticancer Res, 2007. **27**(1a): p. 45-53.
283. Dai, Y., K. Bae, and D.W. Siemann, *Impact of hypoxia on the metastatic potential of human prostate cancer cells.* Int J Radiat Oncol Biol Phys, 2011. **81**(2): p. 521-8.
284. Lyseng-Williamson, K.A. and C. Fenton, *Docetaxel: a review of its use in metastatic breast cancer.* Drugs, 2005. **65**(17): p. 2513-31.
285. Yvon, A.M., P. Wadsworth, and M.A. Jordan, *Taxol suppresses dynamics of individual microtubules in living human tumor cells.* Mol Biol Cell, 1999. **10**(4): p. 947-59.
286. Eisenhauer, E.A. and J.B. Vermorken, *The taxoids. Comparative clinical pharmacology and therapeutic potential.* Drugs, 1998. **55**(1): p. 5-30.
287. Elledge, S.J., Z. Zhou, and J.B. Allen, *Ribonucleotide reductase: regulation, regulation, regulation.* Trends Biochem Sci, 1992. **17**(3): p. 119-23.
288. Cerqueira, N.M., P.A. Fernandes, and M.J. Ramos, *Understanding ribonucleotide reductase inactivation by gemcitabine.* Chemistry, 2007. **13**(30): p. 8507-15.
289. Herrick, J. and B. Sclavi, *Ribonucleotide reductase and the regulation of DNA replication: an old story and an ancient heritage.* Mol Microbiol, 2007. **63**(1): p. 22-34.
290. Skvortsova, I., S. Skvortsov, A. Haidenberger, A. Devries, M. Nevinny-Stickel, M. Saurer, P. Lukas, and T. Seppi, *Effects of paclitaxel and docetaxel on EGFR-expressing human carcinoma cells under normoxic versus hypoxic conditions in vitro.* J Chemother, 2004. **16**(4): p. 372-80.
291. Thews, O., B. Gassner, D.K. Kelleher, G. Schwerdt, and M. Gekle, *Impact of hypoxic and acidic extracellular conditions on cytotoxicity of chemotherapeutic drugs.* Adv Exp Med Biol, 2007. **599**: p. 155-61.
292. Sun, J.D., Q. Liu, D. Ahluwalia, W. Li, F. Meng, Y. Wang, D. Bhupathi, A.S. Ruprell, and C.P. Hart, *Efficacy and safety of the hypoxia-activated prodrug TH-302 in combination with gemcitabine and nab-paclitaxel in human tumor xenograft models of pancreatic cancer.* Cancer Biol Ther, 2015. **16**(3): p. 438-49.
293. Zhao, X., F. Li, Y. Li, H. Wang, H. Ren, J. Chen, G. Nie, and J. Hao, *Co-delivery of HIF1alpha siRNA and gemcitabine via biocompatible lipid-polymer hybrid nanoparticles for effective treatment of pancreatic cancer.* Biomaterials, 2015. **46**: p. 13-25.
294. Zhao, T., H. Ren, L. Jia, J. Chen, W. Xin, F. Yan, J. Li, X. Wang, S. Gao, D. Qian, C. Huang, and J. Hao, *Inhibition of HIF-1alpha by PX-478 enhances the anti-tumor effect of gemcitabine by inducing immunogenic cell death in pancreatic ductal adenocarcinoma.* Oncotarget, 2015. **6**(4): p. 2250-62.

295. Nikolsky, I. and T.V. Serebrovska, *Role of hypoxia in stem cell development and functioning.* Fiziol Zh, 2009. **55**(4): p. 116-30.
296. Coppe, J.P., C.K. Patil, F. Rodier, A. Krtolica, C.M. Beausejour, S. Parrinello, J.G. Hodgson, K. Chin, P.Y. Desprez, and J. Campisi, *A human-like senescence-associated secretory phenotype is conserved in mouse cells dependent on physiological oxygen.* PLoS One, 2010. **5**(2): p. e9188.
297. Althubiti, M., L. Lezina, S. Carrera, R. Jukes-Jones, S.M. Giblett, A. Antonov, N. Barlev, G.S. Saldanha, C.A. Pritchard, K. Cain, and S. Macip, *Characterization of novel markers of senescence and their prognostic potential in cancer.* Cell Death Dis, 2014. **5**: p. e1528.
298. Panieri, E., V. Gogvadze, E. Norberg, R. Venkatesh, S. Orrenius, and B. Zhivotovsky, *Reactive oxygen species generated in different compartments induce cell death, survival, or senescence.* Free Radic Biol Med, 2013. **57**: p. 176-87.
299. Gartel, A.L. and S.K. Radhakrishnan, *Lost in transcription: p21 repression, mechanisms, and consequences.* Cancer Res, 2005. **65**(10): p. 3980-5.
300. Chu, I.M., L. Hengst, and J.M. Slingerland, *The Cdk inhibitor p27 in human cancer: prognostic potential and relevance to anticancer therapy.* Nat Rev Cancer, 2008. **8**(4): p. 253-67.
301. McNeely, S., R. Beckmann, and A.K. Bence Lin, *CHEK again: revisiting the development of CHK1 inhibitors for cancer therapy.* Pharmacol Ther, 2014. **142**(1): p. 1-10.
302. Zhang, Y. and T. Hunter, *Roles of Chk1 in cell biology and cancer therapy.* Int J Cancer, 2014. **134**(5): p. 1013-23.
303. Kerr, M., H.E. Scott, B. Groselj, M.R. Stratford, K. Karaszi, N.L. Sharma, and A.E. Kiltie, *Deoxycytidine kinase expression underpins response to gemcitabine in bladder cancer.* Clin Cancer Res, 2014. **20**(21): p. 5435-45.
304. Young, C.W., G. Schochetman, and D.A. Karnofsky, *Hydroxyurea-induced inhibition of deoxyribonucleotide synthesis: studies in intact cells.* Cancer Res, 1967. **27**(3): p. 526-34.
305. Elford, H.L., *Effect of hydroxyurea on ribonucleotide reductase.* Biochem Biophys Res Commun, 1968. **33**(1): p. 129-35.
306. Committee, J.F., *BNF*. March ed. Vol. 69. 2015, London: Pharmaceutical Press.
307. Zhang, L., V. Sinha, S.T. Forgue, S. Callies, L. Ni, R. Peck, and S.R. Allerheiligen, *Model-based drug development: the road to quantitative pharmacology.* J Pharmacokinet Pharmacodyn, 2006. **33**(3): p. 369-93.
308. Veltkamp, S.A., D. Pluim, M.A. van Eijndhoven, M.J. Bolijn, F.H. Ong, R. Govindarajan, J.D. Unadkat, J.H. Beijnen, and J.H. Schellens, *New insights into the pharmacology and cytotoxicity of gemcitabine and 2',2'-difluorodeoxyuridine.* Mol Cancer Ther, 2008. **7**(8): p. 2415-25.
309. Oettle, H., S. Post, P. Neuhaus, K. Gellert, J. Langrehr, K. Ridwelski, H. Schramm, J. Fahlke, C. Zuelke, C. Burkart, K. Gutberlet, E. Kettner, H. Schmalenberg, K. Weigang-Koehler, W.O. Bechstein, M. Niedergethmann, I. Schmidt-Wolf, L. Roll, B. Doerken, and H. Riess, *Adjuvant chemotherapy with gemcitabine vs observation in patients undergoing curative-intent resection of pancreatic cancer: a randomized controlled trial.* Jama, 2007. **297**(3): p. 267-77.
310. Ferrazzi, E. and L. Stievano, *Gemcitabine: monochemotherapy of breast cancer.* Ann Oncol, 2006. **17 Suppl 5**: p. v169-72.

311. Ghosn, M., H.R. Kourie, E. El Rassy, R. Chebib, F. El Karak, C. Hanna, and D. Nasr, *Optimum chemotherapy for the management of advanced biliary tract cancer.* World J Gastroenterol, 2015. **21**(14): p. 4121-4125.
312. Barlesi, F., C. Chouaid, J. Crequit, H. Le Caer, J.L. Pujol, J. Legodec, A. Vergnenegre, J. Le Treut, E. Fabre-Guillevin, A. Loundou, P. Auquier, M.C. Simeoni, and P.A. Thomas, *A randomized trial comparing adjuvant chemotherapy with gemcitabine plus cisplatin with docetaxel plus cisplatin in patients with completely resected non-small-cell lung cancer with quality of life as the primary objective.* Interact Cardiovasc Thorac Surg, 2015.
313. Wang, H., M. Li, J.J. Rinehart, and R. Zhang, *Pretreatment with dexamethasone increases antitumor activity of carboplatin and gemcitabine in mice bearing human cancer xenografts: in vivo activity, pharmacokinetics, and clinical implications for cancer chemotherapy.* Clin Cancer Res, 2004. **10**(5): p. 1633-44.
314. Ciccolini, J., L. Dahan, N. Andre, A. Evrard, M. Duluc, A. Blesius, C. Yang, S. Giacometti, C. Brunet, C. Raynal, A. Ortiz, N. Frances, A. Iliadis, F. Duffaud, J.F. Seitz, and C. Mercier, *Cytidine deaminase residual activity in serum is a predictive marker of early severe toxicities in adults after gemcitabine-based chemotherapies.* J Clin Oncol, 2010. **28**(1): p. 160-5.
315. Khan, N., H. Hou, S. Hodge, M. Kuppusamy, E.Y. Chen, A. Eastman, P. Kuppusamy, and H.M. Swartz, *Recurrent low-dose chemotherapy to inhibit and oxygenate head and neck tumors.* Adv Exp Med Biol, 2014. **812**: p. 105-11.
316. Zhou, S., Y. Yang, Y. Yang, H. Tao, D. Li, J. Zhang, G. Jiang, and J. Fang, *Combination therapy of VEGF-trap and gemcitabine results in improved anti-tumor efficacy in a mouse lung cancer model.* PLoS One, 2013. **8**(7): p. e68589.
317. Koppe, M.J., W.J. Oyen, R.P. Bleichrodt, A.A. Verhofstad, D.M. Goldenberg, and O.C. Boerman, *Combination therapy using gemcitabine and radioimmunotherapy in nude mice with small peritoneal metastases of colonic origin.* Cancer Biother Radiopharm, 2006. **21**(5): p. 506-14.
318. Francia, G., Y. Shaked, K. Hashimoto, J. Sun, M. Yin, C. Cesta, P. Xu, S. Man, C. Hackl, J. Stewart, M. Uhlik, A.H. Dantzig, F.S. Foster, and R.S. Kerbel, *Low-dose metronomic oral dosing of a prodrug of gemcitabine (LY2334737) causes antitumor effects in the absence of inhibition of systemic vasculogenesis.* Mol Cancer Ther, 2012. **11**(3): p. 680-9.
319. Shipley, L.A., T.J. Brown, J.D. Cornpropst, M. Hamilton, W.D. Daniels, and H.W. Culp, *Metabolism and disposition of gemcitabine, and oncolytic deoxycytidine analog, in mice, rats, and dogs.* Drug Metab Dispos, 1992. **20**(6): p. 849-55.
320. Urien, S., J. Barre, C. Morin, A. Paccaly, G. Montay, and J.P. Tillement, *Docetaxel serum protein binding with high affinity to alpha 1-acid glycoprotein.* Invest New Drugs, 1996. **14**(2): p. 147-51.
321. Baker, S.D., M. Zhao, C.K. Lee, J. Verweij, Y. Zabelina, J.R. Brahmer, A.C. Wolff, A. Sparreboom, and M.A. Carducci, *Comparative pharmacokinetics of weekly and every-three-weeks docetaxel.* Clin Cancer Res, 2004. **10**(6): p. 1976-83.
322. Slaviero, K.A., S.J. Clarke, A.J. McLachlan, E.Y. Blair, and L.P. Rivory, *Population pharmacokinetics of weekly docetaxel in patients with advanced cancer.* Br J Clin Pharmacol, 2004. **57**(1): p. 44-53.
323. Brunsvig, P.F., A. Andersen, S. Aamdal, V. Kristensen, and H. Olsen, *Pharmacokinetic analysis of two different docetaxel dose levels in patients with non-small cell lung cancer treated with docetaxel as monotherapy or with concurrent radiotherapy.* BMC Cancer, 2007. **7**: p. 197.

324. Zahedi, P., R. De Souza, M. Piquette-Miller, and C. Allen, *Docetaxel distribution following intraperitoneal administration in mice.* J Pharm Pharm Sci, 2011. **14**(1): p. 90-9.
325. Galaup, A., P. Opolon, C. Bouquet, H. Li, D. Opolon, M.C. Bissery, T. Tursz, M. Perricaudet, and F. Griscelli, *Combined effects of docetaxel and angiostatin gene therapy in prostate tumor model.* Mol Ther, 2003. **7**(6): p. 731-40.
326. Dykes, D.J., M.C. Bissery, S.D. Harrison, Jr., and W.R. Waud, *Response of human tumor xenografts in athymic nude mice to docetaxel (RP 56976, Taxotere).* Invest New Drugs, 1995. **13**(1): p. 1-11.
327. Yonemura, Y., Y. Endou, E. Bando, K. Kuno, T. Kawamura, M. Kimura, T. Shimada, K. Miyamoto, T. Sasaki, and P.H. Sugarbaker, *Effect of intraperitoneal administration of docetaxel on peritoneal dissemination of gastric cancer.* Cancer Lett, 2004. **210**(2): p. 189-96.
328. Browder, T., C.E. Butterfield, B.M. Kraling, B. Shi, B. Marshall, M.S. O'Reilly, and J. Folkman, *Antiangiogenic scheduling of chemotherapy improves efficacy against experimental drug-resistant cancer.* Cancer Res, 2000. **60**(7): p. 1878-86.
329. Bertolini, F., S. Paul, P. Mancuso, S. Monestiroli, A. Gobbi, Y. Shaked, and R.S. Kerbel, *Maximum tolerable dose and low-dose metronomic chemotherapy have opposite effects on the mobilization and viability of circulating endothelial progenitor cells.* Cancer Res, 2003. **63**(15): p. 4342-6.
330. Dellapasqua, S., F. Bertolini, V. Bagnardi, E. Campagnoli, E. Scarano, R. Torrisi, Y. Shaked, P. Mancuso, A. Goldhirsch, A. Rocca, E. Pietri, and M. Colleoni, *Metronomic cyclophosphamide and capecitabine combined with bevacizumab in advanced breast cancer.* J Clin Oncol, 2008. **26**(30): p. 4899-905.
331. Garcia, A.A., H. Hirte, G. Fleming, D. Yang, D.D. Tsao-Wei, L. Roman, S. Groshen, S. Swenson, F. Markland, D. Gandara, S. Scudder, R. Morgan, H. Chen, H.J. Lenz, and A.M. Oza, *Phase II clinical trial of bevacizumab and low-dose metronomic oral cyclophosphamide in recurrent ovarian cancer: a trial of the California, Chicago, and Princess Margaret Hospital phase II consortia.* J Clin Oncol, 2008. **26**(1): p. 76-82.
332. Lord, R., S. Nair, A. Schache, J. Spicer, N. Somaihah, V. Khoo, and H. Pandha, *Low dose metronomic oral cyclophosphamide for hormone resistant prostate cancer: a phase II study.* J Urol, 2007. **177**(6): p. 2136-40; discussion 2140.
333. Young, S.D., M. Whissell, J.C. Noble, P.O. Cano, P.G. Lopez, and C.J. Germond, *Phase II clinical trial results involving treatment with low-dose daily oral cyclophosphamide, weekly vinblastine, and rofecoxib in patients with advanced solid tumors.* Clin Cancer Res, 2006. **12**(10): p. 3092-8.
334. Shaked, Y., U. Emmenegger, S. Man, D. Cervi, F. Bertolini, Y. Ben-David, and R.S. Kerbel, *Optimal biologic dose of metronomic chemotherapy regimens is associated with maximum antiangiogenic activity.* Blood, 2005. **106**(9): p. 3058-61.
335. Hamano, Y., H. Sugimoto, M.A. Soubasakos, M. Kieran, B.R. Olsen, J. Lawler, A. Sudhakar, and R. Kalluri, *Thrombospondin-1 associated with tumor microenvironment contributes to low-dose cyclophosphamide-mediated endothelial cell apoptosis and tumor growth suppression.* Cancer Res, 2004. **64**(5): p. 1570-4.
336. Specenier, P., G. Guetens, J. Dyck, G. De Boeck, J. Weyler, D. Van den Weyngaert, K. Aelbrecht, and J.B. Vermorken, *Difluorodeoxyuridine plasma concentrations after low-dose gemcitabine during chemoradiation in head and neck cancer patients.* Cancer Chemother Pharmacol, 2011. **68**(1): p. 185-91.

337. Baskar, R., K.A. Lee, R. Yeo, and K.W. Yeoh, *Cancer and radiation therapy: current advances and future directions.* Int J Med Sci, 2012. **9**(3): p. 193-9.
338. Verheij, M., *Clinical biomarkers and imaging for radiotherapy-induced cell death.* Cancer Metastasis Rev, 2008. **27**(3): p. 471-80.
339. Delaney, G., S. Jacob, C. Featherstone, and M. Barton, *The role of radiotherapy in cancer treatment: estimating optimal utilization from a review of evidence-based clinical guidelines.* Cancer, 2005. **104**(6): p. 1129-37.
340. Sher, D.J., *Cost-effectiveness studies in radiation therapy.* Expert Rev Pharmacoecon Outcomes Res, 2010. **10**(5): p. 567-82.
341. Ringborg, U., D. Bergqvist, B. Brorsson, E. Cavallin-Stahl, J. Ceberg, N. Einhorn, J.E. Frodin, J. Jarhult, G. Lamnevik, C. Lindholm, B. Littbrand, A. Norlund, U. Nylen, M. Rosen, H. Svensson, and T.R. Moller, *The Swedish Council on Technology Assessment in Health Care (SBU) systematic overview of radiotherapy for cancer including a prospective survey of radiotherapy practice in Sweden 2001--summary and conclusions.* Acta Oncol, 2003. **42**(5-6): p. 357-65.
342. Lawrence, T.S., A.W. Blackstock, and C. McGinn, *The mechanism of action of radiosensitization of conventional chemotherapeutic agents.* Semin Radiat Oncol, 2003. **13**(1): p. 13-21.
343. Lawrence, T.S., A. Eisbruch, C.J. McGinn, M.T. Fields, and D.S. Shewach, *Radiosensitization by gemcitabine.* Oncology (Williston Park), 1999. **13**(10 Suppl 5): p. 55-60.
344. Kal, H.B., S.Y. El Sharouni, and A.D. Barten-van Rijbroek, *Gemcitabine as a radiosensitizer in undifferentiated tumors.* Anticancer Res, 2006. **26**(1a): p. 139-45.
345. Wouters, A., B. Pauwels, N. Burrows, M. Baay, V. Deschoolmeester, T.N. Vu, K. Laukens, P. Meijnders, D. Van Gestel, K.J. Williams, D. Van den Weyngaert, J.B. Vermorken, P. Pauwels, M. Peeters, and F. Lardon, *The radiosensitising effect of gemcitabine and its main metabolite dFdU under low oxygen conditions is in vitro not dependent on functional HIF-1 protein.* BMC Cancer, 2014. **14**: p. 594.
346. Alvarez, E.A., A.H. Wolfson, J.M. Pearson, M.P. Crisp, L.E. Mendez, N.C. Lambrou, and J.A. Lucci, 3rd, *A phase I study of docetaxel as a radio-sensitizer for locally advanced squamous cell cervical cancer.* Gynecol Oncol, 2009. **113**(2): p. 195-9.
347. Balkman, C.E., T.L. Gieger, M.M. Zgola, L.D. Lewis, and M.C. McEntee, *In Vitro Characterization of Docetaxel as a Radiosensitizer in Canine and Feline Cancer Cell Lines.* Open Journal of Veterinary Medicine, 2012. **Vol.02No.04**: p. 8.
348. Dunne, A.L., C. Mothersill, T. Robson, G.D. Wilson, and D.G. Hirst, *Radiosensitization of colon cancer cell lines by docetaxel: mechanisms of action.* Oncol Res, 2004. **14**(9): p. 447-54.
349. Amorino, G.P., V.M. Hamilton, and H. Choy, *Enhancement of radiation effects by combined docetaxel and carboplatin treatment in vitro.* Radiat Oncol Investig, 1999. **7**(6): p. 343-52.
350. Lin, H.L., T.Y. Liu, G.Y. Chau, W.Y. Lui, and C.W. Chi, *Comparison of 2-methoxyestradiol-induced, docetaxel-induced, and paclitaxel-induced apoptosis in hepatoma cells and its correlation with reactive oxygen species.* Cancer, 2000. **89**(5): p. 983-94.
351. Budman, D.R. and A. Calabro, *In vitro search for synergy and antagonism: evaluation of docetaxel combinations in breast cancer cell lines.* Breast Cancer Res Treat, 2002. **74**(1): p. 41-6.

352. Milas, L., M.M. Milas, and K.A. Mason, *Combination of taxanes with radiation: preclinical studies.* Semin Radiat Oncol, 1999. **9**(2 Suppl 1): p. 12-26.
353. Milas, L., *Docetaxel/radiation combinations: rationale and preclinical findings.* Clin Lung Cancer, 2002. **3 Suppl 2**: p. S29-36.
354. Grant, D.S., T.L. Williams, M. Zahaczewsky, and A.P. Dicker, *Comparison of antiangiogenic activities using paclitaxel (taxol) and docetaxel (taxotere).* Int J Cancer, 2003. **104**(1): p. 121-9.
355. Mason, K.A., N.R. Hunter, M. Milas, J.L. Abbruzzese, and L. Milas, *Docetaxel enhances tumor radioresponse in vivo.* Clin Cancer Res, 1997. **3**(12 Pt 1): p. 2431-8.
356. Mason, K.A., K. Kishi, N. Hunter, L. Buchmiller, T. Akimoto, R. Komaki, and L. Milas, *Effect of docetaxel on the therapeutic ratio of fractionated radiotherapy in vivo.* Clin Cancer Res, 1999. **5**(12): p. 4191-8.
357. Tishler, R.B., C.M. Norris, Jr., A.D. Colevas, C.C. Lamb, D. Karp, P.M. Busse, A. Nixon, R. Frankenthaler, B. Lake-Willcutt, R. Costello, M. Case, and M.R. Posner, *A Phase I/II trial of concurrent docetaxel and radiation after induction chemotherapy in patients with poor prognosis squamous cell carcinoma of the head and neck.* Cancer, 2002. **95**(7): p. 1472-81.
358. Calais, G., E. Bardet, C. Sire, M. Alfonsi, J. Bourhis, B. Rhein, J. Tortochaux, Y.T. Man, H. Auvray, and P. Garaud, *Radiotherapy with concomitant weekly docetaxel for Stages III/IV oropharynx carcinoma. Results of the 98-02 GORTEC Phase II trial.* Int J Radiat Oncol Biol Phys, 2004. **58**(1): p. 161-6.
359. Pauwels, B., J.B. Vermorken, A. Wouters, J. Ides, S. Van Laere, H.A. Lambrechts, G.G. Pattyn, K. Vermeulen, P. Meijnders, and F. Lardon, *The role of apoptotic cell death in the radiosensitising effect of gemcitabine.* Br J Cancer, 2009. **101**(4): p. 628-36.
360. Gregoire, V., M. Beauduin, J.F. Rosier, B. De Coster, M. Bruniaux, M. Octave-Prignot, and P. Scalliet, *Kinetics of mouse jejunum radiosensitization by 2',2'-difluorodeoxycytidine (gemcitabine) and its relationship with pharmacodynamics of DNA synthesis inhibition and cell cycle redistribution in crypt cells.* Br J Cancer, 1997. **76**(10): p. 1315-21.
361. Wachters, F.M., J.W. van Putten, J.G. Maring, M.Z. Zdzienicka, H.J. Groen, and H.H. Kampinga, *Selective targeting of homologous DNA recombination repair by gemcitabine.* Int J Radiat Oncol Biol Phys, 2003. **57**(2): p. 553-62.
362. Kooistra, R., A. Pastink, J.B. Zonneveld, P.H. Lohman, and J.C. Eeken, *The Drosophila melanogaster DmRAD54 gene plays a crucial role in double-strand break repair after P-element excision and acts synergistically with Ku70 in the repair of X-ray damage.* Mol Cell Biol, 1999. **19**(9): p. 6269-75.
363. Essers, J., H. van Steeg, J. de Wit, S.M. Swagemakers, M. Vermeij, J.H. Hoeijmakers, and R. Kanaar, *Homologous and non-homologous recombination differentially affect DNA damage repair in mice.* Embo j, 2000. **19**(7): p. 1703-10.
364. Sutherland, R.M., W.R. Inch, J.A. McCredie, and J. Kruuv, *A multi-component radiation survival curve using an in vitro tumour model.* Int J Radiat Biol Relat Stud Phys Chem Med, 1970. **18**(5): p. 491-5.
365. Schwachofer, J.H., *Multicellular tumor spheroids in radiotherapy research (review).* Anticancer Res, 1990. **10**(4): p. 963-9.
366. Santini, M.T., G. Rainaldi, and P.L. Indovina, *Multicellular tumour spheroids in radiation biology.* Int J Radiat Biol, 1999. **75**(7): p. 787-99.

367. Mayneord, W.V., *On a law of growth of jensen's rat sarcoma.* Am. J. Cancer, 1932. **16**: p. 841–846.
368. Barendsen, G.W., *Dose fractionation, dose rate and iso-effect relationships for normal tissue responses.* Int J Radiat Oncol Biol Phys, 1982. **8**(11): p. 1981-97.
369. Rockne, R., J.K. Rockhill, M. Mrugala, A.M. Spence, I. Kalet, K. Hendrickson, A. Lai, T. Cloughesy, E.C. Alvord, Jr., and K.R. Swanson, *Predicting the efficacy of radiotherapy in individual glioblastoma patients in vivo: a mathematical modeling approach.* Phys Med Biol, 2010. **55**(12): p. 3271-85.
370. Shewach, D.S., T.M. Hahn, E. Chang, L.W. Hertel, and T.S. Lawrence, *Metabolism of 2',2'-difluoro-2'-deoxycytidine and radiation sensitization of human colon carcinoma cells.* Cancer Res, 1994. **54**(12): p. 3218-23.
371. Lawrence, T.S., E.Y. Chang, T.M. Hahn, L.W. Hertel, and D.S. Shewach, *Radiosensitization of pancreatic cancer cells by 2',2'-difluoro-2'-deoxycytidine.* Int J Radiat Oncol Biol Phys, 1996. **34**(4): p. 867-72.
372. Khaitan, D., S. Chandna, M. Arya, and B. Dwarakanath, *Establishment and characterization of multicellular spheroids from a human glioma cell line; Implications for tumor therapy.* J Transl Med, 2006. **4**: p. 12.
373. Landry, J., J.P. Freyer, and R.M. Sutherland, *Shedding of mitotic cells from the surface of multicell spheroids during growth.* Journal of Cellular Physiology, 1981. **106**(1): p. 23-32.
374. Sakata, K., S. Okada, H. Majima, and N. Suzuki, *Cell shedding from x-irradiated multicellular spheroids of human lung carcinomas*. Vol. 167. 1991. 723-5.
375. Menchon, S.A. and C.A. Condat, *Modeling tumor cell shedding.* Eur Biophys J, 2009. **38**(4): p. 479-85.
376. Lawrence, T.S., E.Y. Chang, T.M. Hahn, and D.S. Shewach, *Delayed radiosensitization of human colon carcinoma cells after a brief exposure to 2',2'-difluoro-2'-deoxycytidine (Gemcitabine).* Clin Cancer Res, 1997. **3**(5): p. 777-82.
377. Gregoire, V., M. Beauduin, M. Bruniaux, B. De Coster, M. Octave Prignot, and P. Scalliet, *Radiosensitization of mouse sarcoma cells by fludarabine (F-ara-A) or gemcitabine (dFdC), two nucleoside analogues, is not mediated by an increased induction or a repair inhibition of DNA double-strand breaks as measured by pulsed-field gel electrophoresis.* Int J Radiat Biol, 1998. **73**(5): p. 511-20.
378. Huang, P., K. Ballal, and W. Plunkett, *Biochemical characterization of the protein activity responsible for high molecular weight DNA fragmentation during drug-induced apoptosis.* Cancer Res, 1997. **57**(16): p. 3407-14.